

MODIFICATION OF NANOCCLAY USING
TRANSITION METAL ION AND ITS EFFECT
ON MECHANICAL, PHYSICAL, AND
THERMAL PROPERTIES OF WOOD-PLASTIC
COMPOSITES



SUMIT MANOHAR YADAV

UMP

Doctor of Philosophy

UNIVERSITI MALAYSIA PAHANG

UNIVERSITI MALAYSIA PAHANG

DECLARATION OF THESIS AND COPYRIGHT

Author's Full Name: Sumit Manohar Yadav

Date of Birth : 10-02-1989

Title : Modification of nanoclay using transition metal ion and its effect on mechanical, physical, and thermal properties of wood-plastic composites.

Academic Session: 2016/2017

I declare that this thesis is classified as:

- CONFIDENTIAL** (Contain confidential information under the official secret Act 1997)*
- RESTRICTED** (Contains restricted information as specified by the organization where research was done)*
- OPEN ACCESS** I agree that my thesis to be published as online open access (Full Text)

I acknowledge that Universiti Malaysia Pahang reserve the right as follows:

1. The Thesis is the Property of Universiti Malaysia Pahang
2. The Library of Universiti Malaysia Pahang has the right to make copies for the purpose of research only.
3. The library has the right to make copies of the Thesis for academic exchange.

Certified By:

(Student's Signature)

L4302970
New IC/Passport Number
Date: 03/02/2017

(Supervisor's Signature)

Dr. Kamal Bin Yusoh
Name of Supervisor
Date: 03/02/2017

SUPERVISOR'S DECLARATION

We hereby declare that we have checked this thesis and in our opinion, this thesis is adequate in terms of scope and quality for the award of the degree of PhD in Chemical Engineering.

(Supervisor's Signature)

Full Name : Dr. KAMAL BIN YUSOH

Position : ASSOCIATE PROFESSOR

Date : 3 FEBRUARY 2017

(Co-supervisor's Signature)

Full Name : Dr. ARUN GUPTA

Position : ASSOCIATE PROFESSOR

Date : 3 FEBRUARY 2017



STUDENT'S DECLARATION

I hereby declare that the work in this thesis is based on my original work except for quotations and citation which have been duly acknowledged. I also declare that it has not been previously or concurrently submitted for any other degree at Universiti Malaysia Pahang or any other institutions.

(Author's Signature)

Full Name : SUMIT MANOHAR YADAV

ID Number : PKC 14002

Date : 3 FEBRUARY 2017

MODIFICATION OF NANOCLAY USING TRANSITION METAL IONS AND ITS
EFFECT ON MECHANICAL, PHYSICAL, AND THERMAL PROPERTIES OF WOOD-
PLASTIC COMPOSITES



Thesis submitted in fulfilment of the requirements for the award of the degree Doctor of
Philosophy in Chemical Engineering

Faculty of Chemical and Natural Resources Engineering

UNIVERSITI MALAYSIA PAHANG

JANUARY 2017



*Dedicated to my beloved parents and siblings
for their love and encouragement*

UMP

ACKNOWLEDGEMENTS

Firstly, I would like express my sincere gratitude to my supervisor Dr Kamal Bin Yusoh for his germinal ideas, invaluable guidance, continuous encouragement and constant support in making this research possible. I really appreciate his willingness to always spare time to provide me with the guidance I require to make this research a success.

I would like to thank Universiti Malaysia Pahang for rewarding me DSS (Doctoral Scholarship Scheme) for my financial assistance. My special acknowledgment goes to the Dean, Deputy Dean and all staff of Faculty of Chemical and Natural Resource Engineering, Universiti Malaysia Pahang, and Dr Suriya Kumar who had helped me in many ways and made my stay here a pleasant and unforgettable experience.

It is my pleasure to work with a group of brilliant, warm hearted and lovely group members, Abu Hannifa, Zulhelmi Ismail, and Anis Sakinah. I thank all my friends, in particular, Dr, Ayodele Victor, Mr, Tanveer Khan, Mr, Puranjan Mishra, Mr, Midhun, Mr, Shyam Krishanan, Mr, Pradeep Poddar, Mr, Ravinder Kumar, and Mr, Sharanjit Singh.

Finally, I would also like to acknowledge my sincere indebtedness and gratitude to my parents for their love, dream and sacrifice throughout my life. I really appreciate the consistent encouragement provided to carry on my studies. I am also grateful to my fellow siblings who has guided me throughout my life and provided me with comments and suggestions which were crucial for the successful completion of this study.

Sumit Manohar Yadav
The Author

ABSTRAK

Dalam kajian ini, komposit kayu-plastik (WPCs) telah direka daripada Polypropylene (PP), tepung kayu (WF), acetic Maleic polypropylene dicantumkan (MAPP) dan nanoclay menggunakan extrusion diikuti oleh teknik pengacuan suntikan. Kesan organo, ion montmorilonit (MMT) dan peralihan logam (TMI) nanoclay diubahsuai yang telah dimasukkan ke dalam WPCs telah dibincangkan. The TMI pengubahsuaian bertujuan untuk mencapai penyebaran yang baik nanoclay ke WPCs dengan kurang agglomerates. The TMI-pengubahsuaian nanoclay MMT telah dijalankan dengan menggunakan tembaga (II) klorida. Kandungan nanoclay ke dalam komposit telah berubah pada empat beban yang berbeza (1 hingga 5 peratus berat). Proses pengubahsuaian telah terbukti berjaya sebagai jumlah yang tinggi ion tembaga dikesan di Tenaga Penyebaran X-ray analisis (EDX) dan juga pengedaran nanoclay itu telah diperoleh dalam Field Pelepasan Mikroskop Imbasan Elektron (FESEM). X-Ray Diffraction (XRD) data dengan nilai-nilai d jarak yang lebih tinggi telah diperolehi bagi nanoclay TMI diubahsuai yang menunjukkan bahawa struktur diinterkalasi yang baik telah dicapai. nanoclay TMI diubahsuai menunjukkan suhu degradasi yang lebih tinggi dalam analisis Thermo gravimetrik analisis (TGA) yang menunjukkan bahawa pengubahsuaian nanoclay bertambah baik kestabilan terma. Mikroskop Imbasan Elektron (SEM) mikrograf digambarkan lebih kecil lubang, retak, dan agglomerates dalam WPCs dimuatkan oleh nanoclay TMI diubahsuai kerana pengubahsuaian nanoclay yang membolehkan pengagihan walaupun nanoclay ke dalam komposit. Peningkatan tertinggi dalam kekuatan tegangan telah diperolehi pada 1% berat daripada organo dan nanoclay diperbadankan WPCs TMI diubahsuai. tambahan lagi nanoclay menurun sifat mekanikal yang disebabkan oleh penumpuan nanoclay. Sama seperti sifat-sifat mekanikal permukaan sifat-sifat mekanik dan tingkah laku permukaan rayap telah dipamerkan nilai lebih tinggi pada 1% berat daripada organo dan TMI diubahsuai nanoclay loading ke dalam WPCs. Kestabilan haba juga bertambah baik pada organo dan nanoclay TMI diubahsuai bertetulang WPCs. WPCs diperkukuh oleh organo dan nanoclay TMI diubahsuai kekurangan penyerapan air komposit disebabkan oleh pembentukan keserasian yang lebih tinggi antara nanofiller dan matriks polimer. Kajian pengoptimuman telah dijalankan menggunakan kaedah gerak balas permukaan (RSM). Kekuatan tegangan optimum telah diperolehi sebagai 33.46 MPa pada 72 wt% polypropylene kandungan serat dan 1.38% berat daripada nanoclay.

ABSTRACT

In this study, wood-plastic composites (WPCs) were fabricated from Polypropylene (PP), Wood flour (WF), Maleic anhydride grafted polypropylene (MAPP) and nanoclay using extrusion followed by an injection molding technique. The effect of organoclay, montmorillonite (MMT) and transition metal ion (TMI) modified nanoclay which were incorporated into WPCs was studied. The TMI modification was intended to achieve a good dispersion of the nanoclay into WPCs with fewer agglomerates. The TMI-modification of the MMT nanoclay was carried out using Copper (II) Chloride. The nanoclay content in the composite was varied at four different loadings (1 to 5 weight percentages). The modification process had proved successful, as a high amount of copper ions were detected in the Energy Dispersion X-ray analysis (EDX) and even distribution of the nanoclay was obtained in Field Emission Scanning Electron Microscope (FESEM). X-Ray Diffraction (XRD) data with higher d-spacing values was obtained for TMI-modified nanoclay which suggests that a good intercalated structure has been achieved. TMI-modified nanoclay showed higher degradation temperature in Thermo Gravimetric analysis (TGA) analysis which indicates that modification of nanoclay had improved the thermal stability. Scanning Electron Microscope (SEM) micrographs had illustrated lesser holes, cracks, and agglomerates in WPCs loaded by TMI-modified nanoclay due to the modification of nanoclay which enables an even distribution of the nanoclay into the composite. The highest increase in tensile strength was obtained for 1 wt% of organoclay and TMI-modified nanoclay incorporated WPCs. Further addition of nanoclay had decreased mechanical properties due to the agglomeration of nanoclay. Same like mechanical properties, surface mechanical properties and surface creep behaviour were exhibited with higher value at 1 wt% of organoclay and TMI-modified nanoclay loading into the WPCs. The thermal stability was also improved in the organoclay and TMI-modified nanoclay reinforced WPCs. WPCs reinforced by organoclay and TMI-modified nanoclay decreased the water absorption of composite due to the formation of higher compatibility between nanofiller and the polymer matrix. The optimization study was conducted using a response surface methodology (RSM). The optimum tensile strength was obtained as 33.46 MPa at 72 wt% of polypropylene content and 1.38 wt% of nanoclay.

TABLE OF CONTENTS

DECLARATION	
TITLE PAGE	
ACKNOWLEDGEMENTS	iii
ABSTRAK	iv
ABSTRACT	v
TABLE OF CONTENT	vi
LIST OF TABLES	xiii
LIST OF FIGURES	xv
LIST OF ABBREVIATIONS	xx
CHAPTER 1 INTRODUCTION	1
1.1 Background of study	1
1.2 Problem statement	7
1.3 Objectives of study	8
1.4 Scope of study	8
1.5 Significance of research	10
CHAPTER 2 LITERATURE REVIEW	11
2.1 Introduction	11
2.2 Wood-plastic composites (WPCs)	11
2.3 Components of wood-plastic composites	12
2.3.1 Wood fiber	12
2.3.2 Plastics used to formulate wood-plastic composites	16

2.3.3	Coupling agents	20
2.3.3.1	Classification of coupling agents	21
2.3.4	Wood-plastic composites reinforced by nanofillers	24
2.3.4.1	Nanoclay	26
2.4	Fabrication processes of wood-plastic composites	31
2.4.1	Extrusion processing	32
2.4.2	Compression molding	32
2.4.3	Injection molding	33
2.5	Characterization of wood-plastic composites	35
2.5.1	Morphological characterizations	36
2.5.2	Structural characterization	39
2.6	Properties of wood-plastic composites	41
2.6.1	Mechanical properties	41
2.6.1.1	Surface mechanical properties	42
2.6.2	Physical properties	47
2.6.3	Thermal properties	50
2.7	Optimization of wood-plastic composites using Response surface methodology (RSM)	52
2.8	Summary	54
CHAPTER 3 METHODOLOGY		56
3.1	Introduction	56
3.2	Materials	56
3.2.1	Polypropylene	57
3.2.2	Wood flour	57
3.2.3	Maleic anhydride polypropylene (MAPP)	58
3.2.4	Cloisite 20A	59
3.2.5	Cloisite Na ⁺	60
3.2.6	Copper (II) chloride	61

3.2.7	Methanol	62
3.2.8	Sodium chloride	63
3.3	Methods	63
3.3.1	Montmorillonite (MMT) clay modification using transition ion metal	63
3.3.1.1	Pre-treatment of MMT nanoclay	63
3.3.1.2	Preparation of TMI solution and modification	64
3.4	Characterizations of TMI-modified MMT nanoclay	64
3.4.1	Field emission electron scanning electron microscopy (FESEM) and energy dispersion X-ray analysis (EDX)	64
3.5	Fabrication of nanoclay-based wood-plastic composites	65
3.5.1	Mixing	65
3.5.2	Extrusion	66
3.5.3	Pelletizing	67
3.5.4	Injection molding	67
3.6	Characterization of wood-plastic composites	68
3.6.1	Scanning electron microscopy (SEM)	68
3.6.2	Transmission electron microscope (TEM)	69
3.6.3	X-ray diffraction (XRD)	69
3.6.4	Fourier transform infrared spectroscopy (FTIR)	70
3.7	Properties of wood-plastic composite	70
3.7.1	Mechanical properties	70
3.7.1.1	Tensile testing	71
3.7.1.2	Flexural testing	71
3.7.1.3	Izod impact test	72
3.7.2	Physical properties	73

3.7.2.1	Density	73
3.7.2.2	Water absorption	73
3.7.3	Thermal analysis	74
3.7.3.1	Thermal gravimetric analysis (TGA)	74
3.7.3.2	Differential scanning Calorimetry (DSC)	74
3.7.4	Surface mechanical properties studied by nanoindentation	75
3.7.5	Creep test studied by nanoindentation	78
3.8	Optimization of TMI-modified based wood-plastic composite by Response surface methodology (RSM)	79
3.8.1	Fractional factorial design – screening of process parameters	79
3.8.2	Experimental design and optimization	80
CHAPTER 4 RESULTS AND DISCUSSION		82
4.1	Introduction	82
4.2	Wood-plastic composite reinforced by organoclay	82
4.2.1	Characterization of wood-plastic composite reinforced by organoclay	82
4.2.1.1	Morphological characterizations	82
4.2.1.2	Structural characterizations	88
4.2.2	Mechanical properties	92
4.2.2.1	Tensile properties	92
4.2.2.2	Flexural properties	95
4.2.2.3	Elongation at break	97
4.2.2.4	Izod impact test	98
4.2.3	Physical properties	100
4.2.3.1	Water absorption	100

4.2.4	Thermal properties	102
4.2.4.1	Thermal degradation	102
4.2.4.2	Crystallization behaviour	105
4.3	Modification of pristine (MMT) nanoclay and its application in wood-plastic composite	109
4.3.1	Modification of MMT nanoclay	109
4.3.1.1	Mechanism of transition ion (TMI) modification	109
4.3.2	Characterization TMI-modified MMT nanoclay	112
4.3.2.1	Elemental analysis	112
4.3.2.2	Morphological characterization	114
4.3.2.3	Structural characterization	115
4.3.3	Characterization of wood-plastic composite reinforced by pristine and modified nanoclay	116
4.3.3.1	Morphological characterizations	116
4.3.3.2	Structural characterizations	121
4.3.4	Mechanical properties	126
4.3.4.1	Tensile properties	126
4.3.4.2	Flexural properties	130
4.3.4.3	Elongation at break	132
4.3.4.4	Izod impact test	134
4.3.5	Physical properties	135
4.3.5.1	Density	136
4.3.5.2	Water absorption	137
4.3.6	Thermal properties	139
4.3.6.1	Thermal degradation	140
4.3.6.2	Crystallization behaviour	145

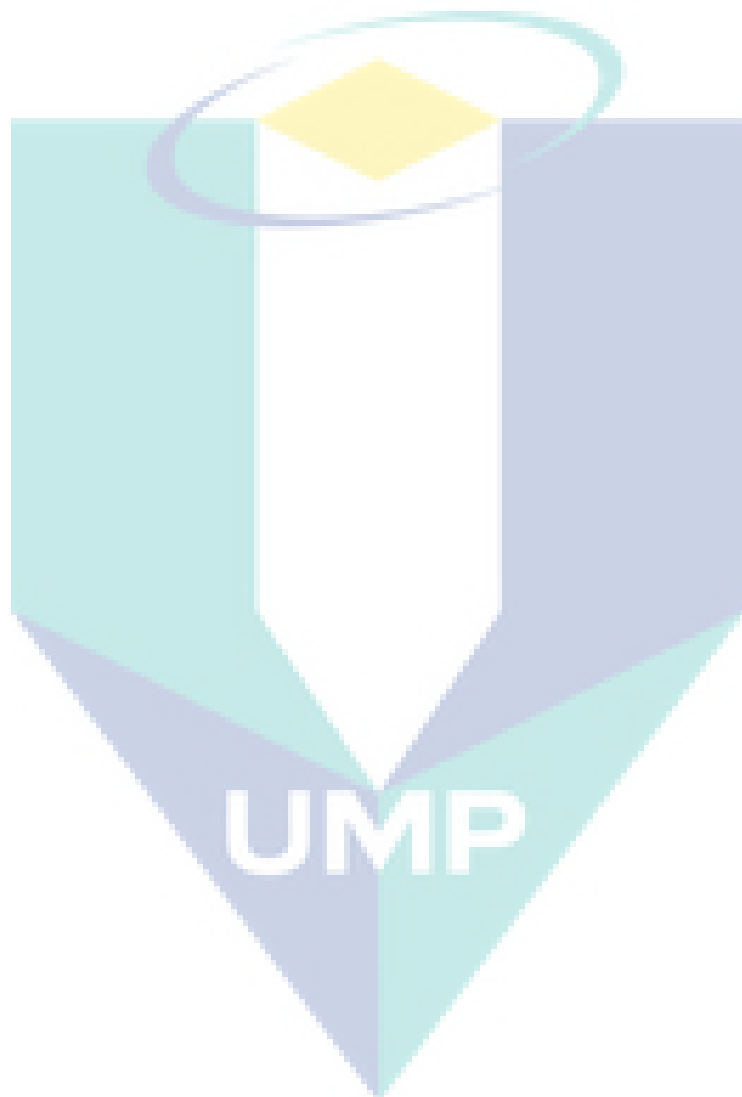
4.4	Subsurface mechanical properties of wood-plastic composite studied by nanoindentation	149
4.4.1	Introduction	149
4.4.2	Wood-plastic composite reinforced by C20 organoclay	149
4.4.3	Wood-plastic composite reinforced by pristine nanoclay (WPC/MMT) and TMI-modified nanoclay (WPC/MMT Cu)	152
4.5	Subsurface creep behaviour of wood-plastic composite studied by nanoindentation	157
4.5.1	Introduction	157
4.5.2	Creep behaviour of wood-plastic composite reinforced by C20 organoclay	157
4.5.3	Creep behaviour of wood-plastic composite reinforced by pristine nanoclay (WPC/MMT) and TMI-modified nanoclay (WPC/MMT Cu)	162
4.6	Optimization of TMI-modified nanoclay based wood-plastic composite by Response surface methodology (RSM)	168
4.6.1	Screening of wood-plastic composite parameters by fractional factorial design (FFD)	168
4.6.2	Augmentation of central composite design (CCD)	175
4.6.3	Fitting model and analysis variance	176
4.6.4	Adequate check model	178
4.6.5	Optimization condition for Response surface methodology (RSM)	179
4.6.6	Model validation and experimental confirmation	180
CHAPTER 5 CONCLUSION AND RECOMMENDATIONS		182
5.1	Conclusions	182
5.2	Recommendations	184
REFERENCES		186
APPENDIX A		206

APPENDIX B

210

PUBLICATIONS

211



LIST OF TABLES

Table	Title	Page
2.1	Effect of Pine Wood Flour Particle Size on Performance of Wood- filled Polypropylene Composite (Sihombing et al., 2012)	16
2.2	Summary of material properties for WPC (Gardner and Murdock, 2002)	19
2.3	Example of atomic groups with their IR absorption wavelengths (Bhattacharya et al., 2008)	39
2.4	Maximum water absorption for different formulations (Ghasemi and Kord, 2009)	48
2.5	Weight percentage of OWS/PCR-HDPE composites at different temperatures (Ratanawilai et al., 2012)	51
3.1	Physical and chemical properties of PP	57
3.2	Physical and chemical properties of MAPP	58
3.3	Physical and chemical properties of organoclay	59
3.4	Physical and chemical properties of montmorillonite	60
3.5	Physical and chemical properties of Copper (II) chloride	61
3.6	Physical and chemical properties of methanol	62
3.7	Physical and chemical properties of Sodium chloride	63
3.8	The composition of designed formulations	66
3.9	Temperature parameter for extrusion of wood-plastic composites	66
3.10	Temperature parameter for injection molding of wood-plastic composites	67
3.11	Parameters used in SEM analysis	69
3.12	Factors and respected ranges decided for the screening experiment	79
3.13	Experimental design for screening	80
3.14	Factors and respected ranges decided for the central composite design	81
4.1	Tentative FTIR peaks Assignments of Wood-plastic composite with different content of C20 organoclay	89
4.2	The value of angular spacing, d and reflection angle, 2θ of the PP, WPC and WPC with different content of C20 organoclay	91

4.3	Weight percentage of PP, WPC without nanoclay and WPC containing different percentages of C20 organoclay at different temperatures	104
4.4	DSC result of neat PP and WPC containing different loading of C20 organoclay	107
4.5	EDX studies of MMT and MMT Cu with elemental weight and atomic percentages	113
4.6	Tentative FTIR peaks Assignments of Wood-plastic composite with different content of MMT and MMT Cu	123
4.7	The value of angular spacing, d and reflection angle, 2θ of the PP, WPC and WPC with different content of MMT and MMT Cu	126
4.8	Thermogravimetric properties of WPC with different MMT and MMT Cu nanoclay loading	143
4.9	DSC result of neat PP and WPC with different loading of MMT and MMT Cu nanoclay	148
4.10	Hardness and modulus values of PP, WPC, WPC with C20 nanoclay loading	152
4.11	Hardness and modulus values of PP, WPC, WPC with MMT nanoclay loading	156
4.12	Hardness and modulus values of PP, WPC, WPC with MMT Cu nanoclay loading	156
4.13	Fitting parameters from Eq. (4.1) for polypropylene, WPC, and WPC/C20 from indentation creep experiment	161
4.14	Fitting parameters from Eq. (4.1) for polypropylene, WPC, WPC/MMT and WPC/MMT Cu from indentation creep experiment	167
4.15	Factors and respected ranges for screening experiment	168
4.16	Factorial design with response	169
4.17	Analysis of variance (ANOVA) table for the screening experiment of experimental factors with actual units and experimental responses	170
4.18	Statistical summary of screening result	171
4.19	Central composite design (CCD) with response	176
4.20	Analysis of variance (ANOVA) table of the quadratic model for tensile strength	177
4.21	Coefficient of variation, R^2 , and adequate precision of the model	177
4.22	Optimum condition obtained from RSM	181

LIST OF FIGURES

Figure	Title	Page
1.1	Types of nanocomposite morphologies (Kornmann, 2001)	5
2.1	Structure of wood fibers (Jayaraman, 2003)	14
2.2	Schematic illustration of the wood fiber swelling process (Wang, 2007)	20
2.3	Classification of coupling agents (Lei et al., 2015)	21
2.4	The reaction of cellulose fibers with MAPP (Keener et al., 2004)	22
2.5	Structure of nanoclay (Hetzer and De Kee, 2008)	27
2.6	Schematic diagram of an ion exchange reaction (Fisher, 2003)	28
2.7	Relative properties for extruded and injection molded WPC made with HDPE and chemo-thermo-mechanical pulp (CTMP) fibers (average for three fiber sizes) (Migneault et al., 2009)	35
2.8	SEM micrographs of tensile fracture surfaces of WPC with 6 wt% of nanoclay (a and b) and WPC with 2 wt% of nanoclay (c and d) (Chavooshi et al., 2014)	37
2.9	TEM of HDPE/nanoclay composites: (a) with 3 wt% of nanoclay and (b) with 5 wt% of nanoclay (Faruk and Matuana, 2008)	38
2.10	XRD patterns of the nanoclay content at $2\theta = 1$ to 10° (Ahmad et al., 2015)	41
2.11	Schematic of tips used in instrumented indentation. (a) A sharp pyramidal tip is often modelled as a cone with $\theta = 70.3^\circ$, (b) A spherical tip is defined by its radius R, and a characteristic strain may be defined as a/R . (c) SEM image of a diamond Berkovich indenter (Pelletier et al., 2008)	43
2.12	Three creep regimes of conventional creep curve which are (A) primary creep region; (B) secondary creep region; and (C) tertiary creep region (Cahn and Lifshitz, 2013)	46
2.13	Indentation creep curve diagram exhibiting the two regimes which are (A) primary creep region and (B) secondary creep region (Cahn and Lifshitz, (2013)	47
3.1	Injection molded dumbbell shaped samples	68
3.2	NanoTest nanoindenter	77
3.3	Nanoindentation creep experiment schematic diagram (Yusoh, 2010)	78

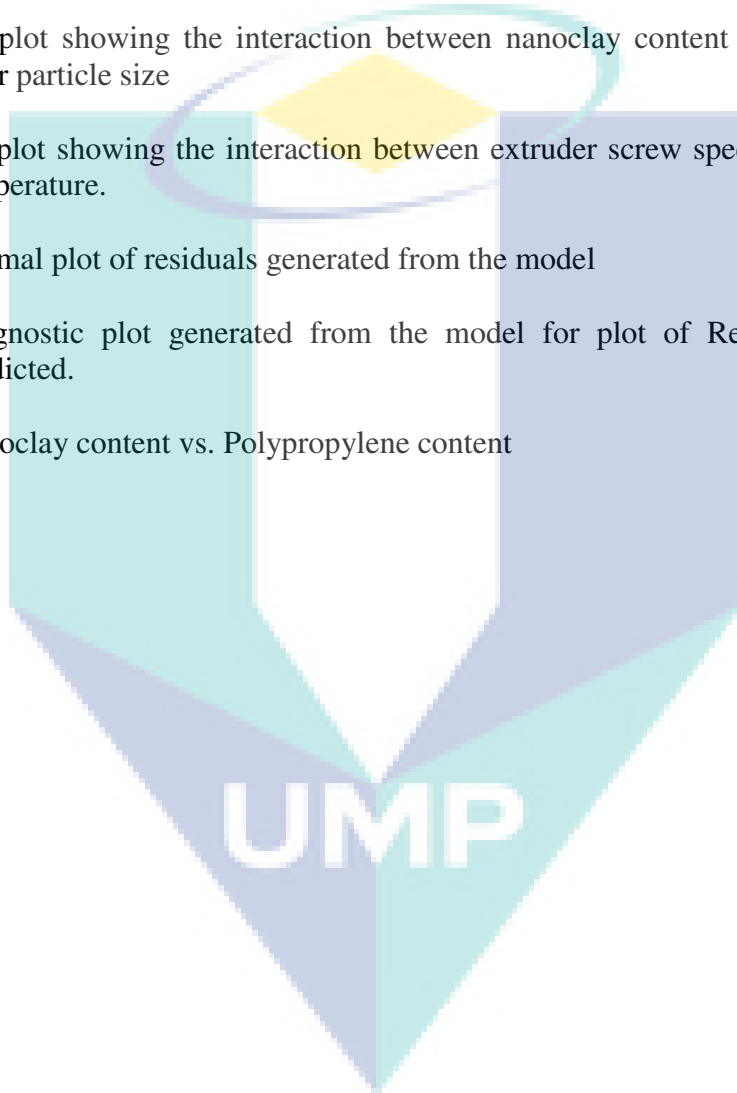
4.1	SEM micrographs of fractures samples of WPC: (a) without C20 (control), (b) with 1wt. %, C20, (c) with 2.5 wt. %, C20, and (d) with 4 wt. %, C20 (200 X), (e) with 5 wt. %, C20 (200 X), (f) with 4 wt. %, C20 (500 X), (g) with 5 wt. %, C20 (500 X).	85
4.2	TEM micrographs of WPC with (a) 1 wt% C20, (b) 5 wt% C20 (100 nm scale).	87
4.3	FTIR spectra of neat PP, WPC and WPC made with different C20 organoclay content	88
4.4	XRD diffractograms of neat PP, WPC and WPC made with different C20 organoclay content.	90
4.5	The effect of C20 organoclay loading on tensile properties of WPC	94
4.6	Effect of C20 organoclay loading on flexural properties of WPC	96
4.7	Elongation at break of PP, WPC, and WPC with different C20 organoclay content.	97
4.8	Izod impact strength of PP, WPC, and WPC with different C20 organoclay content	99
4.9	Water absorption of the WPC as function of C20 organoclay loading	101
4.10	TGA thermogram of neat PP and WPC made with different C20 organoclay content	103
4.11	DTG curve of neat PP and WPC made with different C20 organoclay content.	105
4.12	DSC curves of neat PP and WPC made with different C20 organoclay content.	106
4.13	Proposed diagram of stacks of platelets that are tightly held together	110
4.14	Proposed diagram of TMI Modification of MMT clay via Cu^{2+}	110
4.15	Mechanism of the modification process (Shamini, 2014)	111
4.16	EDX analysis of MMT (Pristine nanoclay)	112
4.17	EDX analysis of MMT modified with copper chloride	113
4.18	FESEM micrographs of (a, b) MMT and (c, d) MMT Cu	114
4.19	XRD Patterns of pristine Cloisite Na^+ and modified Cloisite Na^+ .	115
4.20	SEM micrographs of WPC with (a) 1 wt%, (b) 2.5 wt%, (c) 4 wt%, and 5 wt% MMT (pristine nanoclay).	117

4.21	SEM micrographs of WPC with (a) 1 wt%, (b) 2.5 wt%, (c) 4 wt%, (d) 5 wt% (lower magnification 200 X) and (e) 4 wt%, (f) 5 wt% (higher magnification 500 X) MMT Cu (modified nanoclay)	118
4.22	TEM micrographs of WPC with (a) 1 wt% MMT, (b) 5 wt% MMT, (c) 1 wt% MMT Cu, and (d) 5 wt% MMT Cu (100 nm scale)	120
4.23	FTIR spectra of neat PP, WPC and WPC/MMT made with different content of nanoclay	121
4.24	FTIR spectra of neat PP, WPC and WPC/MMT Cu made with different content of nanoclay	122
4.25	XRD diffractograms of neat PP, WPC and WPC/MMT made with different content of nanoclay	124
4.26	XRD diffractograms of neat PP, WPC and WPC/MMT Cu made with different content of nanoclay	125
4.27	The effect of MMT and MMT Cu nanoclay loading on tensile strength of WPC.	128
4.28	Tensile modulus of PP, WPC, and WPC with different content of MMT and MMT Cu nanoclay	129
4.29	The effect of MMT and MMT Cu nanoclay loading on flexural strength of WPC.	130
4.30	Flexural modulus of PP, WPC, and WPC with different content of MMT and MMT Cu nanoclay	132
4.31	Elongation at break of PP, WPC, and WPC with different content of MMT and MMT Cu of nanoclay	133
4.32	Izod impact strength of PP, WPC, and WPC with different content of MMT and MMT Cu of nanoclay	135
4.33	Density of PP, WPC and WPC with different content of MMT and MMT Cu of nanoclay	136
4.34	Water absorption of the WPC as function of pristine nanoclay loading	138
4.35	Water absorption of the WPC as function of modified nanoclay loading	139
4.36	TGA thermogram of neat PP and WPC made with different pristine (MMT) nanoclay content	141
4.37	TGA thermogram of neat PP and WPC made with different modified	142

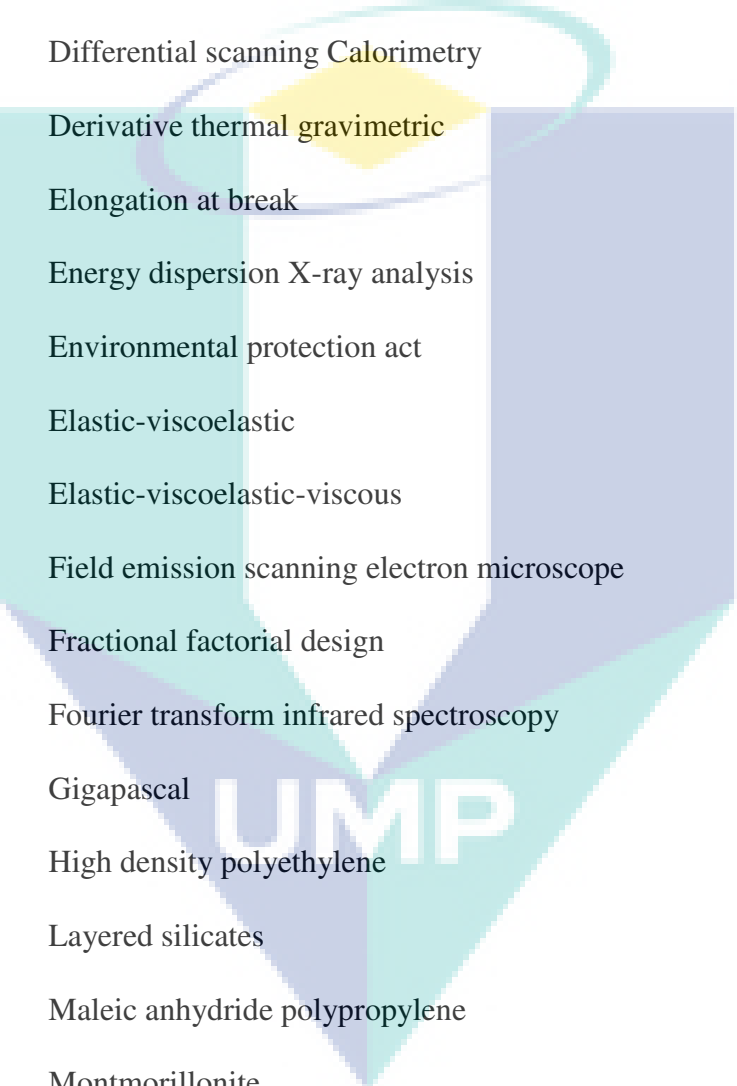
(MMT Cu) nanoclay content

4.38	DTG curve of neat PP and WPC made with different pristine nanoclay content	144
4.39	DTG curve of neat PP and WPC made with different content of modified nanoclay	145
4.40	DSC curves of neat PP and WPC made with different content of pristine nanoclay	146
4.41	DSC curves of neat PP and WPC made with different content of modified nanoclay	147
4.42	Typical indentation load–displacement curves for PP, WPC and WPC with different modified nanoclay concentrations	150
4.43	Hardness of PP, WPC and WPC with different C20 nanoclay loading	151
4.44	Elastic modulus of PP, WPC and WPC with different C20 nanoclay loading	151
4.45	Load-displacement curves of indentation for PP, WPC and WPC with different pristine nanoclay concentrations	153
4.46	Load-displacement curves of indentation for PP, WPC and WPC with different modified nanoclay concentrations	154
4.47	Hardness of PP, pristine and modified nanoclay based WPC as a function of nanoclay loading	155
4.48	Elastic modulus of PP, pristine and modified nanoclay based WPC as a function of nanoclay loading	155
4.49	Creep strain rate versus creep time for PP, WPC and WPC/C20 with different nanoclay concentrations	158
4.50	Creep versus time for PP, WPC and WPC/C20 with different nanoclay concentrations. Solid black line is experimental data and the thin red line is fitting results by Eq. (4.1)	160
4.51	Creep strain rate versus creep time for PP, WPC and WPC/MMT with different nanoclay concentrations	163
4.52	Creep strain rate versus creep time for PP, WPC and WPC/MMT Cu with different nanoclay concentrations	164
4.53	Creep versus time for WPC/MMT with different nanoclay concentrations. Solid black line is experimental data and the thin red line is fitting results by Eq. (4.1)	165

4.54	Creep versus time for WPC/MMT Cu with different nanoclay concentrations. Solid black line is experimental data and the thin red line is fitting results by Eq. (4.1)	166
4.55	3D plot showing the interaction between polypropylene content and nanoclay.	172
4.56	3D plot showing the interaction between polypropylene content and wood flour particle size	173
4.57	3D plot showing the interaction between nanoclay content and wood flour particle size	174
4.58	3D plot showing the interaction between extruder screw speed and die temperature.	175
4.59	Normal plot of residuals generated from the model	178
4.60	Diagnostic plot generated from the model for plot of Residual vs. Predicted.	179
4.61	Nanoclay content vs. Polypropylene content	180



LIST OF ABBREVIATIONS AND SYMBOLS



ABS	Acrylonitrile-butadienstyrene
ASTM	American society for testing and materials
CCA	Copper arsenate
CCD	Central composite design
DSC	Differential scanning Calorimetry
DTG	Derivative thermal gravimetric
EB	Elongation at break
EDX	Energy dispersion X-ray analysis
EPA	Environmental protection act
EVE	Elastic-viscoelastic
EVEV	Elastic-viscoelastic-viscous
FESEM	Field emission scanning electron microscope
FFD	Fractional factorial design
FTIR	Fourier transform infrared spectroscopy
GPa	Gigapascal
HDPE	High density polyethylene
LS	Layered silicates
MAPP	Maleic anhydride polypropylene
MMT	Montmorillonite
mN	Millinewton
MPa	Megapascal
PE	Polyethylene
PP	Polypropylene
PS	Polystyrene

PVC	Polyvinyl chloride
RSM	Response surface methodology
RW	Residual weight
SEM	Scanning electron microscopy
TEM	Transmission electron microscopy
TGA	Thermogravimetric analysis
T_m	Melting point
T_{max}	Maximum temperature
TMI	Transition metal ion
UV	Ultraviolet
WPC	Wood-plastic composite
WPC/MMT	Wood-plastic composite reinforced by pristine nanoclay
WPC/MMT Cu	Wood-plastic composite reinforced by TMI-modified nanoclay
WPC/NC	Wood-plastic composite containing nanoclay
WPC-1	Wood-plastic composite reinforced by 1 wt% nanoclay
WPC-2.5	Wood-plastic composite reinforced by 2.5 wt% nanoclay
WPC-4	Wood-plastic composite reinforced by 4 wt% nanoclay
WPC-5	Wood-plastic composite reinforced by 5 wt% nanoclay
X_c	Crystallinity
XRD	X-ray diffraction

CHAPTER 1

INTRODUCTION

1.1 Background of study

Wood has numerous advantages as an engineering material. Nonetheless, wood, like other natural products can be degraded by fungus and assaulted by termites. Moreover, the dimensional stability of wood is strongly influenced by the relative humidity in the environment. Due to these disadvantages, wood has to be occasionally treated with some hazardous chemicals like chromated copper arsenate (CCA) to prevent degradation; CCA-treated wood was phased out of the building products market by the Environmental Protection Agency (EPA) at the end of December 2004 (Yeh, 2007). This law, importantly, promotes the development of alternative materials such as wood plastic composites (WPCs).

The term WPCs generally mean compounding of wood flour (WF) with thermoplastic polymers such as polystyrene (PS), polyethylene (PE), polypropylene (PP), poly vinyl chloride (PVC), or acrylonitrile-butadienestyrene (ABS). However, the wood fiber loading in the polymer matrix is high, the smell and appearance of wood-plastic composite are similar to natural timber (wood). WPCs were at first delivered in the United States in 1983. Among others, American Woodstock, now a sector of Lear Cooperation in Sheboygan, Wisconsin, began to compound PP-based wood plastic composites using Italian extrusion advancement. The compounded products were extruded into flat sheets and later that framed into various shapes for interior automotive panelling (Schut, 2004).

WPCs can be produced by various procedures relying upon the purchaser's requirement (Schut, 2004). WF is all around recognized by fillers for WPCs preparation since it is not excessive and effortlessly available. By loading wood flour as filler, the strength and stiffness of plastics can be extended. WF also makes less scratched spot to an extruder as contrast with the mineral fillers such as talc and glass fiber. Then again, for development related products such as door sills, railing spindles, railing shafts, and windows and non-improvement related WPCs including automotive parts and furniture segments and these have been produced by injection molding industries. The capacity to use recycled plastics in WPCs is practically reasonable, and there is a general acknowledgment that WPCs are exceptionally solid and resistance to rot (decay), besides the wood particulates are relied upon to be totally typified by plastic.

As per the plastic news (2012), Southeast Asia's little wood plastic composite industry is anticipated to grow 10 percent a year through 2017, accomplishing 55,000 metric huge amount of generation, as showed by another study that cases to be the first to focus on WPCs in that area. The WPCs industries from Indonesia to Thailand are significantly more export oriented than Europe, and is seeing opportunities for export development as expenses in China ascend, as demonstrated by the evaluation "WPC Market in Southeast Asia 2011," by Asta Eder Composites Consulting. While the Southeast Asian WPCs industries remain small by correlation, Chinese capacity is estimated around 1 million metric tons. The region's improvement from 2008 to 2011 outpaced Europe at a near period of Europe's advancement, the report said. Sometime around between 2008 and 2011, SE Asian WPCs creation accomplished 34,000 metric tons and the report depicted fast advancement.

The properties, process limit and generation rate of WPCs can be upgraded fundamentally if appropriate additives are used. Plastics, for example, HDPE and PP have attributed to assimilate less moisture than wood in the indigenous habitat. Along these lines, WPCs are less impacted by moisture and indicates better dimensional stability and fungus/termite resistance than strong wood since WF particulates are embodied by the polymer matrix. Since thermoplastic polymers like PP and HDPE are non-polar (hydrophobic) materials while WF particulates are polar (hydrophilic) materials, there is a high probability of getting poor adhesion between WF and polymer

bringing about low flexural and tensile strength of the WPCs (Lu et al., 2000). In order to improve the attachment between WF and plastics, maleic anhydride grafted polymers are for the most part acquainted as a compatibilizer by upgrading the strength of WPCs. Additionally, when the bonding of wood flour and plastics is enhanced, the rate of water absorption is also reduced within the sight of the coupling agent.

The generation rate of WPCs can be altogether extended when lubricants such as zinc stearate or unsaturated fats are incorporated in the assembling process. Lubricants stifle edge tearing and melt fracture phenomena occur during the extrusion process. For the most part, the density of WPCs is higher than that of solid wood and this constrains restricts the application of wood-plastic composite. The density of WPCs can be diminished by as much as 30% by including a blowing agent that makes the density of WPCs like natural timber. The fungus resistance of WPCs is upgraded by including biocides. WPCs can be colored adequately by including colorants. Adding an UV stabilizer can improve the UV stability and weather capacity of WPCs. Since the significant utilizations of WPCs are in development, flammability of WPCs is another worry and fire retardants are used for the reason. Antioxidants are also applied here to keep polymer from degrading during assembling process. Finally, some filler, for example, glass fiber, talc, calcium carbonate and nanoclay are recommended as the second filler in the WPCs to upgrade mechanical properties and creep resistance (Sherman, 2004).

1.1.2 Polymer Nanocomposites

Like every single other composite, a "nanocomposite" is defined as a two or more phase system where, one phase is dispersed into the other phase (one phase is in nano range). Although polymer-clay interactions have been studied during the sixties and the mid-seventies, the idea of polymer-clay nanocomposites was not proposed until the mid-nineties (Kornmann, 2001). The idea of polymer-layered silicate nanocomposites was proposed by Toyota in the mid 90's, utilizing Nylon-6 as the polymer matrix. The first report from the Toyota research group brought up that adding a small amount of layered silicates to nylon prompts significant enhancements in thermal and mechanical properties. These improvements include high moduli, expanded

strength, improved heat distortion temperature, decreased gas permeability, and lessened flammability (Ray and Okamoto, 2003). These features pulled in tremendous interest from both the academic and industry. These days, efforts are being made all around to produce polymer-layered silicate nanocomposites utilizing a wide range of polymers.

Among the various layered silicates tried, montmorillonite is the effective nanofiller because it has a plate-like structure and a high aspect ratio to give a gigantic surface area. In addition, montmorillonite is abundant in nature. A montmorillonite platelet normally incorporates aluminum or magnesia atoms in the center point of an octahedral sheet which is fused with two external silica tetrahedron layers. This sandwich structure is known as a unit layer. The idealized structure of a montmorillonite unit layer is given in Figure 1.1. The thickness of a unit layer is around 1 nanometer and the lateral dimensions of the platelet range from a several hundred nanometers to a several thousands of nanometers. Typically, however, clays are made of numerous such layers stacked in parallel to each other and held together by Van der Waals strengths.

In numerous types of nanoclay, the lateral Si^{4+} atoms are halfway supplanted by trivalent atoms such as Al^{3+} and/or the central Al^{3+} atoms are also supplanted by some divalent atoms such as Fe^{2+} and Mg^{2+} . Hence, the absence of positive charges on the clay platelet surface is typically remunerated by adsorbing Na^+ and Ca^{2+} ions present in water. These cations can be exchanged by different cations that are present in solution. This property of clay makes it conceivable to supplant inorganic cations on the unit layer surface with organic cations by ion exchange mechanism, and this makes the clay build up an affinity for an organic phase such as polymer. The typical cations utilized as a part of clay modification include: primary, secondary, tertiary and quaternary alkylammonium or alkylphosphonium cations. These cations act as surfactants and lower the surface energy of the inorganic host. Thus, the wetting characteristics of the polymer matrix are improved, and this results in an extensive interlayer spacing. Sometimes, the cations on the surface of the layered silicate can start the polymerization of monomers to enhance the bond strength between the layered silicate surface and polymer (Ray and Okamoto, 2003).

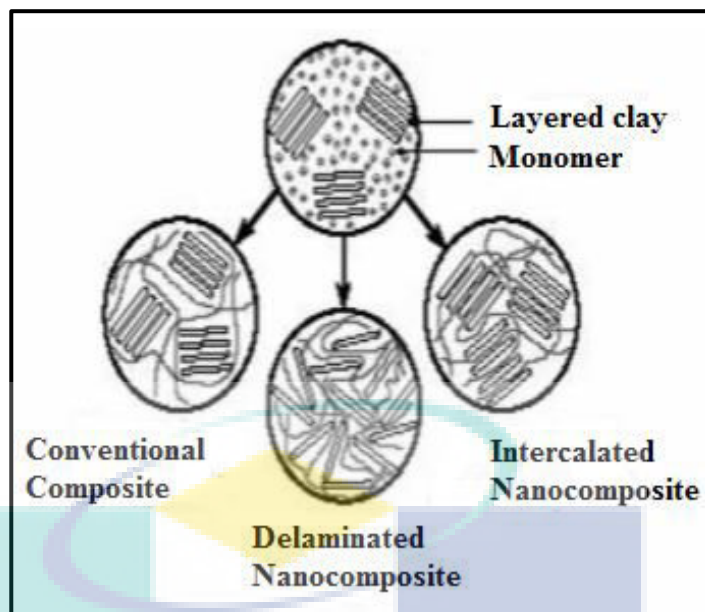


Figure 1.1 Types of nanocomposite morphologies

Source: Kornmann (2001).

Nanoclay-filled polymers are classified as one of three kinds of composites in light of their morphology: conventional composite, intercalated composite or exfoliated/delaminated composite. This classification is determined by the connection of polymer and clay. At the point when the polymer chains are not ready to enter through the holes between the unit clay platelets, the stacks of clay stay in the original aggregates, and this is known as a conventional or microscopic composite. In some other polymer-clay composites, polymer chains are intercalated into unit clay platelet holes however the platelets are still not ready to exfoliate in the polymers. This kind of structure is called intercalated composite. At the point when the clay platelets are randomly dispersed into polymers and the gaps between every platelet are expanded, this structure is called exfoliated or delaminated composite. A schematic graph of these morphologies appears in Figure 1.1. Among these three types of morphologies, exfoliated morphology is accepted to give the maximum advantage because of its well dispersion and produces a high surface area (around $750 \text{ m}^2/\text{g}$) (Dennis et al., 2001). Property improvement is decided by the molecular level interactions between clay surface and polymer. Since montmorillonite clay platelets exhibit the biggest surface area in exfoliated morphology, the property improvement of polymer nanocomposite is exceptionally huge even with small clay loading.

Although organically modified nanoclay are frequently utilized, it was accounted by Nawani et al. (2007) that these organoclay has inadequate activity because of the degradation of the organic surfactants in their structure whereby the organic surfactants such as the quaternary amine surfactant begins to decompose via the Hoffman elimination process above 170 °C. Hoffman elimination is a procedure where quaternary ammonium salts undergo E2 elimination (the reaction transforms 2 sp³ C atoms into sp² C atoms) when heated. This is seen to hinder the property progression of the nanocomposites formed particularly its thermal and barrier properties. As a part of this study, the utilization of transition metal ions (TMI) as a modifier for the montmorillonite nanoclay was studied.

The TMI modification was applied to change the nature of the clay which is hydrophilic as this specific nature makes poor blending and interaction with most polymer matrix that are hydrophobic (Olphen, 1977, Giannelis, 1996). Aside from that, the structure of the layered silicate comprises of stacks that are held firmly by electrostatic powers and it is crucial for the nanoclay to undergo modification before the preparation of nanocomposites. Nanoclay that is not modified would not be viable as it will not have the capacity to interact with the polymer matrix (Silva, 2012). Naturally occurring Layered Silicates (LS) comprises of cations that are not firmly bound to the nanoclay surface and transition metal ions (TMI) are utilized to exchange the cations present in the clay. This procedure isolates the nanoclay platelets with the goal that they should be all the more effectively intercalated or exfoliated, and also enables the clay to be more compatible with a wide range of polymer matrix. The transition metal ion that was selected in this work was copper (Cu) ion.

1.1.3 Sub-Surface Mechanical and Creep behaviour of WPCs

Due to the nano dimensions of nanofillers which are normally in the range of nanometre size and dimensions, nanofillers have forced a huge challenge for experimental equipment to describe their functions in the WPC. However significant improvement in WPC incorporated by nanofillers has been made but their dispersion mechanism and load transfer are still not thoroughly understood. Tensile test have been widely applied to study the mechanical properties and elastic/plastic deformation

nanofiller based polymer composites, with respect to the conventional mechanical testing. Because of the load and displacement resolution restrictions of microscopic tensile tester, the observations of the stress behaviour at the nanoscale level are relatively impossible (Dutta et al., 2004). Fabrication of a tensile test specimen might create surface flaws and surface stress/strain concentration on the tensile specimen, due to this it becomes difficult to study the deformation behaviour and mechanical properties of composite at the nano level (Oliver and Pharr, 1992). To study the effect of nanofillers on deformation behaviour and the mechanical properties of materials, then the nanoindentation technique is the most reliable, accurate and advance technique (Dutta et al., 2004).

This study aims to determine the effect of pristine, organoclay and TMI-modified nanoclay with different concentrations as a reinforced agent and its effect on the properties of WPCs.

1.2 Problem Statement

The highly hydrophilic nature of the lignocelluloses materials makes them incompatible with the thermoplastics which are highly hydrophobic during the fabrication process. It leads to poorer interfacial bonding between thermoplastics and wood flour, and more worse of the composite properties. Moreover, the high moisture absorption of natural fibers may bring dimensional instability of the subsequent composite and weakened the interfacial bond (Lee and Wang, 2006).

Pristine MMT is a hydrophilic phyllosilicate which makes poor blending and interaction with a large portion of the polymer matrix which are hydrophobic in nature. Thus, the modification of MMT is important to enhance the compatibility of MMT with polymers. Apart from that, the structure of the pristine MMT comprises of stacks that are held firmly by electrostatic powers and it is critical for the nanoclay to undergo modification before the preparation of composites. In addition, organically modified nanoclay begins to decompose via the Hoffman disposal process as above 170 °C.

The TMI modification has been used to change the nature of the nanoclay which is hydrophilic. Naturally occurring MMT comprises of cations that are not strongly bound to the nanoclay surface and transition metal ions (TMI) are utilized to exchange the cations present in the nanoclay. This procedure isolates the nanoclay in order for them to be more easily intercalated or exfoliated, and also enables the nanoclay to be more compatible with a wide range of polymer matrix.

1.3 Objectives

1. To fabricate and study the performance of wood plastic composite (WPC) reinforced by organoclay.
2. To modify the conventionally obtained montmorillonite nanoclay (MMT) by TMI which is Cu^{2+} ion.
3. To characterize the wood-plastic composites reinforced by pristine and TMI-modified nanoclay.
4. To study the sub-surface mechanical properties and sub-surface creep behaviour of wood-plastic composite reinforced by organoclay, pristine and TMI-modified nanoclay by means of nanoindentation technique.
5. To optimize the fabrication condition (Polypropylene content, nanoclay content, wood flour size, extruder screw speed, and extruder die temperature) for wood-plastic composite reinforced by TMI-modified nanoclay.

1.4 Scope of Study

A general scope or an experimental framework of this thesis was established by underlining the steps taken to achieve the objectives of the proposed research. Following are the designed scopes that were seen as a guidance and assistance in achieving the research objectives of this work.

1. To fabricate and study the performance of polypropylene (PP) based wood plastic composites (WPCs) made from kempas wood flour (WF) via extrusion followed by injection molding process. The morphology, composition and structure of WPCs made from organoclay (Cloisite® 20A) were characterized using Scanning electron microscopy (SEM), Transmission electron microscopy (TEM), Fourier transform infrared spectroscopy (FTIR), and X-ray diffraction (XRD). The mechanical study of organoclay reinforced WPCs was performed using Universal Testing Machine and impact tester. The barrier properties of the samples were measured by immersing samples into water for certain period of time.
2. The modification of the MMT nanoclay was carried out using the transition metal ion which was copper (II) chloride ion. The characterization of the TMI-modified nanoclay was executed using Field Scanning Electron Microscope (FESEM), Energy dispersion X-ray analysis (EDX), Thermogravimetric analysis (TGA) and X-ray diffraction (XRD).
3. The morphology, composition and structure of WPC made from pristine and TMI-modified nanoclay were characterized using Scanning electron microscopy (SEM), Transmission electron microscopy (TEM), Fourier transform infrared spectroscopy (FTIR), and X-ray diffraction (XRD). The thermal stability of the WPCs reinforced by pristine (WPC/MMT) and modified nanoclay (WPC/MM Cu) samples was investigated by using Thermo Gravimetric analysis (TGA), and differential scanning calorimetry (DSC). The mechanical study of the WPC/MMT and WPC/MMT Cu was carried out via Universal Testing Machine and impact tester.
4. Nanoindentation technique was used to study the sub-surface mechanical properties and sub-surface creep behavior of WPCs reinforced by organoclay, pristine and TMI-modified nanoclay. The hardness, elastic modulus and creep resistance of WPC were measured using nanoindentation test data.
5. The optimization of best fabrication condition for WPC/MMT Cu was carried out by using response surface methodology (RSM) software. The tensile strength effects of fabricated WPC/MMT Cu were optimized using the central composite design (CCD).

1.5 Significance of Research

The main aim of this research is to study the use of low cost resources for the fabrication of WPCs. Fabrication of new kind of WPCs using nanofillers to improve overall properties is considered as added value in industrial applications. However, nanoclay based WPCs has attracted a lot of attention because of its high surface area, low density, high Young modulus, easy availability and low cost of nanoclay.

Nanoclay is the focus of advanced research due to its outstanding mechanical, thermal, and electrical properties, when used as nanofillers with polymers, especially in polypropylene matrix. Nanoclay enriched WPCs have wide applications such as in the development of flame retardant composite, composite with high mechanical properties, composites with high thermal and dimensional stability, and bio-based composites.

In addition, in this research, it was aimed to obtain well dispersed nanoclay into the WPCs to minimize the nanoclay agglomerations and hinder the deterioration of the WPCs properties. In order to aid this effort, TMIs modification was done on the pristine nanoclay to create a good compatibility with WPCs and to ensure that a homogeneous dispersion of the nanoclay has been achieved.

The study of wood-plastic composites reinforced by nanoclay is an interesting topic which has been studied extensively, however to the best of our knowledge, there are no reports to date that studied the properties of WPCs reinforced by TMIs modified nanoclay. Although there are reports on the improved properties using MMT nanoclay, the nanoclay used are modified by the supplier and is often classified as Cloisite 10A, 15A, 20A and 30B. In this work, the MMT clay was modified using copper ions before it was incorporated into the WPCs. Properties of the WPCs that were studied include mechanical, sub-surface mechanical, sub-surface creep behaviour, thermal and barrier. It is to be noted that there are no previous work on the sub-surface mechanical properties and sub-surface creep behaviour of WPCs reinforced by nanoclay using nanoindentation technique. It is presumed that the incorporation of TMI-modified nanoclay will be able to generate a new class of nanocomposites with improved properties

CHAPTER 2

LITERATURE REVIEW

2.1 Introduction

This chapter provides a brief insight of the relevant studies and research on wood-plastic composite such as different components of wood-plastic composite, manufacturing process of wood-plastic composites, different properties of wood-plastic composite. To understand the topic better, some related information such as different kind of polymers and nanofillers are also discussed. In the end of this chapter the gaps in existing research is analysed and discussed.

2.2 Wood-Plastic Composites

The wood plastic composite (WPCs) is a hybrid material basically from woody materials and thermosets plastics or thermoplastics. A thermoset polymer (or plastic), is a petrochemical material that irreversibly cures, while the thermoplastic is a material which becomes soft when heated and hard when cooled and it can be reused. Lately, an increasing interest has concentrated on wood plastic composites (WPCs) reinforced with wood fiber or other lignocellulosic based materials (Panthapulakkal et al., 2006). The polypropylene (PP), polyethylene (PE) and polyvinyl chloride (PVC) are the widely utilized thermoplastics for WPC.

WPCs started as a modern idea in Italy in the 1970s, and popularized in North America in the early 1990s. By the beginning the 21st century it was spreading to India, Singapore, Malaysia, Japan and China (Ashori, 2008). Wood-plastic composites (WPCs) consolidate the best properties of the neat component and thereby exhibit

outstanding performance. Moreover, WPCs have the advantage of good dimensional stability (i.e., lower water uptake and better strength against fungi and insects compared with wood) during their lifetime (Arao et al., 2014). WPCs are thus utilized as a part of construction engineering.

The fabrication process of WPCs usually occurs in two stages i.e., the compounding and the forming. During the fabrication the wood and other different substances are incorporated into a molten thermoplastic to produce a homogeneous composite material. The composite material is then shaped into a product and the common forming techniques are profile extrusion (extruding molten composite through a die), injection molding, and compression molding (pressing molten composite between two mould parts) (Clemons, 2002).

The WPCs has emerged as an important group of engineering materials during the past decade and have become prevalent in many building applications including decking, docks, landscaping timbers, and fencing and also replaces the pressure-treated solid lumber (Morrell et al., 2009). The WPCs are receiving a great consideration in academic and industrial areas because of their favourable properties like low density, renewability, recyclability and also better mechanical properties (Alamri and Low, 2013). The better stability and ideal mechanical properties have turned WPCs into a favoured building material (Salah and Mokhtar, 2009). However, wood flour and thermoplastics have a diverse nature, thereby imposing severe incompatibility during the assembling process and leads to weaker interfacial adhesion between thermoplastics and wood flour (Lei et al., 2015).

2.3 Components of Wood-Plastic Composites

2.3.1 Wood Fibers

Wood fibers generally contain cellulose, hemi-cellulose, pectin, lignin, water soluble ingredients, and wax (John and Thomas, 2008). The actual arrangement of these materials in wood fiber, however, differs from species to species. Here, water soluble constituents and wax are considered as extractives since cellulose, hemi-cellulose, and

lignin are thought to be the fundamental components with respect to their physical properties (John and Thomas, 2008). Generally, more than half of wood fibers are cellulose. Wood fiber can be considered to be composites of empty cellulose fibrils held together by a lignin and hemicellulose matrix (Jayaraman, 2003). It can be seen from Figure 2.1, the cell wall in a wood fiber is not a homogenous membrane.

The moduli of cellulose-based materials are altogether different from each other. For instance, the Young's modulus of strong wood is around 10GPa. By appropriate pulping process the modulus of a single pulp fiber can be as high as 40GPa. Microfibrils can be isolated from pulp fiber after mechanical disintegration and hydrolysis. The modulus of microfibrils is around 70GPa. At last, the modulus of cellulose nano crystals is acquired by hypothetical computation, and this could be as high as 250GPa (Gassan and Bledzki, 2000). From the same literature the moduli estimations of wood fiber ranges from 10 to 90GPa (Gassan and Bledzki, 2000). From these numbers, it can be said that it is sensible to compound WF with plastics to expand the modulus of resins of interest because the modulus of wood fiber (40GPa) is much higher than that of generally plastics. The high moduli of wood fiber make these great applicants as plastic reinforcement.

Wood fibers have various points of interest and weaknesses. The developing interest for wood fibers is mostly because of their efficient production with few requirements for equipment and low specific weight, which results in a higher specific strength and stiffness (Kim et al., 2006). They also exhibit more secure handling and working conditions contrasted with engineered rein-forcements (John and Thomas, 2008). Wood fibers are nonabrasive to blending and molding equipment, which can contribute to cost diminishments. The most fascinating aspect about wood fibers is their positive environmental impact. Wood fibers are renewable resources with generation requiring little energy. They are carbon dioxide neutral i.e. they do not return overabundance carbon dioxide into the climate when they are treated with the soil or combusted. The preparing environment is friendly with better working conditions and therefore there will be a decreased dermal and respiratory irritation. Wood fibers have high electrical resistance. The empty cell structure gives great acoustic protecting properties. The overall accessibility is an additional factor (John and Thomas, 2008).

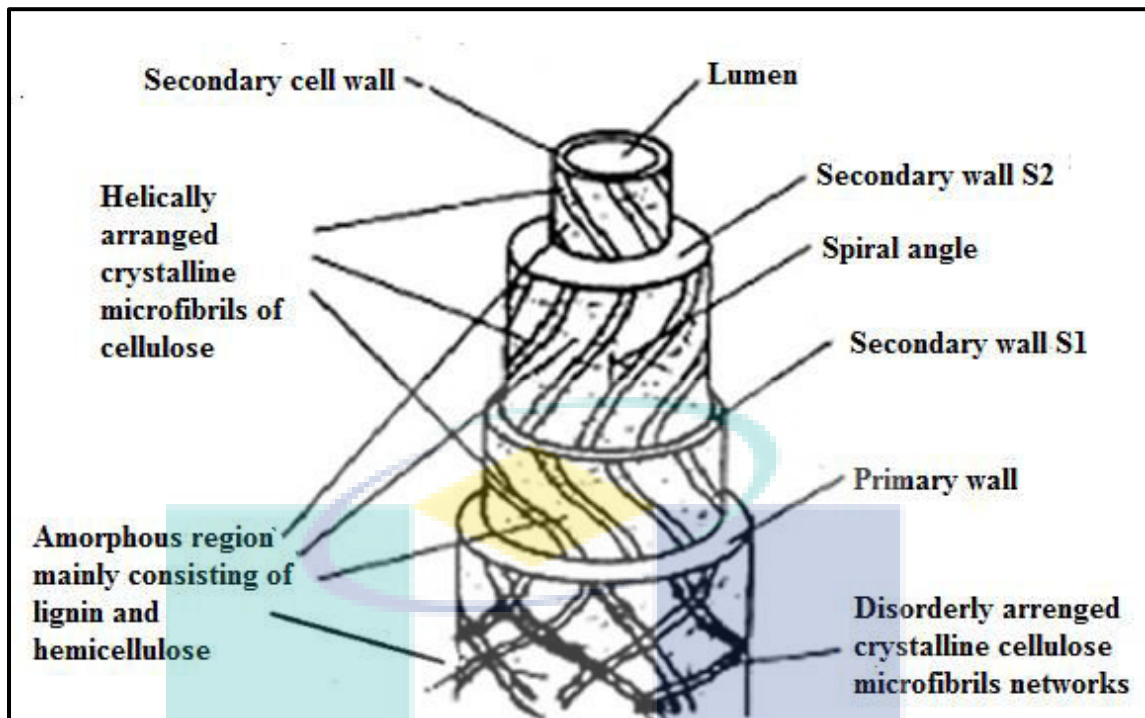


Figure 2.1 Structure of wood fiber
 Source: Jayaraman (2003).

However certain disadvantages, such as tendency to form aggregates while compounding, low thermal stability, high moisture absorption, greatly reduces the capability of wood fiber to be utilized as reinforcement for polymers (Kim et al., 2006). The high water absorption of wood leads to swelling and presence of voids at the interface (permeable items), which results in poor mechanical properties and decrease dimensional instability of composites.

One of the major drawbacks of wood fibers is the weak compatibility shown between the fibers and the polymeric matrices, which results in non-uniform dispersion of fibers inside the matrix and poor mechanical properties. Wood and plastic resemble oil and water, and does not blend well. Most polymers, particularly thermoplastics, are nonpolar ("hydrophobic", repulsing water) substances, which are not perfect with polar ("hydrophilic", it retains water) wood fiber and, therefore, poor bonding between polymer and fiber in WPCs can come about (Ashori, 2008). Another issue is the processing temperature that limits the choice of matrix material. Wood fibers are made of different organic materials (primarily cellulose, and additionally hemicellulose and lignin) and therefore their thermal treatment leads to a various physical and substance

changes. Thermal degradation of those fibers leads to poor organoleptic properties such as odour's and colours and also the reduction of their mechanical properties. It additionally brings about the generation of gaseous products, when processing happens at temperatures above 200 °C, which can cause high porosity, low density and decreased mechanical properties (Georgopoulos et al., 2005).

Wood components, utilized as a part of polymer composites have a large variety of shapes and can be utilized alone or in combinations. The properties of the final product are dictated by the sizes, shapes and characteristics of wood fibers. These incorporate surface chemistry (e.g. waxes and silica) and fiber aspect ratio specifically. Aspect ratio implies the average length over distance across (diameter) of the fibers which change from species to species. For instance, softwood fibers (spruce) are more adaptable contrasted with fibers derived from aspen or birch (hardwoods) (Ashori, 2008). Furthermore, different factors such as size of fibers, morphological structure, thickness, chemical compositions, density, fiber rate, and amount and kind of bonding agent (if any) are essential for the strength properties of WPC. The mechanical properties of wood fibers depend on the pulping procedure even inside the same species (Wenhan Ren, Dan Zhang, Ge Wang, 2014).

Koompassia malaccensis or locally known as kempas, is one of the major hard wood species in South-East Asia. It is a phenomenal prime source for flooring, constructions and plywood manufacturing in Malaysia and numerous other South-East Asia nations (Lee et al., 2011). The mechanical properties of kempas wood are as follow; modulus of rupture-122 MPa, elastic modulus-20.09 GPa, and hardness-7,800 N (Gan et al., 2000).

There were two fundamental alternatives of wood material, i.e. wood flour and wood fiber. In fact, wood's flour is more generally accessible than wood fiber, alongside its reportedly less expensive. Furthermore, wood's flour is generally free flowing and much less demanding to be prepared, (such as feeding and handling process) rather than wood fiber, even though fiber type gives somewhat better performance (Sihombing et al., 2012). The wood's flour is however accessible in numerous sizes, from 20 mesh (coarse) to 400 mesh (additional fine), yet the 40 mesh size is the most widely

recognized one. For a large portion of uses, a satisfactory result composition based on criteria between price, performance, and ease of processing were the wood's flour with size of 40 mesh as shown in Table 2.1.

Table 2.1 Effect of Pine Wood Flour Particle Size on Performance of Wood- filled Polypropylene Composite

Mesh Size	Notched Izod Impact (J/M)	Tensile Strength (MPa)	Bending Stiffness (GPa)
20 (841 microns)	27	23.3	2.98
40 (400 microns)	21	24.8	3.12
80 (177 microns)	19	24.4	3.10
120 (125 microns)	17	24.2	2.84

Source: Sihombing et al., (2012).

2.3.2 Plastics used to formulate Wood-Plastic Composites

Because WF will be burnt when processing temperature is above 200°C, the plastic utilized as the matrix as a part of WPCs are limited. Polyethylene (PE), polyvinyl chloride (PVC), and polypropylene (PP) are the most widely recognized matrix materials in WPCs (Wolcott, 1999). This is because the cost of these plastics is lower than that of other engineering plastics and their processing temperature is lower than 200°C.

Panthapulakkal and Sain, (2007) manufactured composites from HDPE and wheat straw. They observed that wheat straw filled HDPE composite exhibited superior mechanical properties. The impact of photo stabilizer on the properties of HDPE/wood flour composites exposed to natural weathering was examined by Taib et al., (2010).

The study revealed that the addition of ultraviolet stabilizer (UVA) delayed and minimized the adverse impact of natural weathering on HDPE/WF composites.

The impact of water environment on the sorption characteristics of LDPE composites incorporated with pineapple-leaf fibers (PALF/LDPE) has been studied by George et al., (2000) by immersion of PALF/LDPE composite in distilled water at 28, 50 and 70°C. It was found that the fiber/matrix bonding became weak with increasing moisture content, resulting in interfacial failure. Mechanical properties diminished after introduction to water. Wenhan Ren, Dan Zhang, Ge Wang, (2014) investigated the thermal and mechanical properties of HDPE composites reinforced with bamboo fibers (BF) and bamboo pulp fibers (BPF). The results indicated that BPF improved the thermal and mechanical properties of the HDPE based composites more than BF.

The utilization of saline innovation in crosslinking composites of wood flour (pine wood flour) and HDPE has been examined by Bengtsson et al., (2005). A boiling test in water followed by tensile testing demonstrated that the crosslinked composites were less susceptible to water uptake contrasted with the non-crosslinked composites. Besides, the decline in tensile strength of crosslinked composites was not as significant as with respect to the non-crosslinked composites. Scanning electron microscopy showed better compatibility and adhesion between the HDPE and wood flour for crosslinked composites. However, polyethylene has some disadvantages such as high thermal expansion, poor weathering resistance, poor temperature capability, degradation over short-time periods of exposure (less than 3 months) (Gavilan et al., 2007).

PVC is another common plastic utilized as a part of WPC. Unlike to HDPE and PP, the molecular structure of PVC is such that it is hydrophilic. Therefore, PVC is more compatible with WF. Furthermore, PVC contains chlorine which acts as a fire resistant in plastics. As a result of this, the combustibility of PVC-based WPCs will be less as in contrast with HDPE or PP-based WPCs. However, PVC is often referred to as the "Poison plastic" and this is because of the poison (dioxins), it can be discharged when exposed to fire, during manufacturing (Yeh, 2007). The materials which contain poisons can be dangerous to the market of PVC-based WPCs.

The thermal decomposition, mechanical properties and flame retardancy of PVC-WF/zinc borate (ZB) composites were researched by Fang et al., (2013). The authors are of the conclusion that WF betterly affected flame performance of PVC but had little impact on smoke suppression. In contrast, the incorporation of ZB had little effect on fire retardancy of WF-PVC and demonstrated some negative effect on the strength properties of WF-PVC. In another examination, Bishay et al., (2011) studied the thermal and mechanical properties of PVC composites loaded with different concentration of aluminium powder. It was found, that mechanical strength values decrease with increasing the aluminium powder content. They also observed that the thermal stability of composite samples increases with increasing aluminium content.

PP plays a prominent role in the WPCs market. The advantage of PP is that it has marginally higher stiffness than HDPE (Yeh and Gupta, 2008a). PP based WPCs simply provides another choice for WPCs. Arao et al., (2014) used fire retardants to improve the fire performance of PP/WF composites. The study revealed that the tensile strength and modulus of the composites reduced with the loading of retardants. Bhaskar et al., (2012) evaluated the properties of PP/WF (pine wood flour) wood plastic composites. They concluded that the incorporation of MAPP coupling agent in composite formulation improved the interfacial bonding between matrix and wood flour and stability of WPC.

Effect of polarity parameters on the mechanical properties of PP/short banana fiber (BF) was investigated by Paul et al., (2010). It was found that the polarity of BF decreased after chemical treatment. The enhanced fiber/matrix interaction was evident from the improved tensile and flexural properties. In another study Thio et al., (2004) have studied the effect of interfacial adhesion strength on the mechanical properties and toughness of PP/glass particles composites. The tensile strength of reinforced PP increased with increasing adhesion strength and impact toughness increased with weaker adhesion. Fabiyi et al., (2008) researched the effects of outside and accelerated weathering on the chemical change and visual appearance of WPC formulations based on HDPE and PP were explored. The researchers are of the assessment that the HDPE-based WPC revealed decreased lightening, carbonyl concentrations and wood content loss when compared with PP-based WPC.

According to the Fan et al., (2003) hydrophobic nature of PP that lead to quick drying, relatively low static, and resistance to staining and to many chemicals. Moreover, PP is relatively cheap in price as compared to the others plastics.

Some other plastics which have processing temperature lower than 200°C, such as Acrylonitrile butadiene styrene (ABS) and polystyrene (PS) have not been broadly utilized as a part of WPC, because of its limited ductility (impact strength < 35 J/m and elongation at break < 2.5%). Note that fillers which exist in the polymer act as stress concentrators and can reduce impact strength of plastics (Yeh, 2007). ABS may have more opportunities in WPC because of its hydrophilic nature and its mechanical properties are greatly improved than those of HDPE, PVC and PP. The issue here is that cost of ABS is higher than that of other plastics (Griswold, 2006).

Table 2.2 Summary of material properties for WPC (assuming a 50 or 60% WF)

Matrix	Flexural MOE (mm psi)	Flexural MOR (psi)	Tensile strength (psi)	Shear strength (psi)	Hardness (Ibs)
PE	0.1-0.26	1500-3700	200-2200	200-800	N/A
PP	0.6-0.8	4,000-5,000	1700-1800	1300-1400	3,000
PVC	0.7-0.8	5,000-6,000	3,000-4,000	1500-1700	2500

Source: Gardner and Murdock (2002)

2.3.3 Coupling agents

As can be seen from Figure 2.2, the chemical structure of cellulose contains enormous amounts of hydroxyl groups. These hydrophilic hydroxyl groups absorb water molecule effortlessly and swell the wood fiber. A schematic representation of the swelling process is portrayed in Figure (Wang, 2007). As appeared, the hydroxyl groups on various wood fibers form hydrogen bonds and, as a result, WF aggregates easily.

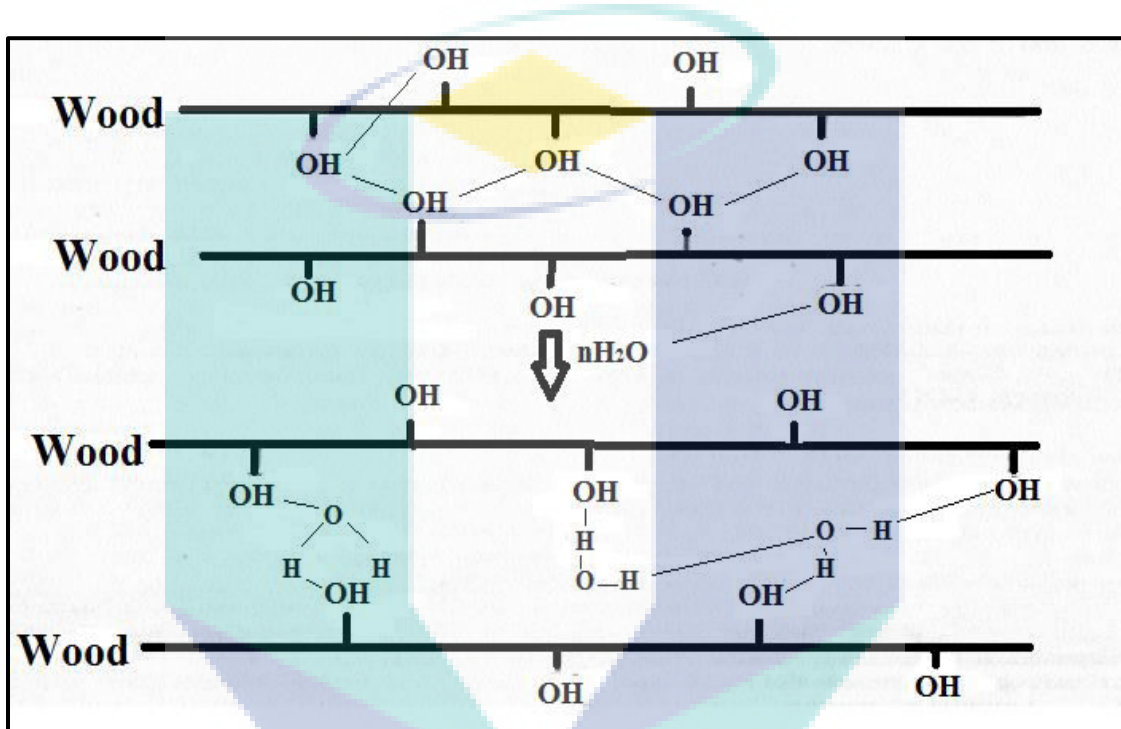


Figure 2.2 Schematic illustration of the wood fiber swelling process.

Source: Wang (2007).

Chemical "coupling" or "compatibilizing" agents have been utilized to enhance the affinity, dispersion and bonding between thermoplastics and wood fibers (Kim et al., 2006). It is normally a type of polymers that are employed to treat a surface so bonding happens between it and other surfaces. It is generally applied in small quantities. Coupling agents are added substance (additives) which contain both polar groups that can react or interact with hydroxyl groups of cellulose and non-polar chain area. They bring down the surface energy of wood fiber, and make it non-polar, more like the plastic matrix (Rude, 2007). They acts as bridges that connect wood fiber and polymer

matrix by forming one or more of the following mechanisms: covalent bonds and secondary bonding, (such as hydrogen bonding) (Rude, 2007).

Coupling agents advance the adhesion and the dispersion of wood fibers in polymer matrix, other than enhancing mechanical properties (Sihombing et al., 2012). Therefore, chemical treatments can be considered in changing the properties of wood fibers. The coupling agent is chemically bonded with hydrophilic fiber and mixed by wetting in the polymer chain (Yang et al., 2014).

2.3.3.1 Classification of Coupling agents;

Coupling agents are classified into organic, inorganic and organic-inorganic groups.

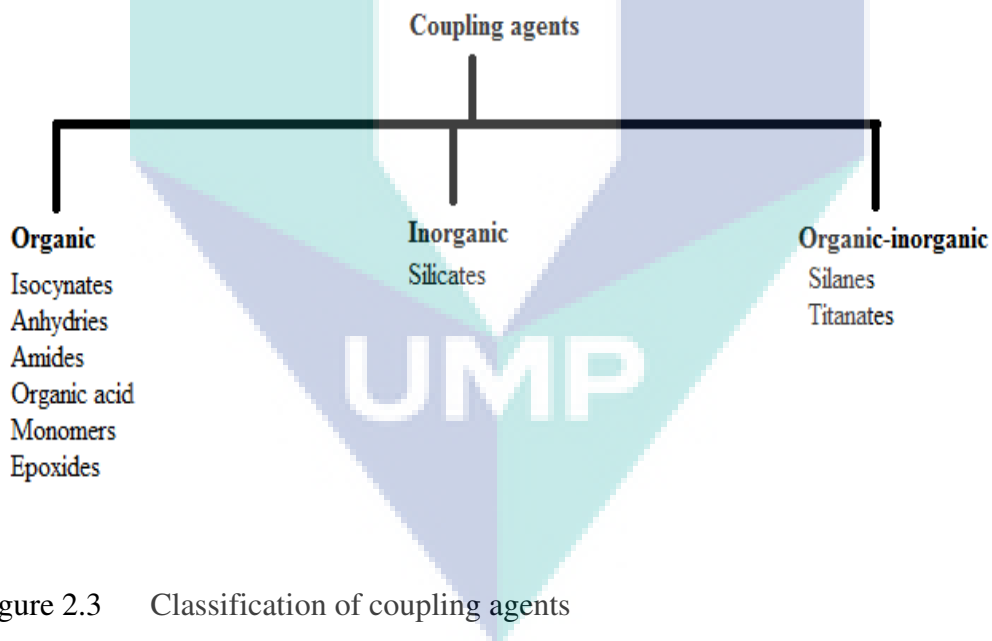


Figure 2.3 Classification of coupling agents

Source: Lei et al., (2015).

Generally, organic and organic-inorganic coupling agents are utilized to compatibilize WF and polymer matrix (Kord and Kiakojouri, 2011). Organic coupling agents in WPC typically have bio- or multifunctional groups in their molecular structure. These functional groups, such as (- N=C=O) of isocyanate, [-(CO)₂O-] of maleic anhydrides interact with the polar groups [mainly hydroxyl groups (- OH)] of cellulose

and lignin to form covalent or hydrogen bonding (Lei et al., 2015). Figure 2.3 shows the classification of coupling agents.

Silanes are recognised as efficient coupling agents widely utilized as a part of composites and adhesion formulation. Xie et al., (2010) consider Silanes (Trialkoxysilanes) as the most useful and effective coupling agent since it forms solid covalent bonds with wood-OH groups. The addition of Trialkoxysilanes to the matrix can build the interfacial bonding between fiber and polymer matrix furthermore it enhances the mechanical and outdoor performance of the subsequent fiber/polymer composites (Xie et al., 2010). The incorporation of Trialkoxysilanes increases crystallinity of the composites (Salmah et al., 2007). In an interesting research Metin et al., (2004) used three different types of saline coupling agents; 3-aminopropyltriethoxysilane (AMPTES), methyltriethoxysilane (MTES), and 3-mercaptopropyltrimethoxysilane (MPTMS) at four different concentrations (0.5 – 2 wt %) in PP/natural zeolite composites. Saline treatment indicated significant improvements in mechanical properties of the composites. Scanning electron microscopy studies also exhibited better dispersion of saline treated filler particles in the PP matrix.

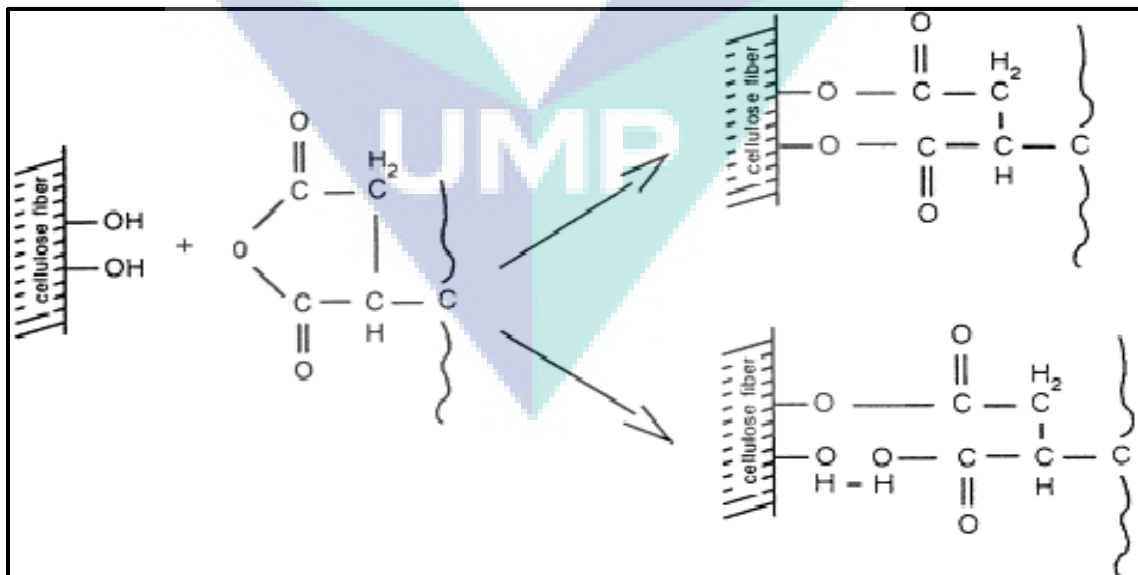


Figure 2.4 The reaction of cellulose fibers with MAPP

Source: Keener et al., (2004).

Maleic anhydride polypropylene (MAPP) is the most widely utilized coupling agent in the WPC due to its accessibility and its capacity to enhance the strength of WPC (Li et al., 2007). However, MAPP is not suitable for other polymers such as polyethylene, poly vinyl chloride. The treatment of cellulose fibers with MAPP copolymers gives covalent bond over the interface as seen in Figure 2.4.

Ashori and Nourbakhsh, (2011) used MAPP as a coupling agent for the surface modification of poplar wood flour. It has been found that the use of 5 and 7.5 wt % of MAPP leads to better interaction, decreases in the water absorption and slow penetration of moisture in the composites. Asgary et al., (2013) had studied the effect of MAPP coupling agent on the old newsprint/polypropylene nanocomposites. They observed that loading of MAPP in the composite shows improved tensile properties than composite loaded with 0 wt% MAPP. The tensile and flexural properties are significantly enhanced when 3 wt% MAPP were added in to the composite.

Analysts have also investigated the incorporation of MAPP as a coupling specialist in jute/PP composites (Doan et al., 2006). They observed that the addition of 2 wt % MAPP to PP matrix can significantly improve the adhesion strength with jute fibers and in the mechanical properties of composites. Khalid et al., (2006) have investigated the use of MAPP as coupling agent for the PP-oil palm empty fruit bunch fiber (EFBF) biocomposites. It was found that 2 wt % MAPP concentrations gave the best result for the PP-EFBB biocomposites. There was a dramatic increase in tensile and impact strength of PP-EFBB biocomposites than control sample. However, with further loading of MAPP from 2 to 7 wt % had decreased the tensile and impact properties of biocomposites.

Ndiaye and Tidjani, (2012) studied the effect of MAPP and oxidized polypropylene (OPP) coupling agents on the thermal properties of wood flour/polypropylene composites. They observed that 3 wt % MAPP loading in the composites improved the thermal behaviour of the composites than OPP coupling agent. In another study, Zhou et al., (2013) used MAPP as coupling agent to concentrate on the effect of coupling agent on rheological behaviour of bamboo powder-PP foamed composites. Addition of MAPP in the composites enhanced the rheological behaviour of

bamboo powder-PP foamed composites. FTIR and XRS results revealed that the interfacial compatibility of the MAPP treated composites was enhanced. XRD results demonstrated that the degree of crystallinity increased from 21.05 % to 26.52% after modification with MAPP.

2.3.4 Wood-Plastic Composites reinforced by Nano-fillers

Nowadays for the amendment of WPCs properties, nanofillers are being consistently used as great potential filler materials (J. Njuguna, 2008). The term nanometer is utilized to define nanometer scale items (10^{-9} m). A nanometer is equal to billionth of a meter and they are smaller than the wavelength length of visible light (Kamel, 2007). The nanofillers application in the field of composites has set up new patterns of prospect to overwhelm the limitations of conventional micrometer scale, since the nano scale fillers are free from defects (Azeredo, 2009). The surface area of nanofillers is larger than micro-scale filler surface area. Nanocomposites shows more interphase region than micro composites (Schadler et al., 2007). Nanofillers demonstrate better reinforcement for composites production because they have high aspect ratio (proportion of largest to smallest dimension) (Magaraphan et al., 2001).

Graphene is two dimensional allotrope of carbon, made by single layer of carbon atoms and bonded by SP^2 orbitals into hexagonal two-dimensional crystal lattice (Shabnam Sheshmani, Alireza Ashori, 2013). Fabrication of wood plastic composites using Graphene nanoplatelets (GNPs) were studied by Sheshmani and Ashori, (2013). They tested the physical, mechanical and thermal properties of composite and observed the impact of GNPs on these properties of composite as a reinforcing agent. It was found that the impact strength, tensile and flexural properties were improved by loading of GNPs filler into the composite. Physical properties were also improved by reinforcing GNPs filler into the composite. Composites loaded with GNPs degraded at maximum temperature compared with neat polypropylene and control sample.

Kamar et al., (2015) used GNPs as nanofiller in glass fiber/epoxy composites to investigate the ability of GNPs to improve the interlaminar mechanical properties of glass fiber/epoxy composites. Flexural test showed a 29 % improvement in flexural

strength with the loading of only 0.25 wt % GNPs. At the same concentration, fracture toughness testing exhibited a 25 % improvement. In another study, Chaharmahali et al., (2014) explored the effect of GNPs on the mechanical and physical properties of bagasse/polypropylene composites. It was seen that when only 0.1 wt % of GNPs was added, tensile and flexural properties reached at maximum values, while the notched impact strength was slightly decreased. Loading of GNPs did not change the average water absorption and thickness swelling, compared to the control sample.

In an interesting work, Yue et al., (2014) mixed carbon nanotubes (CNTs) and graphene nanoplatelets (GNPs) into an epoxy matrix at different ratios and studied the effect of CNTs:GNPs ratios on the mechanical and electrical properties of the composites. The combination of CNTs and GNPs synergistically increased flexural properties and decreased the electrical percolation threshold for the epoxy composites.

Carbon nanotubes (CNTs) are among the most examined nano scale materials, because it's unique functional properties such as high chemical resistance, high mechanical and water resistance, high thermal and electrical conductivity (Kordkheili et al., 2012). CNTs have made huge progress in the most of the areas of science and technology (Ashori et al., 2012) and it is widely being utilized as reinforcement in polymer, wood and cement based composites. CNTs have two types, single cylindrical walls (SWCNTs) and multiple walls (MWCNTs) (Kordkheili et al., 2013). Mechanical and physical properties of experimental composites fabricated from LDPE, WF and single-walled carbon nanotubes (SWCNTs) was studied by Kordkheili et al., (2013). It was found that the water absorption and thickness swelling of the composites had reduced with increased amount of SWCNTs (from 1 to 3 wt %) in the composites. The mechanical properties of LDPE/WF composites significantly improved with increased percentage of CNTs and MAPE in the composites. Composites having 2 wt% SWCNTs and 3 wt % MAPE revealed the highest impact strength.

In another study, Asgary et al., (2013) investigated the effect of multi walled carbon nanotubes (MWCNTs) as reinforcing agent on the physical and mechanical properties of old newsprint (ONP)/PP composites. The results of strength measurement indicated that Izod impact strength improved significantly when 1.5 wt % MWCNTs

was loaded while flexural and tensile properties reached their maximum when 2.5 wt % MWCNTs was added in the composites. Both physical and mechanical properties were improved when 3 wt% MAPP coupling agent was applied. In this work, MWCNTs were compounded with PVC, WF (populus WF) and foaming agent in an internal mixer by Farsheh et al., (2011). The experimental results indicated that because of MWCNTs the density of foamed composites was not affected by chemical foaming agent. Tensile strength and modulus were increased by up to 20% and 23% respectively. Also, water absorption and thickness swelling were decreased as compared with control samples (without MWCNTs).

Ashori et al., (2012) investigated the effects of MWCNTs as a reinforcing agent, on the physical and mechanical properties of bagasse/HDPE composites. MAPE was added as a coupling agent. The authors are of the opinion that tensile and flexural properties were improved when 1.5 wt% MWCNTs were added. Addition of MWCNTs reduced the impact strength and water absorption of the composites. Both physical and mechanical properties were improved when 4 wt% MAPE was loaded. Some of the researchers have also fabricated cement composites from MWCNTs and bagasse fibers (Kordkheili et al., 2012). They are also evaluated mechanical and physical properties of experimental cement panels. The results of measurement showed that, panels having 0.5 wt% MWCNTs revealed the highest impact strength and flexural modulus. With increasing amount of MWCNTs in the composites, the water absorption and thickness swelling of composite were reduced.

3.2.4.1 Nanoclay

Nanoclays are nano form (nanoparticles) of layered mineral silicates. It is derived from montmorillonite, a mineral deposit that has layered structure of dimension around 1 nm thick and a specific surface range of 700-800 m²/g. It is a weathering product synthesized by disintegration and chemical decomposition of volcanic rocks with fine texture of particle size under 0.002 mm (2 micron) (Cairns-Smith, 1986).

Nanoclay structures are classified into two main types one is 1:1 kaolinite type and other 2:1 layer silicates. As appeared in Figure 2.5, both contain stacks of layers

held together by hydrogen bond (as in 1:1) or by interlayer cations (as in 2:1). Kaolinite 1:1 comprises of metal-hydroxide and silicon-oxygen network of sheets combined by hydrogen bonding. The 2:1 layer silicates include mica, smectite, vermiculite, and chlorite. Smectite group is further separated into the montmorillonite (MMT), saponite, nontronite, and hectorite species (Brindley and Brown, 1980; Moore and Reynolds, 1989; Hetzer and De Kee, 2008).

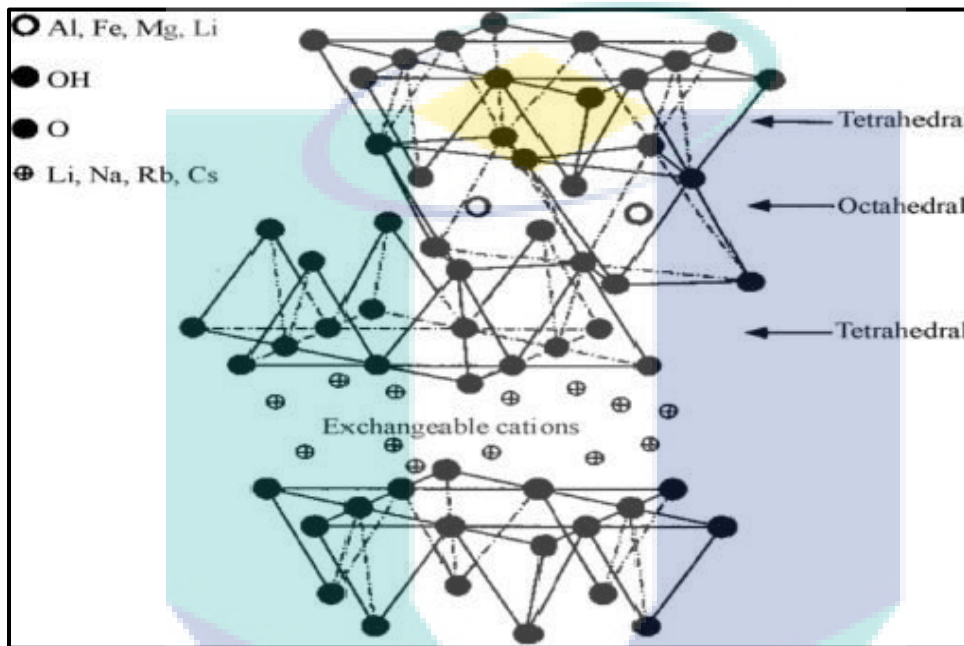


Figure 2.5 Structure of nanoclay

Source: Hetzer and De Kee (2008).

Nanoclays are presently being used to enhance modulus, tensile strength, barrier properties, flame resistance and thermal properties of many plastics. Among these layered silicates, MMT is generally utilized as reinforcement for the polymer-clay nanocomposite synthesis because it is eco-friendly, readily accessible in large quantity at low cost and its intercalation chemistry is well understood (Tjong, 2009). One of the prime advantage of using nanoclay particles in polymer matrix is the considerable increment in the mechanical properties with addition of less amount of nanofiller (< 10 wt %) (Chavooshi et al., 2014).

Organically Modified (organoclay) Layered Silicates

LS are known to be hydrophilic materials and it should be made compatible with hydrophobic polymers, it needs to experience chemical modification as it is only accordant to hydrophilic polymers in its pristine state. This is a big disadvantage as the most of the polymers carry the hydrophobic nature. Without organic treatment, LS will only be able to disperse and phase separate in within the polar polymers.

The organic treatment is generally carried out through ion exchange between inorganic sodium cations on the clay surface with the desired organic cation that is more reactive such as the primary, secondary, tertiary and quaternary alkylammonium or alkylphosphonium cations. In the ion exchange process, the inorganic (sodium) ions are exchanged with more voluminous organic onium cations and it results in extending the gap between the single sheets. The polymeric movements between them are empowered through this and the surface properties of every single sheet are changed from being hydrophilic to hydrophobic as appears in Figure 2.6 (Fischer, 2003).

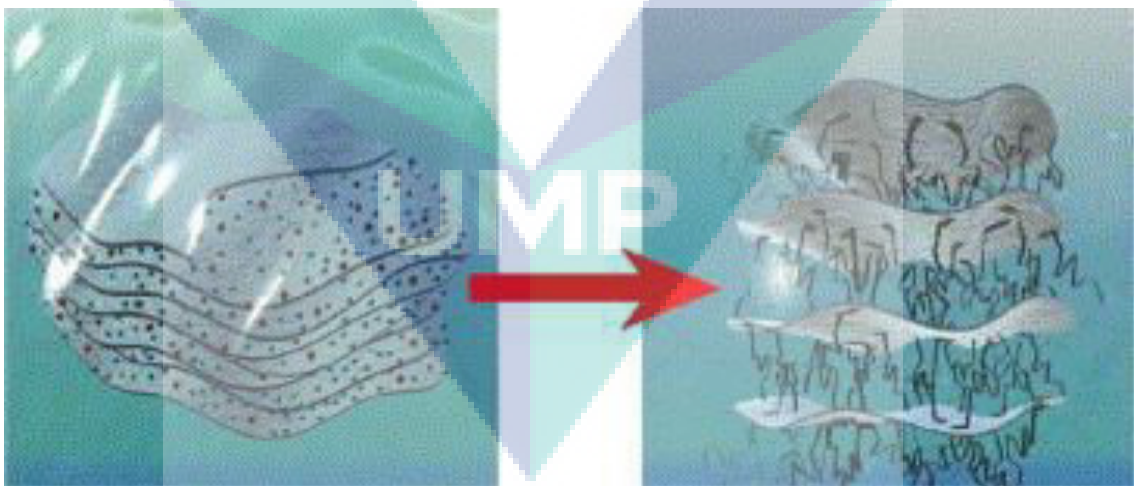


Figure 2.6 Schematic diagram of an ion exchange reaction

Source: Fisher (2003).

Alkylammonium or alkylphosphonium cations in organic silicates (OLS) enhance the wetting characteristics and intercalation with the polymer matrix by decreasing the surface energy of the inorganic host. To improve the strength of the

interface between the inorganic and the polymer matrix, alkylammonium or alkylphosphonium cations offer functional groups that can react with the polymer matrix, or sometimes initiate the polymerization of monomers (Okamata, 2006). There are several types of modification that can be possible such as treating the LS with transition metal ions or clay surface treatment using quaternary ammonium salts. Lee et al., (2008) incorporated nanoclay (Cloisite® 15A) into WF/PP composites in the presence of MAPP coupling agent. They observed that the addition of clay improved the thermal stability of the composites. Tensile strength and modulus indicated maximum values, when 3 wt% nanoclay was loaded in the composites.

In this research, the effect of nanoclay (Cloisite® 20A) and MAPP coupling agent loading on the mechanical properties and water absorption of PP/WF (Poplar WF) composites were investigated by Ashori and Nourbakhsh, (2011). The maximum tensile and flexural strength (increased by 46 % compared to the pure PP) were achieved in the composites, when 3 wt % nanoclay and 7.5 wt % MAPP were added. It was also observed that the addition of nanoclay decreased water absorption of the composites. The impact of nanoclay (Cloisite® 15A) reinforcement on withdrawal strength of fasteners and long-term physical properties before and after the immersion of PP/Medium density fiber board (MDF) dust composites was investigated by Chavooshi et al., (2014). As the nanoclay content increased the long-term water absorption (WA) and thickness swelling (TS) was decreased. Composite with 2wt% nanoclay exhibited Maximum withdrawal strength of fasteners (screws and nails).

Kord and Kiakojouri, (2011) explored the effect of nanoclay (Cloisite 30B) dispersion on mechanical and physical properties of PP/WF (beech tree WF)/glass fiber composites. They determined that the tensile properties of composites increased with increase of nanoclay up to 4 wt% and then decreased. However, the water uptake and impact strength of composites reduced with increasing the nanoclay contents. Long-term water absorption behaviour of PP/WF (beech tree WF)/nanoclay (30B) hybrid nanocomposites was evaluated by Ghasemi and Kord, (2009) In the presence of MAPP coupling agent. The result showed that the water absorption reduced by increasing nanoclay and MAPP (4 wt %) contents. The mechanism of water absorption of the composites followed under the study of the kinetics of a Fickian diffusion process.

In an interesting study, Deka and Maji, (2010) had blended HDPE, LDPE, PP, and PVC (in the ratio of 2:2:2:1) with Nals (Phargamites karka) WF and various concentration of nanoclay (nanomer) to determine the effect of compatibilizer and nanoclay on the properties of polymer blend/WF composites. Polyethylene co-glycidyl methacrylate (PE-co-GMA) was used as a compatibilizer. Composites incorporated with 3 wt % nanoclay and 5 wt % compatibilizer showed highest mechanical properties. Hardness, thermal stability and water uptake improved significantly with loading of nanoclay to polymer/WF composites.

Chemical foaming agent [Azodicarbonamide (AZD)] and nanoclay (Cloisite 15A) content influences the foaming and mechanical-physical properties of HDPE/wheat straw flour (WSF) composites (Babaei et al., 2014). The cellular structure results revealed that by increasing the AZD content from 2 to 4 phr (parts per hundred), the average cell density and size increased whereas the foam density displayed a reduction to 21.7% and by adding nanoclay up to 5 phr, density increased and the cell size decreased. The thickness swelling and water absorption increased to 26% and 19.3% respectively, when the AZD content was increased from 0 to 4 phr. The mechanical properties of HDPE/WSF composites were reduced by loading AZD and it was enhanced by incorporating 2 phr of nanoclay.

Alamri and Low, (2013) produced wood-plastic composite from epoxy resin, recycled cellulose fiber (RCF) and nanoclay (30B). They studied that the effect of water absorption on mechanical properties of composite. Result showed the dramatic reduction in flexural modulus, flexural strength and fracture toughness when samples were exposed to moisture for long time. The effect of water absorption on the mechanical properties of composite was slightly reduced after adding nanoclay into the composite.

LS whether organically modified or not have a hierarchical morphology defined by three general levels of structures which are the crystallite, primary particles and agglomerates. The crystallites are generally referred as tactoids composed of 100 individual layers stacked together; the primary particles consist of thick face to face stacking of individual tactoids and lastly the weak agglomerations. In fabricating WPC,

it is essential to ensure that there is no disruption of the tactoids and primary particles in order to achieve a homogeneous dispersion. It is crucial to accomplish a uniform distribution of the LS in the polymer matrix.

Transition Metal Ions (TMI) Modified Layered Silicates

The modification of LS with transition metal ions (TMI) are not widely investigated to date when contrasted with modification using organic surfactants. Although organically modified clay (organoclay) are often used, it was reported by Nawani et al. (2007) that these organoclay has insufficient activity because of the degradation of the organic surfactants in their structure whereby the organic components such as the quaternary amine surfactant begins to decompose through the Hoffman elimination process above 170 °C. Hoffman elimination is a process where quaternary ammonium salts undergo E2 elimination (the reaction transforms 2 sp³ C atoms into sp² C atoms) when heated. This is seen to hinder the property advancement of the nanocomposites particularly its thermal and barrier properties. It is assumed that small amount of catalytically active TMI salts in the clay may bring some significance in charring process of the WPC in which the development of carbonaceous-silicate chars during burning can reduce gas permeability and enhance thermal stability. The weak compatibility between the polymer host and the clay while fabricating the nanocomposites is also believed to be overcome through this modification process. It is summarized that the modification process enables penetration of the polymer chains in between the LS with ease due to the separation of the clay platelets that makes the intercalation or exfoliation process to be accomplished.

2.4 Fabrication (compounding) Processes of Wood-Plastic Composites

Extrusion, compression molding, injection molding and pultrusion are the common compounding processes of wood-plastic composite (Gebhardt, 2011). Drying of wood fibers or wood flour is an important preparation of wood-plastic composite production because the processing and final product quality wood-plastic composite samples can be affected by water content of wood.

2.4.1 Extrusion Processing

The extruder process is one of main compounding process of wood-plastic composite. To melt the polymer matrix and mix or blend the wood fiber, polymer and other additives in a compounding process is the fundamental objective of extruder. (1) Single screw, (2) co-rotating twin screw, (3) counter-rotating twin screw, and (4) Woodtruder are four main types of extrusion system basically used to fabricate WPC profile (Gardner et al., 2015).

Bengtsson and Oksman, (2006) used dried wood flour (pine) before compounding process at 100°C to achieve a moisture content of 0.03%. The co-rotating twin-screw extruder was used at temperature from 165 to 200°C to feed the HDPE and dried wood flour. In another study, Balasuriya et al., (2001) utilized a twin-screw extruder to blend HDPE with up to 70 wt% wood flakes (pine) to fabricate WPC. High flexural and tensile strength of twin-screw compounded composites loading up to 50 wt% wood flakes, demonstrated the melt blending is a superior processing method than mechanical mixing. The melt blending resulted in improved flake wetting, and thusly enhanced mechanical properties of the composites.

Due to the periodic and desorption of moisture, WPCs undergoes cyclic dimensional changer. Application of coupling agent into the composite can improve mechanical integrity. Moreover, it can be improve by using better processing of composites. Yeh and Gupta, (2008) produced PP based wood-plastic using twin-screw extruder. The co-rotating twin-screw extruder was used at temperature from 170 to 190°C to feed the PP and dried wood flour. At the extruder end a rectangular die was used. The properties were seen to be similar, at the 40 wt% wood flour content but even in the absence of coupling agent the lower rates of moisture absorption showed by using long residence time and average screw or low rotation speeds.

2.4.2 Compression Molding Process

The compression molding process is a molding technique in which preheated polymer and cellulosic material are put into an open, heated mold cavity. The mold is

shut with a top plug and pressure is applied to force the materials to contact all areas of the mold. All through the process the pressure and heat are kept up until the polymer has cured. Compression molding has been assessed for many years and has been utilized widely in the manufacture of automobile composite parts (Holbery and Houston, 2006).

In compression molding process, compounding step can be eliminated and mixing and molding can be done in one step (Jayaraman, 2003). This will permit minimizing length reduction of the fibers and the time the fibers spend at high temperature. In this method the cellulose fibers get distributed evenly between polymer films and then the “sandwich” is created by pressing in a compression molder at sufficient time and temperature. Korol, (2012) prepared composites from poultry feather fiber by mixing with polypropylene and then passing them through a hot oven at a fast rate to melt the PP fibers but not degrade the poultry fibers and a formed a prepreg. After then the prepreg is compression-molded into the laminate plates under pressure (4.44 MPa) and temperature (180 °C) (Barone et al., 2005). Johnson et al., (2008) used compression molding process under pressure 5.5 MPa and temperature 170 °C to produce WPCs from wetlaid lyocell, wood flour and PP. Lyocell fiber-reinforced PP composites manufactured from the compression molding process revealed comparable flexural and tensile properties as melt-processed (injection-molded) rayon-reinforced PP composites.

However, still unsolved and often studied issue during compression molding is the reorientation of the fibers during processing. Surface void formation is still a major issue, particularly for application in automotive industry. Such voids require expensive treatment to empower good appearance after painting (Odenberger et al., 2004). It is extremely important to understand the mechanism of reorientation since the final fiber orientation and distribution has strong impact on the tensile properties. An appropriately designed mold can ensure greater unidirectional alignment avoiding void formations.

2.4.3 Injection Molding

Injection molding is used to manufacture wood-plastic composite samples by requiring no finishing step. It is also used to obtain dumbbell shaped tensile samples.

There have additionally been reports examining injection molding to produce WPC microcellular foams (Gosseling, 2006) as well as injection molding used to fabricate WPC from biopolymers (Sykacek et al., 2009).

Karmaker and Youngquist, (1996) fabricated composites from PP and jute fibers using injection molding technique with temperature range 170 °C in feed zone, 180 °C in melt zone and 190 °C in die zone. Injection molding caused a high fiber attrition bringing about an average fiber length of 390 and 350 μm for compositions with and without coupling agent. Bouafif et al., (2009), manufactured WPC in a two phase process. In the initial phase of process, to compound HDPE with wood particles into pellets, they used a co-rotating twin-screw extruder at temperatures from 180 °C to 190 °C. Followed by extrusion process they used injection molding machine to obtain dog-bone shaped WPC specimen. Migneault et al., (2009), have studied a comparison between two fabrication process of WPCs which are extrusion and injection molding process. Melting, molding and cooling are the common steps they found in both the compounding process. However, process parameters in both the processes are different. Cooling rate, shear stress, shear strain, pressure, temperature and time are the process parameters. Besides, they reasoned, in injection molding shearing and pressure are higher than an extrusion (Figure 2.7).

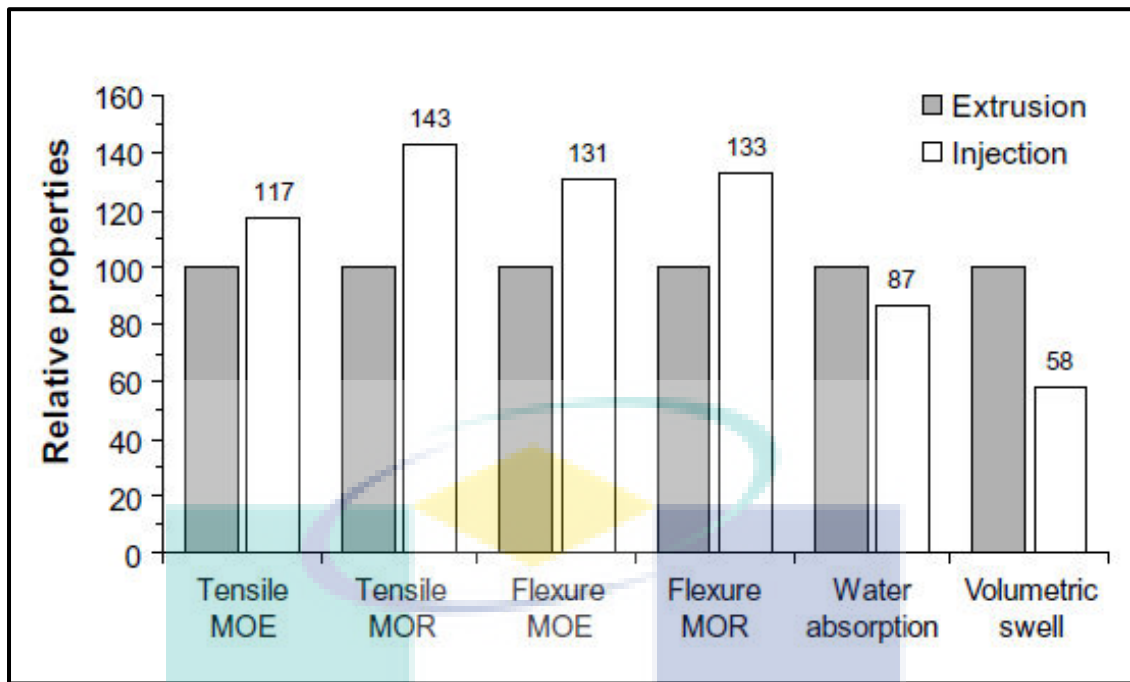


Figure 2.7 Relative properties for extruded and injection molded WPC made with HDPE and chemo-thermo-mechanical pulp (CTMP) fibers (average for three fiber sizes)

Source: Migneault et al., (2009).

Stark et al., (2004) used extrusion and injection molding process to fabricate WPC from HDPE and 50% wood flour. They concluded that injection molded samples exhibited higher flexural strength and density than extruded samples. The authors are of the opinion that injection molding process created better interfacial contact between polymer and wood fiber, resulting in higher density and therefore more strength. Clemons and Iback, (2004) manufactured WPC from 50% of 40-mesh pine flour and HDPE using extrusion and injection molding process and studied moisture sorption behavior of samples. They reasoned that extruded process samples absorbed more water compared to the injection molded samples.

2.5 Characterization of Wood-Plastic Composites

The improvement in properties of the wood-plastic composite is most often determined by the dispersion of the fillers and nanofillers into the composite. Enhancements in the chemical and physical properties of nanoclay based wood-plastic

composite are usually dependent on the intercalation of the silicates layers. The morphological, structural and functional structure of the nanoclay dispersion can be investigated and analyzed through the characterization studies such as scanning electron microscope (SEM), transmission electron microscope (TEM), Fourier transform infrared spectroscopy (FTIR), and x-ray diffraction (XRD).

2.5.1 Morphological Characterizations

In SEM analysis, a very fine electron incident beam is scanned across the surface of the sample through scattered electrons and this electrons produces a signal that is transformed into a two dimensional image of the sample's morphology (Etmimi, 2012). In the general SEM, the electrons are emitted from the electron source and accelerated in a space that comprises of a negative electric potential and an anode electrode at ground electric potential. The material's surface at the ground electric potential is then scanned with electron beam (Todokoro et al., 1999) which results in electrons and x-rays being ejected from the sample whereby this electrons and x-rays are then converted into a signal that produces the final image.

Scanning Electron Microscopy (SEM) is widely utilized to study morphology, structural and surface properties of fractured WPC surfaces. SEM uses secondary electrons generated from either thermal or field emitting cathode (Seegerholm, 2007). It is an important microscopic imaging technique for research in which high resolution images are crucial for analysis of morphological features. In plenty investigations focusing on interfacial mechanical characteristics of WPC, SEM images of the fractured surfaces were used to examine the interfacial features and predict the bonding strength based on whether the wood particles were pulled out of the matrix or broken (Ray et al., 2002). SEM images of exposed surfaces of WPC specimens before and after exposure and qualitatively correlate to the damage resulted from weathering process (Stark et al., 2004).

Royan et al., (2014) manufactured WPCs from recycled HDPE and Rice husk and studied the morphology of the composites. SEM micrographs exhibited better interfacial bonding between the fiber and polymer matrix. Zahedi et al., (2005) had used

SEM to determine the dispersion of nanoclay (Cloisite 15A) into the WPC. In their study, the SEM examination of the fracture surface of the models did not portray any mineral domains. Chavooshi et al., (2014) had fabricated WPC from PP, WF, MAPP and nanoclay (Cloisite 15A) and evaluated the morphology of the composites by using SEM analysis. They observed that high loading of nanoclay into the composites gets agglomerate easily as shown in Figure 2.8.

Morphological study by SEM can only verify the presence of agglomerates in the polymer host up to a certain level of view magnifications. In order to investigate whether intercalation or exfoliation of the nanoclay has occurred, morphological characterizations such as TEM have to be employed.

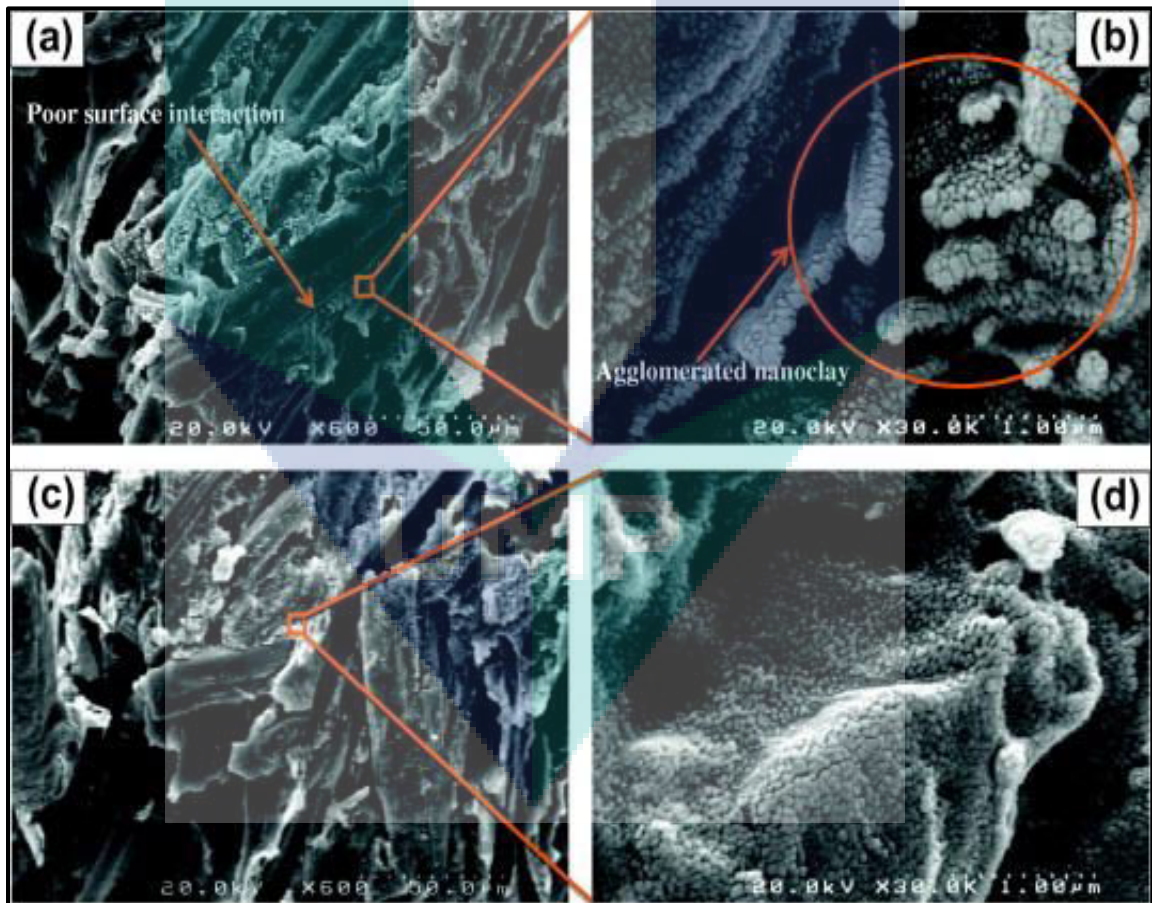


Figure 2.8 SEM micrographs of tensile fracture surfaces of WPC with 6 wt% of nanoclay (a and b) and WPC with 2 wt% of nanoclay (c and d)

Source: Chavooshi et al., (2014).

TEM is a characterization study that is employed to visually see the morphology of WPC at the nanometer scale. To focus and direct thermal electron are accelerated by applying high voltage to form an electron beam from the electron gun to penetrate the sample, it uses electromagnetic lenses. The images that can be seen on a fluorescent screen are formed by the electromagnetic lenses. Due to the ability to visually determine the pattern of the clay dispersion in the polymer matrix, TEM analysis is more advantageous as compared to SEM (Ismail, 2013).

Faruk and Matuana (2008) used TEM in order to gain an insight into the latter feature of the Organoclay (Cloisite 15A) dispersed into the HDPE/WF (maple spp) WPC. The superstructure of the organoclay dispersion consisted of separate nanoclay layers. Agglomerates of the tactoids with a variety of size were present in the WPC as shown in Figure 2.9.

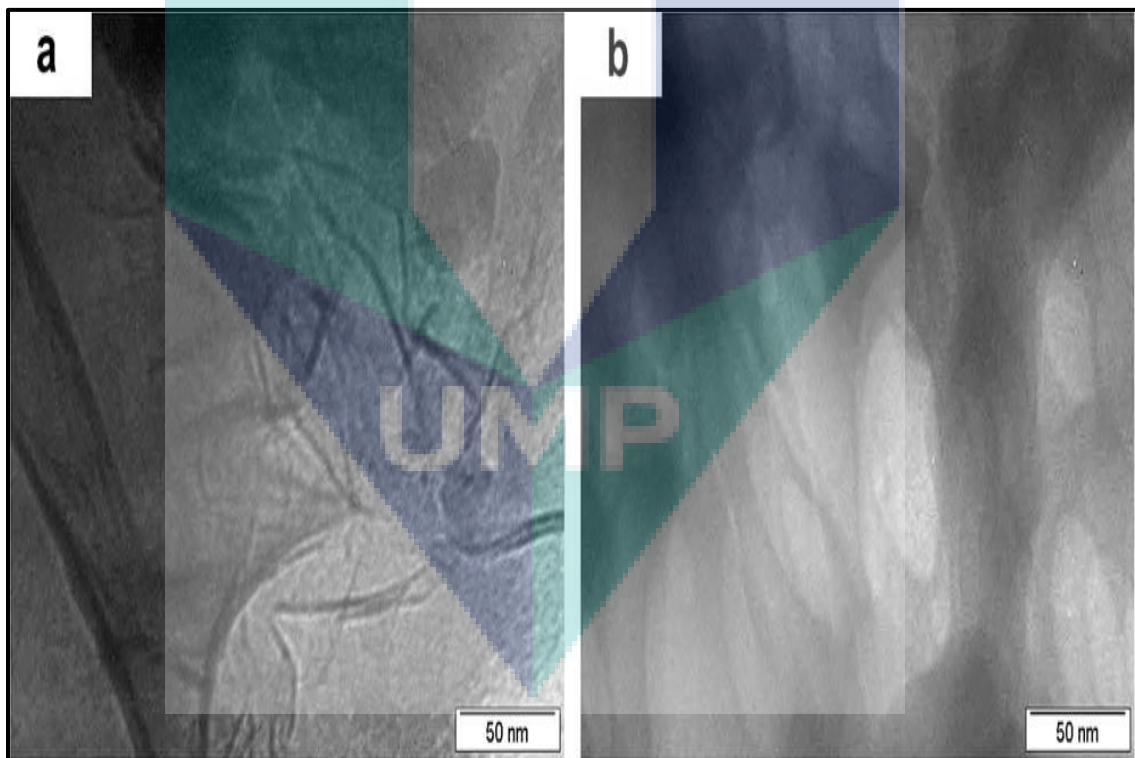


Figure 2.9 TEM of HDPE/nanoclay composites: (a) with 3 wt% of nanoclay and (b) with 5 wt% of nanoclay

Source: Faruk and Matuana (2008).

2.5.2 Structural Characterizations

Fourier Transform Infrared Spectroscopy (FTIR) is a technique that exploits the vibration response of molecules because of infrared (IR) radiation. Molecules absorb energies that relate to their frequency and transmit the unabsorbed frequencies when they are presented to IR and these unabsorbed frequencies are recorded by a detector which enables the identification of molecules by matching the wavelength of the molecule with the frequency to those definitely known (Bhattacharya et al., 2008). The particular bonds inside their molecule and their corresponding wavelength are recorded in Table 2.3.

Table 2.3 Example of atomic groups with their IR absorption wavelengths

Molecules	Absorption wavelength (cm ⁻¹)
C=O	1870-1650
O-H	3640-3250
C-OH	1160-1030
C-H	2980-2850
N-H	3460-3280

Source: Bhattacharya et al., (2008).

Ruijun et al., (2010) used FTIR to explore the chemical structure of WPC reinforced with organoclay (Cloisite 20A). In light of the spectrum obtained from their example, the IR groups at 3480 cm⁻¹ and 3320 cm⁻¹ were related to the hydrogen bonded N-H stretching and the free N-H stretching in the PP respectively. Free of hydrogen bonding carbonyl caused the band at 1733 cm⁻¹ while hydrogen bonded carbonyls resulted in the 1703 cm⁻¹ band. The IR band at 1050 cm⁻¹ is related to the silica oxide (Si-O). The Si-O band showed that nanoclay was able to disperse into the WPC.

X-Ray Diffraction (XRD) is a more commonly used technique to determine the distance between the galleries or interlayer spacing, d_{001} in the clay structure (Utrucki, 2004). The spacing between the ordered crystalline layers of the organoclay is measured using the Bragg's Law.

$$n\lambda = 2d \sin \theta \quad (2.1)$$

Where:

d = Space between layers of the clay

λ = Wavelength of the X-ray

θ = Angle at the maximum point of the first peak into a spectrum

n = Order of diffraction

Intensity of the diffracted x-ray is measured as a component of the diffraction angle 2θ whereby the pattern is used to distinguish the specimen's crystalline phases and to measure its structural properties. The change in the spacing can be utilized to determine the type of polymer nanocomposites formed such as immiscible; no d-spacing changes, decomposed; d-spacing decreased, intercalated; d-spacing increase and exfoliated; d-spacing outside of angle ray diffraction (Utrucki, 2004).

Ahmad et al., (2015) employed XRD to determine the d-spacing for the WPC reinforced with different content of organoclay (Cloisite 30B) as appears in Figure 2.10. According to their results the $2\theta = 4.75^\circ$ peak is related to neat clay with $d_{001} = 18.58 \text{ \AA}$. In a 2% nanoclay sample, the peak moved to a lower angle ($2\theta = 1.83^\circ$; $d_{001} = 48.22 \text{ \AA}$), which suggested the formation of intercalation morphology. The peak corresponds to 4% nanoclay appeared at $2\theta = 1.95^\circ$; $d_{001} = 45.25 \text{ \AA}$. This information demonstrated that the order of intercalation was higher at 2 % nanoclay than at 4 % nanoclay loading. Thus, one reason behind the achievement of an intercalated structure in these nanocomposites could be better dispersion of the nanoclay throughout the polymer matrix.

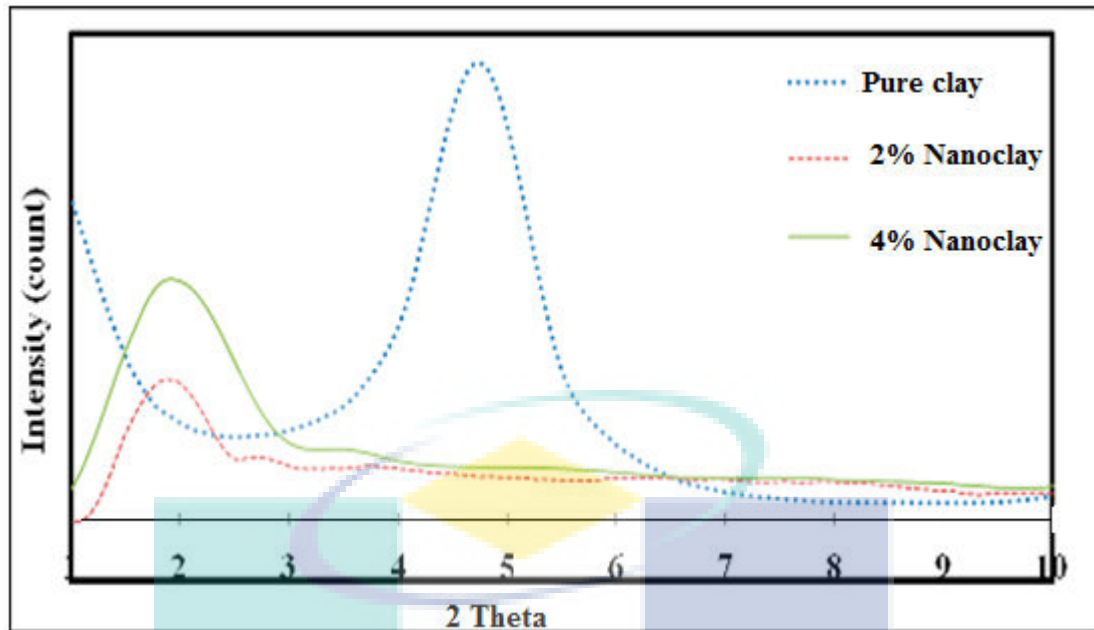


Figure 2.10 XRD patterns of the nanoclay content at $2\theta = 1$ to 10°
 Source: Ahmad et al., (2015).

2.6 Properties of Wood-Plastic Composites

2.6.1 Mechanical Properties of WPCs

High potential of material to deform plastically by initiation of a very large number of microscopic yield events can be improved by the toughness or hardness of material (Dobрева et al., 2006). Initiation of small plastic zones induced by stress concentration of particles, initiation of a large number of micro cracks by short fibers or inorganic particles and cavitation at the surface of (or inside) particles affects the mechanical properties of material. The deformation of the polymer matrix between the particles caused by voids which are produced due to the poorly dispersed and weakly bonded particles.

Dobрева et al., (2006) manufactured composite from PP, wood flour, styrene-butadiene rubber and MAPP and studied the mechanical and deformation mechanisms of composite. They observed that the composite containing 10 wt% wood fiber and 10 wt% MAPP showing improved yield stress, impact strength and young's modulus. The modulus of composite can be improved by adding high stiffness fillers but can reduce

the elongation at break. Bouafif et al., (2009) are of the opinion that the composites filled higher wood fiber size produced higher strength and elasticity but lower energy to break and elongation. The stiffness and tensile strength of composite improved by increasing wood fiber content into the composite but reduced the energy at an elongation.

In an another study, Kuo et al., (2009) fabricated wood-plastic composite using injection molding and investigated material compositions effects on the mechanical properties of composite. They used wood flour (47%), plastic matrix (47%), MAPP (3) and zinc stearate (3) in WPC composition. They found that LDPE and PP-based WPC showed higher tensile strength and modulus of rupture than those of neat LDPE and PP themselves. The addition of flame retardants (magnesium hydroxide) in WF (poplar)/PP composites affect the mechanical properties of the composites. Marginal reduction in the mechanical properties of PP/WF composites was seen with addition of flame retardants (magnesium hydroxide) (Sain et al., 2004). Water absorption of natural fiber/PP composites by immersing the samples in water at three different temperature, 23, 50, and 70°C was observed by Espert et al., (2004). They concluded that after water absorption test composites showed decreased tensile properties. In addition to this, water absorption test samples demonstrated high loss in mechanical properties compared to the dry samples.

2.6.1.1 Sub-Surface Mechanical and Creep behaviour of WPCs

To test mechanical properties of metal at submicron length scale then nanoindentation has set up as a standard method and it is progressively being applied to polymeric materials. The measurement of the mechanical properties such as hardness and modulus particularly with increased demand of nanomaterial technology requires such a precise tool in measuring and interpreting those properties. A wide range of indentation tests was developed to complete such requirements of measurements. Recently it has become easier in indentation understanding in hardness and elastic modulus, as well as creep and scratch properties directly from the load and displacement curve because of computational power (Goldstone et al., 2007).

Nanoindentation is a sophisticated technique that is suitable for the subsurface mechanical properties of variety of materials by providing a wealth of valuable quantitative information (Oliver and Pharr, 1992). The deformation phenomena of materials at small length and load scales utilizing indenter by application of a load, is the mechanism of this nanoindentation technique. The combination of both visco and elastic contribution to the total indentation depth represents the indentation depth variation.

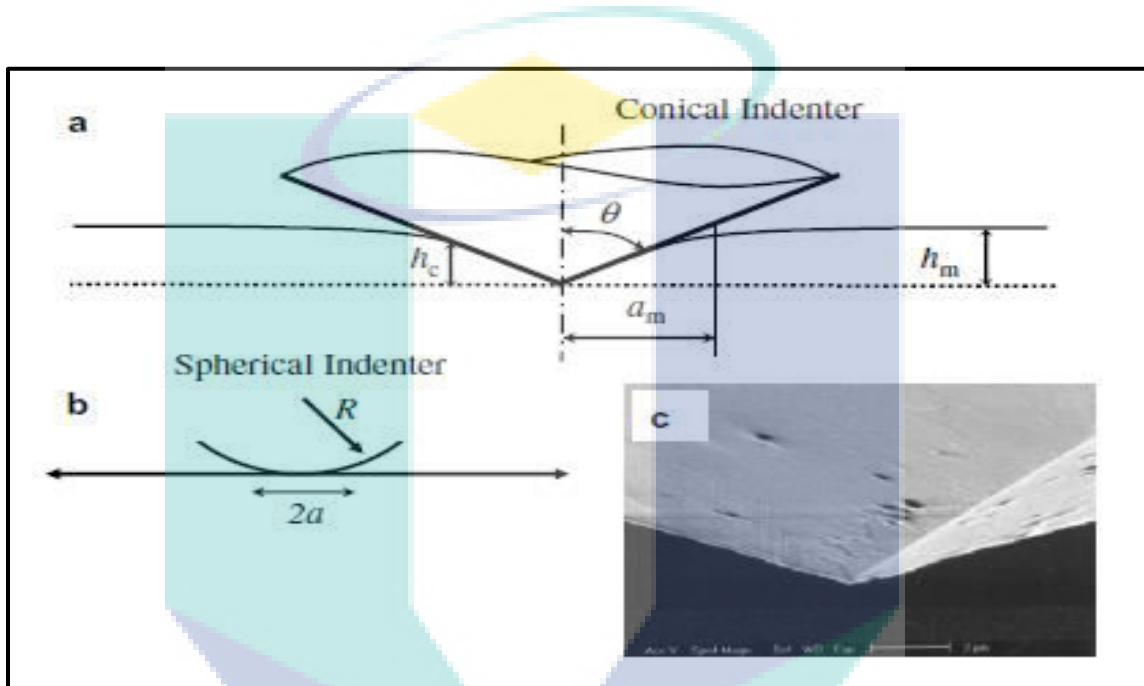


Figure 2.11 Schematic of tips used in instrumented indentation. (a) A sharp pyramidal tip is often modelled as a cone with $\theta = 70.3^\circ$, (b) A spherical tip is defined by its radius R , and a characteristic strain may be defined as a/R . (c) SEM image of a diamond Berkovich indenter

Source: Pelletier et al., (2008).

Generally, there are three different types of indenter tips that are utilized as part of nanoindentation test analysis and experiments are exhibited in Figure 2.11. The first type of indenter tip is sharp, shown in Figure 2.11 (a) and second one is spherical, shown in Figure 2.11 (b). With regard to the first order both the types of indenter are suited for various types of tests. For instance, improving the extraction of elastic-plastic properties of material, the self-comparability of a sharp tip makes it more favourable for analysis of ductile materials. As far as more complex system is concerned in which a small strain elastic deformation is optimum for simpler analysis, but yet has been

utilized as a part of removing elastic plastic properties as well the spherical indenter tip has been widely used to overcome this issue. The spherical tip indenter has been also used for brittle materials. The last type indenter which is a diamond Berkovich indenter is depicted in Figure 2.11 (c).

Load and displacement are measured as the indenter tip is forced into the test materials surface with desirable loading and unloading profile, while a particular nanoindentation analysis. To obtain the mechanical properties utilizing information from the indentation tests, several models have been proposed. A method to measure elastic modulus from the unloading curve and hardness from the loading curve, assuming that the contact remains constant as the indenter is withdrawn and that the unloading curve is straight was investigated by Doerner and Nix (1986). Utilizing the relationship between contact area, elastic modulus and initial slope of the unloading curve, Cheng et al (2004) have depicted a way to measure the hardness and modulus of the materials. To reveal the fact that the indentation unloading curve is even at the onset of unloading are not linear, the Doerner and Nix model was refined by Oliver and Pharr (1992). Using models for indentation of a flat elastic body by a rigid tip of simple geometry, the vertical displacement of the contact periphery can be described is the basic assumption of the Oliver and Pharr examination. The Oliver and Pharr method has been adopted in commercial instruments and experienced various in modifications.

Nanoindentation Creep Test

Many types of work have been performed on the deformation behavior and the mechanical properties of polymer nanocomposites (Jin et al., 2006). However, the viscoelastic behavior of nanocomposites such as stress relaxation and creep is still not completely investigated. With regard to nature of polymeric materials then it is viscoelastic materials which properties are inadequate with the time. For instance, creep of material, it is subjected to a stress beneath its yield stress and it is a time-dependent plastic deformation of a material. The mobility of the polymer chains is completely responsible for the deformation process of material under load. The chain mobility of polymer is subject to the temperature and the time. The use of polymer and polymer-based materials can be affected by the time dependent creep deformation (Messersmith and Giannelis, 1995).

The investigation of viscoelastic behavior of polymer nanocomposites particularly in creep is shown a few literatures. It should be one of the major issues in developing the polymer nanocomposites that creep is quite related with the service life and safety of materials. Due to the limitation of polymer mobility and strong interface interaction between the nanofiller and polymer chains, loading of nanofiller into the polymer matrix could contribute to the retardant of the process of creep or slows down the creep rate. The creep rate of steel enhanced significantly at high temperatures and decreased its creep rate, when nano-sized carbonitride was added.

Polyethylene/MMT layer silicate films were synthesized by Ranade et al. (2005). They found that loading of small amount of MMT clay improved creep resistance of the polymers. The circular nanoparticles with low filler content can improve creep resistance of polyamide 66; this comparable result was reported by Zhang et al. (2004). Introduction of 1 vol% nanoparticles in polypropylene nanocomposites decreased the creep strain and creep rate by 46% and 80% respectively, contrasted with the neat matrix. However, these discoveries usually implement tensile creep test which is reasonably well developed for bulk materials. At submicron scale, to study the mechanical properties of materials is still not achievable. Oliver and Parr (1992) proposed the use of depth sensing indentation in creep test under the condition of constant load. A comparative technique by using nanoindentation equipment was further executed by Mayo and Nix (1988). Utilizing nanoindentation technique and modeling they studied, experimental methodologies of creep property in bulk and subsurface of PU nanocomposites.

Creep behaviour Theory

In the conventional creep test, the test may not necessarily be continued to rupture of the specimen and the elongation of the specimen is measured as a function of duration. As a function of the test span to give the creep curve, the creep strain (the expansion in specimen length as a percentage of the initial length) is plotted, for every test. The three regimes; an area of decreasing creep rate (primary creep), an area in which the creep rate is more or less steady (secondary creep), and an area in which the creep rate increases (tertiary creep) until crack (rupture) of the specimen occurs are

demonstrated in Figure 2.12. It is a schematic figure of a particular tensile creep curve. However, in an indentation creep test the indentation load in all probability leads just to the primary and secondary creep for polymeric materials. Tensile creep test is not quite same as an indentation creep test. It can be seen from Figure 2.13 a typical diagram of indentation creep. All in all, the rupture can't be seen during indentation tests.

Tensile test and indentation creep test have some contrasts. As far as number of samples are concerned, then number of samples require for conventional tensile creep test because each and every specimen can be tested just at one stress and one temperature. It is sometimes hard to obtain desired information because of possible microstructure varieties among the samples. Indentation creep is used to stay away from this trouble, in which similar like hardness test mechanism up to some extent, a smaller indenter is penetrated into the surface of the specimen. However, in indentation creep test, the depth of penetration is measured under a consistent external load forced on the indenter, not like hardness tests in which the size of indent is measured. Indentation creep test is time consuming test as well as it provides a lot of information in a short period (Cahn and Lifshitz, 2013).

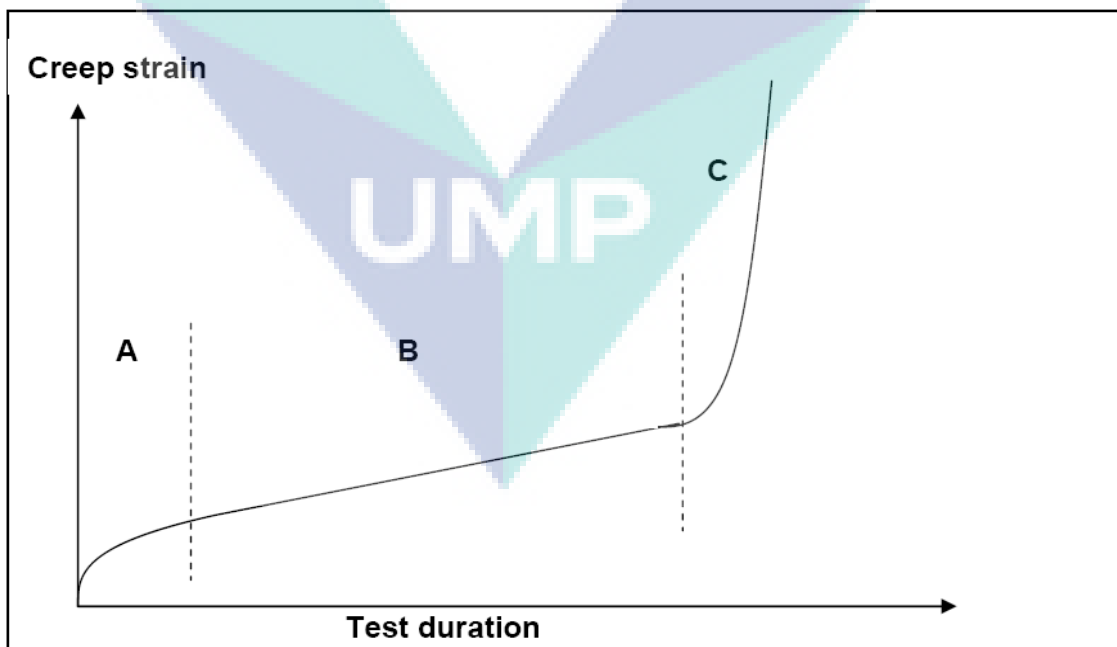


Figure 2.12 Three creep regimes of conventional creep curve which are (A) primary creep region; (B) secondary creep region; and (C) tertiary creep region.

Source: Cahn and Lifshitz (2013).

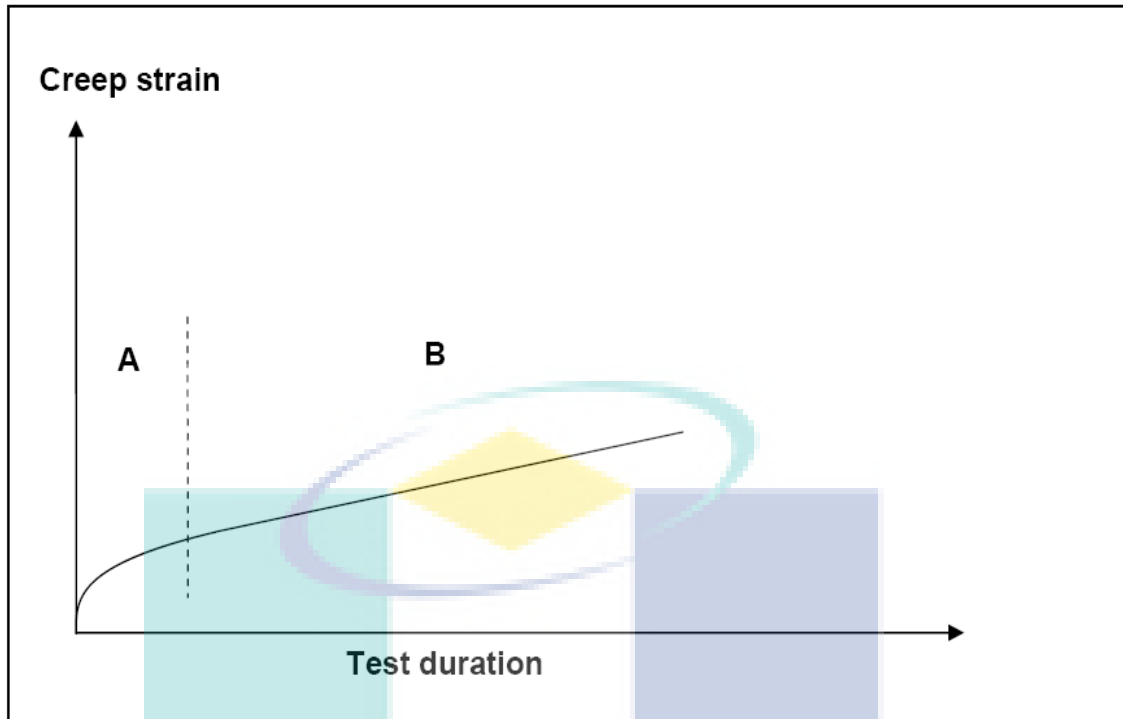


Figure 2.13 Indentation creep curve diagram exhibiting the two regimes which are (A) primary creep region and (B) secondary creep region

Source: Cahn and Lifshitz (2013).

2.6.2 Physical Properties of WPCs

New application and end uses of WPCs for flooring, decking, outdoor facilities, window frames and various construction materials, and their exposure to atmosphere or contact with aqueous media have made it essential to investigate the physical properties of these materials. Physical properties are like water absorption, thickness swelling, biological resistance, flame retardancy, density. Physical properties are generally connected to material structure and performances, so the measurement of physical property changes can be used to evaluate material structural changes. Physical properties are most important characteristics of WPC exposed to the environmental conditions that determine their end use application (Markarian, 2008).

Kamdem et al., (2004) have studied some physical properties of WPC made of recycled HDPE and from with and without CCA (Chromated copper arsenate) treated red pine WF. Authors are of the opinion that the biological durability and the photo-

protection were improved for samples loading CCA-treated WF. In this study, Ghasemi and Kord, (2009) investigated the long-term water absorption of WPC manufactured from PP/WF (Beech)/nanoclay (Cloisite® 30B)/MAPP. The long-term water absorption of the composites was evaluated by their immersion in water at room temperature for long period (3000 h). The result showed that water absorption of composites reduced with increasing nanoclay content and adding MAPP as revealed in Table 2.4.

Table 2.4 Maximum water absorption for different formulations

Sample code (PP/WF/MAPP/Nanoclay)	Maximum water absorption (%)
50P/50W	14.2861
50P/50W/2M	14.0547
50P/50W/2M/3N	13.8785
50P/50W/2M/6N	14.4081

Source: Ghasemi and Kord, (2009).

Effects of species, wood type and fiber size on the water absorption of WPC was evaluated by Bouafif et al., (2008). Researchers found that the water absorption of WPC slightly varied among species and increased with increasing fiber size but to a negligible extent as compared with other wood-based composites and solid wood. This study deals with the fabrication of composites from sawdust and recycled polyethylene terephthalate (PET) at different ratios by flat-pressed method. The water absorption and thickness swelling were measured after 24 hours of immersion in water at 25, 50, and 75°C temperature. It was seen that the water absorption and thickness swelling increased when PET content reduced in the composites and testing water temperature increased (Rahman et al., 2013).

Ayrilmis et al., (2011) observed the effect of a thermal-treatment method on the dimensional stability of flat-pressed WPC containing wood fiber (eucalyptus). The

present study exhibited that the water absorption and thickness swelling of WPC samples are significantly reduced with the increasing treatment of temperature and time. Jordens et al., (2010) employed terahertz time-domain spectroscopy to investigate the sorption of water into WPC. The dielectric properties of the WPC were determined for frequencies between 0.2 and 1.0 THz for varying water contents. The result suggests that this technique is ideal tool for a non-destructive, contactless determination of the water content.

Stark et al., (2010) used oxygen index and cone calorimeter tests to study the fire performance of WF (pine)/PE composites, and compared the results with unfilled PE and solid wood. Researchers then studied the effect of five additive-type fire retardants on fire performance of WPC. Ammonium polyphosphate and magnesium hydroxide highly improved the fire performance of WPC as compared to bromine based and zinc borate fire retardants. Moisture sorption and decay resistance of HDPE based WPC manufactured from poplar, Douglas-fir, black locust, white oak, and ponderosa pine were evaluated by Fabiyi et al., (2011). Dimensional stability of WPCs made from poplar was poor whereas black locust performed well. However, *Trametes versicolor* (white rot) produced significantly higher weight losses on HDPE/poplar composites while HDPE/Douglas-fir composites were less susceptible to this fungus. The effect of water absorption on the mechanical properties of nanoclay (Cloisite® 30B) filled recycled cellulose fiber epoxy hybrid nanocomposites was evaluated by Alamri and Low, (2013). They observed that as the nanoclay loading increased water absorption was found to reduce. As a result of water absorption flexural properties and fracture toughness tremendously decreased. However, after immersion in water the impact toughness and impact strength of composite were increased.

This work concerns the preparation and physical study HDPE/WF WPC. Fire retardants (ammonium polyphosphate) and light stabilizer (HALS) were added to improve the fire retardancy and durability of the composites. The fire retardant worsened the outdoor durability. However, WPC with stabilized fire retarded indicated much lower fading than non-stabilized non-fire retarded composites (Garcia et al., 2009). Stark et al., (2004) have investigated the weathering characteristics of WF (Pandora pine)/HDPE composites. The samples were weathered in a weathering

apparatus (xenon-arc) for 1000, 2000, and 3000 h and then analysed for colour fade and loss of flexural strength. Results indicated that composites with large wood component at the surface experienced a higher percentage of total loss in flexural strength after weathering.

2.6.3 Thermal Properties of WPCs

It is important to study the thermal properties of the wood-plastic composite to know the processing and uses of these composites. The degradation of the cellulosic materials can produce undesirable effects on the properties of composites, because the fabrication of wood-plastic composite requires the mixing of wood fibers and matrix at high temperature. Thermogravimetric analysis (TGA) and Differential scanning Calorimetry (DSC) are the most widely used techniques for thermal analysis.

Ndiaye and Tidjani, (2012) have studied the effect of coupling agent (MAPP) on thermal behaviour of WF (pine)/PP composites. The thermal degradation behaviour of the composites was (T_m , T_p , and T_c) characterized by TGA. The result indicated that the degradation temperature of the composites shifted to slightly higher values after addition of coupling agent in the composites. The effect of hexagonal boron nitride (h-BN) on thermal properties of injection molded WPCs prepared from WF (poplar) and HDPE with 3 wt % coupling agent (MAPE) was evaluated by Ayilmis et al., (2014). The DSC analysis showed that the crystallinity, melting enthalpy, and crystallization enthalpy of WPC increased with increasing h-BN content. Farhadinejad et al., (2012) introduced nano wollastonite in wood fibrils/PP WPCs, to study the effect of nano wollastonite on thermal properties of composites. Thermal properties of the obtained composites were characterized by different techniques such as TGA, DSC, limited oxygen index, and oxidative induction time. They observed that the introduction of nano wollastonite increased the thermal stability and crystallinity in the composites because of high specific area of nano wollastonite.

In this work, 30% particles of iron wood (*Xylia xylocarpa*) were mixed with recycled polypropylene foam (RPPF) with two different additives glycerol as a plasticizer and MAPP as a compatibilizer. The thermal behaviour of composites was

characterized by TGA. The result showed that composites containing plasticizer and compatibilizer have shown a great influence on thermal behaviour of composites as compared to a composites without these additives (Tajan et al., 2008). Ratanawilai et al., (2012) determined the thermal properties of oil palm wood sawdust (OWS) reinforced post-consumer polyethylene composites using TGA technique. It was found that the thermal stability of the composites slightly decreased with higher OWS content as exhibited in Table 2.5.

Table 2.5 Weight percentage of OWS/PCR-HDPE composites at different temperatures

Temperature (°C)	Weight (%)		
	OWS (30%)	OWS (40%)	OWS (50%)
100	98.8	98.4	97.7
200	98.4	97.8	96.9
300	93.4	91.5	89.2
400	80.9	74.0	67.7
500	38.8	36.2	34.5
600	9.6	11.8	14.4

Source: Ratanawilai et al., (2012).

Gwon et al., (2010) prepared WPC from PP, chemically treated WF and talc to investigate the thermal behaviour of WPC using DSC technique. It was found that melting enthalpy had decreased by addition of fillers because of the decreased amount of the crystallisable resin and the interference of the fillers for crystallization process. Li et al., (2014) used bamboo charcoal (BC) to enhance the thermal property of LDPE/WF WPC. Researchers used TGA technique to analyse thermal behaviour of composites. They concluded that the addition of BC improved 30% and 50% wt loss temperature. Hasan et al., (2011) characterized the thermal degradation of WPC with TGA. It was observed that the degradation temperatures shifted to higher values after addition of 3 wt% of MAPP. The largest improvement on the thermal stability of composites was achieved when 2.5 wt% of nanoclay was added.

2.7 Optimization of Wood-Plastic Composites using Response Surface Methodology (RSM)

In order to receive the maximum benefits for a product, a process or a system optimization process has been used to enhance the working ability. One factor influences at a time on an experimental response has been checked by optimization. In this optimization method the other parameters are kept as a constant level whereas only one parameter is changed. This optimization method is known as one-variable-at a time. It does not exclude the impact of interactive factor among the variables examined is the major drawback of it. This optimization method does not show the full effect on response parameter. The experiment on number expansion is essential to perform the research, which results in the increment of cost and time and in addition an expansion in the utilization of materials is another drawback of this one-factor optimization method (Bezerra et al., 2008).

In order to tackle this issue, the analytical process optimization has been completed by utilizing multivariate statistic technique. Response surface methodology (RSM) is amongst the most concerned multivariate techniques utilized as a part of analytical optimization. RSM depends on the fit of a polynomial equation to the experimental information, which must portray the behaviour of data set with the objective of making statistical previsions (Bezerra et al., 2008). It is an accumulation of statistic and mathematic. When a response or a set of responses of interest are affected by several variables, RSM can be well applied. To simultaneously optimize the levels of these variables to achieve the best system performance is the goal of this analytical process.

It is important to choose an experimental design that will determine which experiments should be applied in the experimental before the beginning of the RSM methodology. When the information set does not present curvature, experimental plans (designs) for first-arrange models (e.g., factorial design) can be utilized (Bas and Boyaci, 2007). Experimental designs for quadratic response surfaces should be used such as Box–Behnken, focal (central) composite, three levels factorial, and Doehlert designs.

Herrmann et al., 2000 studied Polyethylene terephthalate (PET) - based wood-plastic composite. Four operational factors that influence flexural and tensile strength of PET-based WPC were determined. Particle size of the filler was assumed as uncontrollable factor. It's worth to mention that milling and sieving of wood flour to a expected size is exceptionally costly. Using response surface methodology with regards to dual robust design (Zang et al., 2005), researchers concluded that the level of these three operational controllable factors had increased tensile and flexural strength of wood-plastic composite. There has been some work on improving properties of wood-plastic composite with various methodologies. The injection molded pp-based wood-plastic composite was examined by Yeh and Gupta, (2008). They observed that while maintaining the same mechanical properties the water absorption rate can be reduced by changing operational conditions. Factorial design employed for experiments and analysis of variance (ANOVA) was used to analyse experimental data.

The application of a micro-multiobjective genetic algorithm, which was applied in optimizing the design of a PP-based wood-plastic composite profile, was evaluated by Soury et al., (2009). To decrease the overall weight of the product and to keep up adequate capacity was the fundamental objective of this study. The impact of changing the combination of a wood-plastic composite with recycled polypropylene (RPP), on mechanical and physical properties was determined by Yang et al., (2012). Particle size of filler, lubricant content, dose of coupling agent and the mass ratio of the wood and RPP were taken as parameters. According to the study, tensile and flexural strength enhanced as well as water absorption decreased by using small size particle sawdust (> 125 microns). Javier et al., (2015) have concentrated on the optimization of flexural and tensile strength of WPC fabricated from sawdust and polyethylene-terephthalate. To develop the working conditions that provide ideal properties of the wood-plastic composite with minimal variance was the objective of this work. Fiber particle size was taken as a noise factor. The RSM by contour lines, in a combined design of experiment was applied.

2.8 Summary of Literature Review

Selection of polymer matrix is the most important factor in WPC. The selected polymer matrix should be available at low cost, good in performance and non-hazardous to the environment. Polypropylene (PP) is widely used in the WPC because of its availability and better properties. PP has slightly higher stiffness than HDPE.

The higher strength and stiffness of wood fibers/flour makes them good candidates as plastic reinforcements. However, the thermal instability nature of WF places an upper limit on the processing temperature. Other intrinsic properties such as quality variation and low resistance to moisture also limit the applications of WF. The most important problem is, the poor compatibility exhibited between the hydrophilic WF and the polymeric matrices, which results in non-uniform dispersion of fibers within the matrix and poor mechanical properties.

Coupling agents have been employed in to the composite, in order to improve compatibility between thermoplastics matrices and wood flour. Substances, commonly polymers that are utilized as a part of small amount to treat a surface so adhesion occurs between it and other surfaces such type of substance is known as coupling agent. Maleic anhydride polypropylene coupling agent is popular in the research and industry because of its effectiveness and availability.

Nano-particles or nano-fillers are presently considered as great potential filler materials for the amendment of mechanical and physical properties of wood plastic composites. Nano-scale filler offers larger effective surface area than micro-scale filler. As a result, there is more interphase region in nanocomposites than in micro composites. Among all nanofiller, nanoclays are widely used as nanofiller in WPC because it is eco-friendly, readily available in large quantity and inexpensive. However, Pristine MMT is a hydrophilic phyllosilicate which creates poor mixing and interaction with most of the polymer matrix which are hydrophobic in nature. The TMI (Transition Metal Ions) modification has been widely used to change the nature of the nanoclay which is hydrophilic.

Fabrication or manufacturing of WPC is the important aspect of WPC production. Manufacturing methods like compression molding, pultrusion have some limitations. Extrusion and injection molding are most widely used manufacturing processes in WPC due their effectiveness.

With regard to the characterizations then SEM, TEM, FTIR, and XRD are useful to characterize the WPC. Mechanical properties, physical properties, thermal properties testing can be applied to determine the performance of WPC. In addition to this, at nano stage, to study deformation behavior and the mechanical properties of composite becomes hard, because of the surface strain and surface flaws concentration might be introduced by manufactured tensile test specimen. The nanoindentation method is the most exact and propels technique to assess the effect of nanofillers on deformation behaviour and the mechanical properties of WPC.

This research aims to fabricate the wood-plastic from polypropylene, wood flour, MAPP coupling agent with Organoclay and pristine nanoclay which are highly economically viable. The pristine nanoclay is modified by The TMI (Transition Metal Ions) modification method which is simple, versatile and commercially scalable method. This nanoclay can be used to improve the various properties of WPC.

The logo for UMP (Universiti Malaysia Perlis) is a large, stylized letter 'V' shape. The left side of the 'V' is light blue, the right side is teal, and the bottom point is a darker blue. The letters 'UMP' are written in white, bold, sans-serif font across the center of the 'V'.

CHAPTER 3

METHODOLOGY

3.1 Introduction

This chapter compiles all the materials and methods used in this study. The grade of polymer, size of wood flour, type of coupling agent and nanoclay used during this research would be described in this chapter. In addition, the experimental work carried out in order to understand the effect of incorporation of nanofiller on the mechanical properties, physical properties, viscoelastic and thermal behaviour of wood-plastic composites would also be included to outline the designed experimental work.

3.2 Materials

During the preparation of wood-plastic composites, an industrial grade of thermoplastic polypropylene was used as the polymer matrix while Organoclay Cloisite® 20A and marketed montmorillonite clay (MMT) under the registered name Cloisite® Na⁺ were incorporated as nano scaled filler. The modification process was conducted using copper (II) chloride as a transition metal ion. Analytical grade methanol was used in the TMI modification process. The characteristics and the properties of the material used would be further explained in this section.

3.2.1 Polypropylene (PP)

In this work, a commercial grade of PP under the grade name G 112 which was supplied by Polypropylene Malaysia Sdn, Bhd (Malaysia). The physical and chemical features of PP are listed in Table 3.1.

Table 3.1 Physical and chemical properties of PP

Constituent	value
Physical state	solid
Appearance	granules
Colour	colourless
Odour	slight
Density (g/cm ³)	0.91
Melting point (°C)	166
Solubility in water	insoluble
Tensile strength (MPa)	33
Flexural strength (MPa)	1553

3.2.2 Wood flour (WF)

In this research work, freshly prepared Wood flour of *Koompassia malaccensis* supplied by Leong Seng, Sawmill, Gambang, Malaysia. As far as preparation is concern before compounding, firstly, the fresh wood flour was dried at 105 °C for 48 hours. The dried wood flour was then milled down to particle size of 40 mesh (400 micron). The sieved wood flour was kept in a container for subsequent use.

3.2.3 Maleic anhydride polypropylene (MAPP)

In this study, MAPP was used as a coupling agent with trade name Polybond 3200, which was supplied by Chemtura, China. The physical and chemical features of MAPP are listed in Table 3.2.

Table 3.2 Physical and chemical properties of MAPP

Constituent	value
Physical state	solid
Appearance	granules
Colour	colourless
Odour	slight
Density (g/cm ³)	0.90
Melting point (°C)	156
Solubility in water	insoluble
Tensile strength (MPa)	22
Flexural strength (MPa)	880

UMP

3.2.4 Cloisite® 20A

In this study, Cloisite® 20A organoclay was used as one of the nanofiller. It is organically modified nanoclay used as an additive for plastics composites to improve various physical and mechanical properties. The organoclay was supplied by Southern Clay Products (Rockwood additives, Ltd). The physical and the chemical traits of the organoclay are listed in Table 3.3.

Table 3.3 Physical and chemical properties of organoclay

Constituent	value
Commercial name	Cloisite® 20A
Physical state	solid
Form	powder
Colour	off white
Density (g/cc)	1.77
Organic modifier	Dimethyl, dehydrogenated tallow, quaternary ammonium (2M2HT)
X-ray data (Å)	$d_{001} = 24.2$
Cation exchange capacity (meq/100g)	95

3.2.5 Cloisite Na⁺

In this research, Cloisite Na⁺ was selected as the pristine nanoclay. It is a natural montmorillonite (MMT) used as an additive for plastics to improve various properties such as reinforcement and barrier. The MMT was supplied by Southern Clay Products (Rockwood additives, Ltd). The physical and the chemical traits of the MMT clay are listed in Table 3.4.

Table 3.4 Physical and chemical properties of montmorillonite

Constituent	value
Commercial name	Cloisite® Na ⁺
Physical state	solid
Form	powder
Colour	tan
Density (g/cc)	1.77
Moisture (wt%)	4-9
X-ray data (Å)	d ₀₀₁ = 11.7
Odour	mild

3.2.6 Copper (II) chloride

In this research, Copper (II) Chloride was used in the modification process of the pristine MMT clay via ion exchange method and it was purchased from Fisher Scientific (M) Sdn. Bhd. The physical and chemical properties of Copper (II) Chloride are laid out in Tables 3.5.

Table 3.5 Physical and chemical properties of Copper (II) chloride

Constituent	value
Physical state	liquid
Molecular formula	CuCl ₂
Form	crystalline powder
Colour	brown
Relative density (g/cm ³ at 20° C)	3,386
Melting point (°C)	620
Boiling point (°C)	993
Molecular weight (g/mol)	134.45

3.2.7 Methanol

In the modification process of the montmorillonite clay, methanol was used as the solvent and it was supplied by Fisher Scientific (M) Sdn. Bhd. The chemical and the physical properties of methanol are contained in Table 3.6.

Table 3.6 Physical and chemical properties of methanol

Constituent	value
Physical state	liquid
Molecular formula	CH ₃ OH
Odour	mild
Colour	clear
Vapour pressure (mmHg at 20° C)	128
Melting point at 101.3 kpa (°C)	64.7
Boiling point (°C)	99.3
Molecular weight (g/mol)	32.04

3.2.8 Sodium chloride

In the modification process of the montmorillonite clay, sodium chloride was used as the solution to ensure the removal of exchangeable ion contaminants from pristine nanoclay and it was supplied by Fisher Scientific (M) Sdn. Bhd. The chemical and the physical properties of methanol are contained in Table 3.7.

Table 3.7 Physical and chemical properties of sodium chloride

Constituent	value
Physical state	liquid
Molecular formula	NaCl
Odour	odourless
Colour	colourless
Density (g/cm ³)	2.16
Melting point (°C)	801
Boiling point (°C)	1,413
Molecular weight (g/mol ⁻¹)	58.44

3.3 Methods

3.3.1 Montmorillonite (MMT) clay modification using Transition Metal Ion

In this research, one of the main objectives that were given much emphasis was the modification of the MMT nanoclay through ion exchange process using transition metal ion. This step was taken to ensure the homogeneous dispersion of the clay into the polymer matrix. The experimental works of the modification process are explained in a two steps process as following.

3.3.1.1 Pre-treatment of MMT Clay

At the initial stage of modification, the nanoclay sample was thoroughly washed with methanol in order to remove the excess surfactants and the impurities in it.

Initially, the clay sample was added into methanol which was the solvent in this process at a ratio of 2g of clay to 40 ml of methanol and the clay suspension was stirred vigorously for 24 hours under room temperature (Nawani et al., 2007). It was noticed that the nanoclay started swelling during the stirring process resulting in a viscous slurry solution later on. The slurry was kept in 1 M NaCl solution for 48 h to ensure the removal of exchangeable ion contaminants. The slurry was then filtered and dried in vacuum oven for 12 hours at 80 °C. The pore size of filter paper was 11 µm.

3.3.1.2 Preparation of TMI solution and Modification

Followed to the pre-treatment process, the washed and dried samples of clay were placed in 0.30M of the desired metal ion salt using the same solvent in the washing process for the ion exchange to occur. Copper chloride was employed as a metal ion in this study. The required weight of the material to produce 1600 ml of the TMI solution with 0.3M was 64.52 gram.

In the TMI-modification process, 80g of pre-treated nanoclay was used for 1600ml of the metal ion solution. Initially, the required amount of the salt and the pre-treated nanoclay was added into methanol and the solution was stirred for 36 hours (Nawani et al., 2007) at room temperature. The nanoclay suspension was kept in a closed container as a preventive measurement to solvent evaporation. The nanoclay samples were then filtered washed and, dried for 12 hours at 80 °C in a vacuum oven after the TMI treatment. Pestle and mortar were used to make powder of dried nanoclay samples.

3.4 Characterization of TMI-modified MMT nanoclay

3.4.1 Field Emission Scanning Electron Microscopy (FESEM) and Energy Dispersion X-ray analysis (EDX)

In this study, Field emission scanning electron microscopy (FESEM) and energy dispersion x-ray analysis (EDX) were used to analyze the modification process. Field emission scanning electron microscopy (FESEM) was engaged in this study to

understand the distribution of the nanoclay particles and to check the size of nanoclay particles after modification process. Before observation the samples were coated with gold by a vacuum sputter. The presence of the copper ions and elemental composition of modified Cloisite Na⁺ were confirmed using energy dispersion x-ray analysis (EDX). In addition, EDX was employed to trace metals in the TMI-modified nanoclay to ensure that the ion exchange has occurred successfully during the modification process.

3.5 Fabrication of Nanoclay-based Wood-Plastic Composites

After a successful TMI modification process, the wood-plastic composites were prepared by using polypropylene, wood flour, Maleic anhydride grafted polypropylene (MAPP), Organoclay/MMT/TMI-modified nanoclay. The stages involved in the composite fabrication process are as described below:

3.5.1 Mixing

Mixing of polymer matrix, wood flour, MAPP and different types of nanoclay in the various formulations were all done manually. The desired weight (wt%) of each component was weighed out on a laboratory four digits analytical balance. These were mixed together accordingly as shown in Tables 3.8. WF and MAPP content was kept as a constant in the composite. The reason behind this, the low content of WF is easy to process during the compounding. In addition, the high concentration of WF creates agglomerates, which restricts the stress transfer between WF and polymer matrix (Guo et al., 2012). On the other hand, the excess amount of a coupling agent acts as an inhibitor rather than a promoter of adhesion (Lu et al., 2000). This is attributed to the plasticization effect of coupling agent. It is difficult to obtain better dispersion of coupling agent at high loading and thus resulted in poor mechanical properties.

Table 3.8 The composition of designed formulations

Samples	Polypropylene (wt.%)	Wood flour (wt.%)	MAPP (wt.%)	Nanoclay
PP	100	0	0	0
WPC	78	20	2	0
WPC-1	77	20	2	1
WPC-2.5	75.5	20	2	2.5
WPC-4	74	20	2	4
WPC-5	73	20	2	5

3.5.2 Extrusion

For the extrusion process, a single screw extruder (Brabender GmbH & Co. KG, Germany) was used. The extruder was initially set at a temperature of around 300 °C in order to burn out all left over materials after which the temperature was set at the required operating condition and purging was carried out using pure PP so as to avoid contamination with other materials. During the extrusion process, the compounding was done based on the mixing formulations as listed above and as shown in Tables 3.8. The mixed formulations were compounded in a four temperature zone extrusion process in order to obtain a homogenous mixture of the materials with the help of the counter rotating effect of the single screw extruder moving at a speed range of 50 rpm. To overcome void formation, all materials were initially dried at 80 °C for 24 h prior to extrusion. The processing temperature parameter for the extrusion process is as shown in Table 3.9.

Table 3.9 Temperature parameter for extrusion of wood-plastic composites

Zone	Temperature profile
Feed zone	190 °C
Melting zone	185 °C, 180 °C
Die zone	170 °C

3.5.3 Pelletizing

Pelletizing was carried out simultaneously with the extrusion process, with a fixed length pelletizing machine. This was done in a speed of 3 rpm to obtain pellets of about 3 mm length which is needed to be fed into the barrel of the injection molding machine.

3.5.4 Injection Molding

Around 3 mm length uniform pellets from the pelletizing machine were further dried at 80 °C in for 24 h in preparation for injection molding so as to make them moisture free. Injection molding was done with the help of injection molding machine (model- DR BOY 22M). Test sample were prepared according to ASTM D638-IV as shown in Figure 3.1. The cooling time was 20 seconds, clamping pressure was 160 bars, injection pressure was 100 bars and plasticizing back pressure was 5 bars. The operating temperature parameter for the injection molding stage is as shown in Table 3.10.

Table 3.10 Temperature parameter for injection molding of wood-plastic composites

Zone	Temperature profile
Feed zone	190 °C
Melting zone	185 °C, 180 °C
Nozzle	170 °C



Figure 3.1 Injection molded dumbbell shaped samples

3.6 Characterization of Wood-Plastic Composites

This section would be dedicated for describing the characterization techniques used in order to understand the structural and morphological behaviour of the wood-plastic composites. The characterization of the composites was engaged using Scanning Electron Microscopy (SEM), Transmission Electron Microscopy (TEM), X-Ray Diffraction (XRD), and Transform Infrared (FTIR).

3.6.1 Scanning Electron Microscopy (SEM)

In this study, SEM was used to determine the distribution of nanoclay particles and compatibility between the fillers and the matrix in the composites. The samples were prepared by cutting a small piece from the fracture tensile samples of wood-plastic composites and these small pieces of composites were placed on a specimen holder and it was coated with platinum particles using BALTEC SCD 005 Sputter Coater. The coating was done to provide conductivity, protecting the samples from the beam damage and to eliminate charging issues. Once the sample had been coated successfully,

it was attached to stub and transferred to the SEM chamber for the analysis. SEM was performed in a ZEISS EVO 50 Scanning Electron Microscope. The setup parameters that were used in this analysis are shown in Table 3.11

Table 3.11 Parameters used in SEM analysis

Parameters	ranges
EHT	5-10 kv
I probe	80 pA
WD	10 mm
Magnification	200x – 500x

3.6.2 Transmission Electron Microscope (TEM)

In this research, TEM analysis was employed with scale bar of 100 nm to study the distribution of nanoclay insight the composites. Wood-plastic composites samples powder was used for TEM analysis. Composites powder was mixed in water and then placed on 400mesh copper grids. The analysis was conducted using a ZEISS LIBRA 120 instrument with 120 kv accelerating voltage.

3.6.3 X-Ray Diffraction (XRD)

In this study, Rigaku Miniflex II (Japan) X-Ray Diffractometer is used to analyze the structure of the TMI-modified nanoclay and wood-plastic composites samples. Before analysis WPCs samples were powdered using grinder and dried in oven at 105 °C for 2 hours. The tube current of the X-ray generator and the working voltage were 15 mA and 30 kV, respectively. The XRD pattern of modified nanoclay WPCs samples was obtained ($\lambda = 0.15406$ radiation choke nm) at room temperature. The extent of intercalation that has occurred in the composites was determined by measuring the inter-gallery spacing, d_{001} that existed between the monomer chain and the layered silicates. The diffractograms obtained in the 2θ range of 3-20° at a rate of 1°/min.

The d-spacing (d) of the interlayer gallery of the MMT, TMI modified MMT and the nanoclay based wood-plastic composites was calculated using Bragg's Law equation.

$$n\lambda = 2d \sin\theta \quad (3.1)$$

Where:

d = Space between layers of the clay

λ = Wavelength of the X-ray which is

θ = Angle at the maximum point of the first peak into a spectrum

n = Order of diffraction

3.6.4 Fourier Transform Infrared (FTIR)

In this study, FTIR analysis was used to examine the structural and functional groups present into the nanoclay based wood-plastic composites. This functional group analysis was carried out by Perkin Elmer spectrum 100 Model of Fourier transforms infrared spectrophotometer using the standard KBr technique. As far as preparation is concerned then, samples were first mixed with KBr 1 to 100 % by weight ratio and formed as pellets. Formed pellets were scanned on FTIR spectrometer. The averages of more than 50 scans were taken at 2 cm^{-1} resolution in the wavelength range of $4000 - 0 \text{ cm}^{-1}$.

3.7 Properties of Wood-Plastic Composites

Sub sequential to the structural and morphological study, the wood-plastic composites samples are then tested in order to analyse and understand the advancement in their properties over control sample (WPC without nanoclay) and neat polypropylene. In this segment of the thesis, the testing methods that assisted in studying the mechanical, physical and thermal studies of the wood-plastic composites are discussed.

3.7.1 Mechanical Properties Testing

In this work, the mechanical properties testing that were done on the wood-plastic composites samples were tensile, flexural and impact testing whereby three mechanical properties were obtained from tensile testing which were the tensile

strength, tensile modulus and elongation at break. Flexural strength and flexural modulus were obtained from flexural testing and impact strength from impact testing.

3.7.1.1 Tensile Testing of Composites

Tensile test samples were prepared according to ASTM 638-08: Standard Test Method for Tensile Properties of Plastics. Tensile testing was carried out using an Instron universal testing machine (model-3369) with load cell of 5 KN at a crosshead speed of 5 mm/min. 65 mm gauge length was used for testing. All the reported values for the tests were the average values of 5 specimens. The tensile strength of composite sample was calculated from the maximum load (F_{max} in N) and cross sectional area (m^2) as follows:

$$\sigma_t = \frac{F_{max}}{A} \quad (3.2)$$

Where, A = cross sectional area (m^2), F_{max} = Maximum (peak) load.

Percentage elongation which defines the percentage increase in length of test specimen at its breaking point was also calculated for each test sample using the following relation:

$$\% \text{ Elongation} = \frac{L - L_o}{L_o} \times 100 \quad (3.3)$$

Where, L_o and L are the initial measured length (m) and length at breaking point (m) of test sample respectively.

3.7.1.2 Flexural Testing of Composites

Flexural testing otherwise referred to as 3 point bending test was carried out to determine the force required to bend the composites sample under a 3 point loading, as well as its resistance to elastic deformation under an applied force (flexural modulus).

Flexural testing was carried out in line with ASTM D790-97 standard using an Instron universal testing machine (model- 3369) with static load cell of 5 KN. The dimensions of test sample were 65 mm x 3.4 mm x 10 mm and cross head speed was set at 5 mm/min with support kept at 50 mm apart. Testing was done at room temperature. Flexural strength can be calculated using the relation below:

$$\sigma = \frac{3 FL}{2 b d^2} \quad (3.4)$$

Where, F = Load (Force) at fracture point, L = length of support span, b = width of test sample and d = thickness of test sample.

The flexural modulus is given by the slope of the linear area of the stress-strain curve. It can however be calculated using the relation:

$$E_f = \frac{L^3 m}{4 b d^3} \quad (3.5)$$

Where, E_f = Flexural modulus (MPa), L = length of support span (mm), m = slope, b = Width of test sample (mm) and d = Depth of test sample (mm).

3.7.1.3 Izod Impact Testing of Composites

To fabricate high quality composite material, then impact resistance is the most essential property to consider. Materials have tendency to absorb applied forces and this tendency is based on the application, these could be drops, blows, falling things and collisions. The toughness of the material represents the impact properties of polymeric materials.

In this study, Impact testing was conducted according to ASTM D256 Plastics-Determination of Izod impact strength. Rectangular impact test samples were prepared using an injection moulding machine (model- DR BOY 22M) with dimension 55 mm x 3.3 mm x 10 mm. Testing was carried out using a Instron impact tester (model- CEAST

9050) with an impact velocity of 3.04 m/s and hammer weight of 0.168 kg. Average of five replicate samples were taken for each composite type to obtain the impact strength.

3.7.2 Physical properties

In this study, the physical properties analyses that were applied on the wood-plastic composites samples were density and wood absorption.

3.7.2.1 Density

Measurement of density was conducted according to ASTM D 792. Specimens were dried for 24 hrs at 105 °C. Five specimens were tested and their average values were reported. The value of the density was calculated using the following equation:

$$\rho = \frac{m_d}{V} \quad (3.6)$$

where ρ is the density, v is the volume and m_d is the dry of specimen.

3.7.2.2 Water Absorption

Water absorption analysis was carried out on injection moulded tensile bar sample of composites so as to study the moisture absorption capacity of composites reinforced with Organoclay, MMT and TMI-modified MMT. In addition, to examine the effect of different types of nanoclay on water absorption capacity of composites. The water absorption (WA) test was conducted in accordance with ASTM D 570. The weight of each specimen was measured before testing and conditioned samples of each composite type were soaked in distilled water at room temperature for 15 and 30 days. Samples were removed from the water, patted dry and then measured again. Each value obtained represented the average of 5 samples. The value of the water absorption in percentage was calculated using the following equation:

$$WA(t) = \frac{W(t)-W_0}{W_0} \times 100 \quad (3.7)$$

where WA (t) is the water absorption (%) at time t, W₀ is the oven dried weight and W (t) is the weight of specimen at a given immersion time t.

3.7.3 Thermal Analysis

There were three types of thermal analysis done in this research to study the thermal effects of the incorporation of nanoclay into the wood-plastic composites. Thermal Gravimetric Analysis (TGA), and Differential Scanning Calorimetry (DSC) were used to study thermal behaviour of composites. The methods employed on these analyses are outlined in this section.

3.7.3.1 Thermal Gravimetric Analysis (TGA)

In this study, TGA analysis was employed to study the thermal behaviour of the wood-plastic composites using a Polymer Laboratories Thermogravimetric Analyzer (TA Instruments, model TAQ500). The equipment was calibrated prior to analysis and for each set of experiment, the pan was cleaned to remove any impurities or residues. Powdered particle samples of approximately 5mg was prepared from the wood-plastic composites sample and the TGA analysis was performed at a ramp rate of 20 °C/min at a temperature range from 30 °C to 900 °C under the influence of nitrogen gas. The evaluation of the TGA curve was completed by using “STARe Excellence Software” of Mettler Toledo. In addition, TGA analysis was also used to ensure that the ion exchange has occurred successfully during the modification process.

3.7.3.2 Differential Scanning Calorimetry (DSC) Analysis

In this research study, differential scanning calorimeter (TA Instruments, model TA-Q1000) was used to determine the influence of nanoclay loading on the crystallization and melting behavior of the wood plastic composites as shown in Figure 3.6. Each sample was heated and cooled at a scanning rate of 10 °C/min under nitrogen atmosphere in order to prevent oxidation. A test sample of 4 to 5 mg was placed in an

aluminum capsule and heated from 20 to 200 °C for each run. The degree of crystallinity of the samples was calculated using the following equation

$$X_c \% = \Delta H_f / \Delta H_f^\circ \times 100, \quad (3.8)$$

where ΔH_f is the heat of fusion determined by DSC, and ΔH_f° is the heat of fusion of completely crystalline PP, which has the value 203 J/g (Lei, 2003).

3.7.4 Sub-surface Mechanical Properties studied by Nanoindentation

In this study, a completely calibrated Nano Test (Micro Materials, Wrexham, UK) was used to perform all nanoindentation tests as depicted in Figure 3.2. Three sided pyramidal based a Berkovich diamond indenter tip was used in this test. Using a suitable adhesive a 1cm×1cm×1000µm catted specimen mounted onto the nanoindentation sample stub and all tests were performed at room temperature. The experimental indentation parameters were same for all measurements. The typical parameters are as follows;

Initial load : 0.10 mN

Maximum load for all indents : 10 mN

Loading and unloading rate (strain rate): 0.50 mN/s

Dwelling time or holding time at maximum load : 180 s

The distance between two indentation points was 30 µm, to avoid the overlapping problem. Average values were obtained from the measurements of 10 indentations.

The hardness and elastic modulus as well as properties like scratch, creep, and residual stress of material are generally measured by nanoindentation test. In nanoindentation testing indenter tip is used to penetrate a material. Force and displacement are measured during performing the typical nanoindentation test. The mechanical properties of the composite or material are generally reflected by variation of load displacement. In this test, Oliver and Pharr method (Oliver and Pharr, 1992) was

used to calculate the hardness and elastic modulus of composite. Ten indentations were performed on each sample of the composite to obtain average values.

Oliver and Pharr method were used to determine the hardness (H) and elastic modulus (E) of composite samples with the help of load displacement information or data. The elastic and plastic deformation of samples occurs when the indenter tip enters into the sample but during unloading of indenter only the elastic portion of the displacement is recovered. Hardness of nanoindentation test is derived as:

$$H = \frac{P_{max}}{A}, \quad (3.9)$$

Where P_{max} is the load measured at peak depth of penetration (h) in an indentation; A is the projected area. For an ideal Berkovich indenter, $A = 24.5h^2$.

The unloading curve information can be used to derive the reduced modulus of the sample. A relationship expressed in the following equation:

$$E_r = \frac{\sqrt{\pi}}{2} \frac{S_{max}}{\sqrt{2}} \quad (3.10)$$

Where E_r is decreased elastic modulus and S_{max} represent the slope of unloading curve at the point of maximum load.

The relationship between reduced modulus, E_r and elastic modulus, E_s , is shown in the following equation (Oliver and Pharr, 1992):

$$\frac{1}{E_r} = \frac{(1-\nu_s)^2}{E_s} + \frac{(1-\nu_i)^2}{E_i} \quad (3.11)$$

where E and ν with subscripts 's' and 'i' are the elastic modulus and Poisson's ratios of the material and the indenter, respectively. E_i is the modulus of the indenter (1141 GPa).

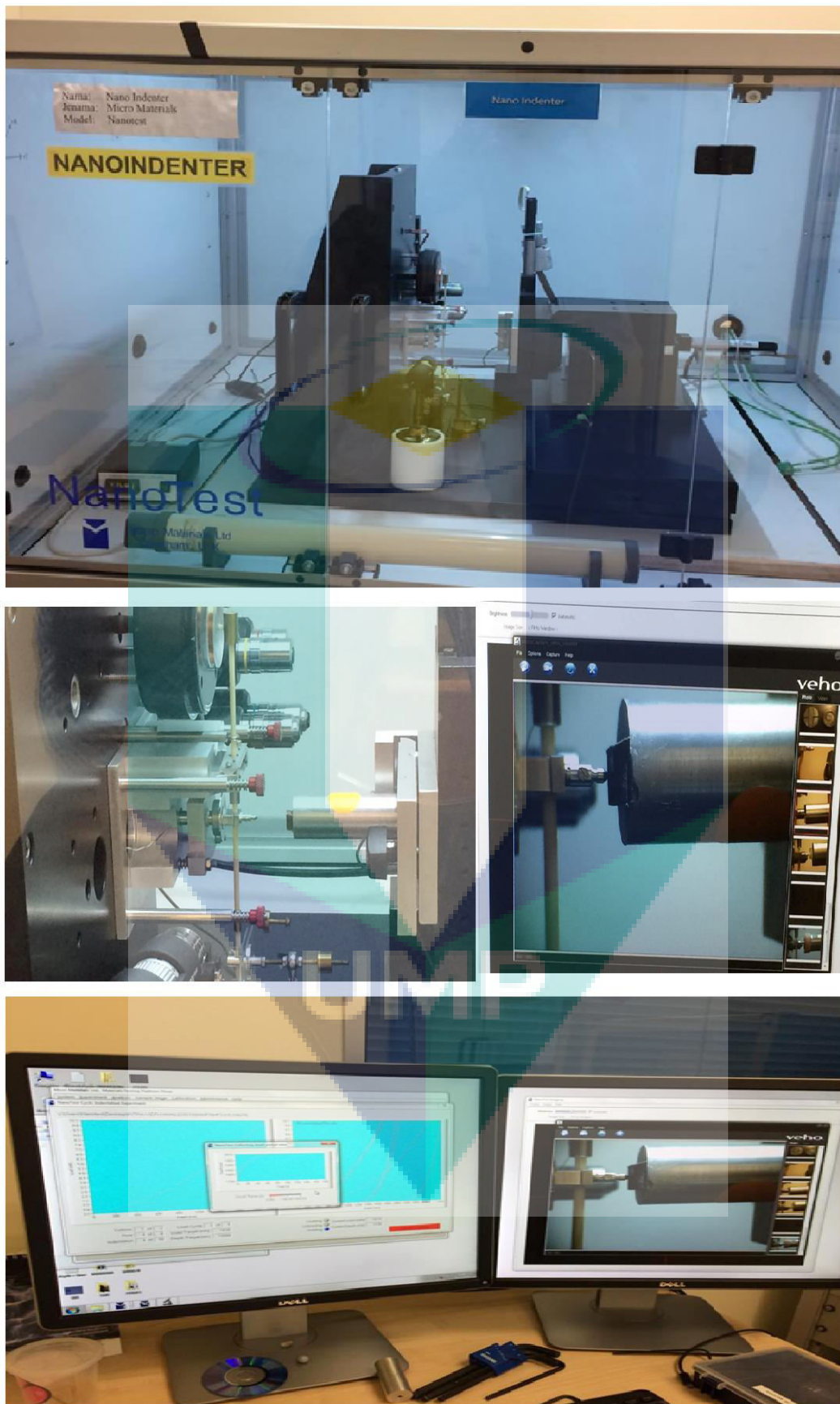


Figure 3.2 NanoTest nanoindenter

3.7.5 Creep Test studied by Nanoindentation

In this research, the Nano Test system (Micro Materials, UK) was used to determine the viscoelastic creep behaviour of the wood-plastic composite. In this system electromagnetic load was applied on the horizontally mounted sample employing a pendulum-based depth-sensing system and the measurements were achieved. The initial and maximum loads of the test were 0.10 and 10mN respectively. Until the indenter tip reached the maximum depth into the composite surface, a 0.50mN/s loading rate was maintained during the incremental increase. To obtain the creep effect of composite, the load was held for 180s before the intender was unloaded. To avoid overlapping of indentation, 30 μm was kept between the indentations. The nanoindentation creep experiment process is shown in Figure 3.3.

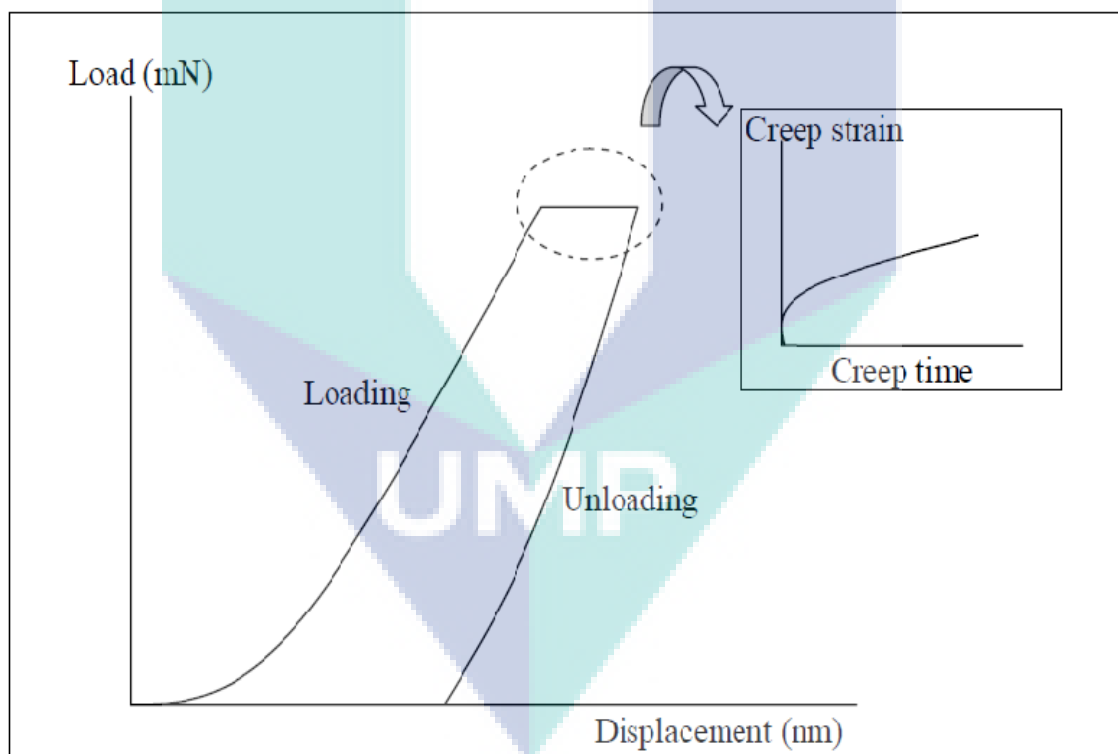


Figure 3.3 Nanoindentation creep experiment schematic diagram

Source: Yusoh (2010).

3.8 Optimization of TMI-modified based Wood-Plastic Composite by Response Surface Methodology (RSM)

3.8.1 Fractional Factorial Design-Screening of Process Parameters

The Design expert software (D \times 7) was used for statistical experimental design and data analysis. Polypropylene content, nanoclay content, wood flour size, extruder die temperature, and extruder screw speed were screened by 2^{5-1} fractional factorial designs (FFD), whereas tensile strength of composites was taken as a response (Javier et al., 2015). The ranges of these parameters were decided from the previous studies, dealing with fabrication wood-plastic composites (Mathuna and Li, 2004a). Screening process of wood-plastic composites parameters was performed between Polypropylene content (73 to 78 wt%), nanoclay content (1 to 5 wt%), wood flour size (400 to 250 μ), extruder die temperature (170 to 190 $^{\circ}$ C), and extruder screw speed (50 to 80 rpm) according to the fractional factorial design generated by Design Expert (D \times 7) software. As per FFD software, total of 16 experiments were performed. All the variables were analysed for their direct as well as interactive influence on tensile strength of wood-plastic composites. The table 3.12 summarizes factors and their ranges and Table 3.13 summarize the experimental design.

Table 3.12 Factors and respected ranges decided for the screening experiment

Factors	Unit	Minimum	Maximum
Polypropylene content	Wt%	73	78
Nanoclay content	Wt%	1	5
Wood flour particle size	μ	250	400
Extruder die temperature	Celsius	170	190
Extruder screw speed	RPM	50	80

Table 3.13 Experimental design for screening

Run	Polypropylene content (%)	Nanoclay content (%)	Wood flour particle size (μ)	Die temperature ($^{\circ}$ C)	Screw speed (rpm)	Response [Tensile strength (MPa)]
1	73.00	1.00	400	170.00	80.00	
2	73.00	5.00	250	190.00	50.00	
3	73.00	1.00	250	190.00	80.00	
4	78.00	1.00	250	170.00	80.00	
5	78.00	5.00	250	170.00	50.00	
6	78.00	5.00	400	190.00	50.00	
7	73.00	5.00	400	170.00	50.00	
8	73.00	1.00	400	190.00	50.00	
9	78.00	1.00	400	190.00	80.00	
10	78.00	5.00	400	170.00	80.00	
11	78.00	5.00	250	190.00	80.00	
12	73.00	5.00	250	170.00	80.00	
13	73.00	5.00	400	190.00	80.00	
14	73.00	1.00	250	170.00	50.00	
15	78.00	1.00	400	170.00	50.00	
16	78.00	1.00	60	190.00	50.00	

3.8.2 Experimental Design and Optimization

In this research, central composite design (CCD) was applied to determine the optimum range of parameters for high tensile strength of woo-plastic composites. All five parameters studied in screening experiment, and among five parameters two showed high influence on tensile strength. Polypropylene content and nanoclay content exhibited high contribution for tensile strength among other parameters. Thus, polypropylene content and nanoclay content were considered for optimization process. Based on the screening result, a new range of parameters were prepared for CCD and it is summarized in table 3.14. In this study, total 13 experiments were performed. The quadratic model for two factors obtained, can be expressed as:

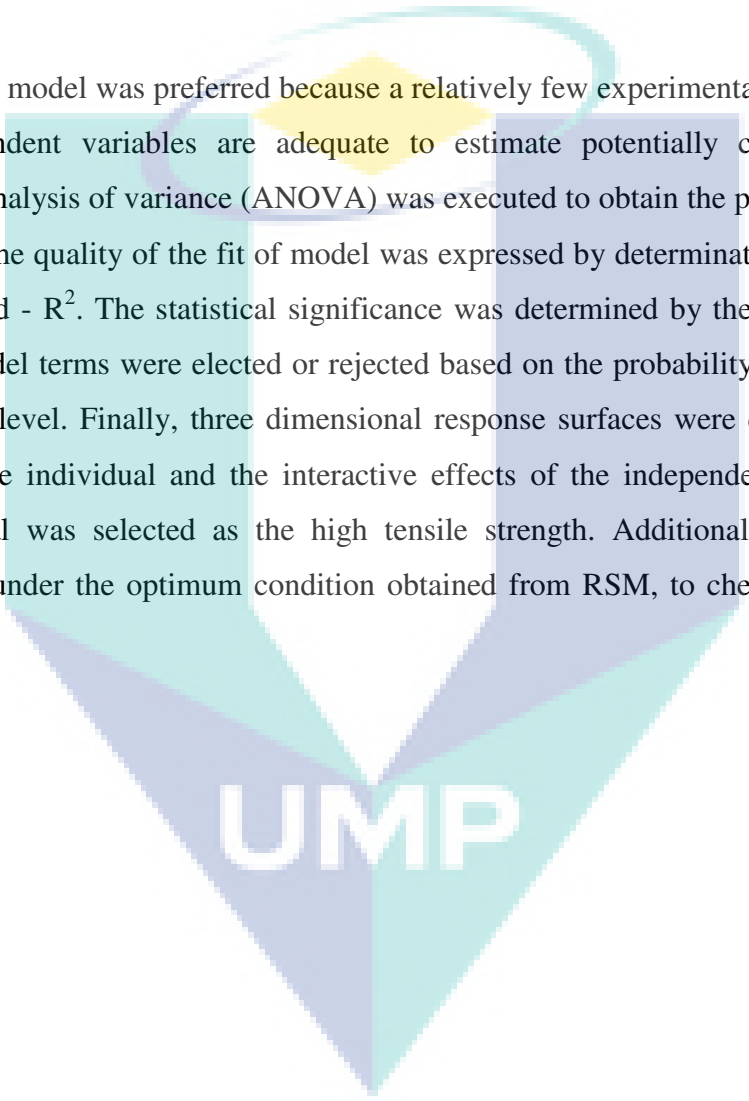
$$y_2 = b_0 + b_1 X_1 + b_2 X_2 + b_{11} X_{11}^2 + b_{22} X_{22}^2 + b_{12} X_{12}^2 \quad (3.12)$$

Where y_2 is the measured response, b_0 is the intercept coefficient, b_{1-2} is a linear coefficient, b_{11-22} is a quadratic coefficient, b_{12} logarithmic coefficient, and x_{1-2} is independent variables.

Table 3.14 Factors and respected ranges decided for the central composite design

Parameters	Units	Actual		Coded	
		Low	High	Low	High
Polypropylene content	Wt%	71	75	-1	1
Nanoclay content	Wt%	0	2	-1	1

This model was preferred because a relatively few experimental combinations of the independent variables are adequate to estimate potentially complex response function. Analysis of variance (ANOVA) was executed to obtain the process factors and response. The quality of the fit of model was expressed by determination coefficient R^2 and adjusted - R^2 . The statistical significance was determined by the F- values and p-values. Model terms were elected or rejected based on the probability values with 95% confidence level. Finally, three dimensional response surfaces were drawn in order to visualize the individual and the interactive effects of the independent variables. The desired goal was selected as the high tensile strength. Additional three runs were performed under the optimum condition obtained from RSM, to check the validity of the model.



CHAPTER 4

RESULTS AND DISCUSSION

4.1 Introduction

This chapter discusses the results obtained from analysis and tests based on Chapter 3. The effectiveness of the organoclay (C20) and TMI-modified nanoclay on the properties of the wood-plastic composites is to be discussed and reviewed in this section. The morphological and structural studies through FESEM-EDX, SEM, TEM, FTIR and XRD are discussed. This chapter is further expanded to the effects of the C 20 organoclay, pristine and modified montmorillonite on the mechanical, physical, thermal and subsurface mechanical properties of the wood-plastic composite.

4.2 Wood-Plastic Composites reinforced by organoclay

This section discusses the structural and morphological analysis of wood-plastic composite reinforced by C20 organoclay. This is segment further extended to the reinforcing effect of C20 organoclay on the different properties of wood-plastic composite.

4.2.1 Characterization of Wood-Plastic Composite reinforced by organoclay

4.2.1.1 Morphological Characterizations

Figure 4.1 shows the Scanning Electron Microscopy (SEM) micrographs of the tensile fracture surfaces of the composite reinforced by C20 organoclay. The significant

improvements in mechanical properties of the composites with incorporation of nanoclay can be supported by SEM micrographs.

The SEM micrographs of the tensile fracture surfaces represents, the distribution and compatibility between the fillers and the matrix. Figure 4.1a corresponds to WPC without C20 Organoclay. As can be seen, there is poor adhesion area, cavity and wood flour particles pull-out; therefore, when stress is applied it causes the gaping holes. This was attributed to the hydrophilic nature of the wood flour particles and its weak homogeneity in the polymer matrix. It could be informed that the interfacial adhesion between the WF and the PP matrix in the composite was poor. Figure 4.1b and c shows fewer holes, cracks, and cavities as compared to WPC sample without nanoclay. Micrographs 4.1b and c corresponds to the WPC containing 1 and 2.5 wt% organoclay, respectively. It suggests that the nanoparticles and matrix were thoroughly mixed. As can be seen in Fig. 4.1b and c there is no separation of the WF particles from the matrix and there was a very good interaction between the components and it can be inferred from the images. The strong adhesion is observed at the interface of the composite. The reason might be due to the well dispersion of organoclay particles into the composite.

As can be seen from Figure 4.1d and e, the composite filled with 4 and 5 wt% C20 organoclay had many holes and cavities remained after the fillers were pulled out of the matrix. Figure 4.1d and 4.1e show the micrographs of WPC at low magnification (200 X). The presence of these holes means that the interfacial bonding between the filler and the matrix polymer is weak and therefore the organoclay could not provide an efficient stress transfer from the matrix. As shown in Figure 4.1f and g, high content of C20 organoclay were easily agglomerated, which is the characteristic of these nanofiller. Figure 4.1f and g show the micrographs of WPC that was loaded with 4 and 5 wt% organoclay at high magnification (500 X). It can be seen clearly from Figure 4.1f and g, the agglomeration of organoclay particles. These aggregates may be related to poor distribution of the nanoclay in the matrix as nanoclay is known to have a very high tendency to agglomerate during the fabrication process due to its lamellae structure (Yapar, 2009). The distinct sphere or large white spot into the composite showed the nanoclay agglomeration. The agglomerates create voids between the polymer matrix and the filler. Thus composite filled with lower content of organoclay showed higher

mechanical properties than composite filled with higher content of organoclay. Hence the formation of voids into the composite reduces the mechanical properties of composite.

Nanoclay has absorption property and it is an absorbent of the coupling agent (Yeh and Gupta 2010). Thus higher content of nanoclay in the composite will increase the coupling agent absorption. In such a case, due to the insufficient coupling agent the composite does not obtain appropriate bonding between the polymer matrix and the lignocellulosic materials. As can be seen from Figure 4.1 d to g, the composite loaded with 4 and 5 wt% organoclay shows the larger nanoclay particles on the fracture area. This is the indication of poor interaction between wood flour and the polypropylene matrix. The comparison between high contain organoclay composite and low contain organoclay composite then the less and smaller pores were seen in composite containing low (1 and 2.5 wt%) organoclay (Figure 4.1 b and c). It means less amount of nanoclay creates more appropriate interaction between polymer matrix and the lignocellulosic material.

Microstructure study of composite determines the mechanical and physical properties of the composites (Naeemian, 2008). However, higher loading (4 and 5 wt%) of nanoclay into the composite will reduce tensile/flexural strength by creating large number of pores, cracks because of the absorbent of the coupling agent. While studying the morphology of polypropylene/lignocellulosic fibers/nanoclay composite by SEM photography Fink et al. 2000 and Huda et al. 2006, found similar results in their work.

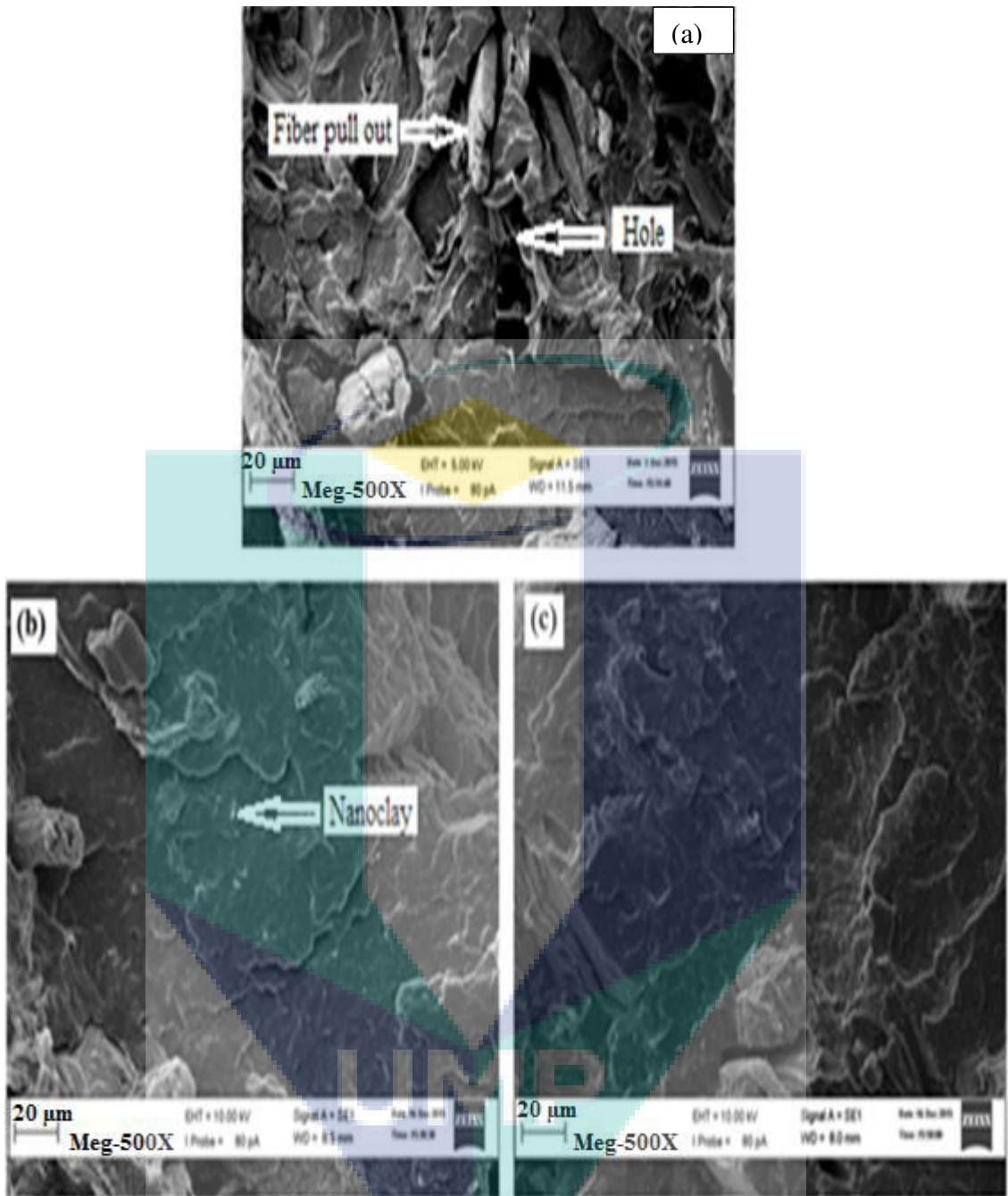
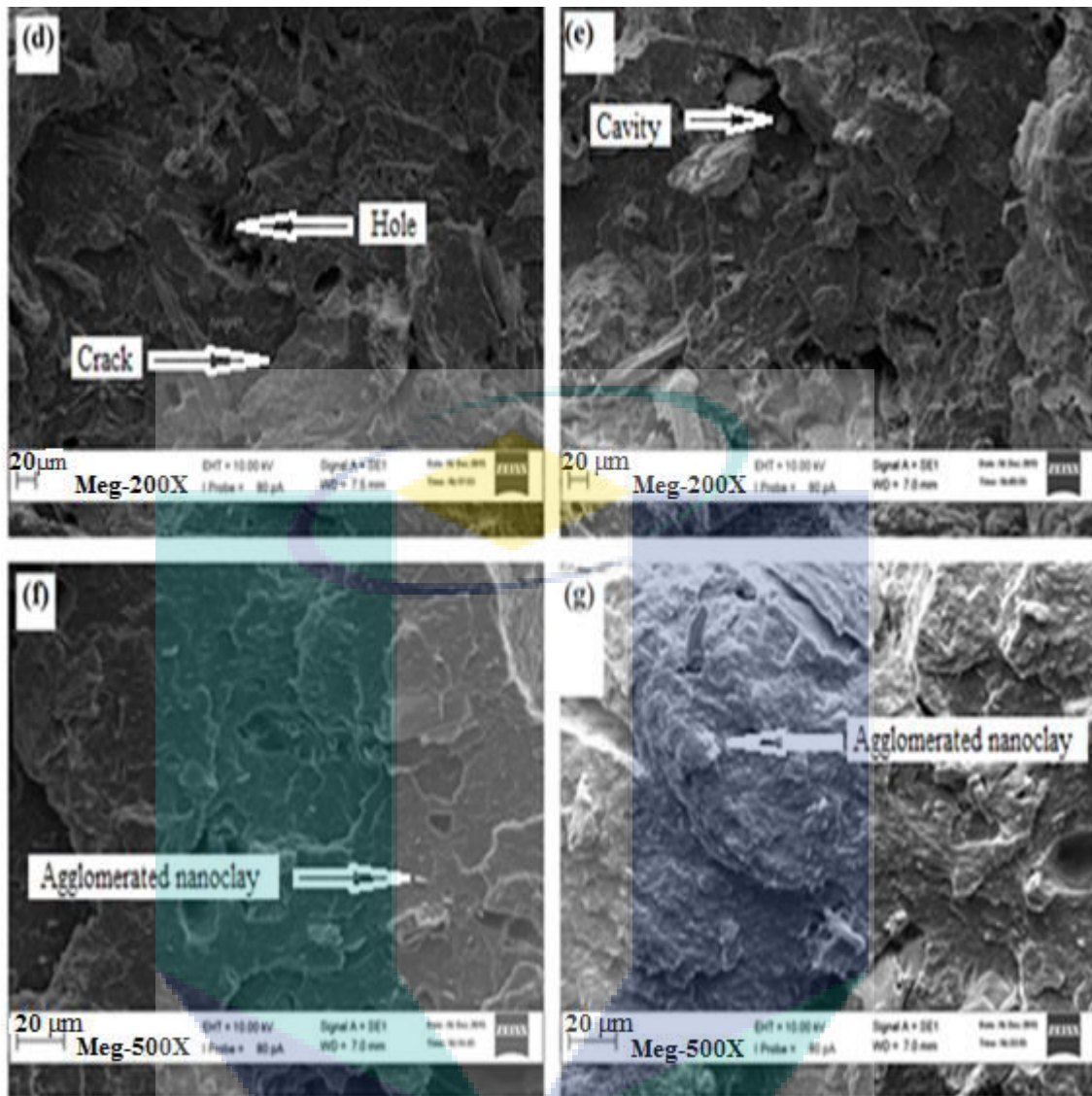


Figure 4.1 SEM micrographs of fractures samples of WPC: (a) without C20 (control), (b) with 1wt. %, C20, (c) with 2.5 wt. %, C20,



and (d) with 4 wt. %, C20 (200 X), (e) with 5 wt. %, C20 (200 X), (f) with 4 wt. %, C20 (500 X), (g) with 5 wt. %, C20 (500 X)

SEM analysis was applied to understand the distribution of nanoclay particles in the polymer matrix. Transmission electron microscopy (TEM) has a more intensive and monochromatic electron beam that create a lesser cross over diameter. This smaller cross over in TEM which is the point at which the electrons are focused when leaving the electron gun as it gives smaller final electron spot thus creating higher resolution. In this study, TEM was conducted to observe more detail structure of nanoclay particles distribution in the composite and to support the SEM analysis.

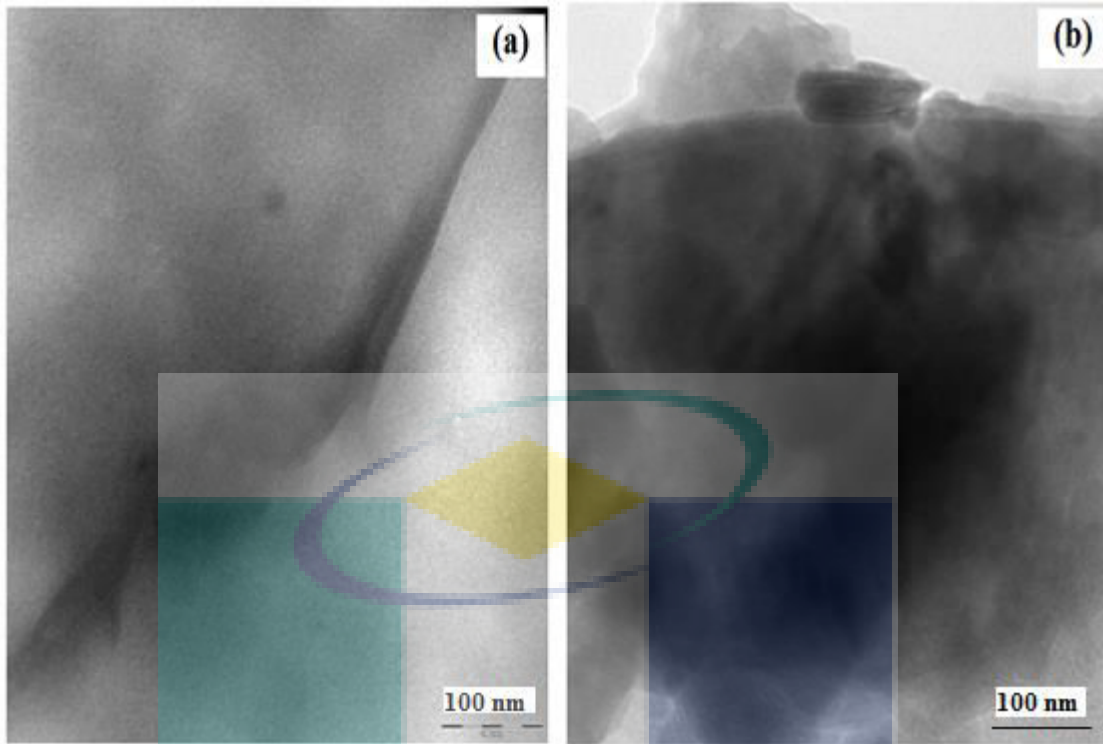


Figure 4.2 TEM micrographs of WPC with (a) 1 wt% C20, (b) 5 wt% C20 (100 nm scale)

Figure 4.2 (a) and (b) show the TEM micrograph of wood-plastic composite with 1 and 5 wt% C20 organoclay. In these micrographs, filamentary dark lines are related to intersection of silicate layers and the light regions correspond to the polymer matrix. As can be seen from the figure 4.2 (a), the nanoclay shows better dispersion and intercalation of nanoclay with PP in the WPC when 1 wt% of nanoclay was loaded into the composite. However, as can be seen in Figure 4.2 (b) with the increase in the level of nanoclay loading to 5 wt%, the size of nanoclay particles became larger or aggregated and reduced the degree of intercalation. In other words at higher loading, organoclay agglomeration occurs and the applied load will be distributed unevenly between non-agglomerated and agglomerated organoclay. It will affect the mechanical properties of composite. Zhao et al., (2006) reported similar examination while investigating the mechanical properties of wood flour/polyvinyl chloride matrix/organoclay composite.

4.2.1.3 Structural Characterizations

In this study, Fourier Transform Infrared (FTIR) spectroscopy was employed to identify whether the C20 organoclay has been embedded in the WPC and chemically bonded to the polymer chains. PP, WPC and WPC with 1, 2.5, 4 and 5 wt% of C20 organoclay were investigated. The chemical changes that occurred upon the incorporation of organoclay into the composite are presented in Figure 4.3. The Infrared absorptions bands that are commonly seen in PP were observed in all six samples in all the four different percentages of the organoclay loading. The characteristic of broad peak that were observed at 3200-3460 cm^{-1} are attributed to the hydrogen bonded (O-H) and O-H stretched in the spectrum of the PP and WPC.

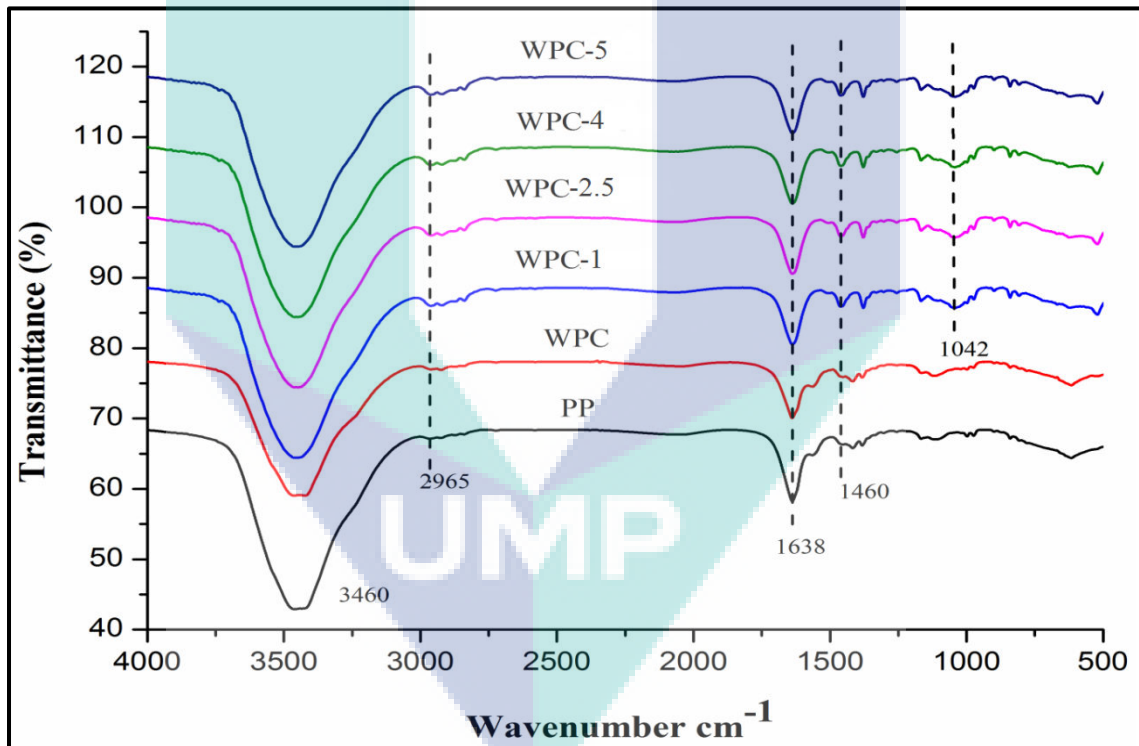


Figure 4.3 FTIR spectra of neat PP, WPC and WPC made with different C20 organoclay content

All composites displayed peaks at around 2850-3000 cm^{-1} . It is expected that these peaks are due to CH stretching, as CH is present in the chemical structures of PP and cellulose fibres stretching (Sgriccia et al., 2008). Similar observation was reported by Awal et al., (2009). The C=O stretching of the acetyl groups is believed to cause the peak

at around 1600-1730 cm^{-1} (Sgriccia et al., 2008). CH_2 bending vibration causes peaks around 1450-1460 cm^{-1} , this peaks are due to the nanoclay vibrations (Alhuthali et al., 2012).

It can be seen in Figure 4.3, WPC contains organoclay showing a peak arising between 1000 and 1110 cm^{-1} is due to Si-O stretching (Stark and Matuana, 2004). These Peaks are the indication of the presence of silica oxide (Si-O) bonds due to the incorporation of the nanoclay silicates in the WPC and this finding is in line with Frankowski et al., (2007). It is known that silica is the dominant constituent of nanoclay whereby it is present in the tetrahedral layer of the clay. The tentative assignments of the main absorption bands of the FTIR analysis are illustrated in Table 4.1.

Table 4.1 Tentative FTIR peaks Assignments of Wood-plastic composite with different content of C20 organoclay

Wavenumber (cm^{-1})	Assignment
3460	Hydrogen bonded (O-H)
2965	Stretching of C-H
1638	Free C= O
1460	CH_2 bending
1042	Bending of Si-O

It can be confirmed from the above visual observation that the layered silicates (Si-O) were able to disperse in WPC. The chemical bonding between the PP grafted onto the nanoparticles would certainly enhance the filler/matrix adhesion in the composite and contribute to its property enhancement.

The X-Ray Diffraction (XRD) analysis was employed in this work to characterize the structure of the samples by determining the interlayer spacing of the samples. The samples were scanned in fixed step size, 0.020 with a step-time of 0.1s in the range of 3-20° however the XRD graphs were plotted based from 0-30° due to the significance found at this point from the analysis. An XRD diffractogram with an intensity of 2 θ was obtained from the scans.

According to Bragg's Law, a decrease in the crystallite size causes an increase in the width of the diffraction and in very small crystallites, there are not enough planes to produce complete destructive interference which results in a broadened peak. Increasing d-spacing results in broadening and shifting the XRD peak towards the lower diffraction angle 2θ and vice versa. Figure 4.4 displays the data obtained from the XRD analysis for each type of samples with a diffraction angle from 3-20° whereas Table 4.2 summarizes the interlayer spaces of the PP, WPC, WPC with different content of C20 organoclay.

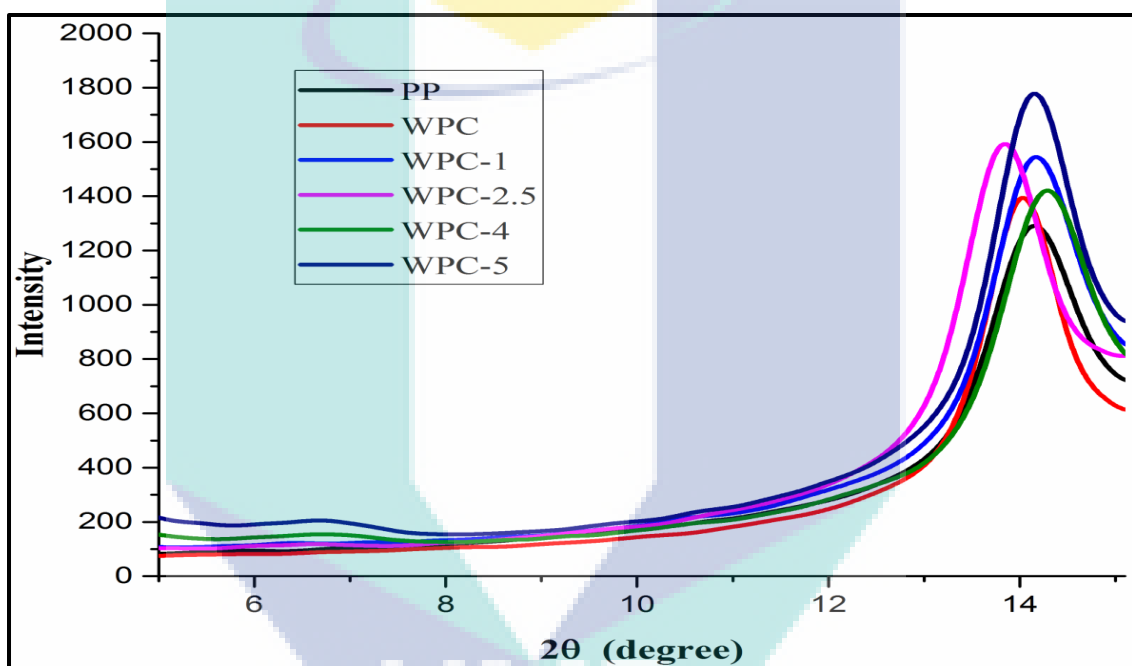


Figure 4.4 XRD diffractograms of neat PP, WPC and WPC made with different C20 organoclay content

From Figure 4.4, it can be noticed that the final structures of the wood-plastic composite were greatly influenced by the organoclay filler content. The structures of the wood-plastic composite incorporated with different concentrations of nanofiller showed a variety of changes in its angular spacing and reflection angle. The XRD pattern obtained were highly dependent on the quantity and the degree of dispersion of nanofiller. Bragg's law states that if nanoclay retains its original structure and the original d-spacing when incorporated into the polymer matrix, the position of the Bragg peak that corresponds to the d-spacing in the XRD diffractogram will remain unchanged whereas if the layered structure is maintained and the d-spacing increases, the Bragg

peak will be shifted to the lower value. The Bragg's peak disappears altogether when the layered structure is disrupted.

The data obtained from analysis has shown that neat PP possessed a visible peak at $2\theta = 14.08^\circ$ with an angular spacing $d = 6.28 \text{ \AA}$, whereas WPC without nanoclay shown a peak at $2\theta = 13.88^\circ$ with an angular spacing $d = 6.37 \text{ nm}$. The addition of wood flour with MAPP gave slightly wider peaks, indicating the improved compatibility of wood flour and PP matrix by adding MAPP and the enhancement of intercalation from the better shear action by adding wood flour during the compounding process (Lee et al., 2008). WPC with 1 wt%, 2.5 wt%, 4 wt% and 5 wt% showed characteristic diffraction peaks at $2\theta = 6.20^\circ$ (d-spacing is 14.23 \AA), $2\theta = 6.25^\circ$ (d-spacing = 14.14 \AA), $2\theta = 6.62^\circ$ (d-spacing is 13.60 \AA) and $2\theta = 6.63^\circ$ (d-spacing = 13.41 \AA) respectively. It can be observed from Figures 4.4 that there are two visible peaks in the XRD diffractograms for the samples with organoclay. The peaks rose at angle 2θ more than 10° are indications that the organoclay particles functioned as nucleating agents that induced the crystallization of the segments in PP. The peaks attained at angle 2θ less than 10° is useful in determining the degree of interaction between the polymer and filler as a shift towards the lower angles, are associated with the intercalation and exfoliation of the polymer between the nanoclay lamellas (Dias et al., (2010).

Table 4.2 The value of angular spacing, d and reflection angle, 2θ of the PP, WPC and WPC with different content of C20 organoclay

Samples	2θ (degree)	d (\AA)
PP	14.08	6.281
WPC	13.88	6.375
WPC-1	6.20	14.23
WPC-2.5	6.25	14.14
WPC-4	6.62	13.60
WPC-5	6.63	13.41

From the data obtained, WPC incorporated with different content of organoclay portrayed a smaller 2θ value than neat PP and WPC without organoclay that corresponds to higher angular spacing which indicates that a successful intercalation process has been achieved. The peaks of the organoclay reinforced WPC which were seen to shift towards a lower value is an indication that an intercalated nanoclay structure has been created.

However, these data showed that the order of intercalation was higher at 1 and 2.5 wt% organoclay than at 4 and 5 wt% organoclay concentration. Thus, one reason for the achievement of an intercalated structure in these composite could be better dispersion of the organoclay particles throughout the wood-plastic composite. Kord, 2012 and Khademi Eslam et al. 2013 exhibited similar results.

4.2.2 Mechanical Properties

In this segment, the mechanical properties of PP, WPC, and WPC with different content of C20 organoclay are discussed.

4.2.2.1 Tensile Properties

The tensile strength of WPC with organoclay was obtained at the breaking point of the material. In order to avoid factors such as molecular weight and processing history that affects the tensile strength values, WPC without organoclay was tested to ensure a more direct comparison with the nanocomposites and by using WPC as a reference, the reliability of the data obtained is believed to have been enhanced.

The matrix properties largely affect the tensile strength of composite. The proper chemical bonding among the composite components is highly dependent on the filler orientation and the low stress concentration. The movement of force into the composite starts from the matrix and then through matrix particles, later it is moved to the filler particles. The content of applying filler should be controlled because it is hard to control and direct the filler particles. The fracture in the interface between the fillers particles

and the matrix perform load transfer between the filler particles and the matrix during the tensile stress (Svab et al., 2005).

Figure 4.5 depicts the tensile strength of PP, WPC, and WPC with various concentration of C20 organoclay. The tensile strength of neat PP is decreased by 17% when WF was added. This is not surprising since it is known that when wood flour is used in thermoplastics, the tensile strength decreases. The higher degree of brittleness is introduced by the incorporation of wood flour in WPC (Yeh et al., 2013). The tensile strength results show that the composites containing 1 wt% of organoclay exhibited the highest value compared to the other samples. The tensile strength value was observed 27.98 MPa for composites made without organoclay, while maximum tensile strength was approximately 32.21 MPa for composites made with 1w% organoclay. Since the quantity, size, apparent coefficient, shape, crystal structure, diffraction of nanofillers and method of their blending with the polymer matrix are the factors which influences the mechanical properties of nanocomposites (Shokrieh and Sonbolestan, 2007; Kord, 2010; Ashori and Nourbakhsh, 2011). Moreover, the tensile strength of composites is mainly influenced by filler fraction and the interfacial adhesion between particles and matrix (Sun et al., 2006). Similar observations were reported by Ashori and Nourbakhsh, (2011) while studying polypropylene/wood flour/nanoclay composite.

The logo for UMP (Universiti Malaysia Perlis) is a large, stylized letter 'U' composed of several overlapping triangles in shades of teal, light blue, and yellow. The letters 'UMP' are printed in white, bold, sans-serif font across the bottom of the 'U' shape.

UMP

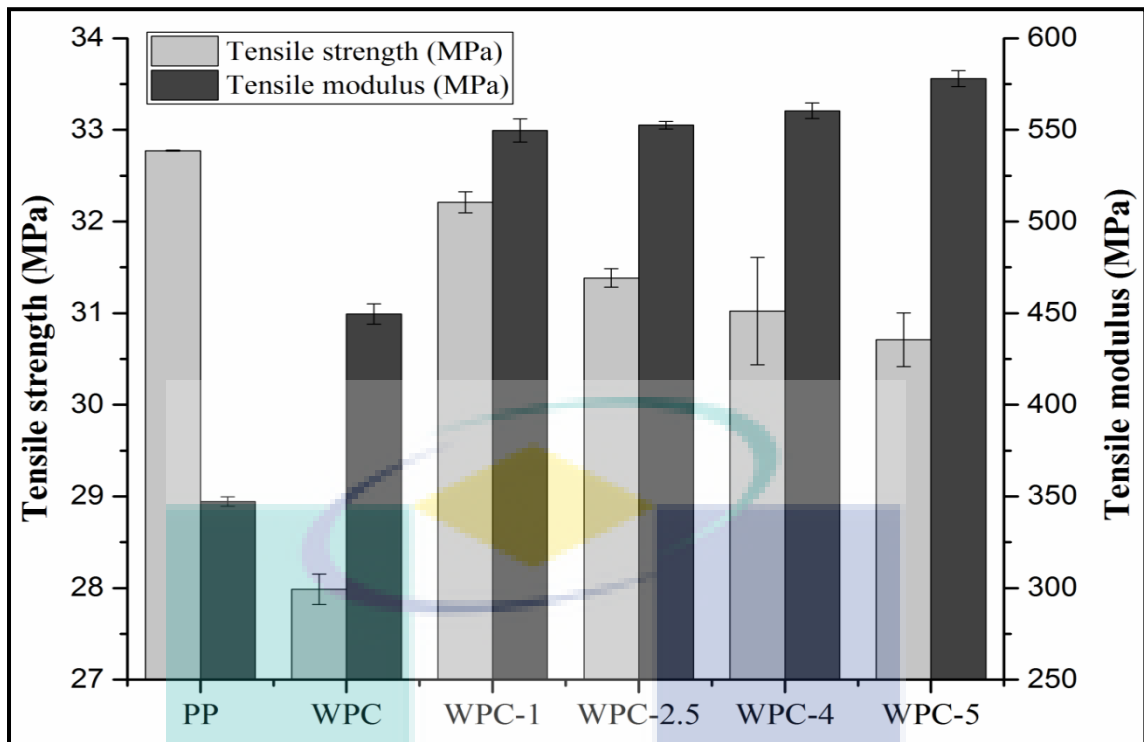


Figure 4.5 The effect of C20 organoclay loading on tensile properties of WPC

In Figure 4.5, it clearly illustrates that unlike 1wt. % of organoclay further addition of organoclay cannot significantly improve the tensile strength due to the agglomeration of nanoparticles. Many research works had discussed the importance of nanoclay dispersion and their impact on mechanical properties of composites (Breton et al., 2004; Coleman et al., 2006).

Furthermore, the tensile modulus of composite was increased over PP when wood flour was incorporated into the PP. It might be due to the lower stiffness of PP than wood flour. Moreover, with increasing organoclay amount into the composite, the tensile modulus of WPC increased. As it could be seen from Figure 4.5, the tensile modulus value was increased by 28.57% compared to control sample (WPC) and reached at 578MPa at 5 wt% of organoclay loading. It might be due to the stack form of nanoclay particles which restricts the mobility of polymer chains and enhances the tensile modulus of composite (Lei et al., 2015). The tensile and flexural modulus can be improved due to the high interfacial contact area and high aspect ratio of nanoclay (Ramos Filho *et al.* 2005, Advani 2007). Moreover, the modulus of individual components affect the modulus of composite (Yildiz and Gumuskaya, 2007).

4.2.2.2 Flexural Properties

The flexural test is the bending resistance of sample when vertical load is applied. In flexural test of plastic, the polymer chains are condensed and compressed at the point where the vertical load is applied. Polymer chains are moves on to the other side during the test. However, the introduction of wood fiber into the polymer matrix reduces the polymer chains mobility and increases the composite strength against bending and breakage (Khosravian, 2009). According to this study, incorporation of wood flour into the PP increased the flexural properties of composite over neat PP.

The composite made with 1 wt% organoclay showed good organoclay dispersion and strong interfacial interactions in the composite, which resulted in high flexural strength by transferring effective stress from matrix to fibers. Another reason is that, as discussed earlier, the quantity, size, apparent coefficient, shape, crystal structure, diffraction of nanofillers and method of their mixing with the polymer matrix affect the mechanical properties of nanocomposites. Therefore, the high apparent coefficient of organoclay particles created an exfoliated and intercalated structure into the composite and increased the flexural strength of composite containing 1 wt% of organoclay. The high apparent coefficient of nanofillers enhances the interface of two phases by playing the role in its reinforcing ability in the composite and improving the flexural strength of composite. Furthermore, the flexural strength of composite increases due to the strong interaction of polymer matrix and nanoclay particles and has created intercalated structure in the nanocomposite (Kord, 2010; Ahmadi and Mohadespour, 2005).

As can be clearly seen from Figure 4.6 that with the increase in organoclay concentration into the composite, the flexural strength is considerably decreased. The maximum value of flexural strength was found at 1wt% of organoclay concentration. Ashori and Nourbakhsh (2011) reported that the flexural strength of composite at higher nanoparticles concentration decreased because of the agglomeration of C20 organoclay particles in to the WPC. The nanoclay dispersion in the polymer matrix is the most important parameter in fabricating the composite. The agglomeration of nanoparticles caused the reduction of mechanical and physical properties of the nanocomposites.

Besides, the increased loading nanoclay from 4 to 5 wt% produced inside-together flocculates resulting in decreased in flexural strength of composite.

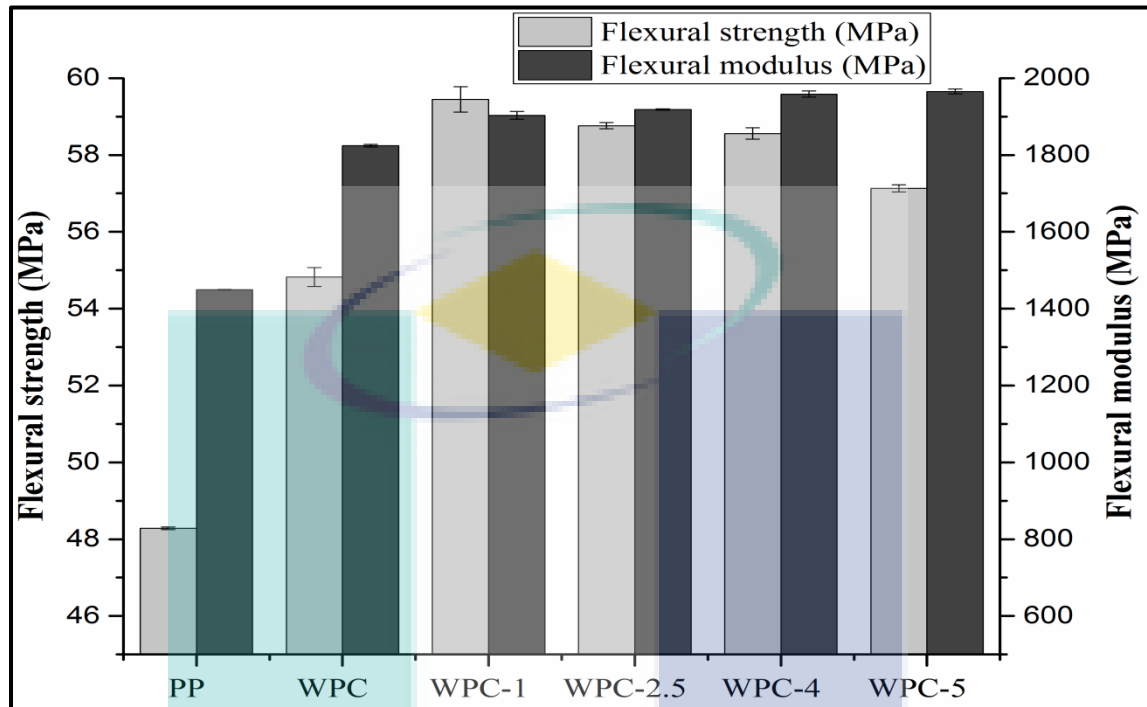


Figure 4.6 Effect of C20 organoclay loading on flexural properties of WPC

The flexural modulus is a measure of resistance to deformation of the composite in bending. Similar like a tensile modulus, the flexural modulus of composite showed significant increment over PP when wood flour was incorporated into the PP. As mentioned earlier, PP has low stiffness than wood flour. As it could be seen from Figure 4.6, increasing organoclay content increased the flexural modulus of composite. Since the wood flour has lower flexural modulus than organoclay (Sheshmani et al., 2013). Moreover, the modulus of individual components affect the flexural modulus of composite (Yildiz and Gumuskaya, 2007). The high aspect ratio of nanofillers increased the wettability of fillers by the matrix and transferred stress from polymer matrix to the fillers.

4.2.2.3 Elongation at break

The elongation at break (EB) is the increase of percentage in length that occurs before the polymer composite sample breaks under strain. It is highly dependent on the interfacial reactions between the polymer matrix and other constituents of composite. There were four different weight percentages that were studied in this experiment which were 1wt%, 2.5 wt%, 4 wt% and 5 wt% C20 organoclay loading. Five samples were tested for each parameter and average mean value was taken. The elongations at break values of the PP and WPC are plotted in Figure 4.7. As can be seen from Figure, the elongation at break value decreased as the addition of wood flour into the PP. The reason might be, as discussed earlier, wood flour introduces higher degree of brittleness in the composite.

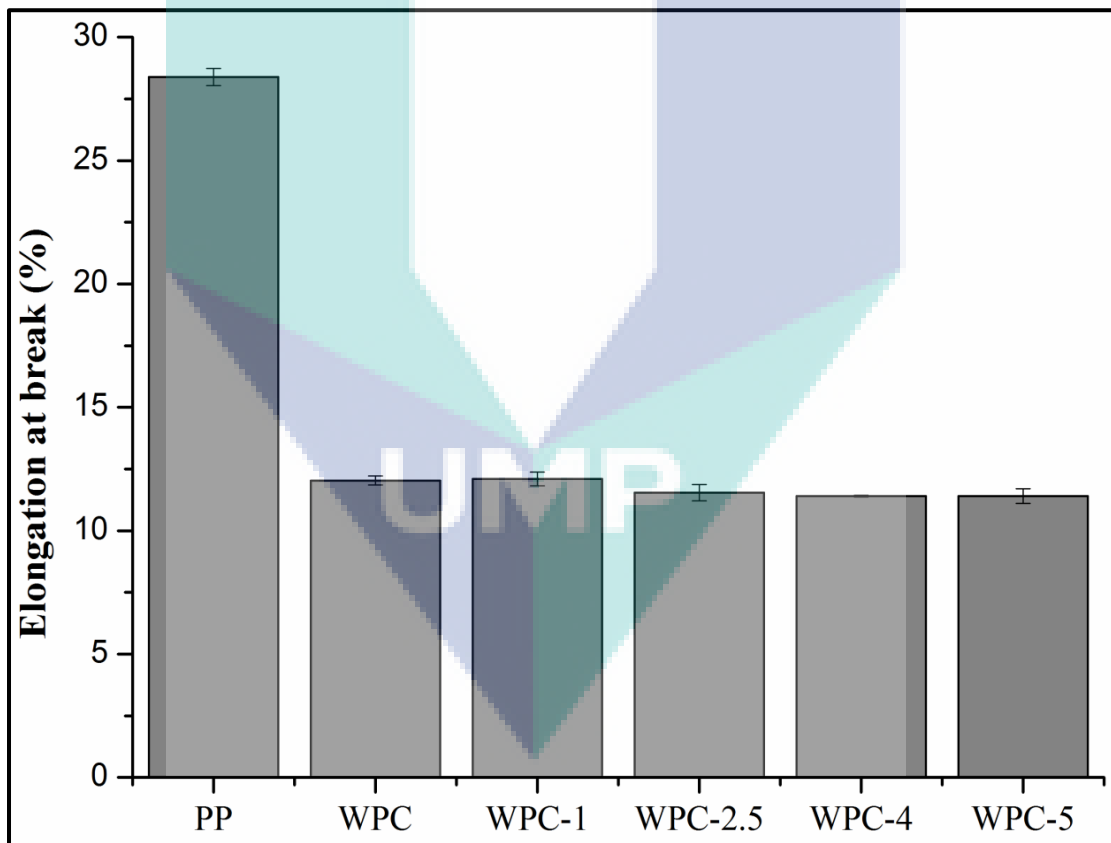


Figure 4.7 Elongation at break of PP, WPC, and WPC with different C20 organoclay content

As observed from Figure, the elongation at break value obtained showed a decreasing trend. WPC and WPC with 1 wt%, 2.5 wt% 4 wt% and 5 wt% organoclay

loading showed a decreasing pattern in its EB values over PP. The elongation at break value of PP was 28.39 %, whereas, WPC and WPC with 1 wt%, 2.5 wt% 4 wt% and 5 wt% organoclay loading exhibited the elongation at break value nearly 12.03%, 12.10%, 11.54%, 11.40%, and 11.40% respectively.

The composites depicted a negative elongation at break effect with the addition of nanoclay. Abraham et al. (2009) mentioned that the incorporation of fillers to the polymer matrix decreases the EB value. When PP is filled with wood flour it shows brittle behaviour, thus the elongation at break of WPC and WPC filled organoclay decreased markedly compared to PP. Ahmadi et al. (2004) stated that the decrease in the EB values in composites may be attributed to the fact that ductility decreased when stiffness is increased by reinforcement. However, WPC with 1 wt% organoclay showed slightly better (0.59 %) improvement over the WPC sample. Further addition of organoclay into the composite decreased the EB value of WPC. This observation is similar to that of the flexural and tensile strengths results of WPC. At 1 wt% organoclay loading, WPC had the higher tensile and flexural strength. However, they were decreased over WPC (control sample) when more organoclay was added into the composite.

4.2.2.4 Izod Impact Strength

The strength of composite materials against the fracture is known as the impact strength of composite material. It represents the toughness and stiffness of material. Properties of matrix, arrangement of filler particles, and dispersion of nanofillers into the composite and especially the matrix and filler particles interaction are the factors which affect the fracture resistance of composite material. The izod impact strengths of PP, WPC, and WPC with different content of C20 organoclay are shown in Figure 4.8. According to the obtained results, when organoclay and wood flour were added into the PP, the impact strength of composite was decreased. The loading of cellulosic fiber and nanoparticles into the matrix increases the brittleness and reduces the toughness which results in reduction of impact strength (Klyosov, 2007; Razavi et al., 2006). Moreover, PP shows higher impact strength than the composite samples.

The independent effect of nanoclay is significant on the WPC impact strength. The test results showed that the impact strength of composite was increased at first, showing higher strength at 1 wt% organoclay content over other WPC. The reason behind this is, that the well dispersion of organoclay into the composite. As, discussed earlier, the dispersion of nanofiller affects the impact strength of the composite. Furthermore, as shown in Figure 4.8, the impact strength of WPC is largely decreased by increasing the amount of nanoclay from 4 to 5 wt%.

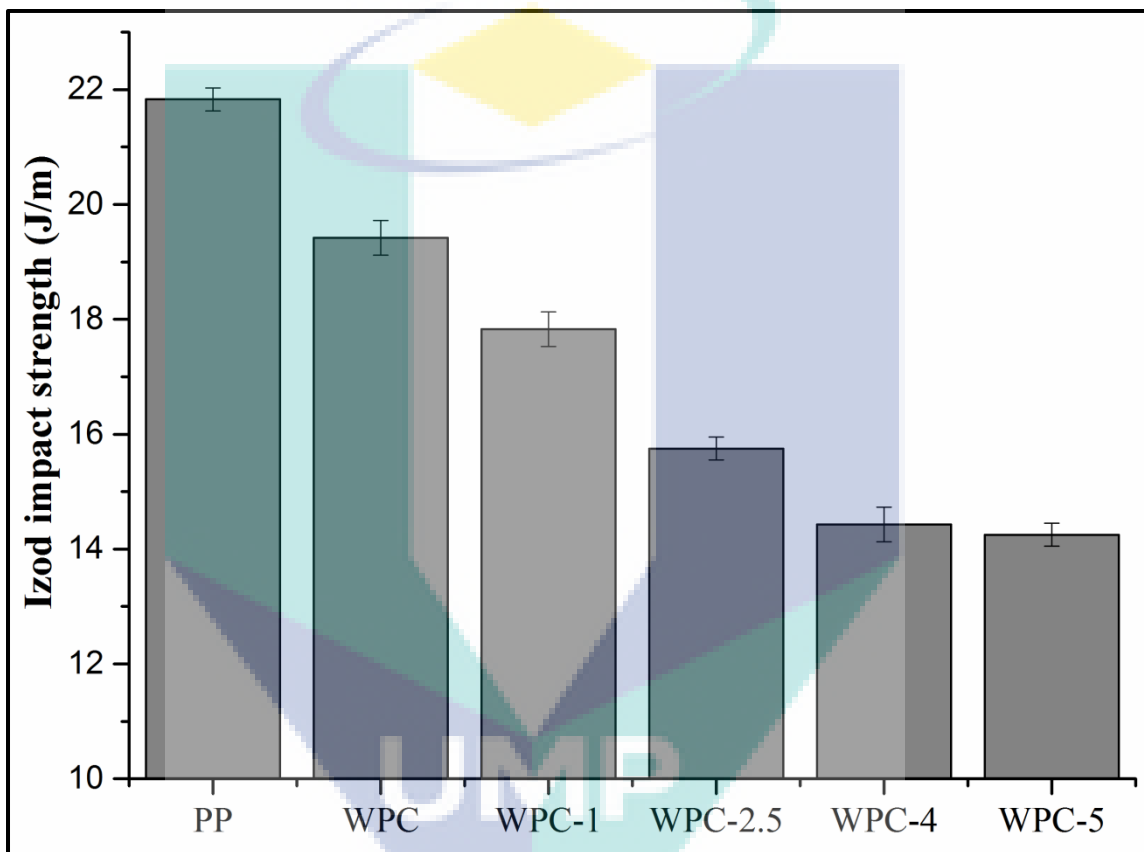


Figure 4.8 Izod impact strength of PP, WPC, and WPC with different C20 organoclay content

The increasing content of organoclay reduced the impact strength of composite; it might be that the starting point of fracture and the stress concentration points were produced by nanoclay particles. Moreover, the high content of nanoparticles absorbs less energy and increases agglomeration (Mohanty and Nayak, 2007). Thus, in the polymer matrix, the high content of organoclay creates the points where they improve the stress concentration and initiate the crack expansion from that point or area (Han et

al., 2008). Lei et al. (2007), Han et al. (2008) and Kord (2010) had reported similar results.

4.2.3 Physical Properties

In this segment, the effect of C20 organoclay reinforcement on physical properties of wood-plastic composite is explored. Water absorption of PP, WPC, and WPC with different concentrations organoclay is discussed.

4.2.3.1 Water Absorption

Besides mechanical properties, water resistance is also important for WPC. The water absorption behaviour is important to investigate the resistance of PP and WPC towards the natural conditions. Figure 4.9 shows the result of 15 and 30 days water absorption of PP, WPC and WPC with different percentage of organoclay loading. The PP absorbed very less amount of water (0.03%) because of its hydrophobic nature. The introduction of wood flour into the PP dramatically increased the water absorption. The hydrophilic nature of wood flour created voids, holes, cracks and microgaps between the matrix and filler, since PP was unable to cover all wood flour. A SEM observation (Fig. 4.1a) was used to confirm this hypothesis. The role of organoclay can be attributed for the different water absorption among all fabricated composites because wood flour concentration was constant (20 wt%) in all blends.

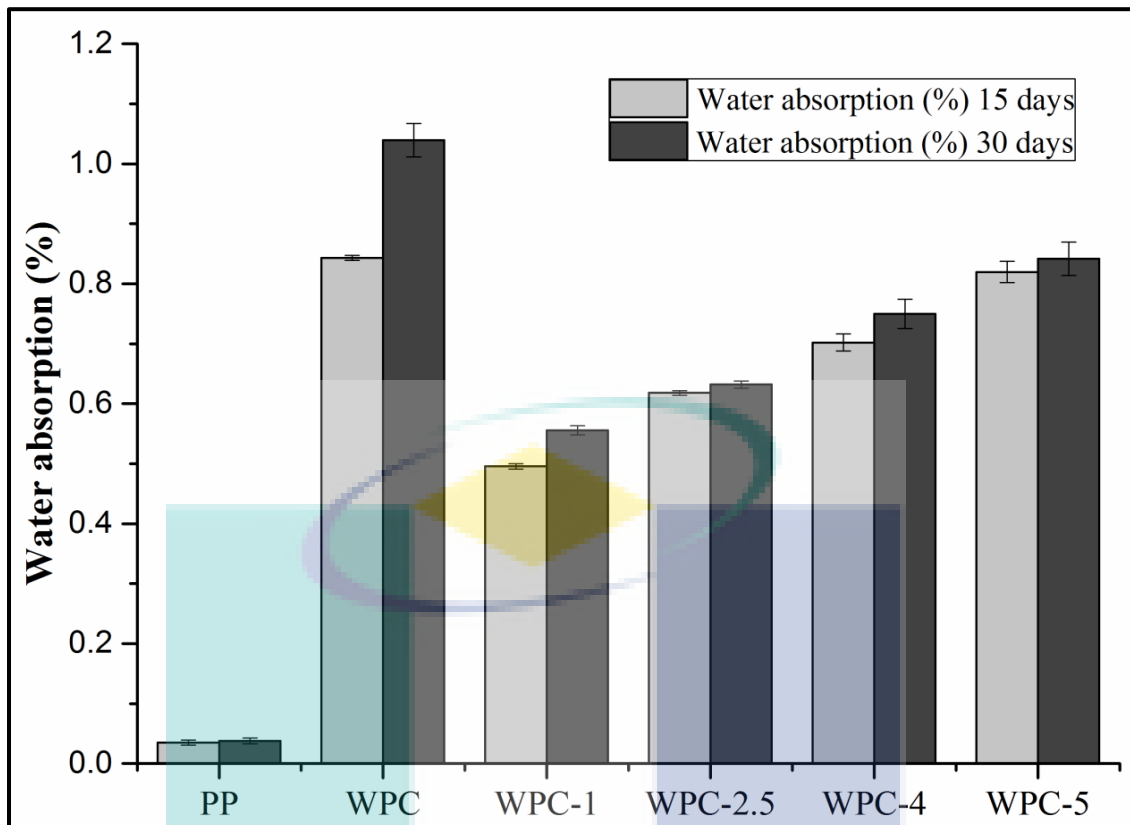


Figure 4.9 Water absorption of the WPC as function of C20 organoclay loading

Less water absorption was shown by WPC sample containing 1 wt% organoclay. However, WPC with 0 wt% organoclay exhibited higher water absorption than organoclay loaded WPC. As compared to the WPC sample then 1 wt% organoclay loaded WPC reduced 70% water uptake in 15 days and 87% water uptake in 30 days over WPC sample. The well dispersion of nanoparticles created good interaction between matrix and the organoclay and had improved the water barrier performance of composite. The well dispersion of nanoparticles was achieved at low content and it was 1 wt%. Das et al. (2000) reported that before occupying the void spaces, water saturates the cell wall of fiber.

However, the water absorption of composite had increased when the nanoclay was reinforced into the composite from the range of 1 wt% to 5 wt%. The water uptake of composite increased by 65% and by 51% in 15 and 30 days water absorption test respectively, when 1 wt% to 5 wt% organoclay was loaded into the composite. The agglomeration of organoclay particles increased the water absorption of composite by creating cracks fractions and porosity during fabrication process. SEM images (Fig.

4.1d-g) were used to confirm this hypothesis. SEM images showed more numbers holes and cracks of sample containing 5 wt% organoclay.

4.2.4 Thermal Properties

Thermal properties of WPC have attracted a significant amount of interest due to the ability of the layered silicates to trigger a tremendous thermal properties improvement. The improvement in the thermal stability of polymers in the presence of layered silicates can be attributed to the rich intercalation of polymer chains into the lamellae of layered silicates. These layered silicates act as an insulator between the heat source and the surface area of the polymer. (Etmimi, 2012). In this research work, the Thermal Gravimetric Analysis (TGA), and Differential Scanning Calorimetry (DSC) were employed to analyse the thermal properties of WPC. The section that follows discusses the results obtained from both the analysis done in order to get a better understanding on the thermal properties of WPC prepared in this work.

4.2.4.1 Thermal Degradation

The investigation of degradation behaviours and the thermal properties of the composite were applied at high temperature, so it is essential to perform TGA analysis. The mixing of matrix and wood fibers (cellulosic materials) at high temperature is the part of wood-plastic composite fabrication process, so the composite properties can be affected by the degradation of cellulosic materials. Figure 4.10 shows the weight loss curves of various composite samples at different temperatures. Table 4.3 shows the decomposition temperature at different weight loss (T_{20} , T_{40} , T_{60} , and T_{80}), maximum degradation temperature (T_{max}) and char content (%) for PP, WPCs and WPCs containing organoclay.

In all the samples, due to the removal of some moisture from the sample, a slow decrease in weight loss was noticed below 100°C. A single mass loss step was shown by PP at 422 °C maximum decomposition temperature. In case of composite loaded with wood flour, the maximum degradation temperature moved to the higher temperature exhibiting that the thermal stability of PP had improved by introducing

wood flour in it. It is worth to mention that the high thermal stability of lignin present in chemical composition wood flour improves the thermal stability of wood flour. According to the Yildiz and Gumus kaya (2007) the most thermally stable components of wood is lignin. Generally, the cellulosic materials thermally decompose between 200°C and 400°C (Fisher et al., 2002). The two decomposition stages were shown by WPC. The thermal degradation of cellulosic components has shown the first peak at 309°C (Fisher et al., 2002), the decomposition of polymer matrix has exhibited the next peak at 435°C.

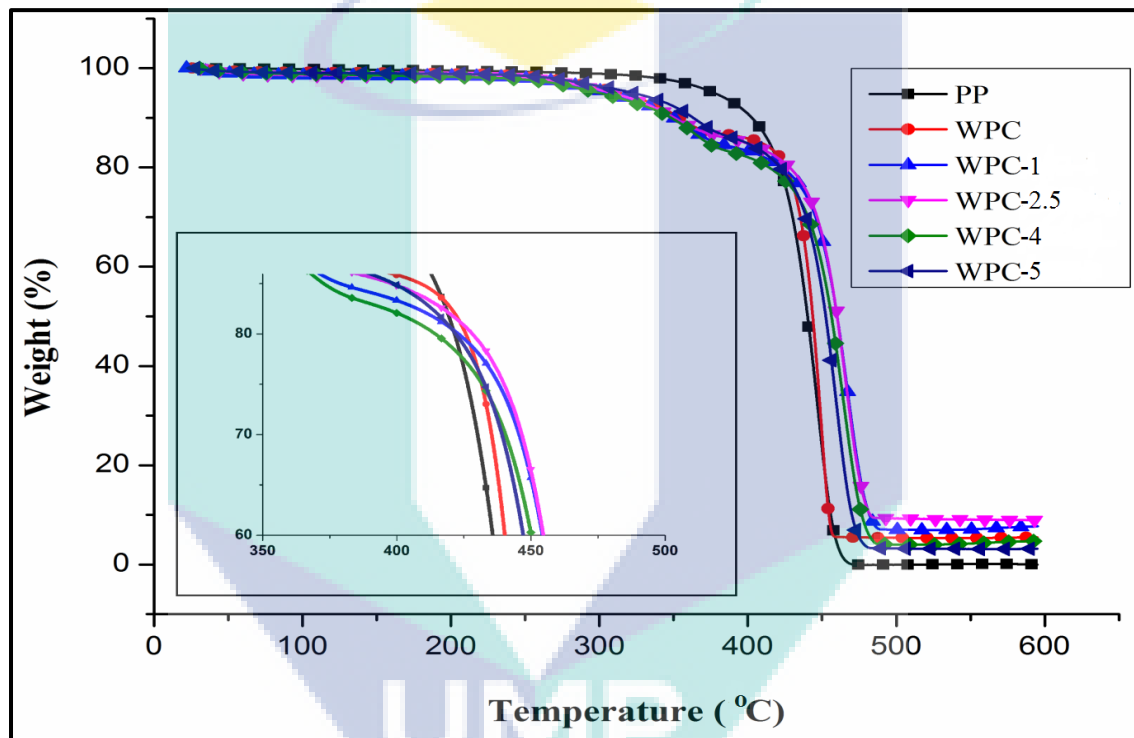


Figure 4.10 TGA thermogram of neat PP and WPC made with different C20 organoclay content

The degradation temperature of wood-plastic composites was increased by incorporating organoclay into the composite as shown in Figure 4.10. The presence of silicate layers in wood plastic composite acted as barrier and delayed the diffusion of degraded volatile products throughout the composite. Thus the loading of organoclay enhanced the thermal degradation temperature of the wood-plastic composite (Qin et al., 2004). The 20 % weight loss temperature of composites was increased by about 8 % as compared to WPC without nanoclay (control sample) when the loading of 2.5 wt % organoclay. Similar like the 20 % weight loss, at 40 %, 60 %, and 80 % weight loss, the organoclay loaded WPCs showed higher degradation temperature than the control

sample and neat PP. The composite with 1wt% of organoclay exhibited maximum degradation temperature (T_{max}) (447°C) among other samples of wood-plastic composites.

However, it was observed that the decomposition temperature values were reduced, due to the higher loading of organoclay into the composite. The reason might be, as discussed earlier, the agglomeration of nanoclay in the composites. Composites provide more area exposure of matrix polymer and could have resulted in more weight loss at lower temperature (Lee et al., 2008).

Table 4.3 Thermogravimetric properties of WPC with different C20 organoclay loading

Composites	T_{20}	T_{40}	T_{60}	T_{80}	T_{max} (°C)	Char (%)
PP	421	435	444	451	422.41	0.00
WPC	425	440	446	451	435.36	5.39
WPC-1	428	457	468	476	447.04	7.01
WPC-2.5	433	448	465	473	446.74	8.96
WPC-4	427	451	460	471	444.20	4.03
WPC-5	426	448	456	464	440.84	3.17

Moreover Derivative Thermal Gravimetric (DTG) was further employed to study the thermal stability of the WPCs which was expected to shed some light on the chemical structure of the composite. Figure 4.11 delineated the DTG of PP and the different types of WPC analysed in this study.

WPCs presented a two-step decomposition process, while polypropylene matrix presented only one-step. The first decomposition step of the WPCs, at 309 °C, corresponds to the decomposition of the wood flour. The second step, at 435 °C, corresponds to the degradation of the propylene group of polypropylene. The loading of organoclay is seen to shift the peak temperature to slightly high values and this shows that the organoclay has a contribution in the decomposition rate. However, with the incorporation of organoclay, two peaks were observed. The first peak may be attributed

to the decomposition of the PP matrix whereas the second peak which is seen at a higher temperature which is due to the PP physicochemical attachment to the nanoparticle's surface.

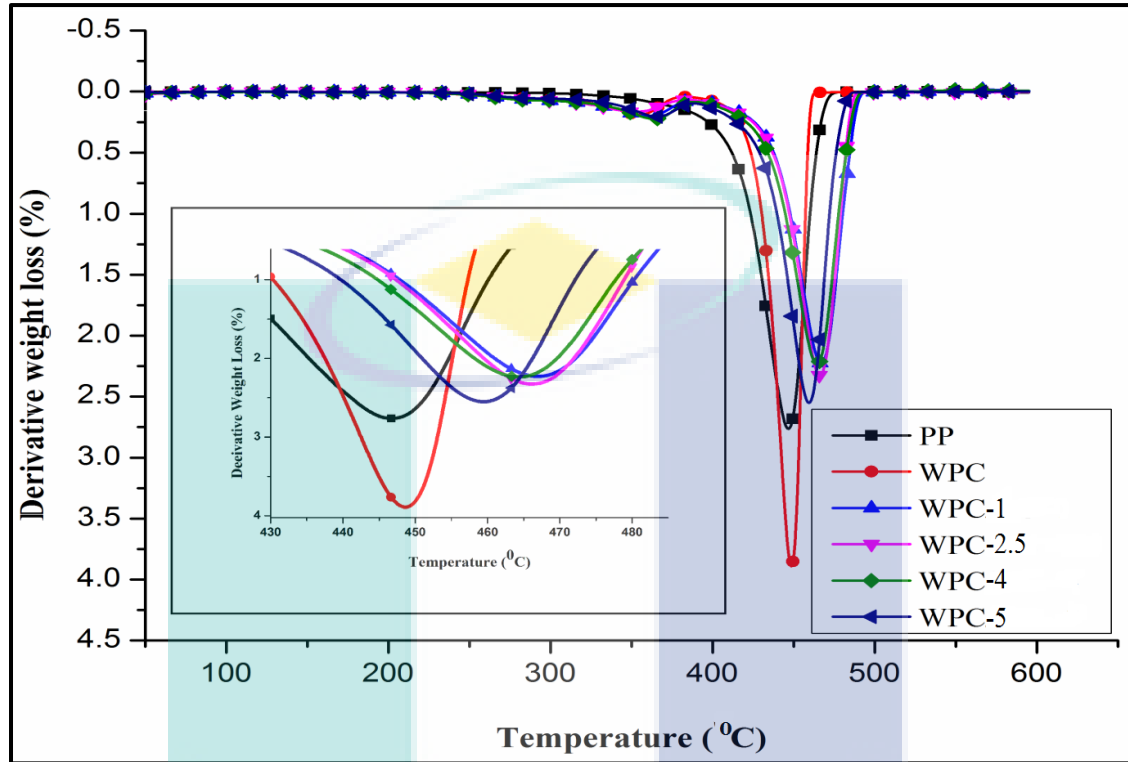


Figure 4.11 DTG curve of neat PP and WPCs made with different C20 organoclay content

The presence of silicate layers in wood plastic composite acted as barrier and delayed the diffusion of degraded volatile products throughout the composite. Thus WPCs containing organoclay improved the thermal stability of composite. Similar observations were reported by Deka and Maji (2010) while exploring the effect of organoclay on PP/Phargamites karka nanocomposite.

4.2.4.2 Crystallization behaviour

Differential Scanning Calorimetry (DSC) is a technique used to study the thermal transitions of a substance when it is being heated. Thermal transitions are the change that takes place in a polymer such as the melting of the crystalline and the glass transition of the substance. Figure 4.12 shows DSC curves of neat PP and WPC with

and without C20 organoclay. Crystallization behavior (melting and crystallization temperature, heat of fusion and crystallinity) of neat PP, WPC and WPC containing nanoclay obtained from DSC experiments is summarized in Table 4.4.

Figure 4.12 illustrates the differential scanning calorimetry thermograms of the wood-plastic composites. The general idea about the melting temperature and the interaction between the organoclay and wood-plastic composites was obtained from the graph. The DSC results exhibit the increased crystallization temperatures of 1 wt% organoclay reinforced composite up to 154.00 °C, in contrast with 149.88 °C for neat PP. The small amount of nanoclay increases the crystallization of PP matrix because the small content of uniformly dispersed nanoclay can act as the effective nucleating agent and thus through the surface-nucleated PP crystalline phase, it has improved the mechanical performance (Mohan et al., 2011). The DSC results shows the nucleating effects, which can relate with mechanical properties for WPCs.

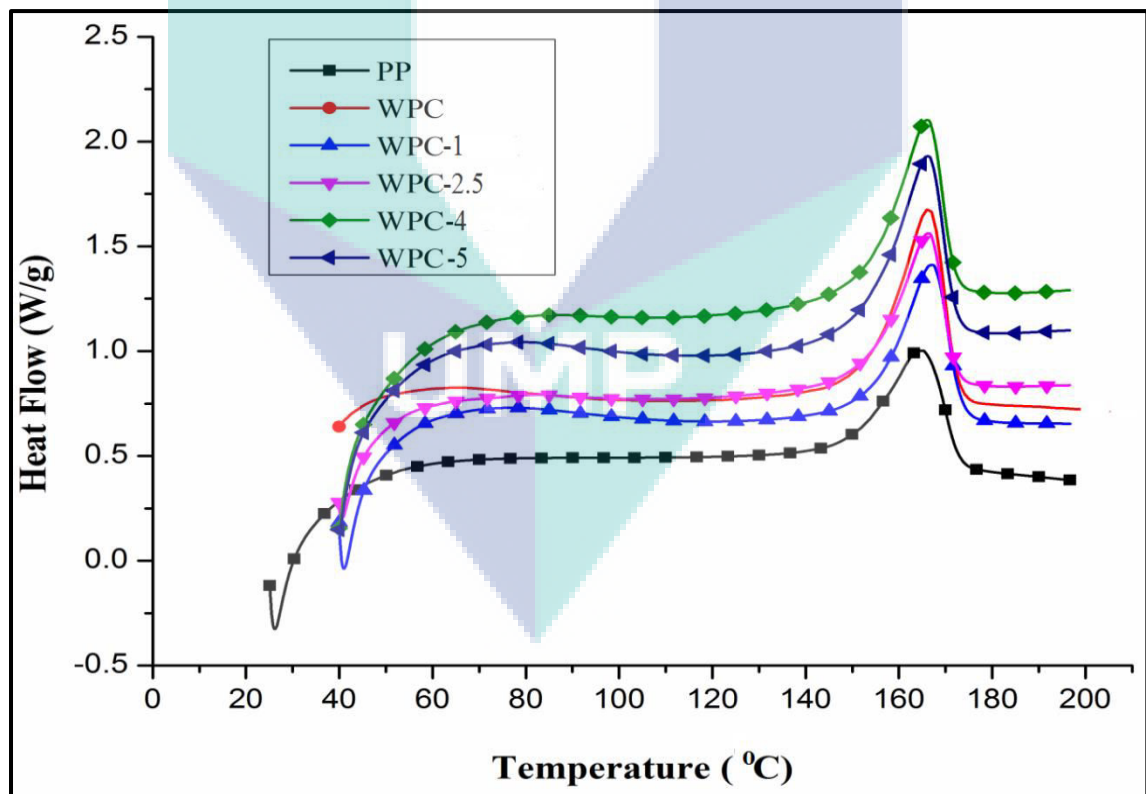


Figure 4.12 DSC curves of neat PP and WPC made with different C20 organoclay content.

All WPC had a higher melting temperature (T_m), compared to the neat PP. Neat PP had the lowest T_m (165.12°C), while WPC with 1 wt% organoclay had the highest T_m (167.06°C). The increased loading level of organoclay had no significant effect on the T_m of the WPC. However, increased loading level of organoclay slightly decreased the T_m of the WPC.

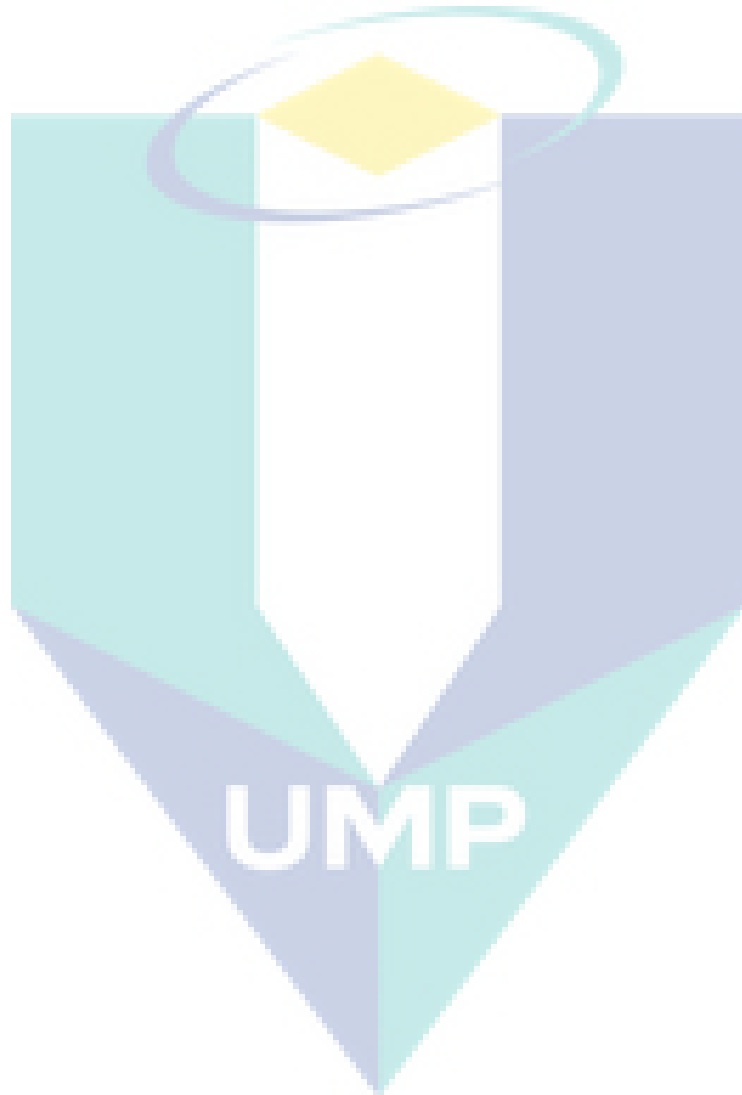
The enthalpy (ΔH_m) of caloric processes shown in Table 4.4 and it was determined at the heating rate of 10°C/min. Neat PP shows 54.80 J/g enthalpy (ΔH_m) value but reduction occurred in ΔH_m value when wood flour was introduced into the neat PP and the value was decreased by 19.57 %. The reason behind this is that the ΔH_m of neat PP is much higher than that of wood flour because in the melting process of composite wood flour had absorbed more heat energy (Wunderlich, 1980). However, the ΔH_m increased from 57.96 to 69.50 J/g when the nanoclay loaded into the composite from the range of 1 to 5 wt%.

Table 4.4 DSC result of neat PP and WPCs containing different loading of C20 organoclay

Composites	Crystalline Temperature (T_c °C)	Melting Temperature (T_m °C)	Heat of Fusion (J/g)	Crystallinity (%)
PP	149.88	165.12	54.80	27
WPC	153.41	166.39	45.83	22.57
WPC-1	154.00	167.06	67.63	33.31
WPC-2.5	153.51	166.35	69.50	34.23
WPC-4	153.01	165.97	55.58	27.37
WPC-5	152.56	166.09	60.01	29.56

As shown in Table 4.4, the crystallinity (X_c) of PP was 27 %. However the crystallinity (X_c) decreased when wood flour was introduced into the neat PP. The addition of wood flour had greatly reduced the X_c . It shows that some factors such as viscosity of hybrids and surface chemistry, the concentration level, and the dispersion of fillers affect the crystallinity (X_c) of composite (Wang et al., 2002).

Meanwhile, an increasing amount of organoclay increased X_c . This is probably due to the interactions between the carbonyl groups of the repeating units of hard segments and the hydroxyl end groups of nanoclay (Biswal et al., 2009). However, at higher loading of nanoclay, X_c gradually decreased. As mentioned earlier, the loading level, the dispersion, and the surface chemistry of filler affects X_c of composites.



4.3 Modification of pristine (MMT) nanoclay and its application in wood-plastic composite

The mechanism of nanoclay modification process and its effectiveness on the wood-plastic composite are discussed in this section. The characterization through FESEM-EDX, SEM, TEM, FTIR, and XRD are discussed. The effect of the pristine and modified nanoclay on the mechanical, physical, and thermal properties of wood-plastic composite is further explored in this segment.

4.3.1 Modification of MMT nanoclay

4.3.1.1 Mechanism of Transition Metal Ion (TMI) Modification

Transition metal ion (TMI) modification was employed on the pristine nanoclay prior to the fabrication of wood-plastic composite. In this modification process, Copper (II) chloride (CuCl_2) was used as transition metal ion to get copper ions. The intension of modification process was to change the nature of the pristine nanoclay which is hydrophilic in order for it to be compatible with the polymer host which is polypropylene (PP). The hydrophilic nature of the nanoclay is caused by the isomorphous substitution of the SiO_4 tetrahedral with $[\text{AlO}_6]^{3-}$ tetrahedral and $[\text{AlO}_6]^{3-}$ octahedral which causes an excess of negative charges within the layers of the sheet and these negative charges are balanced with additional cations such as Ca^{2+} and Na^+ which are located within the layers. The counter ions are shared by two neighbouring platelets which results in this stacks to be held tightly together as shown in Figure 4.13.

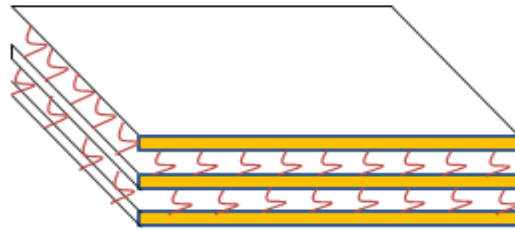
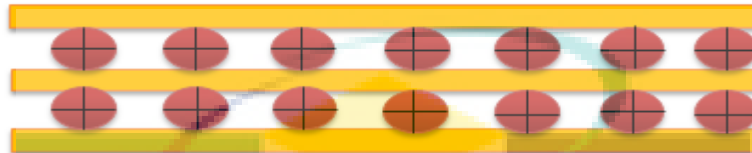


Figure 4.13 Proposed diagram of Stacks of platelets that are tightly held together



Modification of MMT using transition metal ion is seen as a prerequisite for a successful formation of nanoclay based wood-plastic composite. Figure 4.14 shows the cation exchange that took place from the modification process whereas Figure 4.15 shows the mechanism of the nanoclay modification.

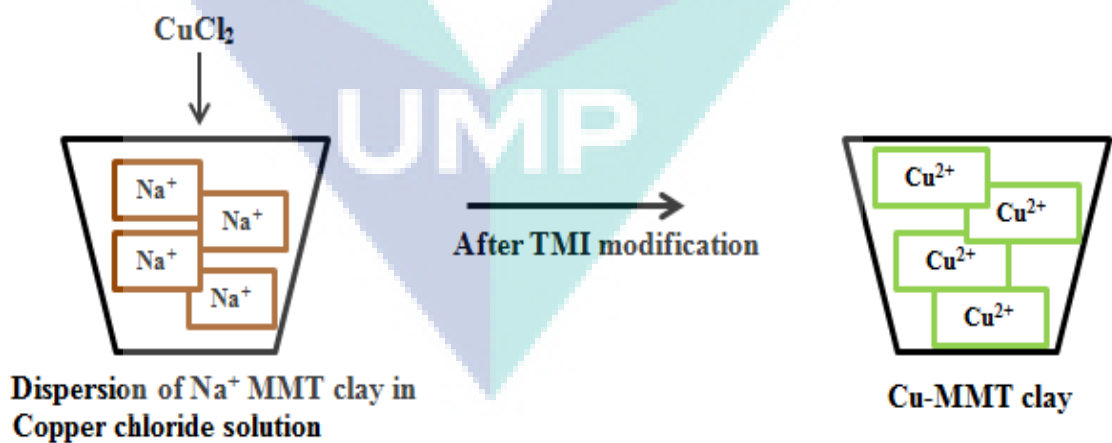


Figure 4.14 Proposed diagram of TMI Modification of MMT clay via Cu^{2+}

When the cations in the MMT nanoclay are exchanged with the copper metal ions, the surface energy of the silicate surface is lowered and wetting with the polymer matrix is improved. The positively charged cations are attached to the surface of the negatively charged silicate layers and results in an increase of the gallery height. The diffusion of the Cu^{2+} ions between the layers alters the surface properties of each single sheet from being hydrophilic to hydrophobic (Pavlidou and Papaspyrides, 2008). A large interlayer spacing which facilitates better intercalation process is obtained as shown in Figure 4.15

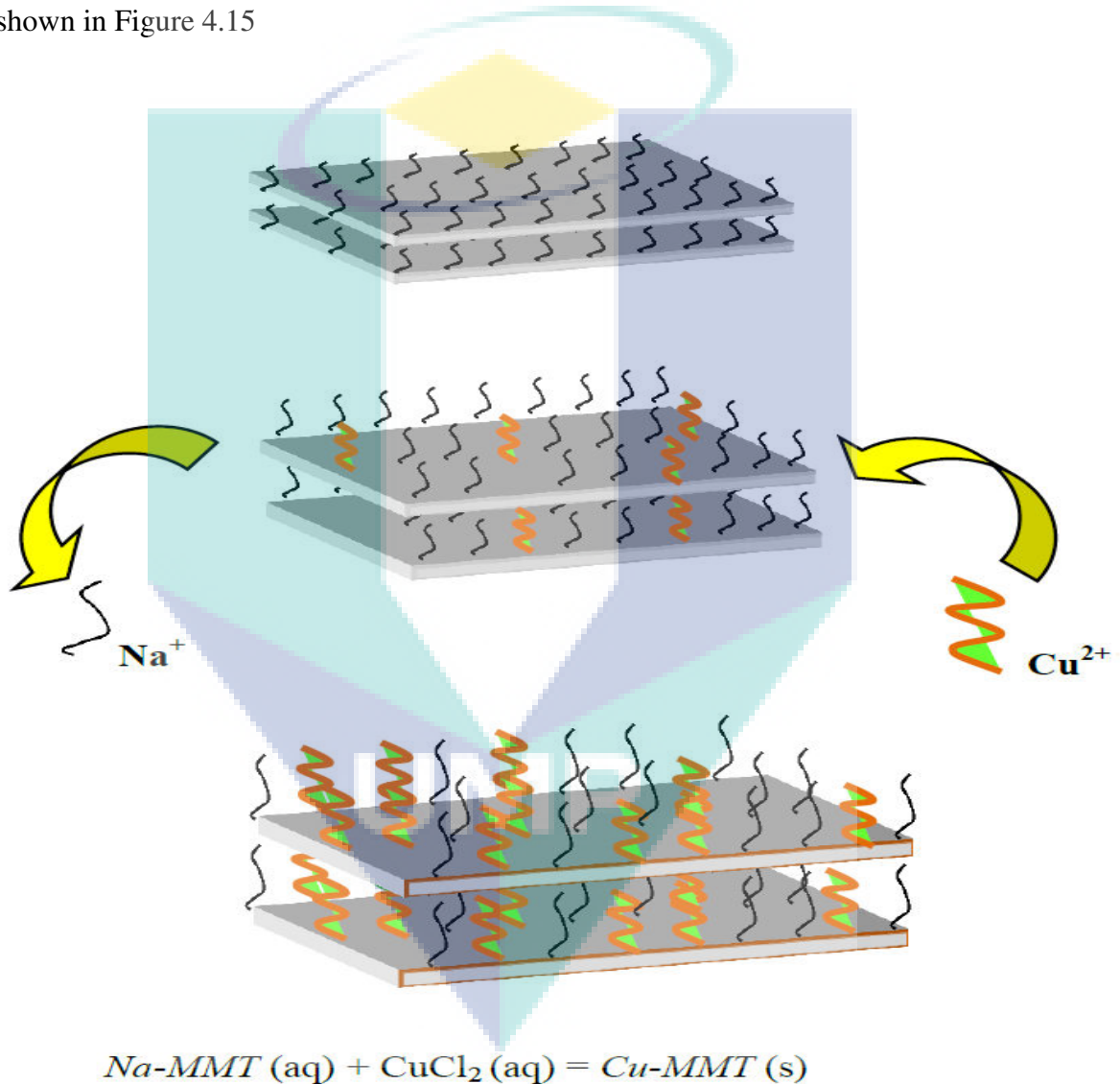


Figure 4.15 Mechanism of the modification process

Source: Shamini (2014).

4.3.2 Characterization of TMI-modified MMT nanoclay

4.3.2.1 Elemental analysis

The presence of the copper ions and elemental composition of modified Cloisite Na⁺ (MMT) were confirmed using energy dispersion x-ray analysis (EDX). It is one of the most notable methods, due to its high detection power and true multi element capabilities. In addition, EDX detection allows measurement at extremely low concentrations and it has an excellent sensitivity which enables it to become a good detector for many trace elements. EDX analysis showed that oxygen (O), carbon (C) sodium (Na) and Silicon (Si) elements are present in MMT (Figure 4.16), while O, C, Si and copper (Cu) are present in copper modified MMT (Figure 4.17).

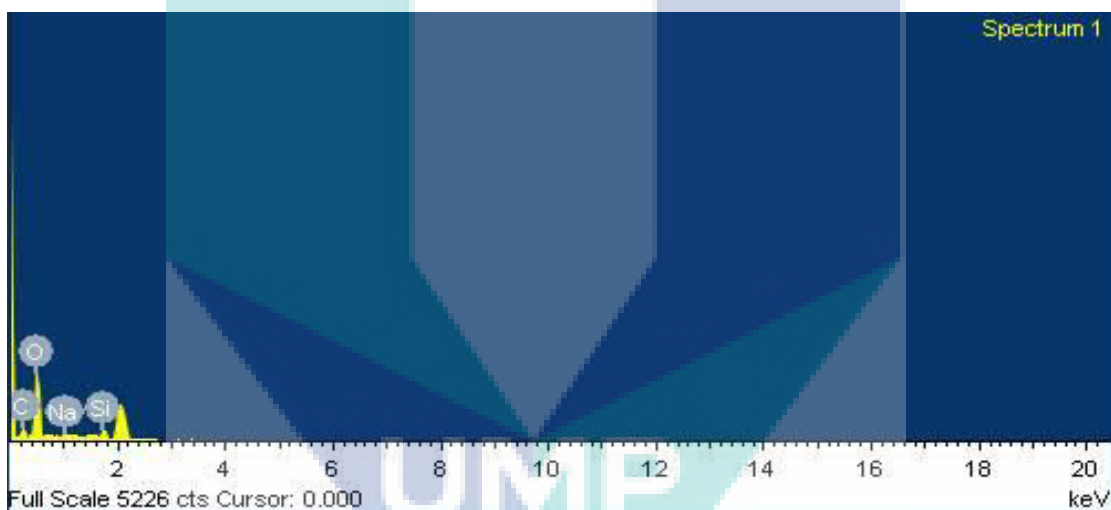


Figure 4.16 EDX analysis of MMT (Pristine nanoclay)

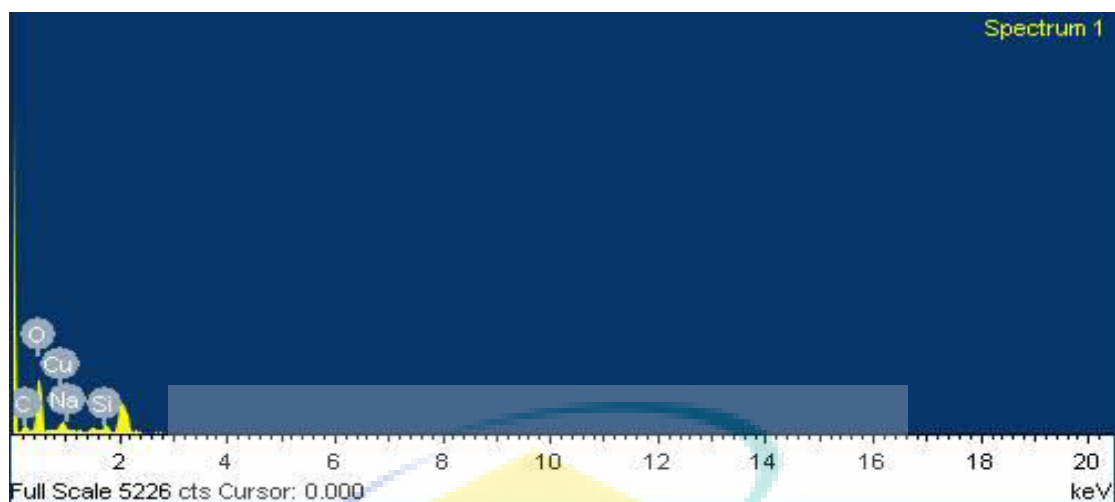


Figure 4.17 EDX analysis of MMT modified with copper chloride

Table 4.5 EDX studies of MMT and MMT Cu with elemental weight and atomic percentages

Element	MMT		MMT Cu	
	Weight %	Atomic %	Weight %	Atomic %
C	10.17	14.21	7.31	11.68
O	70.63	74.14	62.29	74.70
Na	1.22	0.89	0.00	0.00
Si	17.91	10.75	11.63	7.95
Cu	0.00	0.00	18.77	5.67

As can be seen in table 4.5, after TMI-modification process the C, O, and Na components are decreased. The reason might be that the decreases in C, O, and Na components in TMI-modified nanoclay exhibits, that the ion exchange might have taken place. It is conceivable that instead of a complete exchange of surfactant cations in Cloisite Na⁺ (MMT), CuCl₂, may form molecular complexes with them.

From the Figure 4.17 and the data displayed in the Table 4.5, the amount of copper (Cu) were seen in the MMT Cu, which ensures that the modification of the clay was successful in aiding the TMI to be able to displace themselves in the lamellar plane of the layered silicates.

4.3.2.2 Morphological Characterization

Field emission scanning electron microscopy (FESEM) was engaged in this study to understand the distribution of the pristine and TMI-modified nanoclay particles. Figure 4.18 depicts the micrographs obtained for MMT and MMT Cu.

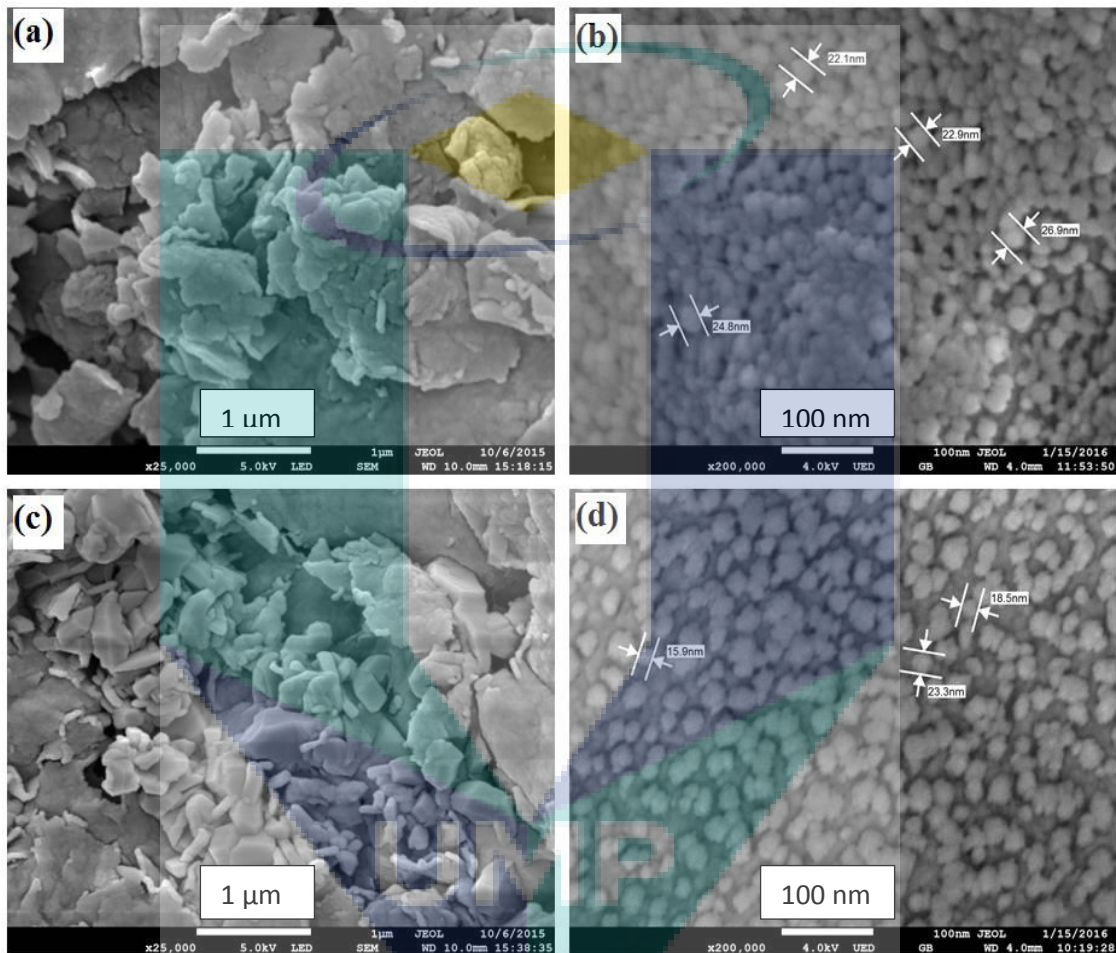


Figure 4.18 FESEM micrographs of (a, b) MMT and (c, d) MMT Cu

It can be seen in Figure 4.18 (a) that pristine MMT nanoclay exists in stacked platelet and forms overlapped layers. These layers could be attributed to the structure of the nanoclay which exists in stacked platelet forms. After the TMI modification process, the nanoclay layers are covered by the metal ion which is copper and appear to have a homogeneous distribution. Furthermore, the nanoclay agglomerations in pristine MMT nanoclay are reduced and numerous separated tactoids are seen in MMT Cu (Fig. 4.18 [c]).

Moreover, the sizes of the nanoclay agglomerates in MMT are reduced after modification process and numerous separated tactoids are seen in MMT Cu as shown in Figure 4.18 (c) with very few smaller agglomerates. The sizes of the pristine MMT tactoids were obtained around 22 to 26 nm (Fig. 4.18 [b]) whereas MMT Cu ranged from 15 nm to 23 nm (Fig. 4.18 [d]). The reduction in the size may be related to the ion exchange between the Na^+ ions from the MMT gallery with the Cu^{2+} from the transition metal ions. The comparison between the pristine Cloisite Na^+ clay and copper modified Cloisite Na^+ clay demonstrates a notable impact of the modification done.

4.3.2.3 Structural Characterization

XRD analysis was further employed to differentiate the structure of the pristine Cloisite Na^+ and the modified Cloisite Na^+ . The samples were scanned in fixed step size 0.020 with a step time of 0.1s in the range of 3-20°. Figure 4.19 shows a comparison of pristine Cloisite Na^+ and Cloisite Na^+ modified with copper (Cu).

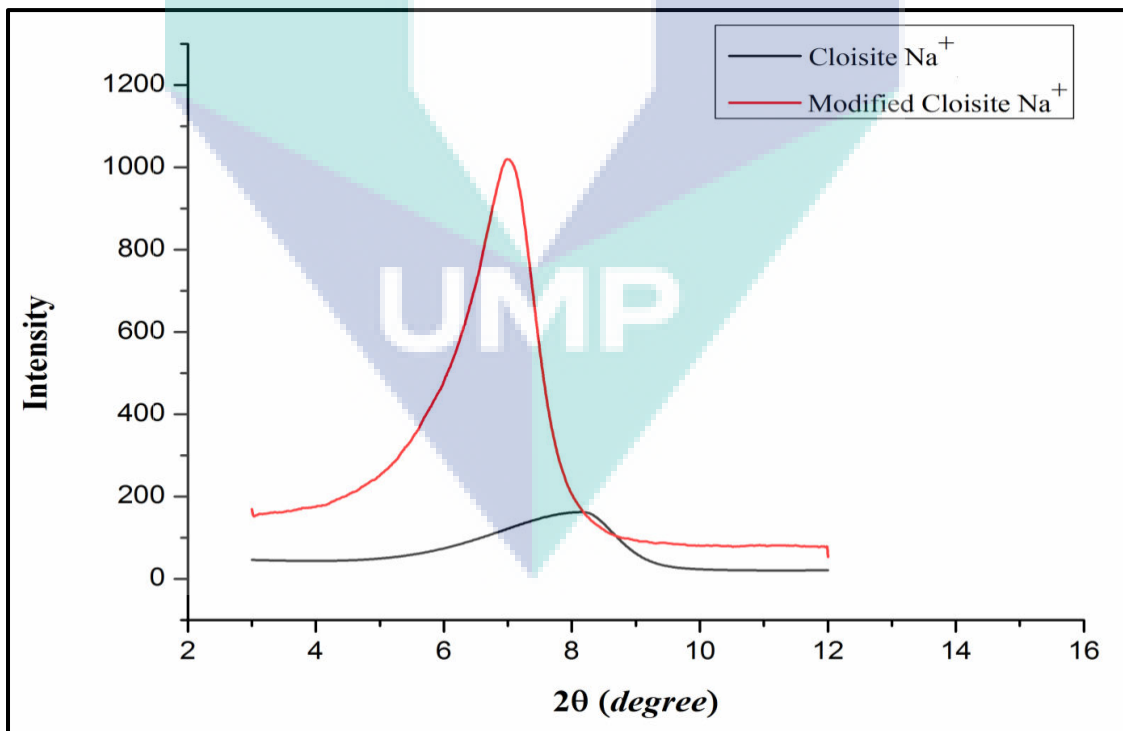


Figure 4.19 XRD Patterns of pristine Cloisite Na^+ and modified Cloisite Na^+

Based on Figure 4.19, the characteristic peak of pristine Cloisite Na⁺ appeared at $2\theta = 8.17^\circ$ and corresponded to the inter layer space of 10.81 Å. The X-ray data obtained for modified Cloisite Na⁺ is seen to shift to a smaller angle towards the left. The characteristic peak of Cloisite Na⁺- Cu was seen at $2\theta = 7.09^\circ$ with an interlayer spacing of 12.45 Å. Increase in the d-spacing of the modified nanoclay indicates that the modified ions were able to intercalate themselves into the gallery of Cloisite Na⁺ and there is a higher tendency for the formation of an exfoliated or intercalated structure during the fabrication with PP and other WPC constituents. Similar observations were reported by Nakas and Kaynak (2009) who stated that a modification of nanoclay improves the interlayer spacing.

4.3.3 Characterization of Wood-Plastic Composites reinforced by Pristine and modified nanoclay

4.3.3.1 Morphological Characterizations

Scanning Electron Microscope (SEM) was used to examine the dispersion of pristine and modified nanoclay inside the composite as well as the interface analysis of WPC. Figure 4.20 (a) and (b) shows the SEM micrograph obtained from WPC with 1 wt% and 2.5 wt% MMT. There were visible WF particles pull out, cracks and holes on the composite surface. This may be caused by the weak compatibility among composite constituents. Furthermore, the effect of incorporation of high loading of pristine nanoclay can be seen in Figures 4.20 (c) and (d). Each sample demonstrated the presence of large aggregates with distinct sphere like grains and this surface morphology may be associated to the layered structure of the MMT nanoclay. Analogous findings were reported by Yapar (2009). The presence of these aggregates may be related to poor distribution of the nanoclay in the matrix as MMT nanoclay is known to have a very high tendency to agglomerate during the fabrication process due to its lamellae structure. Moreover, MMT nanoclay possesses a hydrophilic nature in its pristine state. It is known that PP is a hydrophobic polymer and a homogeneous dispersion of the MMT nanoclay into PP matrix can never be achieved due to the intrinsic incompatibility of hydrophilic layered silicates and hydrophobic polymers (Vaia et al., 1999).

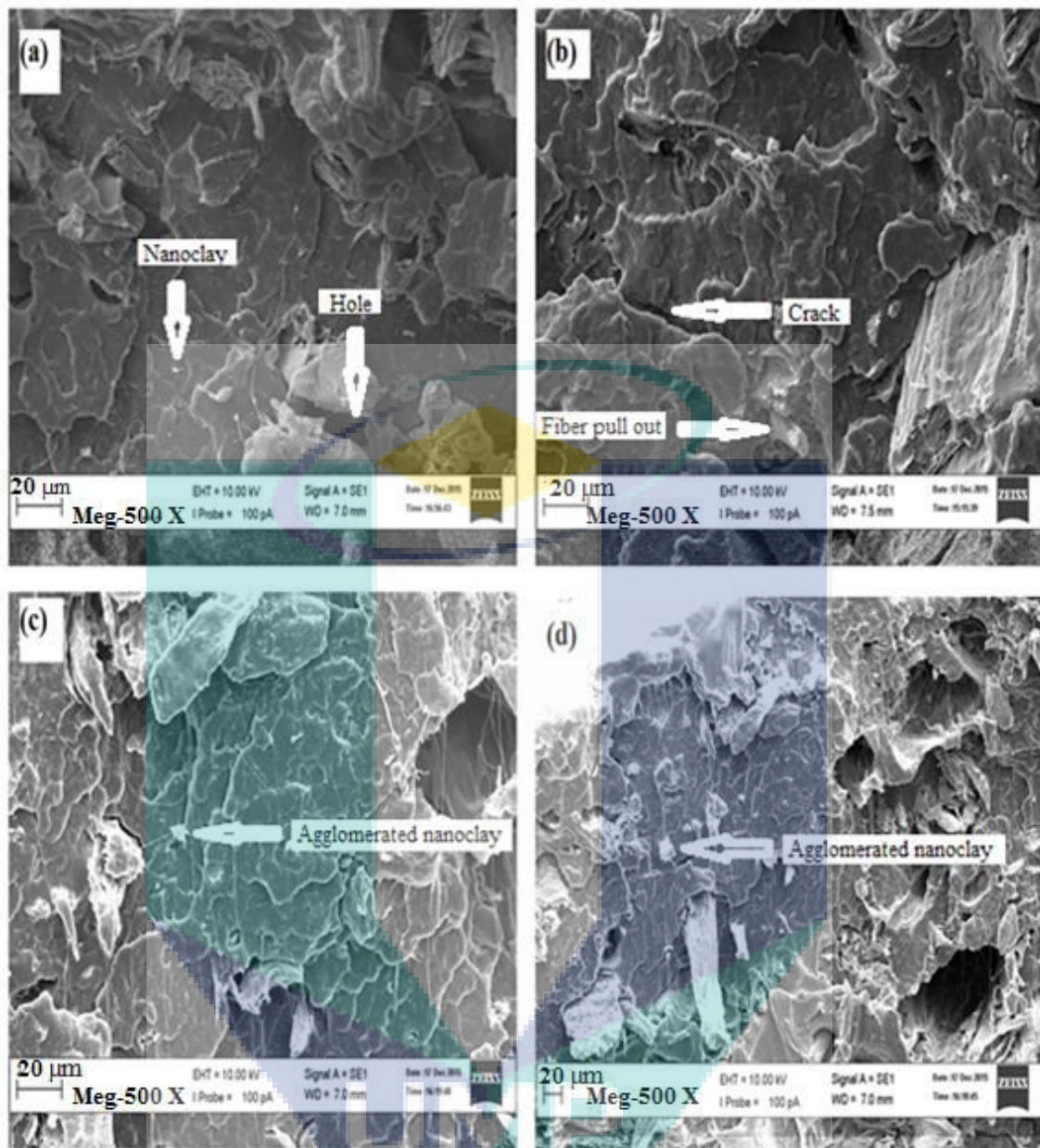


Figure 4.20 SEM micrographs of WPC with (a) 1 wt%, (b) 2.5 wt%, (c) 4 wt%, and 5 wt% MMT (pristine nanoclay)

The TMI modification was carried on the nanoclay in order to develop a better dispersion of the nanoclay in the polymer matrix. The replacement of interlayer cations through ion exchange reactions enables natural nanoclay to be compatible with the polymer matrix (Krishnamoorti et al., 1996).

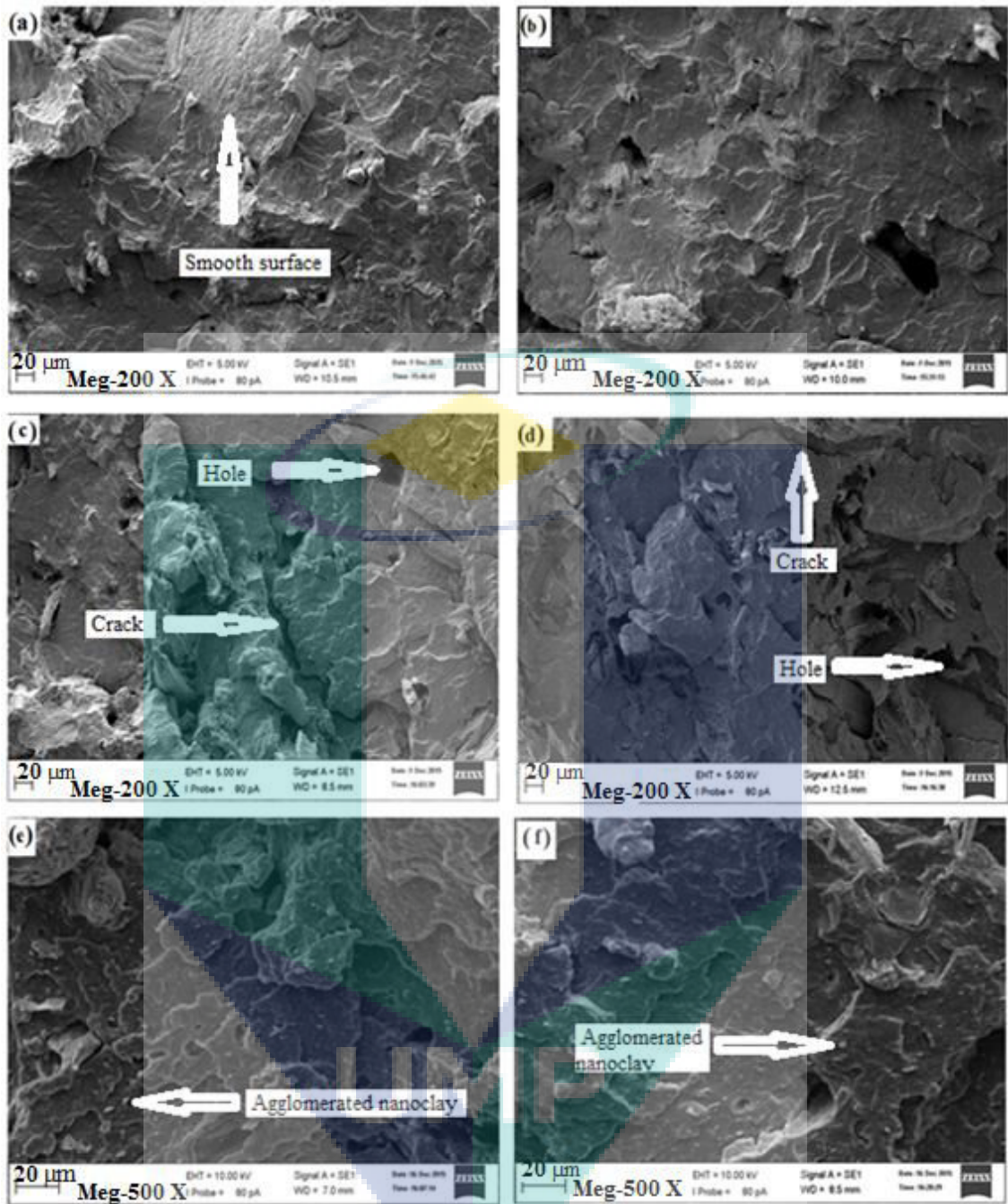


Figure 4.21 SEM micrographs of WPC with (a) 1 wt%, (b) 2.5 wt%, (c) 4 wt%, (d) 5 wt% (lower magnification 200 X) and (e) 4 wt%, (f) 5 wt% (higher magnification 500 X) MMT Cu (modified nanoclay)

The ion exchange reaction with cationic surfactants was able to modify the interlayer interactions by lowering the surface energy of the inorganic component and improve the nanoclays wetting characteristics with the polymer (Bulmstein, 1965 and Theng, 1979). This can indeed be seen in Figures 4.21, (a) and (b) of WPC/MMT Cu whereby the compatibility of the nanoclay were seen to improve. Figures 4.21, (a) and

(b) exhibit the SEM micrographs of WPC with 1 wt% and 2.5 wt% TMI-modified nanoclay. A relatively uniform and smooth surface with less holes and cracks is formed in contrast to the SEM images of WPC/MMT. However, Findings of a report by Dimitry et al. (2010) accounted that the tendency of the nanoclay to distribute itself evenly at high nanoclay loading is seen to be difficult, as with more nanoclay particles, the nanoclays are more prone to agglomerate and this makes it unable to form a uniform dispersion and distribution of the nanoclay in the polymer matrix. The uneven dispersion of nanoclay may create holes and cracks on the composite surface. As can be seen in Figure 4.21 (c) and (d), there were large number of holes and cracks on composite surface. Figure 4.21 (c) and (d) show the SEM micrographs of WPC with 4 wt% and 5 wt% modified nanoclay at lower magnification (200 X). Furthermore, in Figures 4.21 (e) and (f), Flake like images of the nanoclay were detected. As discussed earlier, it was the agglomeration of nanoclay due to the high loading of nanoclay into the composite. Figure 4.21 (e) and (f) show the SEM micrographs of WPC with 4 wt% and 5 wt% modified nanoclay at higher magnification (500 X). Wang et al. (2008) found identical results in their analysis and they justified that the ion exchange reactions that occurred during the TMI modification might have increased the interlayer distance and enabled the assumption that the particles are intercalated with larger distances. The same assumption can be presumed in this work as these nanocomposites did portray an intercalated form which was confirmed in the XRD data from Figure 4.19. Wang et al. (2008) found similar result in their work.

It can be seen from TEM images that the quality of dispersion and distribution of the layered silicates were correlated to the amount of nanoclay loading and the TMI modification done on the nanoclay particles as shown in Figure 4.22. The samples analyzed were WPC with 1 and 5 wt% MMT and WPC with 1 and 5 wt% MMT Cu, and the nanocomposites were magnified to 100 nm in order to obtain a clearer and in depth picture of the nanoclay particles and aggregates. It can be observed that structure of WPC incorporated with 1 wt% MMT as depicted in Figure 4.22(a) as compared to WPC with 1 wt% MMT Cu (Figure 4.22 [c]) shows the dark line of nanoclay. The dark line of nanoclay indicates the agglomerations of the layered silicates.

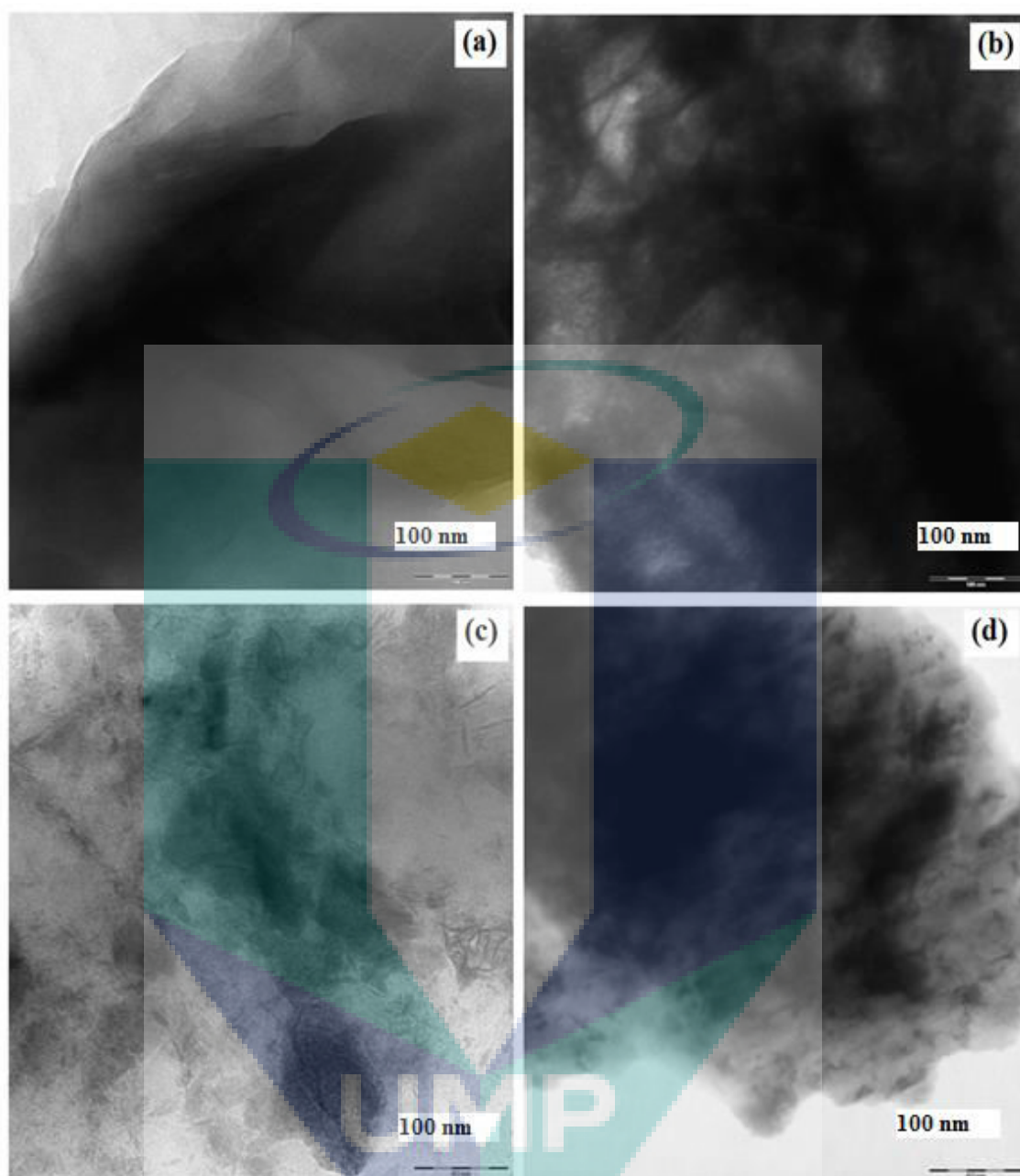


Figure 4.22 TEM micrographs of WPCs with (a) 1 wt% MMT, (b) 5 wt% MMT, (c) 1 wt% MMT Cu, and (d) 5 wt% MMT Cu (100 nm scale)

However, in Figure 4.22 (c), the multi layered nanoclay platelets intercalated with PP in the WPCs and the particles did not flocculate in the sample. It can be observed that the modification done on the nanoclay particles has enhanced its dispersibility on the polymer matrix and helped to lower the surface energy of the host, improved the wetting characteristics and intercalation with the polymer matrix which resulted in larger interlayer spacing as supported by the XRD analysis done. It is worth to mention that the TMI modification on the nanoclay particles has indeed aided in

better dispersion and the ability to create better compatibility between nanoclay and polymer matrix.

Furthermore, Figure 4.22 (b) and (d) shows the TEM images of WPC with 5 wt% MMT and MMT Cu, respectively. As can be seen in Figures, both the images shown the dark lines and the dark spots of nanoclay. It means the size of nanoclay particles became larger and reduced the number of intercalated platelets. As mentioned in SEM result that the high loading of nanoclay are more prone to the agglomeration.

4.3.3.2 Structural Characterizations

In this work, FTIR analysis was carried out to study the chemical structure of WPC/MMT and WPC/MMT Cu and to identify whether the nanoclay has been blended with polymer matrix and chemically bonded with polymer chains. Figure 4.23 and 4.24 show the FTIR spectra of PP, WPC, WPC/MMT and WPC/MMT Cu with different content of nanoclay.

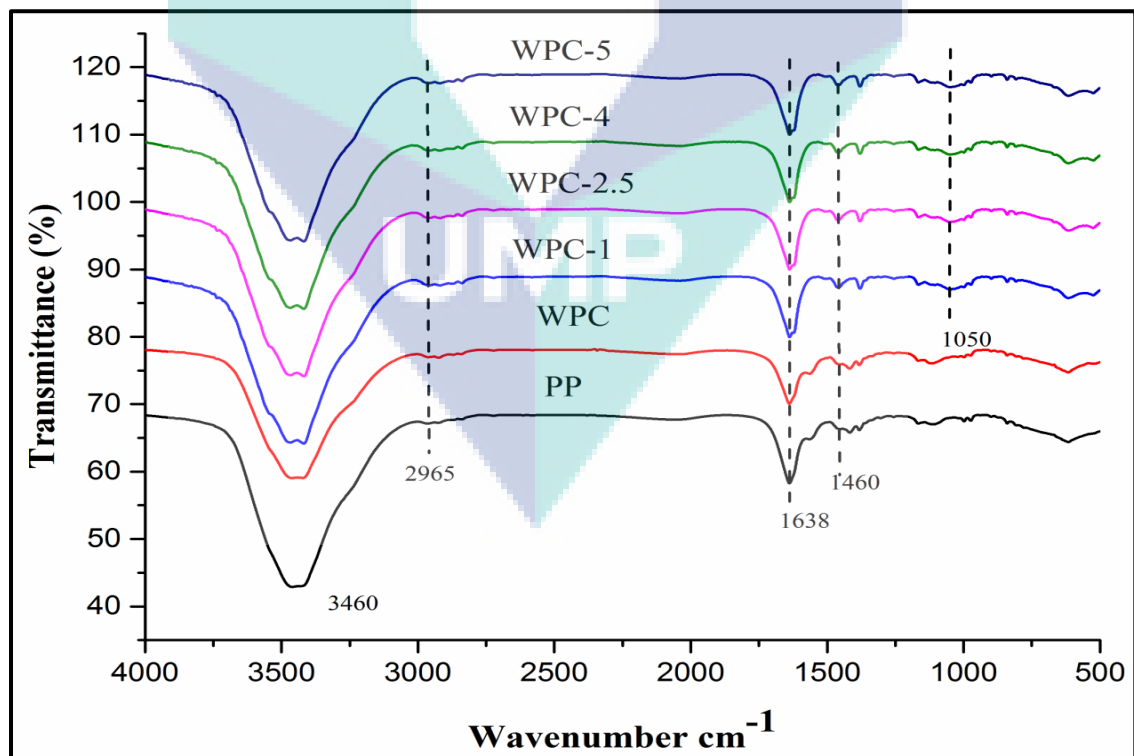


Figure 4.23 FTIR spectra of neat PP, WPC and WPC/MMT made with different content of nanoclay

A strong adsorption peak that were observed at 3200-3460 cm^{-1} shows the hydrogen bonded (O-H) and O-H stretch in the spectrum of the PP and WPC. While the existence of CH stretching can be detected in the region of 2850-3000 cm^{-1} . The peak between 1600-1730 cm^{-1} reveal the C=O stretching of the acetyl groups (Sgriccia et al., 2008). The peak at 1450-1460 cm^{-1} attributed to CH_2 bending vibration. This peak is due to the vibration of nanoclay (Alhuthali et al., 2012). In order to verify this during the formation of WPC/MMT and WPC/MMT Cu all spectra were recorded which are shown in Figure 4.23 and 4.24.

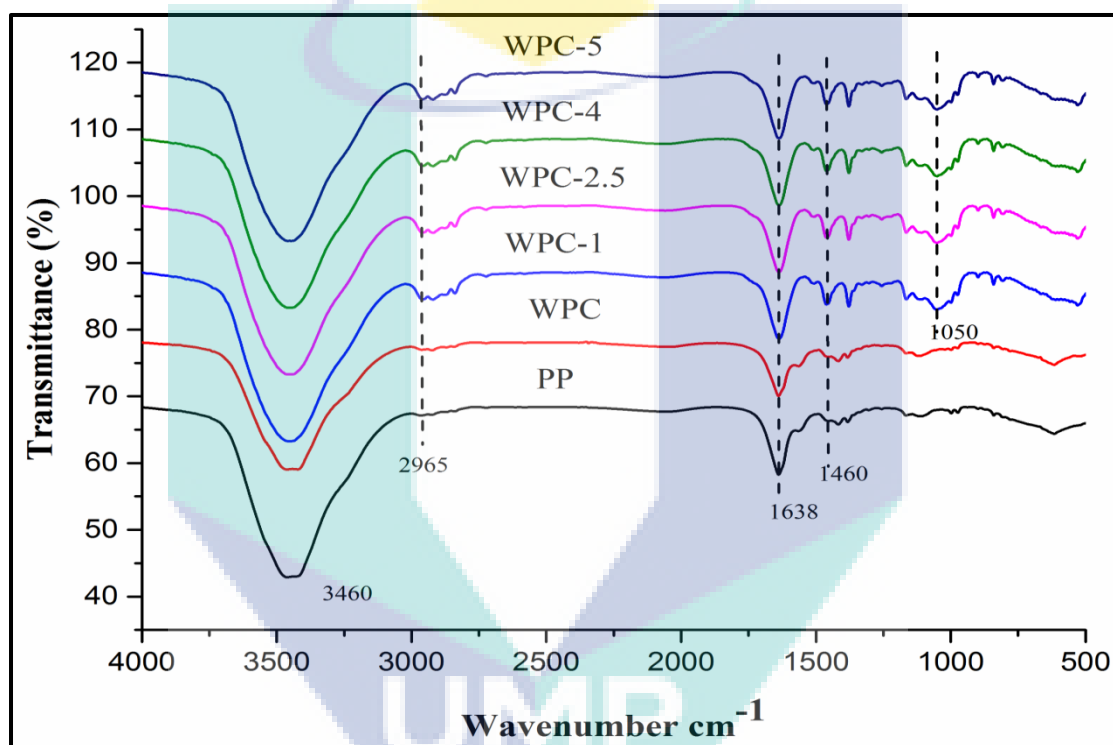


Figure 4.24 FTIR spectra of neat PP, WPC and WPC/MMT Cu made with different content of nanoclay

It is important to mention here, there is an occurrence of an absorption band at 1000-1110 cm^{-1} in figures 4.23 and 4.24. This occurrence is an indication of the existence of silica oxide (Si-O) bond due to the loading of nanoclay silicates into the polymer matrix. Silica is the dominant constituent of MMT whereby it is present in the tetrahedral layer of the clay. The tentative assignments of the main absorption bands of the FTIR analysis are illustrated in Table 4.6.

Table 4.6 Tentative FTIR peaks Assignments of Wood-plastic composite with different content of MMT and MMT Cu

Wavenumber (cm^{-1})	Assignment
3460	Hydrogen bonded (O-H)
2965	Stretching of C-H
1638	Free C=O
1460	CH ₂ bending
1042	Bending of Si-O

It can be concluded from the above visual observation and spectral analyses that the layered silicates (Si-O) were able to disperse in PP. However, as can be seen in figures 4.23 and 4.24, compared to WPC/MMT, there is a difference in the broadness and sharpness of the peak at the area $1000\text{-}1110\text{ cm}^{-1}$. The WPC/MMT Cu has shown sharp and broad peak of layered silicates over WPC/MMT silicates peak. It means, dispersion or mixing of layered silicates in WPC/MMT Cu was more uniform than WPC/MMT. As discussed earlier, TMI modification reduced the sizes of nanoclay tactoids and improved dispersion of nanoparticles into the composites.

From Figures 4.25 and 4.26, it can be observed that the structures of the WPCs were greatly influenced by the modified and pristine MMT filler content. The structures of the WPC incorporated with different types of filler and weight percentage showed a variety of changes in its angular spacing and reflection angle. The XRD pattern obtained, were highly dependent on the quantity and the quality of the filler content.

The data from XRD analysis showed that WPC/MMT with 1 wt%, 2.5 wt%, 4 wt% and 5 wt% showed characteristic diffraction peaks at $2\theta = 6.71^\circ$ (d-spacing is 13.18 Å), $2\theta = 6.31^\circ$ (d-spacing = 14.03 Å), $2\theta = 6.82^\circ$ (d-spacing = 13.44 Å) and $2\theta = 6.83^\circ$ (d-spacing = 13.39 Å) respectively. From the data obtained, WPC incorporated with modified nanoclay portrayed a smaller 2θ value over WPC/MMT that corresponds to

higher angular spacing which indicates that a successful intercalation process has been achieved. WPC/MMT Cu demonstrated reflection angles of 6.61° (d-spacing is 13.82 \AA), 6.02° (d-spacing is 14.63 \AA) 7.18° (d-spacing is 12.88 \AA) and 6.80° (d-spacing is 13.11 \AA) in its 1wt%, 2.5 wt%, 4 wt% and 5 wt% nanoclay loadings.

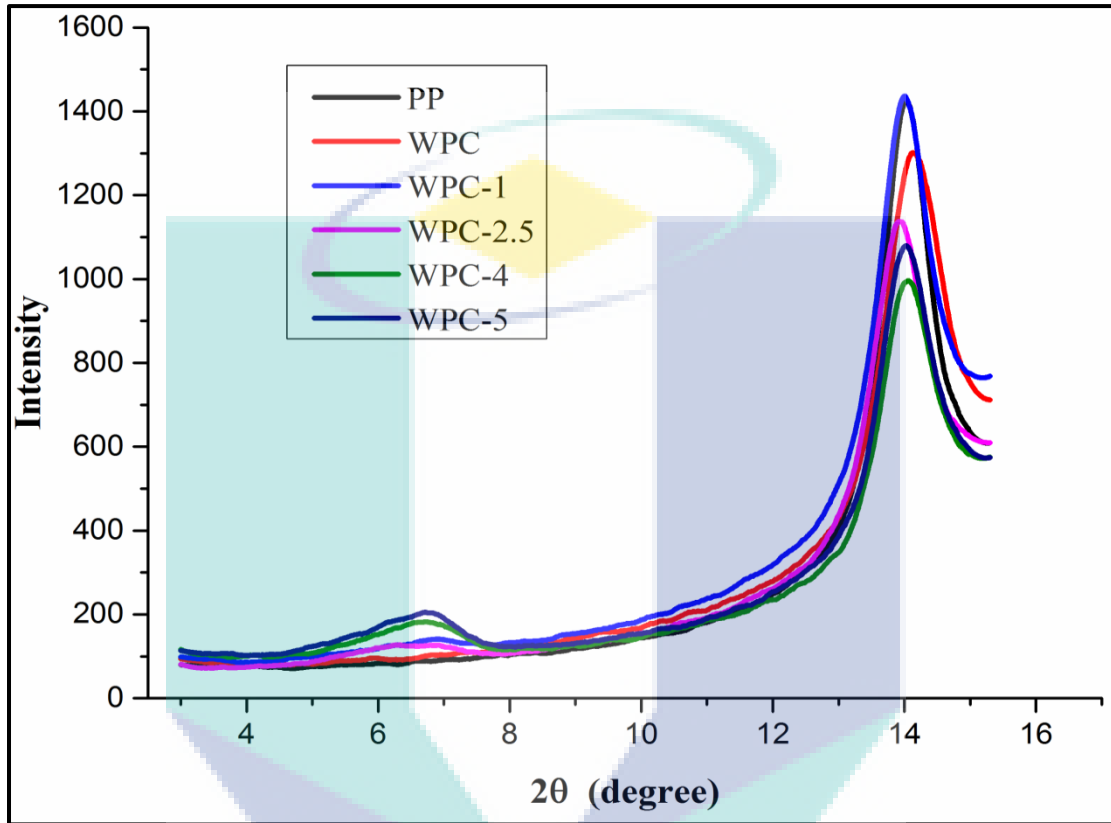


Figure 4.25 XRD diffractograms of neat PP, WPC and WPC/MMT made with different content of nanoclay

The peaks of the modified clay nanocomposites which were seen to shift towards a lower value, it is an indication that an intercalated clay structure has been created. According to Wang and Pinnavaia (1998), the gallery spacing in modified clay becomes larger as a resultant of the longer chain in the nanoclay relative to the conventional nanoclay whereby the extent of gallery expansion is highly dependent on the chain length of the modifier in the interlayer. Nafchi et al., (2015) found that in their work that incorporation of Cloisite 30B into the PP-based WPC shows an increase in the d-spacing of the composite compared to the incorporation of pristine nanoclay.

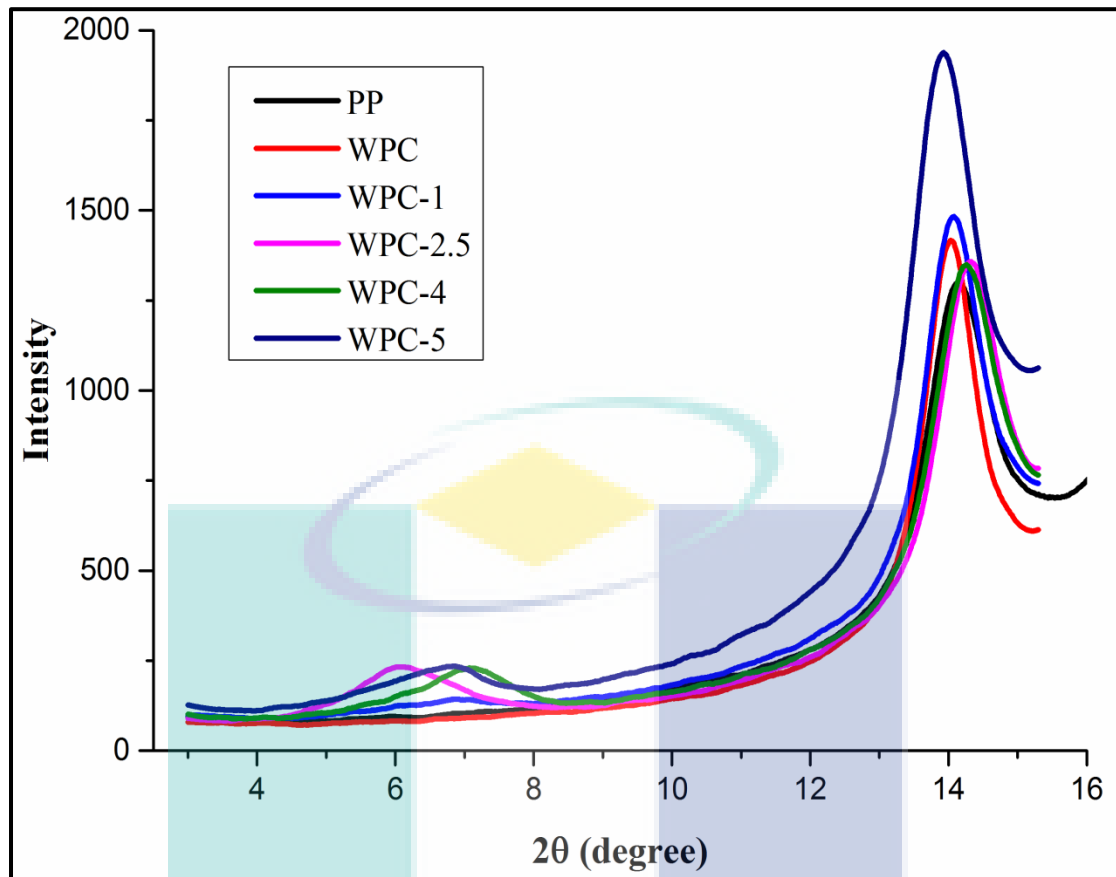


Figure 4.26 XRD diffractograms of neat PP, WPC and WPC/MMT Cu made with different content of nanoclay

According to Nafchi et al., (2015), the modifiers in Cloisite 30B aided in increasing the gallery height and made the layer separation more, as the modifier inside the layer weakens the electrostatic forces between the silicate layers. In this study, the TMI modification process is seen as a method to change the nature of the nanoclay from being hydrophilic to hydrophobic and thus accommodating a higher driving force of the PP into the nanoclay. This resulted in the increase of the d-spacing. The even distribution of the modified MMT clay can be viewed from the TEM images in Figure 4.22 (a) and SEM micrographs from Figures 4.21 (a) and (b) that show the uniform dispersion of the nanoclay into the composite with no visible agglomerates. It can be deduced from this that the TMI modification done has promoted an intercalation process in the nanocomposites. Table 4.7 summarizes the interlayer spaces of the nanocomposites.

Table 4.7 The value of angular spacing, d and reflection angle, 2θ of the PP, WPC and WPC with different content of MMT and MMT Cu

Composite	Nanoclay loading (wt %)	2θ (degree)	d (Å)
PP		14.08	6.28
WPC		13.88	6.37
WPC/MMT	1	6.71	13.18
	2.5	6.31	14.03
	4	6.82	13.44
	5	6.83	13.39
WPC/MMT Cu	1	6.61	13.82
	2.5	6.02	14.63
	4	7.18	12.88
	5	6.81	13.10

4.3.4 Mechanical Properties

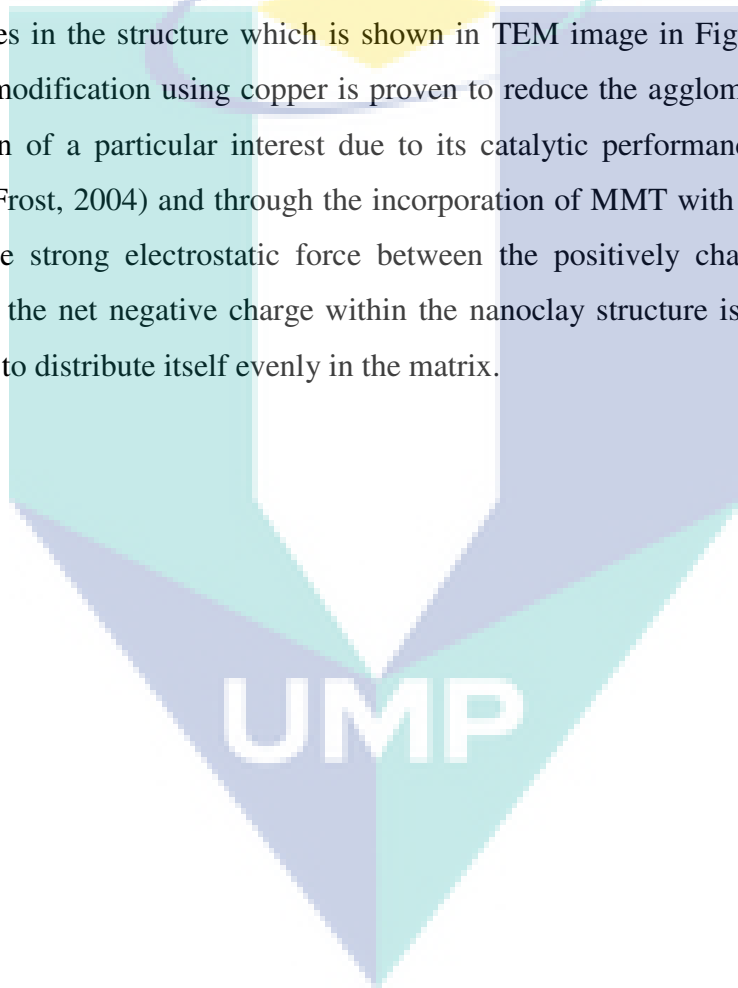
In this section, the mechanical properties of wood-plastic composite with pristine nanoclay and modified clay with copper are discussed.

4.3.4.1 Tensile Properties

According to the results obtained, the incorporation of nanoclay in the WPC promoted an increment in the tensile strength as can be seen in Figure 4.27. WPC/MMT with 1 wt% nanoclay loading exhibited 6% increment in tensile stress compared to WPC without nanoclay. The highest increment among these four different percentages of nanoclay loading was seen on 2.5 wt% WPC/MMT which was 8%. There was not much improvement in the tensile stress of WPC/MMT as compared to WPC/MMT Cu due to the nanoclay agglomerations as shown in the SEM analysis which is shown in Figure 4.20. It can be presumed that the incompatibility of MMT nanoclay with PP was unable to create a good dispersion of these particles in the matrix. Successful strengthening of the interfacial interactions between the dispersed phase and matrix phase could not be achieved in the case of WPC/MMT. Dowling et al. (2006)

anticipated that the modification of the nanoclay reduces the agglomerates and helps to intercalate the MMT platelets.

In line with them, the modification done on the nanoclay did indeed result in higher values of tensile stress over to WPC and WPC/MMT. In general, from the results attained, it can be seen in Figure 4.27, that the tensile stress of WPC/MMT Cu was higher compared to WPC/MMT. The highest leap of 16 % was seen in 1wt% nanoclay loading followed by 14 % increase in 2.5 wt% WPC/MMT Cu as compared to the WPC. The higher increase as compared to WPC/MMT is due to lesser nanoclay agglomerates in the structure which is shown in TEM image in Figure 4.22 (c) and in which the modification using copper is proven to reduce the agglomerates. Copper has always been of a particular interest due to its catalytic performance in the reactions (Ding and Frost, 2004) and through the incorporation of MMT with modified nanoclay into PP, the strong electrostatic force between the positively charged ions that are attracted to the net negative charge within the nanoclay structure is destroyed and the clay is able to distribute itself evenly in the matrix.



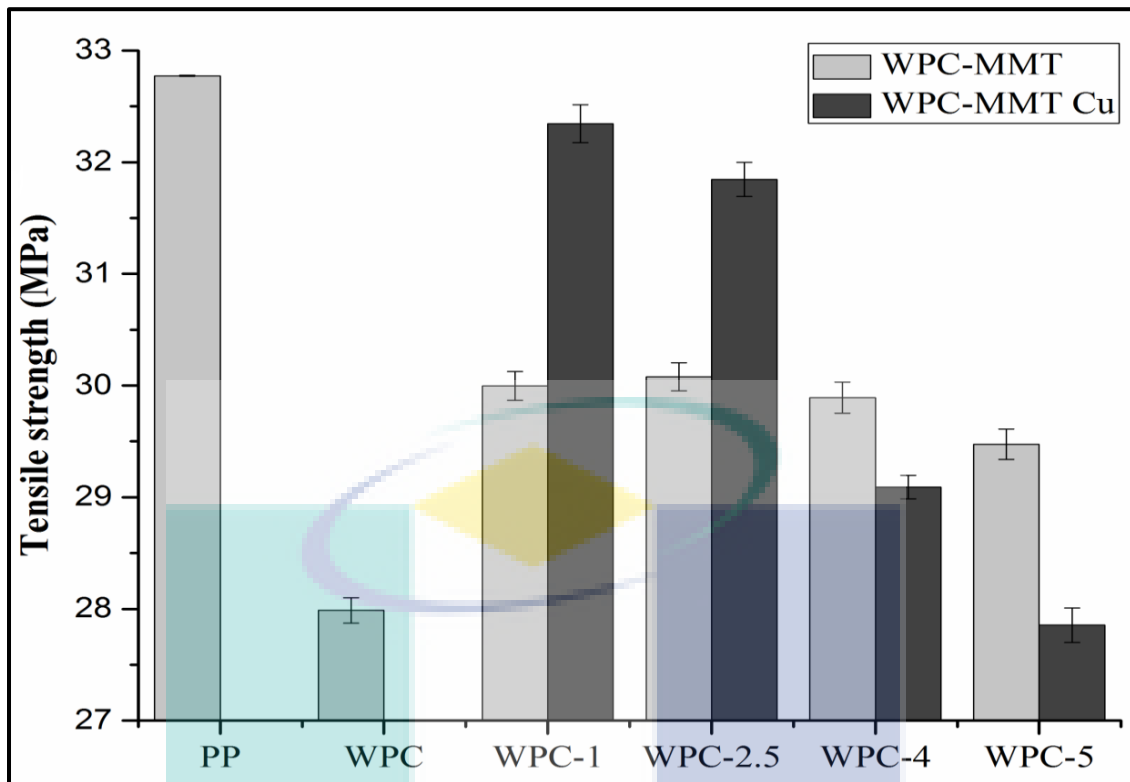


Figure 4.27 The effect of MMT and MMT Cu nanoclay loading on tensile strength of WPC

However, it can be seen from Figure 4.27, a decrement of tensile stress from 1 wt% clay loading to 5 wt% was observed in both WPC/MMT and WPC/MMT Cu. This decrease could be attributed to the high nanoclay content in the matrix in which the nanoclay is more prone to agglomerate rather than being distributed evenly in the matrix. Other researchers who found similar results were Isik et al. (2003) and Chang et al. (2003). They argued that at high nanoclay contents, clay particles agglomerates and act as stress concentrators that decreases the strength. However, in general, it can be seen that the incorporation of modified clay into the WPCs has brought forth significant improvement in the tensile stress.

Furthermore, Figure 4.28 shows the tensile modulus of WPC reinforced by pristine and copper modified nanoclay. As can be seen from figure, with increasing nanoclay (MMT) content into the composite, the tensile modulus of composites had increased. The tensile modulus value was increased by 28.61 % compared to the control sample that had reached at 579.68 MPa at 5 wt% of MMT loading.

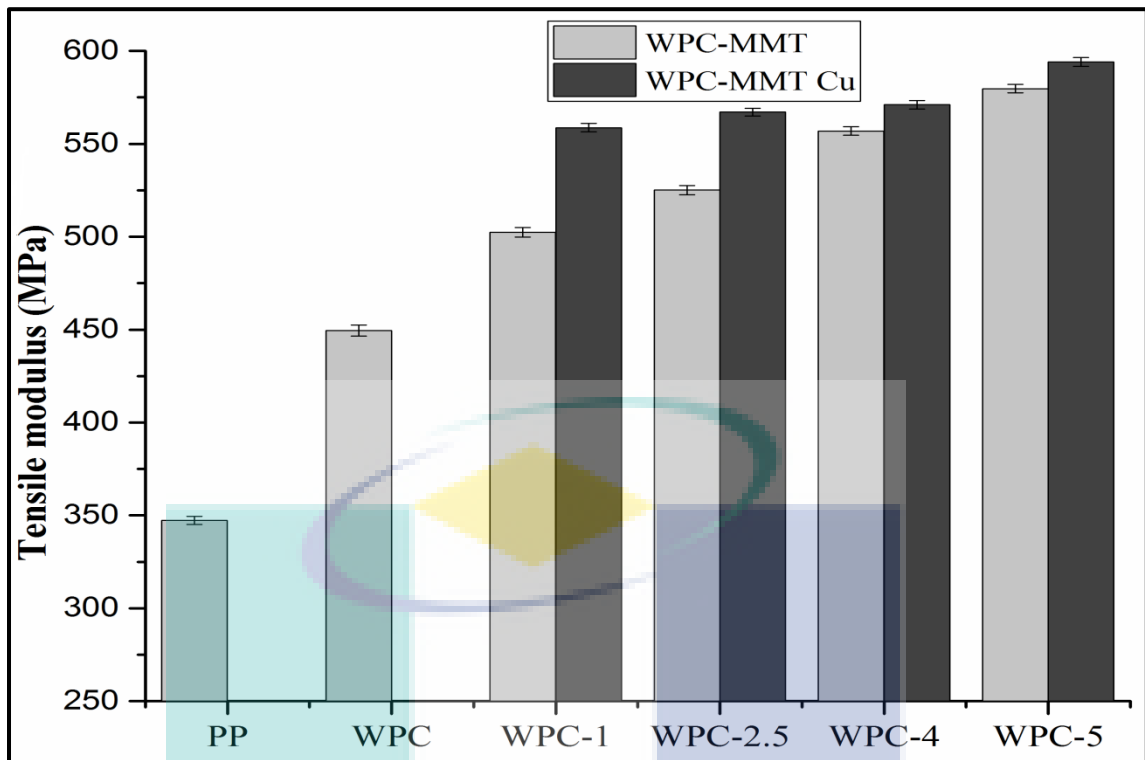


Figure 4.28 Tensile modulus of PP, WPC, and WPC with different content of MMT and MMT Cu nanoclay

However, with the same content of MMT Cu into the WPC, the tensile modulus value increased by 30.01% over WPC and reached at 594.10 MPa. The higher enhancement in WPC/MMT Cu over WPC/MMT might be related to the reduced size of nanoclay particle and their well dispersion into the composite after modification process.

4.2.4.2 Flexural Properties

The flexural strength is always used to characterize the mechanical properties of composites as they provide a simple means of determining the bending response. This test provides significant information on the performance of the composites. The effect of pristine and modified nanoclay addition on the flexural strength of WPC is illustrated in Figure 4.29.

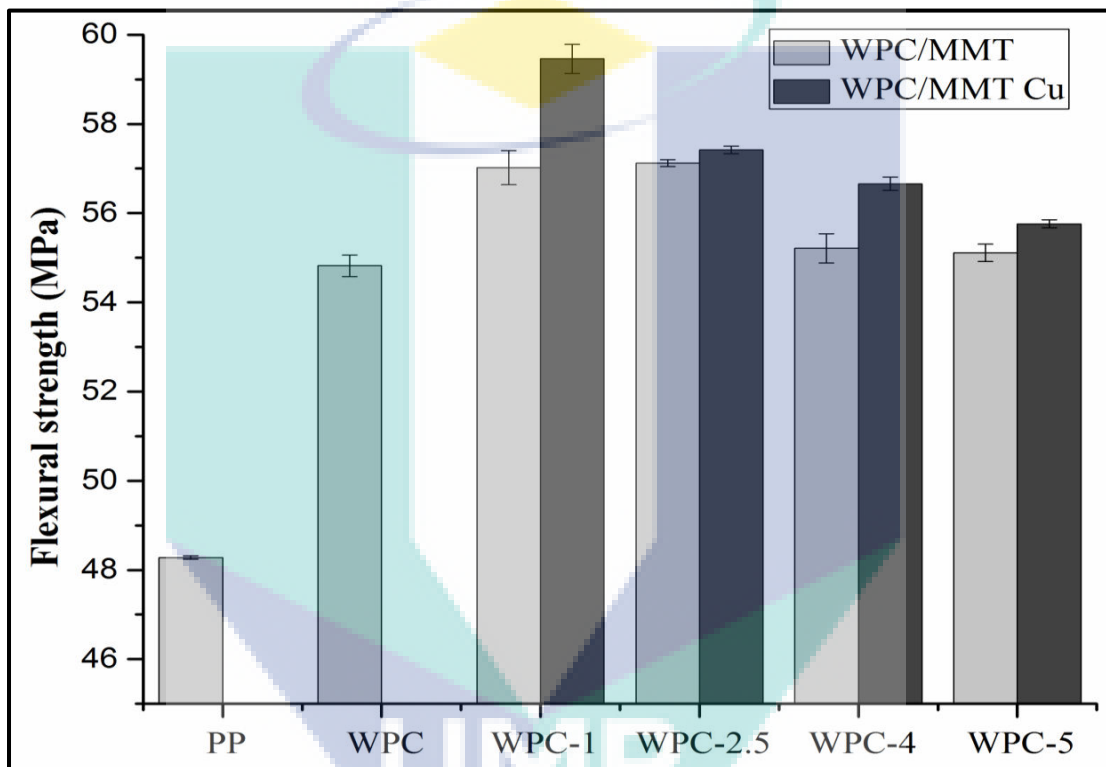


Figure 4.29 The effect of MMT and MMT Cu nanoclay loading on flexural strength of WPC

Experimental results reveal that the flexural strength of composites was increased at the 1 wt% content of MMT nanoclay compared to the WPC sample and it started to decrease as more MMT nanoclay was loaded. The flexural strength of the composite is mainly depended on the interfacial interaction and the properties of constituents (Kordkheili et al., 2012; Najafi et al., 2011). The flexural strength of the WPC has improved from 54.82 MPa in the control to about 57.02 MPa with 1wt% MMT. WPC/MMT with 1 wt% nanoclay loading showed 4% increment in flexural strength compared to WPC. As discussed in tensile strength result, like a tensile

strength, there was no significant enhancement in the flexural stress of WPC/MMT as compared to WPC/MMT Cu due to the nanoclay agglomerations as shown in the Scanning Electron Microscopy (SEM) analysis which is shown in Figure 4.20. The hydrophilic nature of MMT created the incompatibility of MMT nanoclay with PP and therefore it was unable to create a good dispersion of these particles in the matrix.

However, the WPC from copper modified nanoclay has shown higher values of flexural strength as compared to the WPC and WPC/MMT. At 1 wt% loading of modified nanoclay into the WPC showed 9 % increment of flexural strength over WPC. The flexural strength of WPC/MMT Cu at 1 wt% loading of nanoclay was 59.46 MPa. This improvement can be attributed to the better homogeneous dispersion and good interfacial interaction of the nano-particles throughout the matrix, which enabled effective stress transferring from matrix to fibers and then leading to high flexural strength. The higher improvement in WPC/MMT Cu as compared to WPC/MMT is due to lesser nanoclay agglomerates in the composite and modification of MMT is proven to reduce the agglomerates and improve the dispersion of nanoparticle into the composite.

Furthermore, as can be seen in Figure 4.29, with high loading, the nanoclay began to agglomerate, which resulted in poor dispersion in WPC and then the flexural strength started to decrease, so the composite with 5 wt% nanoclay in both WPC/MMT and WPC/MMT Cu revealed the minimum flexural strength, decreased by 4% and 6%, respectively over the WPC with 1 wt% nanoclay. As discussed in previous section that another reason for the lower strength from the addition of the nanoclay at 5 wt% could be related to the absorption of the coupling agent by the nanoclay. Larger amount of the nanoclay increases the absorption of the coupling agent. In this case, the coupling agent does not establish a proper connection between the matrix (polymer) and the lignocellulosic material (Yeh and Gupta, 2010).

As it could be seen from Figure 4.30, increased nanoclay loading increased the flexural modulus of WPC. The high aspect ratio of nanoclay increased the wettability of fillers by the matrix and transferred stress from polymer matrix to the fillers. WPC reinforced by MMT, increased the flexural modulus by 7.3% over WPC and reached at 1958.97 MPa at 5 wt% of nanoclay loading. Whereas, with same loading of MMT Cu

into the composite increased the flexural modulus by 8.05 % over control sample and reached at 1971.74 MPa. As mentioned earlier, modification of nanoclay reduced the size of nanoclay particles and improved the aspect ratio of nanoclay clay particles.

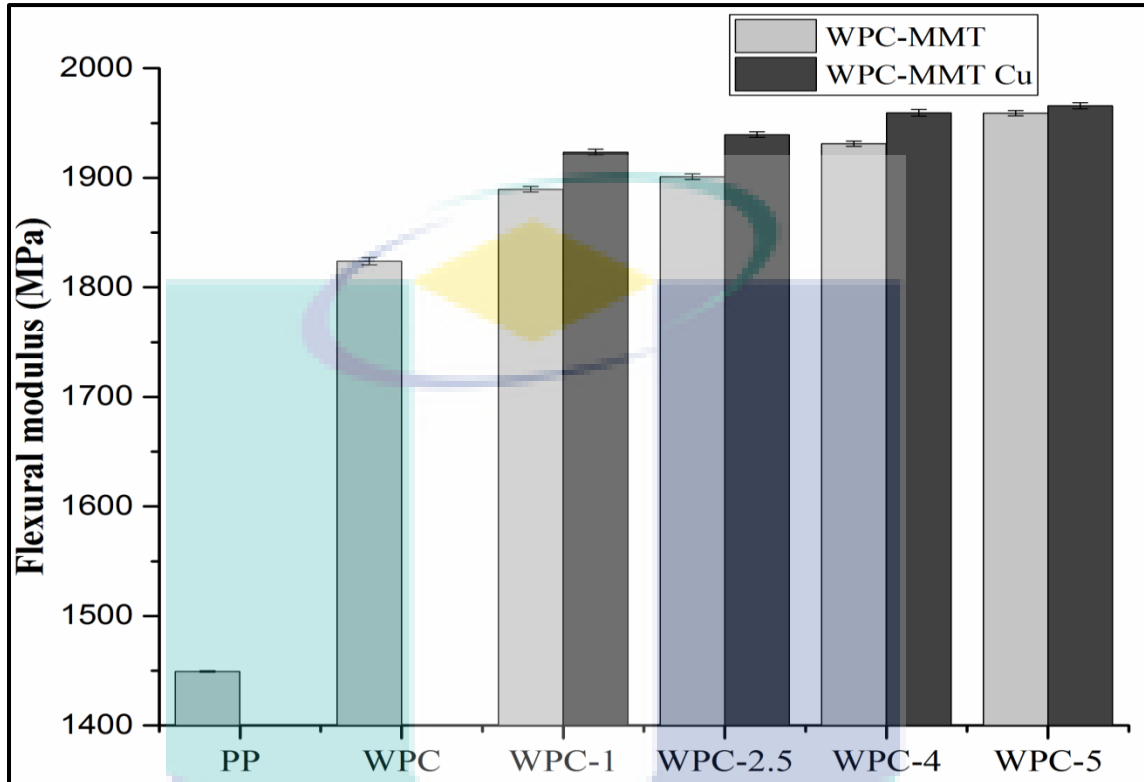


Figure 4.30 Flexural modulus of PP, WPC, and WPC with different content of MMT and MMT Cu

4.2.4.3 Elongation at break

In this work, there were four different weight percentages MMT and MMT Cu that were studied in this experiment which were 1wt%, 2.5 wt%, 4 wt% and 5 wt% nanoclay loading. Five samples were tested for each parameter and average mean value was taken. The elongations at break values of the PP and WPC are plotted in Figure 4.31.

Elongation at break (EB) value is highly dependent on the interfacial reactions between the polymer matrix and the nanoclay and from this work; the trend is noticed to be a direct reduction in percent elongation at break, with respect to increase nanoclay content. WPC/MMT with 1 wt%, 2.5 wt%, 4 wt% and 5 wt% nanoclay loading showed

an decreasing pattern in its EB values over neat PP and which were 175%, 190%, 199%, and 201% respectively whereas WPC/MMT Cu with 1 wt%, 2.5 wt%, 4 wt% and 5 wt% nanoclay incorporation exhibited a decrement of 115%, 124%, 125% and 185% respectively. Like the flexural and tensile strengths of WPC, elongation at break of composite also showed the higher values at 1 wt% nanoclay loading. The decrement observed in WPC/MMT Cu was the lowest over WPC/MMT.

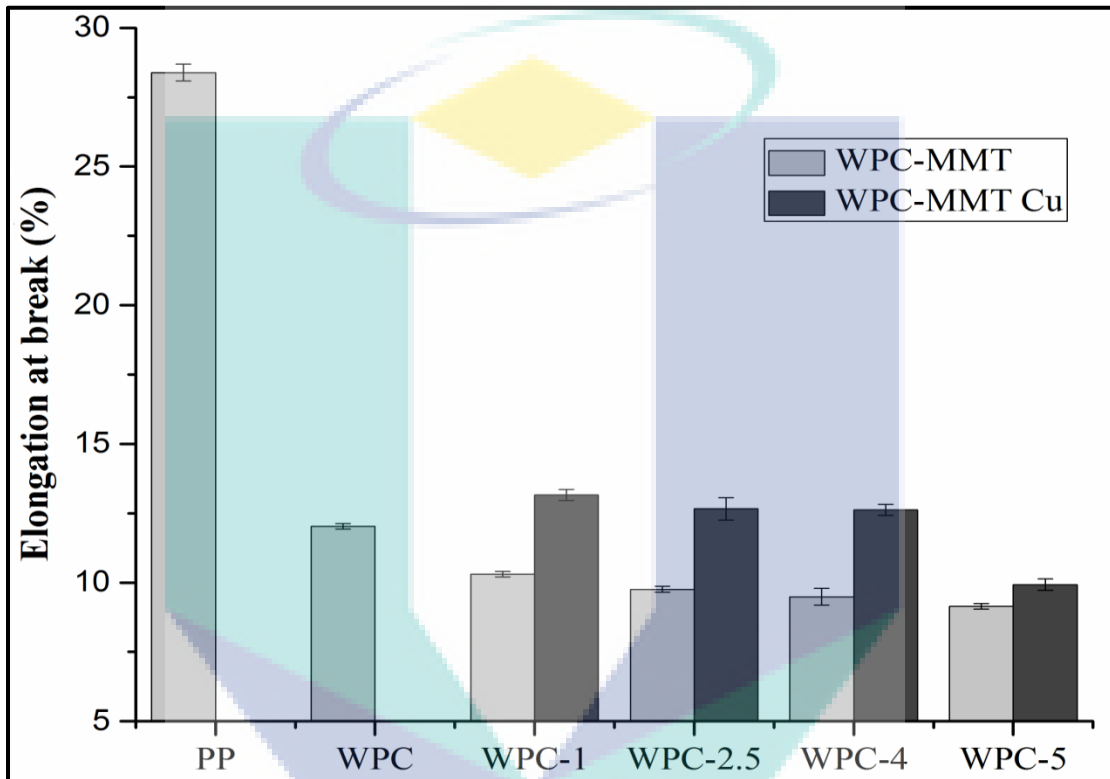


Figure 4.31 Elongation at break of PP, WPC, and WPC with different content of MMT and MMT Cu nanoclay

Abraham et al. (2009) mentioned that the incorporation of fillers to the polymer matrix decreases the EB value however if a good reinforcement can be achieved between the polymer and the filler. The fracture goes from particle to particle rather than following a direct path and the filled polymers move slightly near EB value with neat polymer. It can be observed from the data obtained that WPC with modified nanoclay exhibited higher EB value compared to WPC incorporated with conventional nanoclay and it could be deducted that the TMI modification process did improve the dispersion of the filler into the matrix and a good rearrangement of the filler particles were able to be obtained. Moreover, increasing trend in EB values may also be an

indicative of a good intercalation and phenomena which resulted in high strength reinforcement between the filler and matrix (Varghese et al., 2003). Finnigan et al. (2004) and Yao et al. (2002) reported similar findings in their work.

4.2.4.4 Izod Impact Strength

Impact strength shows the impact resistance of materials against breakage (Sheshmani et al., 2013). Figure 4.32 presents the Impact strength values for PP, WPC and WPC with different content of pristine and modified nanoclay. The test results revealed that the impact strength of composite had increased at first, shown higher strength at 1 wt% nanoclay content over other WPC. Then, the further addition of nanoclay decreased the impact strength. As can be seen in Figure, WPC/MMT with 1 wt%, 2.5 wt%, 4 wt% and 5 wt% nanoclay loading showed an decreasing order in its impact strength values and which were 15.45 J/m, 14.72 J/m, 13.97 J/m, and 11.22 J/m respectively whereas WPC/MMT Cu with same pattern of nanoclay content also exhibited decreased impact strength values which were 17.92 J/m, 15.86 J/m, 15.06 J/m and 12.84 J/m respectively.

Generally, the impact strength decreases, with increasing nanoclay loading (Cheng et al., 2003). As discussed earlier in section, the cause behind this decline might be the stiffening of polymer chains due to the incorporation of nanofiller and the agglomeration of nanoclay, which leads in absorbing less impact energy (Mohanty and Nayak, 2007). This kind of behaviour was also observed by Yeh et al., (2005).

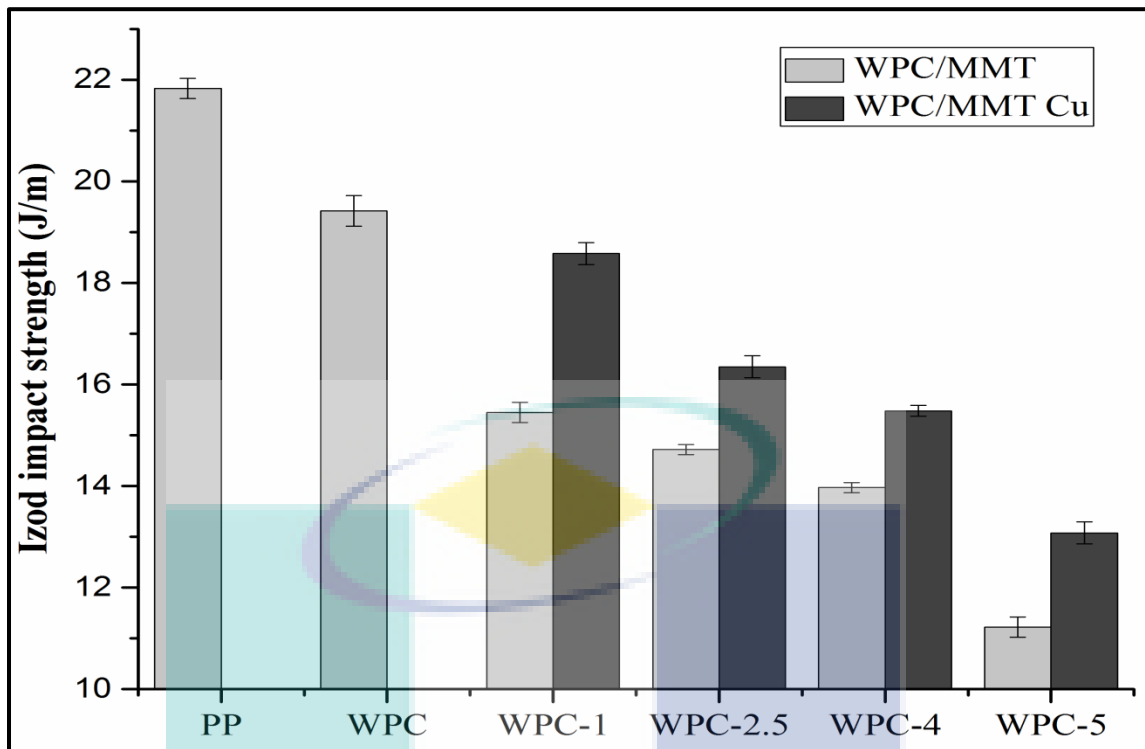


Figure 4.32 Izod impact strength of PP, WPC, and WPC with different content of MMT and MMT Cu nanoclay

However, it can be observed from the obtained data that WPC with modified nanoclay showed highest impact strength values of composite over WPC loaded with pristine or unmodified nanoclay. According to the analysed impact strength results of WPC, it can be concluded that the TMI modification process of pristine nanoclay reduced the agglomeration and improved dispersion of nanoparticles into the composite by reducing the tactoids sizes of nanoclay particles.

4.3.5 Physical Properties

In this segment, the effect of pristine and modified nanoclay reinforcement on physical properties of wood-plastic composite is explored. Density and Water absorption of PP, WPC, and WPC with different concentrations MMT and MMT Cu is discussed.

4.3.5.1 Density

The density of WPCs as a function of nanoclay content is plotted in Figure 4.33. From the Figure, the trend of density variation as a function of nanoclay content can be clearly seen. All WPCs containing nanoclay showed higher densities than neat PP and WPC without nanoclay. Incorporation of nanoclay increased the density of composite. The reason might be that the pore-filling role and well dispersion of nanoclay particles. The better improvement was achieved at 1 wt% of nanoclay. However, loading high content of nanoclay decreases the density of composite. The decrease in density at high content is due to the poor dispersion and agglomeration of nanoclay particles. This result of density is comparable to that of cement reinforced Organoclay composites, where the density of cement composites increased due to the incorporation of an optimum content of nanoclay in cement paste. However, at excessive amount of nanoclay loading, the density of composites decreased. The reduction of density is due to the agglomeration effect of nanoclay particles (Hakamy et al., 2014).

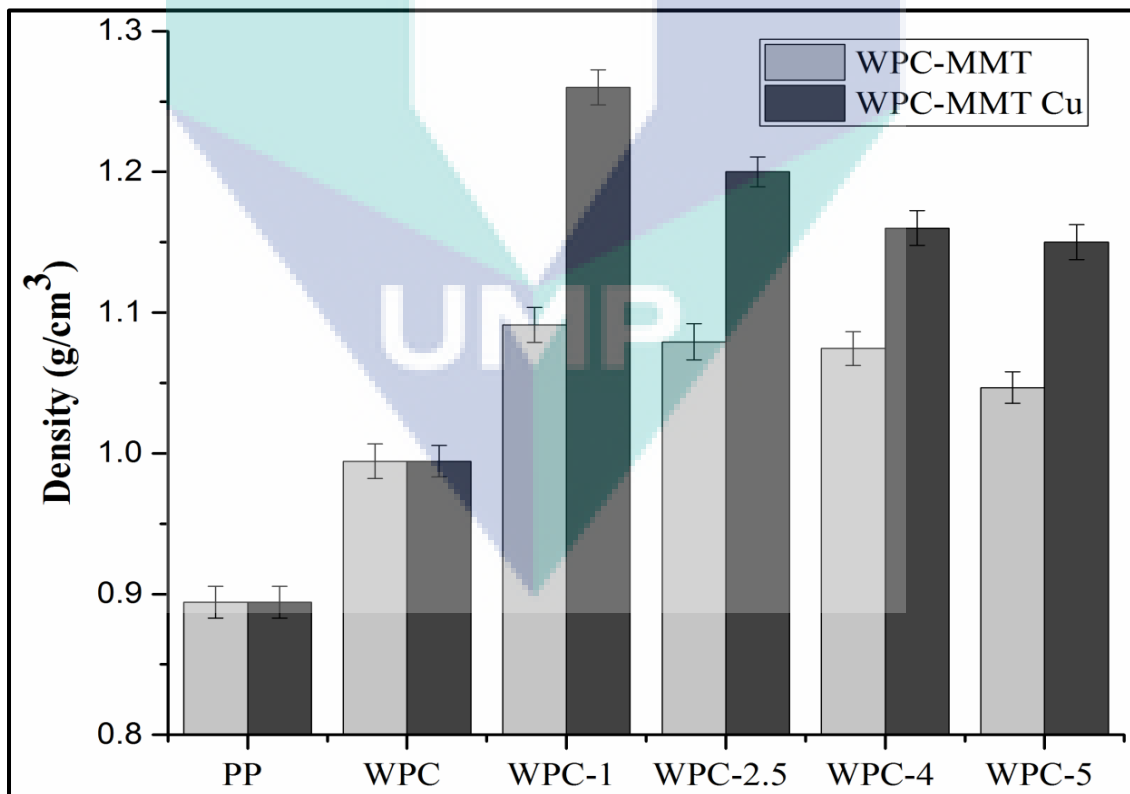


Figure 4.33 Density of PP, WPC and WPC with different content of MMT and MMT Cu nanoclay

However, WPCs made from modified nanoclay showed higher density over unmodified nanoclay-based WPCs. The TMI-modified nanoclay based WPC showed density of 1.26 g/cm^3 at 1 wt% of nanoclay, whereas unmodified nanoclay-based showed density of 1.09 g/cm^3 at same content of nanoclay. The nanoclay modification process reduced the sizes of nanoclay tactoids and promotes better nano particle dispersion, and thus the reduced tactoids sizes of modified nanoclay improved the pore-filling capacity of composites.

4.3.5.2 Water Absorption

Figure 4.34 and 4.35 exhibits the water absorption of PP, WPC and WPC loaded with MMT and MMT Cu after 15 and 30 days immersion in distilled water. Due to the constant level of wood flour (20 wt%) and coupling agent (2 wt%) content in all composites, the different water absorption values can be attributed to the role of nanoclay. It can be seen that neat PP absorbed a very negligible amount of moisture around 0.03% due to its hydrophobic nature. However, the amount of water absorption had suddenly increased with the incorporation of WF into PP. So, the content of wood flour in the composites and the micro gaps, voids and holes between matrix and filler would be ascribed to the water absorption values. With the high loading of WF into WPC would result in creating holes, cracks and gaps between WF and PP, since PP was not able to cover all of the WF, which weakens the interfacial adhesion between wood flour and PP. This hypothesis was confirmed by SEM micrographs (Figure 4.20).

WPC with 1 wt% loading of nanoclay showed the least water absorption in both WPC/MMT and WPC/MMT Cu. At 1 wt% loading MMT in WPC reduced the water uptake by 47% in 15 days water absorption and by 56 % in 30 days water absorption, whereas the same loading of MMT Cu in WPC reduced the water uptake by 76% in 15 days water absorption and by 95 % in 30 days water absorption over WPC sample. The reason might be that well dispersion of nanoclay was achieved for 1 wt%, which gave better interfacial bonding of nanoclay to the matrix and better water barrier performance.

Furthermore, adding excessive amounts of nanoclay increased the water uptake of all the composites. It was attributed to the agglomeration of nanoclay that has increased holes and crack fractions during the compounding process. This hypothesis was also confirmed by SEM images.

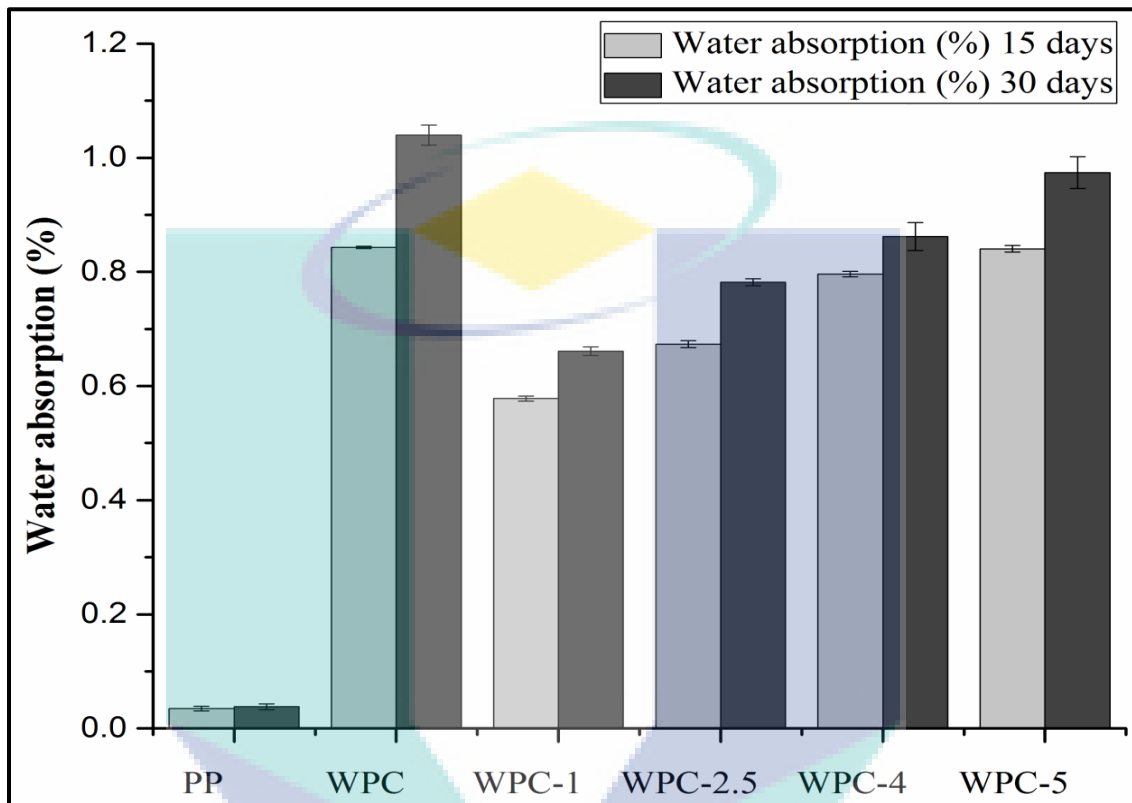


Figure 4.34 Water absorption of the WPC as function of MMT nanoclay loading

However, the results obtained showed that WPC/MMT Cu absorbed less water as compared to the WPC/MMT. The water absorption decreased significantly over WPC, when modified layered silicates was incorporated into the composite. This finding was in line with Mai and Yu (2006). In addition, Gusev and Lusti (2001) reported that a major factor accountable for the barrier property is the changes in the permeability of water due to the transformation of the molecular level in the polymer matrix that is caused by the silicate layers and directly related this to the molecular level interaction between the polymer matrix and the layered silicates. In addition, another reason might be that hydrophilic nature of pristine nanoclay which leads to absorbing more water into the composite.

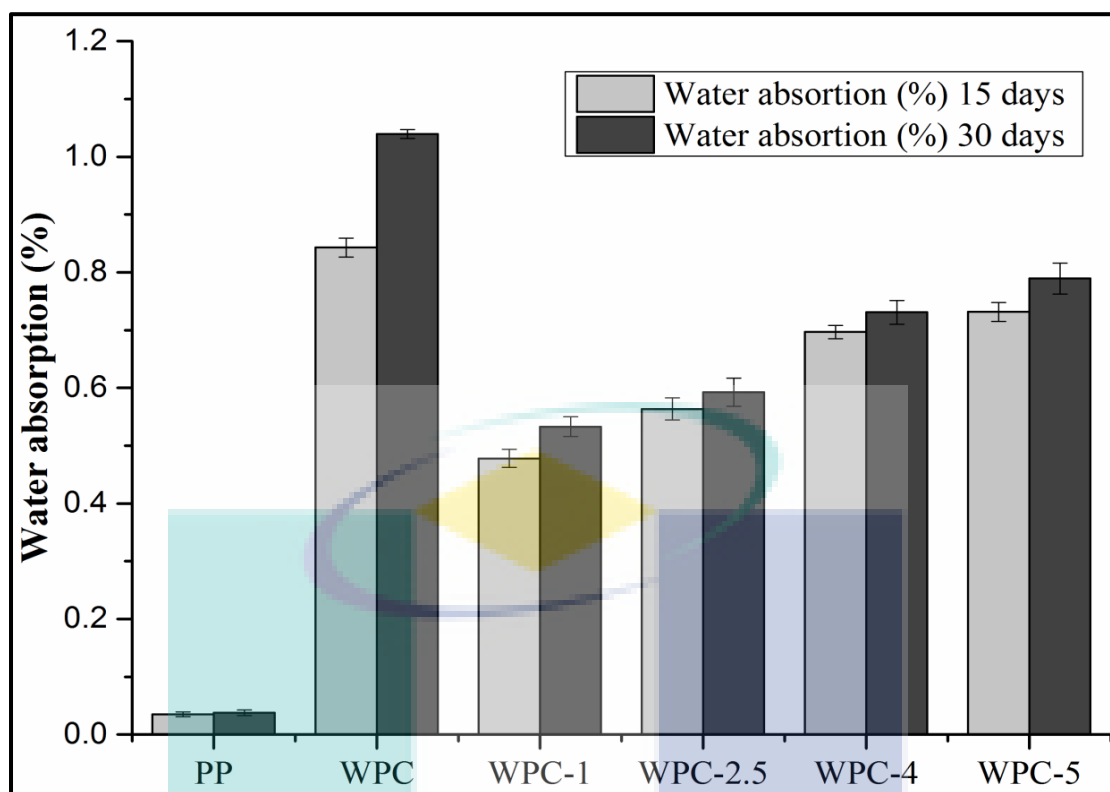


Figure 4.35 Water absorption of the WPC as function of MMT Cu nanoclay loading

It can be examined from Figure 4.35 that WPC/MMT Cu depicted the lowest water absorption over WPC/MMT and which could be associated to the good interaction level between PP and the nanoclay (Layered silicates) as the result of the TMI modification done on the pristine nanoclay. The modification process has clearly enhanced the interaction level by creating an intercalated system as supported by the XRD analysis and further proved by the SEM micrographs.

4.3.6 Thermal Properties

In this research study, the thermal analysis was carried out, to study the effect of pristine nanoclay modification process on the thermal properties of WPC. Thermal Gravimetric Analysis (TGA), and Differential Scanning Calorimetry (DSC) were employed to analyse the thermal properties of WPC/MMT and WPC/MMT Cu. The section that follows, discusses the results obtained from both the analysis done in order to get a better understanding on the thermal properties of WPC prepared in this work.

4.3.6.1 Thermal Degradation behaviour

Thermogravimetry is used in general to measure the change in mass of a sample as a function of temperature or time. In this work, thermal gravimetric analysis (TGA) was conducted to measure the thermal stability of the prepared WPC as a function of temperature. The TGA thermograms of PP, WPC, and WPCs with different percentages of MMT and MMT Cu are illustrated in Figures 4.36 and 4.37 whereas Table 4.8 shows the decomposition temperature at different weight loss (T_{20} , T_{40} , T_{60} , and T_{80}), maximum degradation temperature (T_{max}) and char content (%) for PP, WPCs and WPCs containing pristine and TMI-modified nanoclay.

The incorporation of LS into WPC has enhanced their thermal stability compared to PP and WPC without nanoclay. It can be observed from the data acquired that the degradation temperature at different weight loss (20, 40, 60, and 80 %) of WPC/MMT Cu showed higher degradation temperature than WPC/MMT. Moreover, at 1 wt%, 2.5 wt%, 4 wt% and 5wt% of pristine nanoclay loading into the composites increased the maximum degradation temperature (T_{max}) by 3%, 3%, 2%, and 1.9% respectively whereas the T_{max} of same content TMI-modified nanoclay into the composite was increased by 5%, 4.5%, 2.7%, and 0.9% respectively over the WPC sample without nanoclay. In the cases of WPC/MMT Cu these degradation temperatures are higher than the WPC/MMT. The TGA results obtained proved that the enhancement in the thermal stability is more significant with the incorporation of modified clay.

It can also be observed from the results that degradation temperature of WPC is higher with modified nanoclay compared to conventional nanoclay. This may suggest that the TMI modification done on the nanoclay has played a significant role in exfoliating the layered silicates into the polymer matrix with improved thermal stability. The increase in the stability may be a result of the improved barrier properties in the polymer due to the incorporation of the layered silicates whereby it prevents the penetration of oxygen and thus reduces the oxidation of the resin. Similar results were obtained by Baysal et al., (2013). They analysed the thermal properties of polyurethane and polyurethane–Organoclay nanocomposites and they found that the introduction of organoclay into polymer backbones has increased its thermal stability.

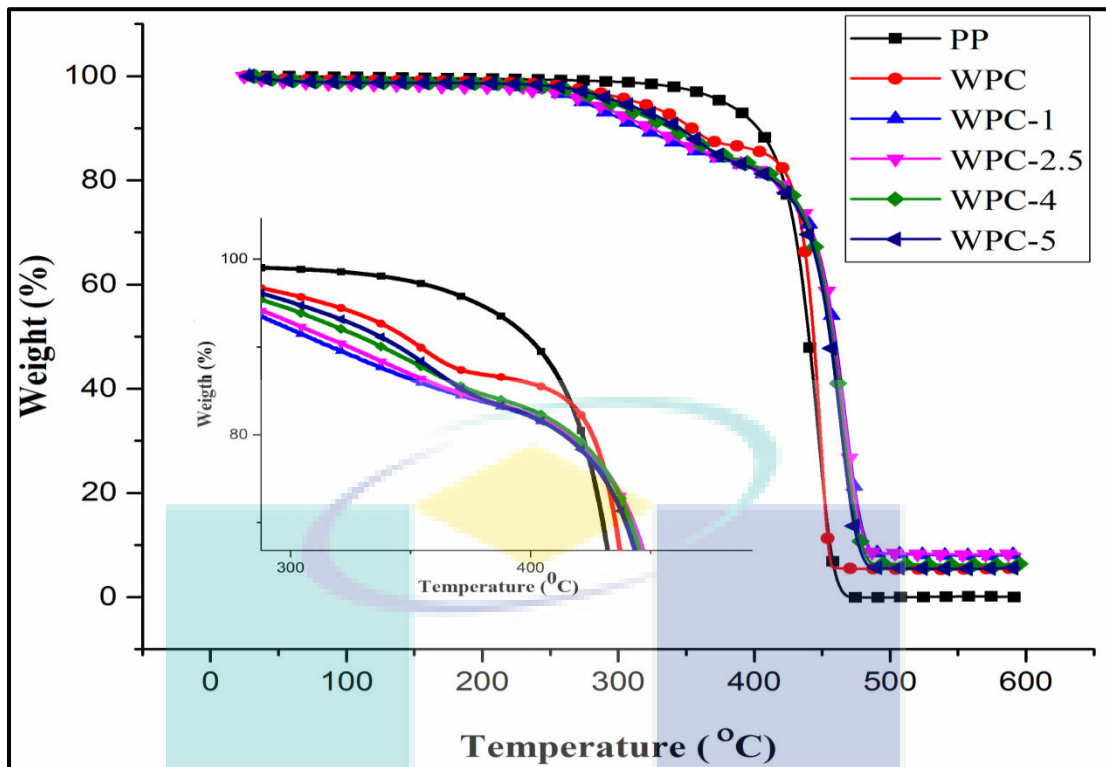


Figure 4.36 TGA thermogram of neat PP and WPC made with different pristine (MMT) nanoclay content

It was observed that the decomposition temperature values were reduced, due to the higher loading of nanoclay into the composite. The reason might be, as discussed earlier, the agglomeration of nanoclay in the composites. Composite provide more area exposure of matrix polymer and could have resulted in more weight loss at a lower temperature (Lee et al., 2008). The well dispersion of nanoclay particles is seen as a heat barrier that enhances the thermal stability of the system as well as forming char residues after thermal decomposition and during the initial stage of the thermal decomposition, the well dispersion of nanoclay is able to shift the decomposition temperature higher (Okamoto, 2003).

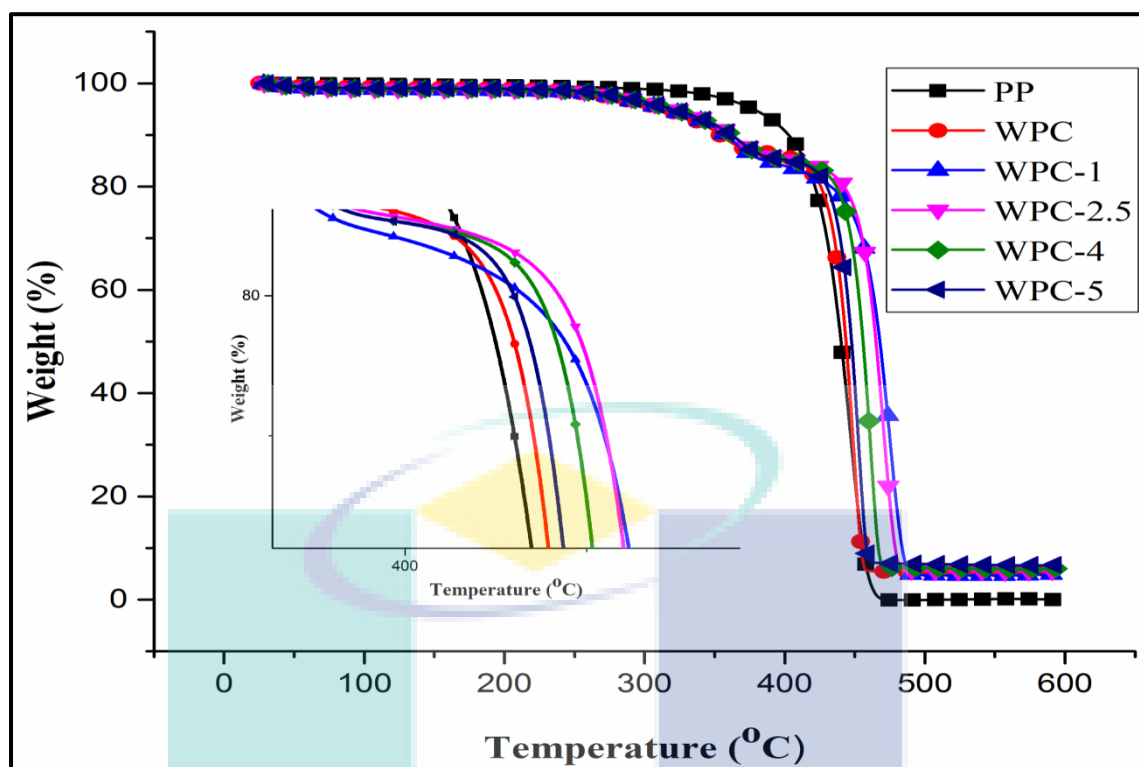


Figure 4.37 TGA thermogram of neat PP and WPC made with different modified (MMT Cu) nanoclay content

From the data gained according to Table 4.8, it can be observed that there are no residue or char for PP, however the charred residue of the WPC increased at increasing nanoclay loading of the layered silicates. The highest char was produced by 2.5 wt% WPC/MMT with 8.19% followed by 1 wt% of WPC/MMT which showed 8.00%. The amounts of char in WPC/MMT Cu were lesser compared to pristine nanoclay incorporated into the matrix. It is known generally, that layered silicates consist of stacking layers and it does not burn easily. This in return results in high char residue however in the case of WPC/MMT Cu, the nanoclay is seen to have intercalated perfectly into the structure of the composites as supported by the XRD analysis. This justifies the lesser amount of the char produced by WPC/MMT Cu.

Table 4.8 Thermogravimetric properties of WPC with different MMT and MMT Cu nanoclay loading

Composites	Nanoclay content (wt%)	T ₂₀	T ₄₀	T ₆₀	T ₈₀	T _{max}	Char (%)
		(°C)					
PP		421	435	444	451	422	0.00
WPC		425	440	446	451	435	5.39
WPC/MMT	1	414	452	464	474	445	8.00
	2.5	415	425	463	473	445	8.19
	4	417	451	462	471	444	6.22
	5	413	449	460	469	443	5.43
WPC/MMT Cu	1	433	462	471	479	457	4.67
	2.5	442	461	468	474	455	5.46
	4	436	452	458	463	447	5.93
	5	430	444	450	455	439	6.73

Derivative thermal gravimetric (DTG) was further applied to study the thermal stability of the PP, WPC, and WPC with MMT and MMT Cu, which was expected to shed some light on the chemical structure of the composite. Figure 4.38 and 4.39 delineated the DTG of PP and the WPC with different content of pristine and modified nanoclay respectively.

UMP

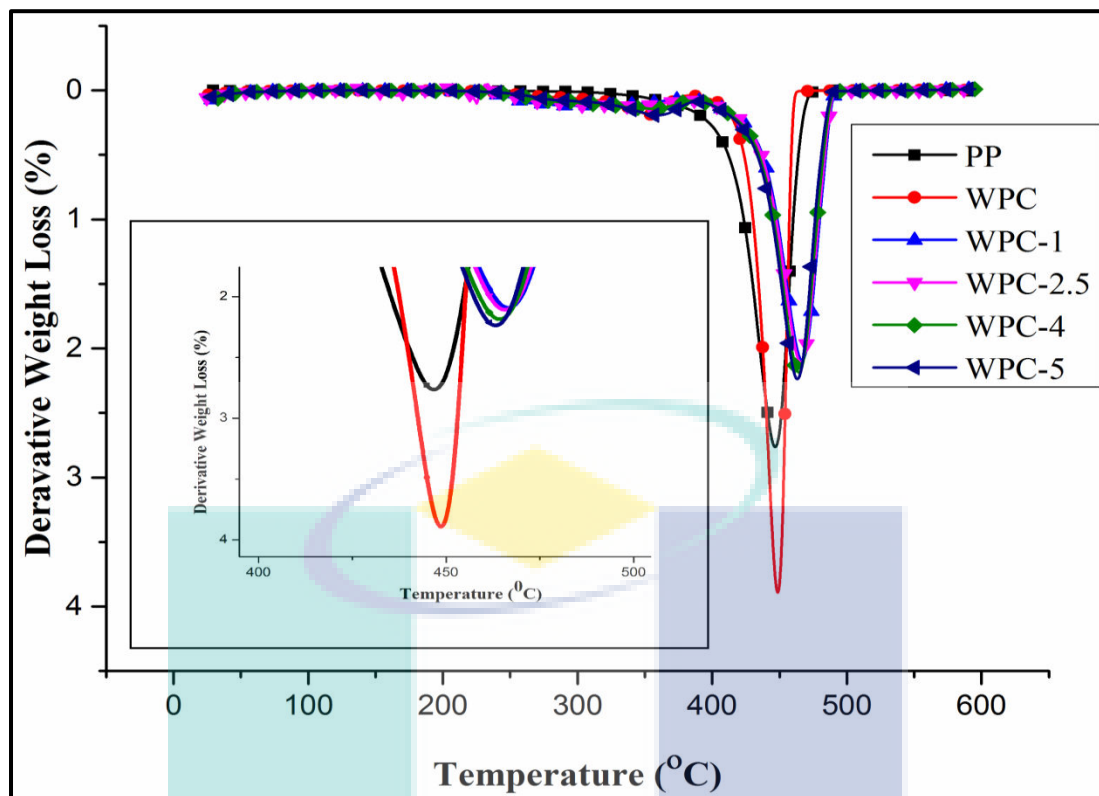


Figure 4.38 DTG curve of neat PP and WPC made with different pristine nanoclay content

Vitkauskienė et al. (2011) reported similar thermal profiles in their study. The incorporation of MMT nanoclay into the polymer matrix is seen to shift the peak temperature to slightly high values and this shows that the nanoclay has a contribution in the decomposition rate. PP incorporated with MMT showed a visible peak at around 450 °C where this occurrence can be related to the decomposition of the silica particles. However, with the addition of clay modified with copper ions, two peaks may be observed especially in the case of WPC/MMT Cu. The first peak may be attributed to the decomposition of the PP matrix whereas the second peak which appeared at a higher temperature is due to the PP physicochemical attachment to the nanoparticle's surface. Similar results were reported by Guo et al. (2007) and they claimed that this phenomenon is an indication of strong chemical bonding between the nanoparticles and the polymer matrix.

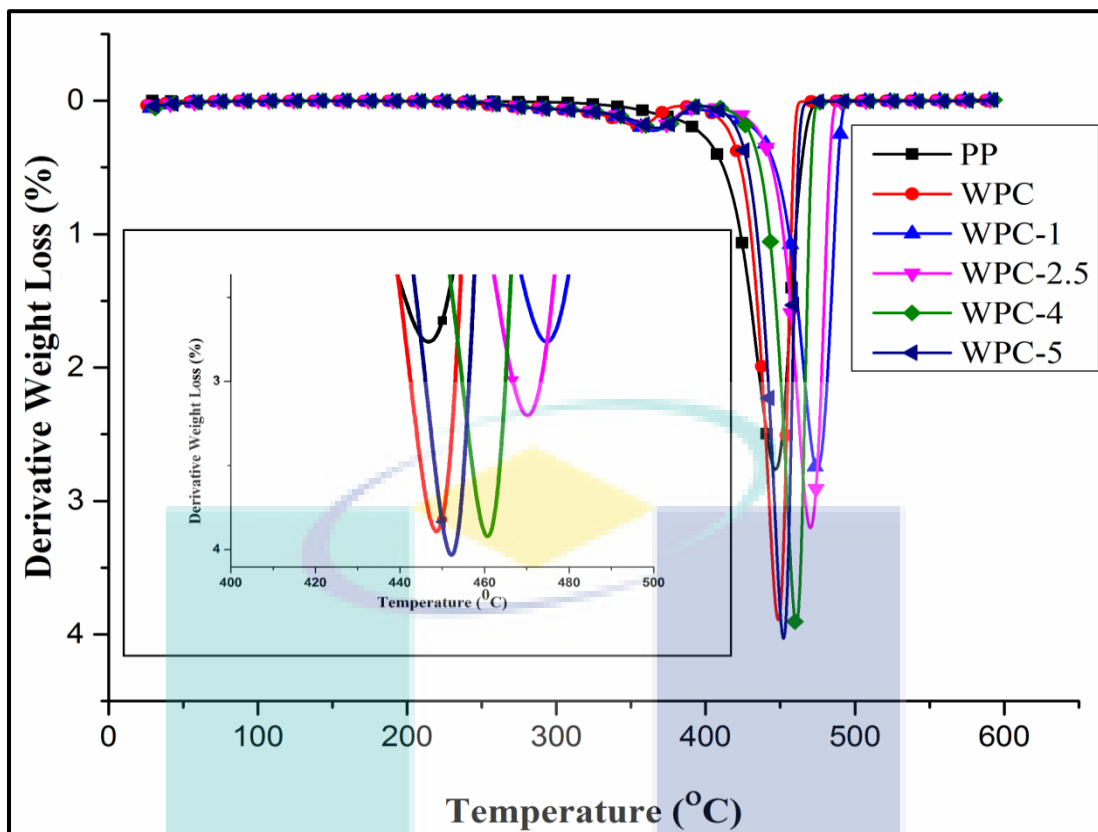


Figure 4.39 DTG curve of neat PP and WPC made with different content of modified nanoclay

4.3.6.2 Crystallization behaviour

Differential Scanning Calorimetry (DSC) is a technique used to study the effect of pristine and modified nanoclay on thermal transitions of a WPC. Polymeric materials are known to melt over a relatively broad range due to its semi crystalline behaviour and the melting range is governed by the structure of the polymer. Figure 4.40 and 4.41 shows DSC curves of neat PP, WPC and WPC with different content of pristine and modified nanoclay. Crystallization behavior (melting and crystallization temperature, heat of fusion and crystallinity) of neat PP, WPC and WPC/NC obtained from DSC experiments is summarized in Table 4.9.

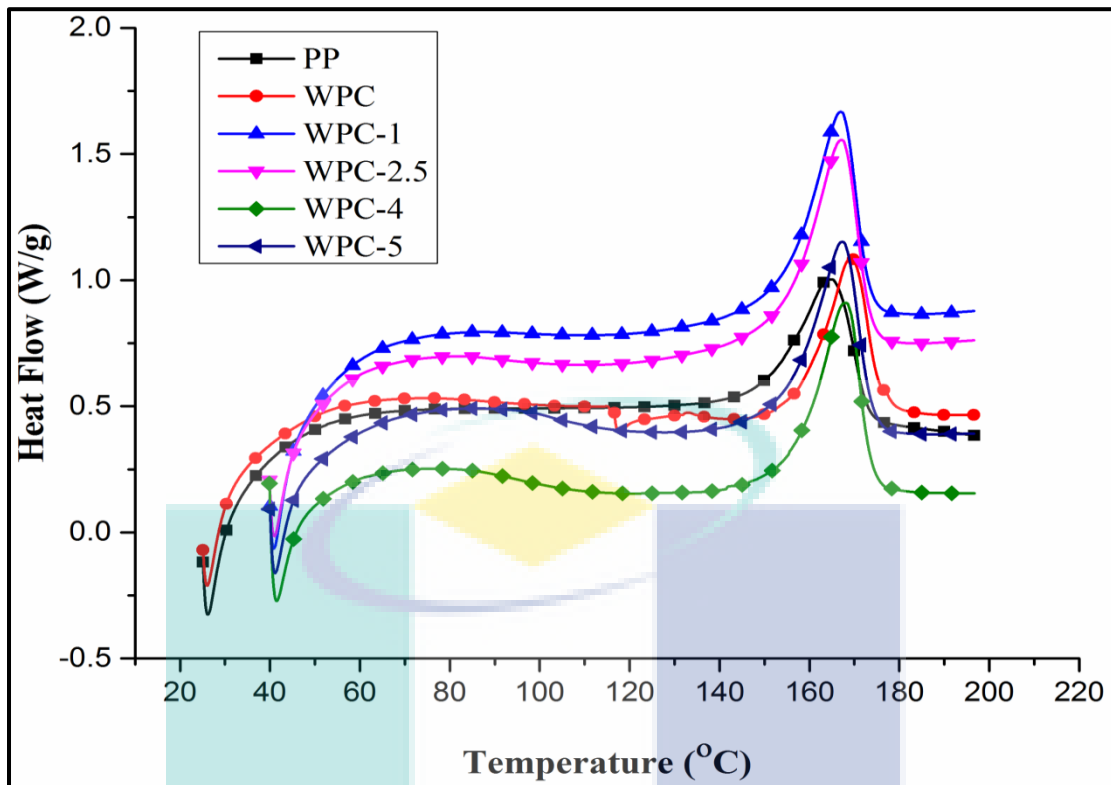


Figure 4.40 DSC curves of neat PP and WPC made with different content of pristine nanoclay

From the results obtained, it can be observed that the crystallization temperature of WPC was increased with the addition of nanoclay into the composite. The DSC results exhibit the increased crystallization temperatures up to 153.60 °C, at 1 wt% of MMT loading into the composite whereas with same content of MMT Cu loading into the composite increased crystalline temperature up to 154.40 °C, in contrast with 149 °C for neat PP and 153.41 °C for WPC without nanoclay.

Furthermore, All WPC showed a higher melting temperature (T_m), compared to the neat PP. Neat PP had the lowest T_m (165.12°C), while WPC with 1 wt% MMT and MMT Cu showed the T_m nearly 166.91°C and 167.59 °C respectively. As discussed in previous DSC result, the increased loading level of nanoclay had no significant effect on the T_m of the WPC. However, increased loading level of nanoclay slightly decreased the T_m of the WPC.

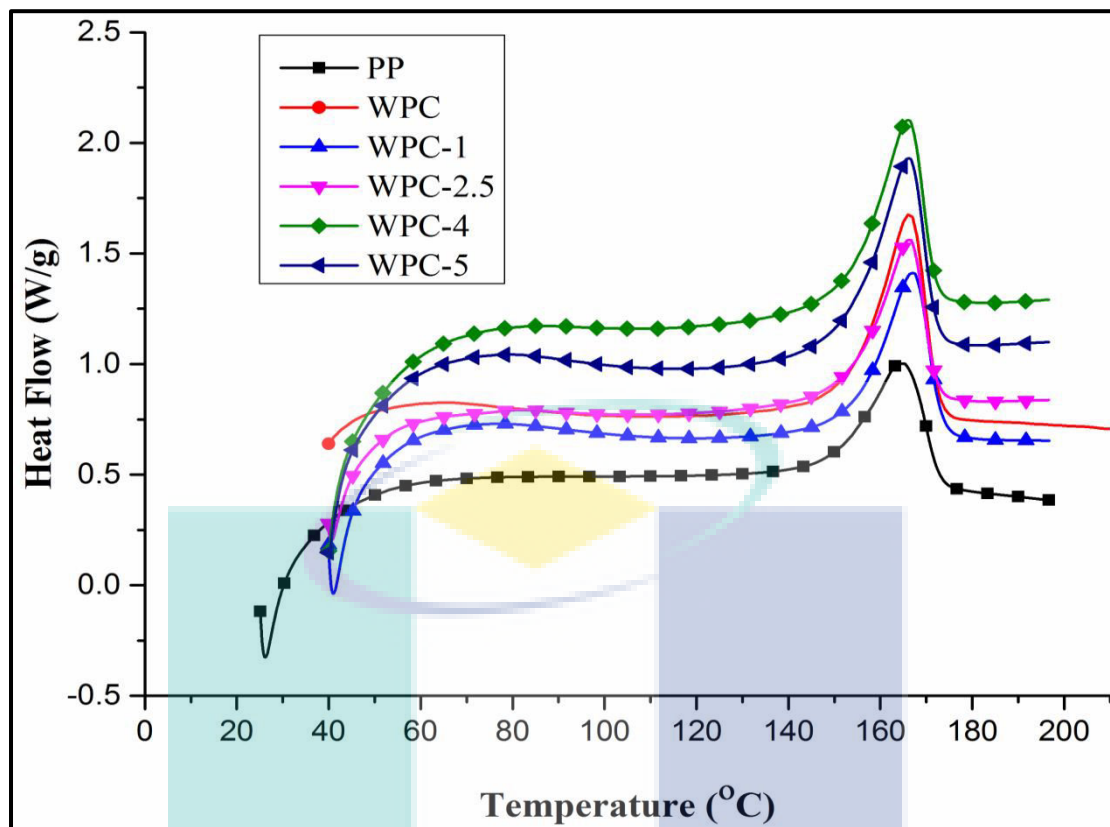


Figure 4.41 DSC curves of neat PP and WPC made with different content of modified nanoclay

As shown in Table 4.9, an increasing amount of nanoclay increased X_c . WPC with 2.5 wt% of MMT and MMT Cu increased the X_c up to 34.08% and 34.45% respectively. This is probably due to the interactions between the carbonyl groups of the repeating units of hard segments and the hydroxyl end groups of nanoclay (Biswal et al., 2009). However, at higher loading of nanoclay, X_c gradually decreased. The reason might be, as discussed earlier, the agglomeration and poor dispersion of nanoclay in composite.

However, from the results obtained, it can be concluded that WPC/MMT cu showed better crystallization behaviour as compared to the WPC/MMT. It could be attributed to the well dispersion of nanoclay into the composite as result of the TMI modification done on the MMT. Generally, well-dispersed nanoclay can act as the effective nucleating agent to accelerate the crystallization behaviour of PP matrix and thus promote the mechanical performance through the surface-nucleated PP crystalline phase (Mohan et al., 2011).

Table 4.9 DSC result of neat PP and WPC with different loading of MMT and MMT Cu nanoclay

Composite	Nanoclay Loading (wt %)	Crystalline temperature (°C)	Melting temperature (°C)	Crystallinity (%)
PP		149.88	165.12	27
WPC		153.41	166.39	22.57
WPC/MMT	1	153.60	166.61	32.33
	2.5	153.53	166.49	34.08
	4	153.39	166.37	29.92
	5	153.21	166.18	28.55
WPC/MMT Cu	1	154.40	167.59	29.60
	2.5	153.45	166.64	34.45
	4	153.18	166.38	34.22
	5	154.27	167.47	27.41

UMP

4.4 Sub-surface mechanical properties of wood-plastic composite studied by nanoindentation

4.4.1 Introduction

Nanoindentation is a more sophisticated technique which provides quantitative qualitative information of subsurface mechanical properties of various materials (Downing et al., 2000; Gao and Mader, 2002). The principle of this technique is based on the local deformation phenomena of materials. This deformation phenomena occurs at small load and scale with help of indenter by application of force or load. The elastic and viscous contribution combination to the total indentation depth represents the variation of indentation depth. Microindentation test has same working principle like nanoindentation test. The nanoindentation test produces indentations from a few micrometers to a few hundred nanometers in size because the loads and probe are smaller in nanoindentation test. This is main difference between microindentation and nanoindentation test.

4.4.2 Wood-Plastic Composite reinforced by C20 organoclay

In subsurface indentation of a material, an indenter penetrates into the material with loaded force. A time of single loading and unloading cycle curve can be used to record the data. The information with respect to the plastic, viscoelastic and elastic behaviour of material can be obtained from subsurface indentation test (Flores and Calleja, 1998).

Figure 4.42 depicted the loading and unloading indentation curve of PP, WPC, and WPC loaded with different concentrations of C20 (organoclay). It can be seen in Figure that the every composites sample shows different mechanical responses. The loading curves are followed by a period of holding time at 180s at which the peak loads are 10mN. The indentation curves of samples are shifted on left with the addition of nanoclay into the composite. It means that the WPC resistance to indentation significantly increases with the addition of organoclay. For the PP and WPC, the indenter reached at the maximum depth of 2129 nm and 1913 nm respectively. The

maximum depth of WPC reached at 1595 nm, when 1 wt% of organoclay had been introduced into the composite. The indentation depth represents the contributions from both plastic and elastic displacements.

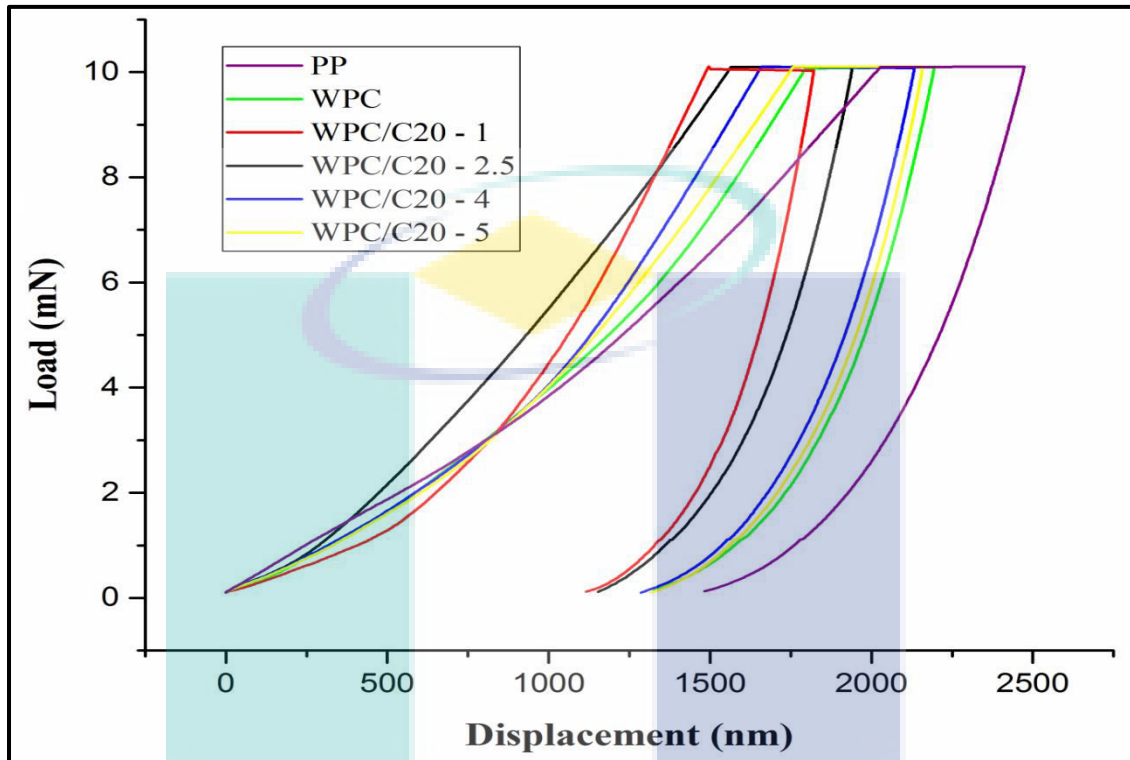


Figure 4.42 Typical indentation load–displacement curves for PP, WPC and WPC with different C20 organoclay concentrations

Unloading curves discontinuity of the neat PP, WPC and WPC/NC noticed at around 0.10mN exhibits a recovery in the composites surface. The incorporation of nanoclay into the WPC, results in the yield strength of the WPCs being increased, as per results obtained by Nanoindentation test.

The resistance of a material to the local deformation represents the hardness value (H) of the composite, whereas the overall stiffness of the composite represents the elastic modulus (E). The obtained nanoindentation test data were used to compute the reduced modulus and hardness values of composite. Equation 3.11 was then used to calculate the elastic modulus of composite. Figure 4.43 and 4.44 show the hardness and modulus plot of PP, WPC, and WPC with different organoclay concentration, respectively. The hardness and modulus of composite were increased over PP when

wood flour was incorporated into the PP as shown in Table 4.10. The reason might be due to the high degree of hardness and stiffness introduced by the incorporation of wood flour in the composite (Yeh et al., 2013).

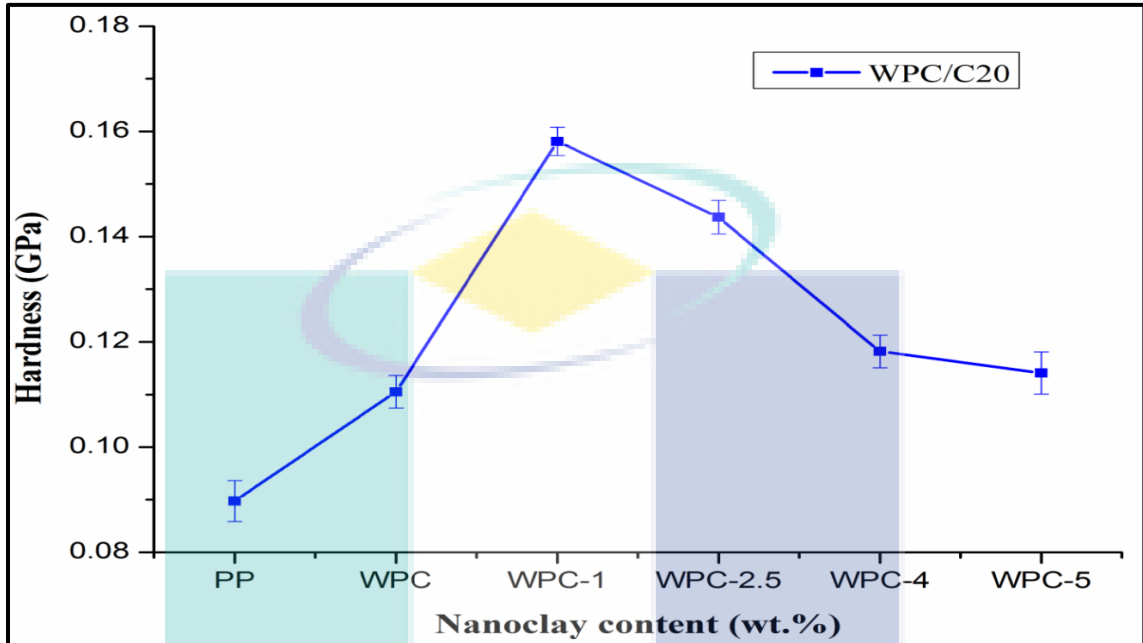


Figure 4.43 Hardness of PP, WPC and WPC with different C20 nanoclay loading

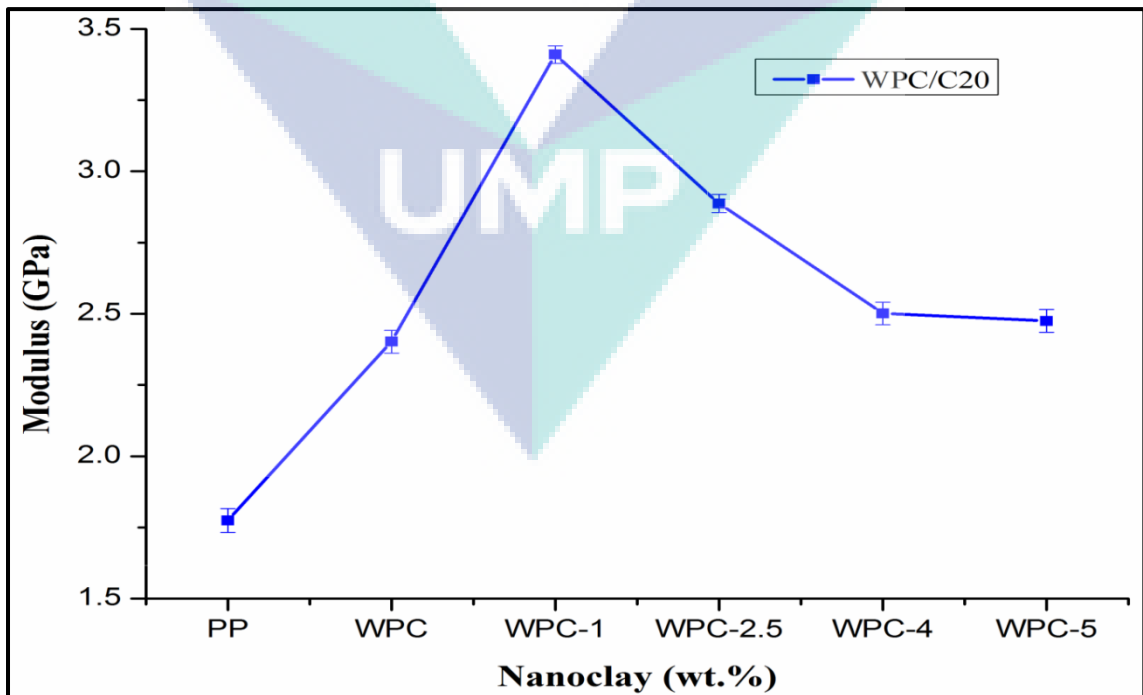


Figure 4.44 Elastic modulus of PP, WPC and WPC with different C20 nanoclay loading

It can be seen from the Figure 4.43 and 4.44 that the loading of organoclay into the composite increased both the hardness and the modulus. With the loading of 1wt% content organoclay, the hardness and modulus had increased nearly 36% and 41%, respectively. However, with high loading, the nanoclay created a poor dispersion in WPC due to agglomeration of nanoparticles and then the hardness and elastic modulus started to reduce, so the composite with 5 wt.% nanoclay revealed the minimum hardness and elastic modulus.

Table 4.10 Hardness and modulus values of PP, WPC, WPC with C20 nanoclay loading

Sample	Hardness (GPa)	Modulus (GPa)
PP	0.089 ± 0.003	1.774 ± 0.04
WPC	0.1105 ± 0.004	2.402 ± 0.04
WPC/C20-1	0.1581 ± 0.003	3.410 ± 0.03
WPC/C20-2.5	0.1437 ± 0.003	2.887 ± 0.03
WPC/C20-4	0.1182 ± 0.002	2.501 ± 0.03
WPC/C20-5	0.1141 ± 0.004	2.475 ± 0.04

4.4.3 Wood-Plastic Composite reinforced by Pristine nanoclay (WPC/MMT) and TMI-modified nanoclay (WPC/MMT Cu)

As can be seen from Figure 4.45 and 4.46, typical loading-unloading curves of indentations for PP, WPC and two types of WPC with 1 wt%, 2.5wt%, 4 wt%, and 5 wt%, of nanoclay content, respectively. The addition of wood flour into the neat PP increased the resistance of composite. This might be attributed to the lower stiffness of PP than wood flour. In addition, the loading of nanoclay into the WPC resulted in its composites surface being more resistant to penetration by an indenter over to that of neat PP and WPC without nanoclay. For the PP and WPC, the indenter reached at the maximum depth of 2129 nm and 1913 nm respectively. The maximum load was 10 mN during the maximum depth. The maximum depth of WPC reached at 1637 nm, when 1 wt% of unmodified nanoclay had been introduced into the composites. With the similar loading of modified nanoclay into the WPC, the average maximum depth of composite (WPC/MMT Cu) reached at 1589 nm, a decrease of around 3 % compared to

unmodified nanoclay-based WPC (WPC/MMT). It means modified nanoclay showed more effective reinforcement. This is due to the modification of nanoclay which promotes the better dispersion of nanoparticles into the composite. Small sizes of modified nanoclay tactoids increase the density and hardness of composite.

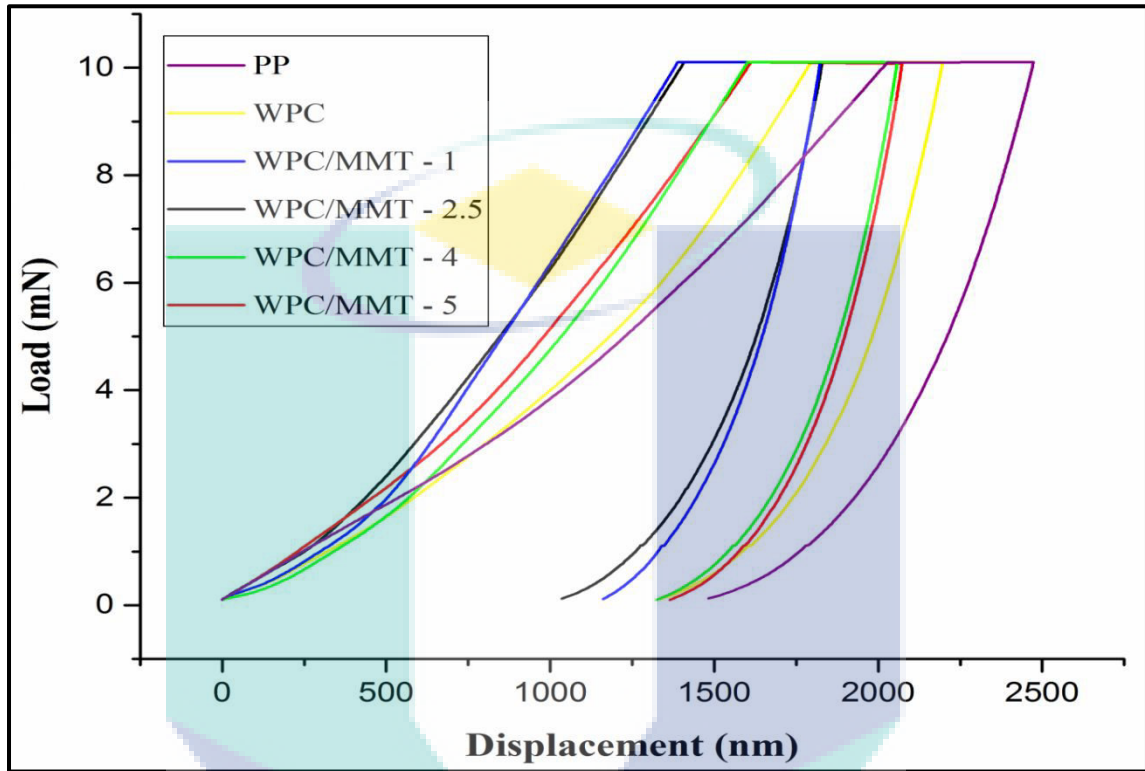


Figure 4.45 Load-displacement curves of indentation for PP, WPC and WPC with different pristine nanoclay concentrations

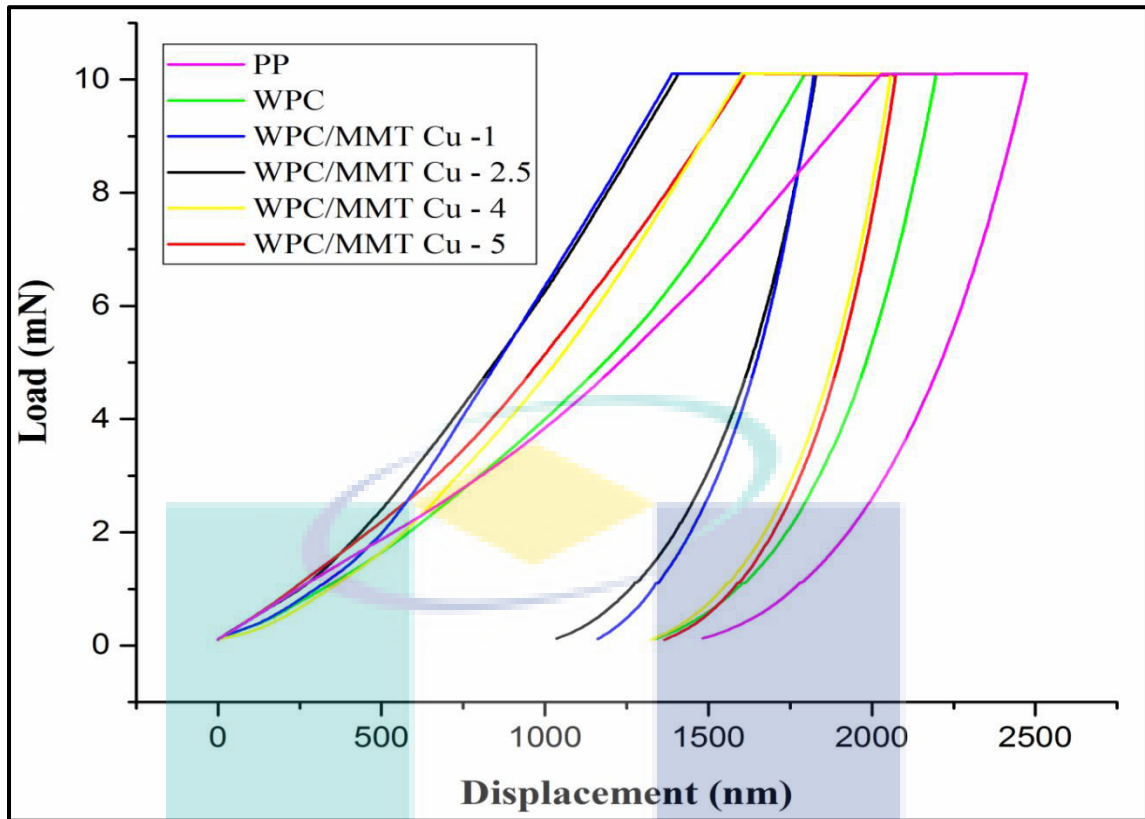


Figure 4.46 Load-displacement curves of indentation for PP, WPC and WPC with different modified nanoclay concentrations

The average value of hardness and elastic modulus of neat PP and the WPC were plotted against nanoclay content in Figures 4.47 and 4.48, respectively. As can be seen in both the figures, loading of nanoclay into the composite has shown positive impact on the mechanical properties of WPC. With the 1.0 wt% loading of nanoclay into the composite: both the elastic modulus and hardness of the composite effectively increased. This improvement might be attributed to the good uniform dispersion and better interfacial interaction of the nanofiller throughout the matrix, which enabled effective stress transferring from the matrix to fibers and then leading to high hardness and elastic modulus. However, with high content, the nanoclay created poor dispersion into the composite due to the agglomeration of nanoparticles and then the hardness and elastic modulus started to decrease, so the composite with 5 wt.% nanoclay revealed the minimum hardness and elastic modulus (Table 4.11 and 4.12).

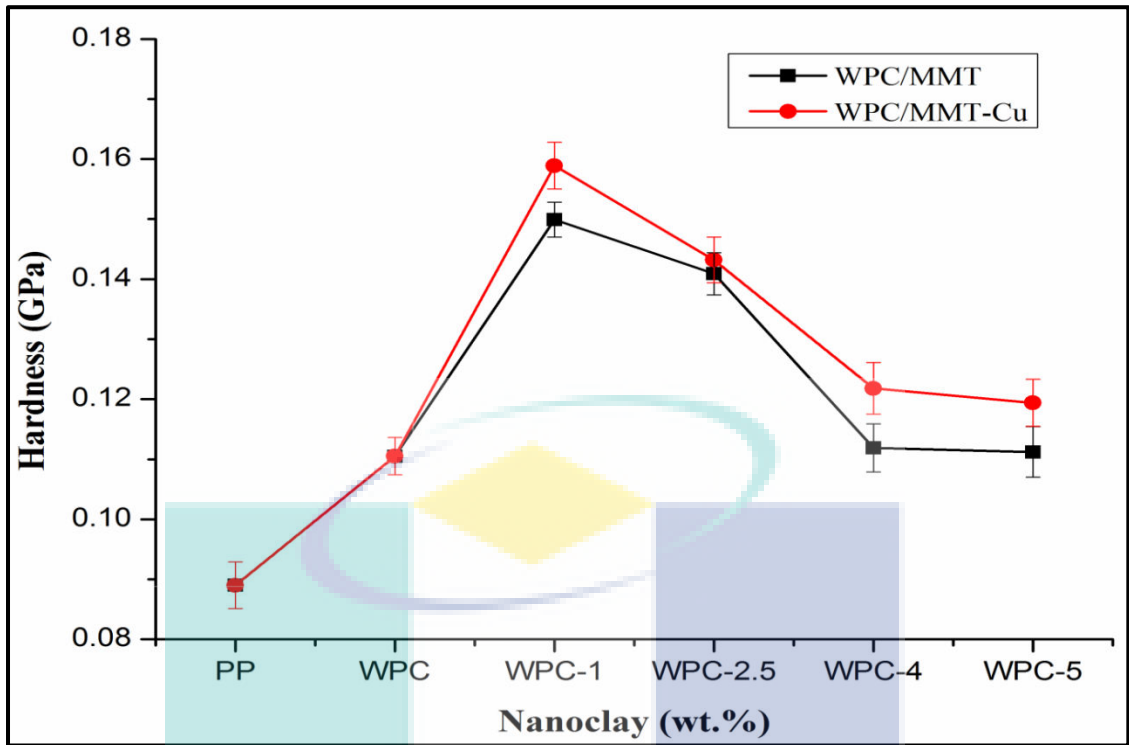


Figure 4.47 Hardness of PP, pristine and modified nanoclay based WPC as a function of nanoclay loading

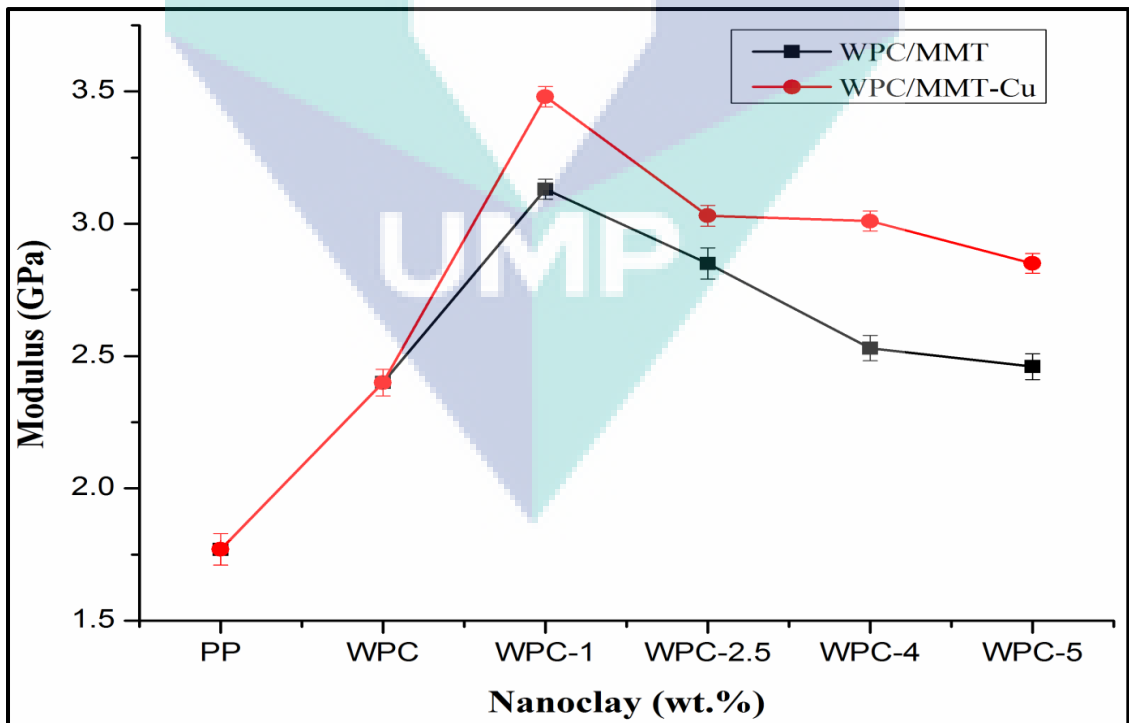


Figure 4.48 Elastic modulus of PP, pristine and modified nanoclay based WPC as a function of nanoclay loading

In addition, with the loading of 1.0 wt% of unmodified nanoclay, the hardness and elastic modulus of the WPC increased by around 35% and 30%, respectively over WPC. With the incorporation of nanoclay, the WPC became stiffer. However, with the addition of same content of TMI-modified nanoclay into the composite, these properties of WPC increased by around 44% and 45% respectively. As discussed earlier, modification of nanoclay improves the overall properties of the composite by improving the dispersion of nanoclay into the composite.

Table 4.11 Hardness and modulus values of PP, WPC, WPC with MMT nanoclay loading

Sample	Hardness (GPa)	Modulus (GPa)
PP	0.089 ± 0.003	1.774 ± 0.04
WPC	0.1105 ± 0.004	2.402 ± 0.04
WPC/MMT-1	0.1499 ± 0.003	3.137 ± 0.05
WPC/MMT-2.5	0.1409 ± 0.003	2.853 ± 0.03
WPC/MMT-4	0.1119 ± 0.003	2.532 ± 0.04
WPC/MMT-5	0.1112 ± 0.004	2.468 ± 0.04

Table 4.12 Hardness and modulus values of PP, WPC, WPC with MMT Cu nanoclay loading

Sample	Hardness (GPa)	Modulus (GPa)
WPC/MMT Cu-1	0.1590 ± 0.002	3.485 ± 0.03
WPC/MMT Cu-2.5	0.1432 ± 0.002	3.034 ± 0.03
WPC/MMT Cu-4	0.1218 ± 0.004	3.016 ± 0.02
WPC/MMT Cu-5	0.1194 ± 0.002	2.842 ± 0.03

4.5 Sub-surface creep behaviour of wood-plastic composite studied by nanoindentation

4.5.1 Introduction

The creep behaviour of neat PP, WPC and WPC with three different kinds of nanoclay using a nanoindentation technique is discussed in this section. The creep performance of neat PP and WPC with different nanoclay content can be characterized by the creep strain under a constant stress.

4.5.2 Creep behaviour of Wood-Plastic Composite reinforced by C20 organoclay

Generally, there are two stages of indentation creep displacement versus time curve. Due to the reorientation and slippage of polymer chains under constant load, the stage which reflects to area of decreasing creep rate is the primary stage or creep. Normally, after a certain period the stage which reflects to more or less persistent creep rate and the creep rate reaches a constant state value known as secondary stage or creep (Cahn, 2005).

The image contains a large, semi-transparent watermark logo for UMP. The logo is a downward-pointing triangle composed of several overlapping colored shapes: a teal triangle on the left, a purple triangle on the right, and a yellow diamond at the top. The letters 'UMP' are printed in white, bold, sans-serif font across the center of the triangle.

UMP

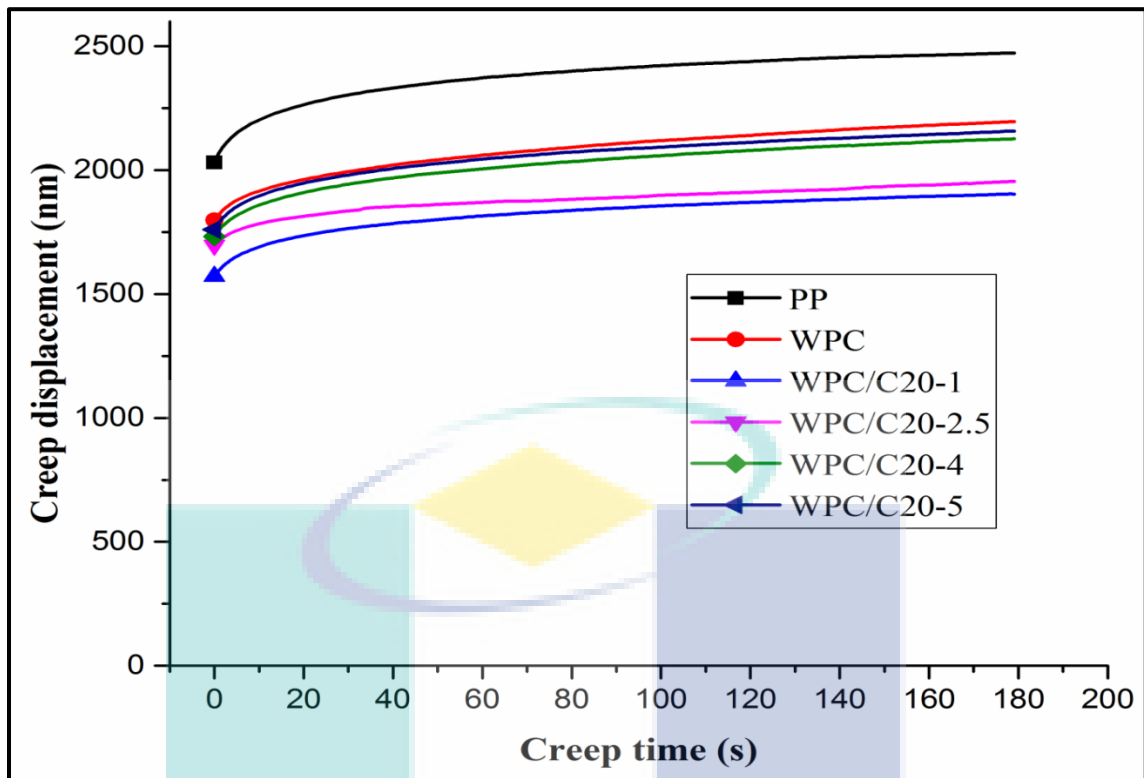


Figure 4.49 Creep displacement rate versus creep time for PP, WPC and WPC/C20 with different nanoclay concentrations

Figure 4.49 depicted the creep displacement results of neat PP, WPC and WPC with different C20 organoclay concentrations. It is observed that the creep deformation decreased with the addition of nanoclay into a composite. Wood-plastic composites reinforced with nanoclay shows lower creep deformation over neat PP and WPC at the same load after 180 seconds. After 180 seconds of creep time, the creep displacement of 1 wt%, 2.5 wt%, 4 wt% and 5 wt% of nanoclay reinforced composite were decreased to 292nm, 242nm, 69nm, and 38nm, respectively, over the WPC. A better interaction of polymer matrix and nanoclay can be contributed to increase in the creep resistance and it is more noticeable with just 1 wt% and 2.5 wt% of nanoclay content. The increment of creep displacement with 4 wt% and 5 wt% of nanoclay content might be attributed by the nanoclay agglomerates formation into the composite.

This result is comparable to that of nylon 66 (PA66) reinforced nanoclay nanocomposites whereby after a high loading of nanoclay, the improving impact of nanoclay was consistently reduced. The high concentration of nanoclay could change

the morphology or microstructure of the polymer matrix, which could have adversely effect on creep behaviour of composites (Shen et al., 2004).

A generalized elastic-viscoelastic (EVE) model which is refined form of elastic-viscoelastic-viscous (EVEV) model (Yang et al., 2004) was used to modelling the obtained results of creep test. The EVE model was applied to obtain a deeper insight into the creep response of nanoclay addition to the WPC. This model is a combination of a series of spring and dashpot which define the total displacement during indentation creep test. According to this model, during the indentation the creep deformation can be expressed as:

$$h = h_{in} \frac{P_o}{E_o A_o} + \sum_i^n \frac{P_o h_{in}}{E_i A_o} (1 - e^{-E_i t/n_i}) = h_e + \sum_i^n h_i (1 - e^{-t/\tau_i}) \quad (4.1)$$

where, the indentation creep displacement represented by h . h_{in} stands for virtual length which is used to express the indentation strain as $in \ \epsilon = h/h_{in}$ and its value is equal to the elasticplastic displacement. P_o and E_o represent the persistence indentation load for the indentation creep test and the elastic modulus of material respectively. At the beginning of the indentation creep test, the initial contact area is presented by A_o . The calibrated indenter area function can be used to express the A_o .

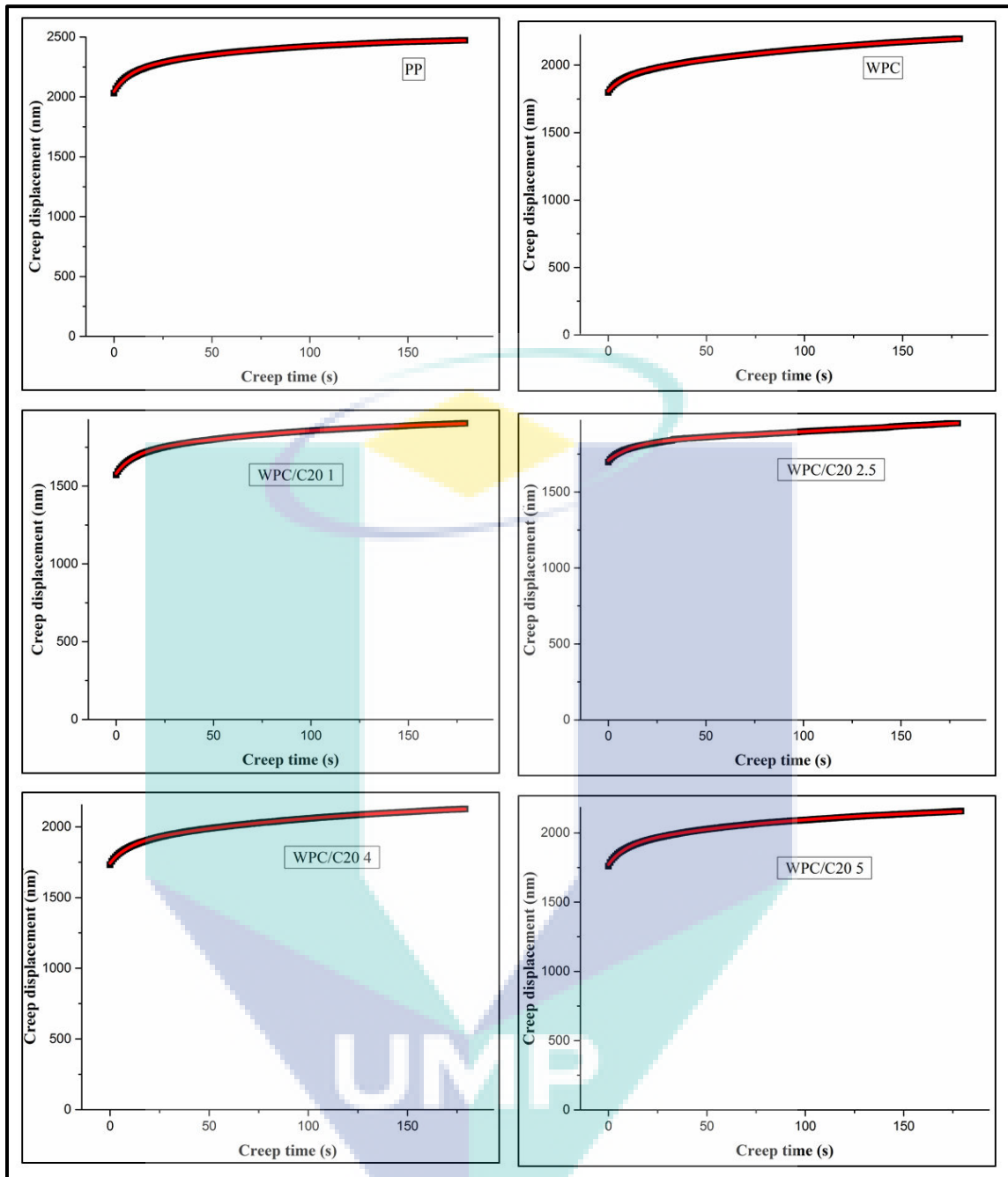


Figure 4.50 Creep displacement versus time for PP, WPC and WPC/C20 with different nanoclay concentrations. Solid black line is experimental data and the thin red line is fitting results by Eq. (4.1)

For the i th Kelvin unit in the model E_i is the elastic modulus and η_i is the viscosity coefficient. The n stands for the numbers of the Kelvin units, with the value of $n=2$ whereas t is the creep time (Yang et al., 2004). The viscoelastic deformation controlled by the exponential terms during creep, according to the equation and the deformation which are instantaneous displacement resulting from the elastic

deformation of the materials during loading are the two contributions to the deformation which should be included in an indentation creep test.

This model can be applicable to the indentation creep data for the PP, WPC and nanoclay-based wood plastic composite. A satisfactory agreement of model with the indentation creep data of PP, WPC and WPC with different concentrations of C20 organoclay is depicted in Figures 4.50.

Table 4.13 Fitting parameters from Eq. (4.1) for polypropylene, WPC, and WPC/C20 from indentation creep experiment

Parameters	WPC/C20					
	PP	WPC	1 wt%	2.5 wt	4 wt%	5wt%
h_e (nm)	2045	1807	1580	1709	1743	1772
h_1 (nm)	467	455	118	126	291	315
τ_1 (s)	474	323	13	96	103	118
h_2 (nm)	283	144	230	234	235	240
τ_2 (s)	9.66	9.30	8.30	8.33	8.63	8.80

Table 4.13 describes the fitting results based on Equation 4.1 for the indentation creep test of PP, WPC and WPC with different content of C20 nanoclay using a Berkovich indenter tip. According to the result, the value of instantaneous displacement, h_e , which is obtained by the elastic deformation, illustrates some decrement when loading of wood flour into the neat polypropylene. The hardness and stiffness of wood flour possibly retards the initial process of creep. Whereas, the incorporation of the nanoclay into the composite significantly decreased the initial creep process. At the initial stage due to elastic deformation, the retardation of creep process is improved by the loading of nanoclay into the composite. Nevertheless, the higher loading of nanoclay to 4 and 5 wt% of content induced a higher initial displacement at the early stage of

creep and increased the elastic deformation. Possibly some changes in the structure of the polymer chains and the agglomeration of nanoclay in the polymer matrix might increase the h_e . According to the above observation, it can be concluded that nanoclay dispersion into the composite has significant role controlling the creep in initial stages.

For viscoelastic behaviour which is represented by h_1 and h_2 , the presence of nanoclay shows dramatic improvement on the creep performance of composite over neat PP and WPC. According to the result, the WPC without nanoclay have lower h_1 and h_2 values than neat PP. Whereas, the values of h_1 and h_2 in WPC with 1wt% nanoclay show a lower viscoelastic deformation compared to neat PP and WPC. The retardation times, τ_1 and τ_2 are the response times indicating that the WPC have lower retardant time than neat PP. In contrast, the retardation time became longer, with increasing nanoclay content into the WPC, particularly in τ_1 , as demonstrated in Table 4.13. A good polymer matrix and nanoclay interactions might decrease the retardation time in the composite.

4.5.3 Creep behaviour of Wood-Plastic Composite reinforced by Pristine nanoclay (WPC/MMT) and TMI-modified nanoclay (WPC/MMT Cu)

For the WPC/MMT as illustrated in Figure 4.51, the WPC with different content of MMT shows particularly lower creep strain over neat PP and WPC at the same load after 180 seconds. The introduction of nanoclay into the WPC effectively improved in their creep resistance as their creep strains were significantly decreased by 15 % (1wt% MMT), 13% (2.5 wt% MMT), 0.81% (4 wt% MMT) and 0.92% (5 wt% MMT) respectively. The restriction effects by the presence of nanoclay had reduced the creep strain.

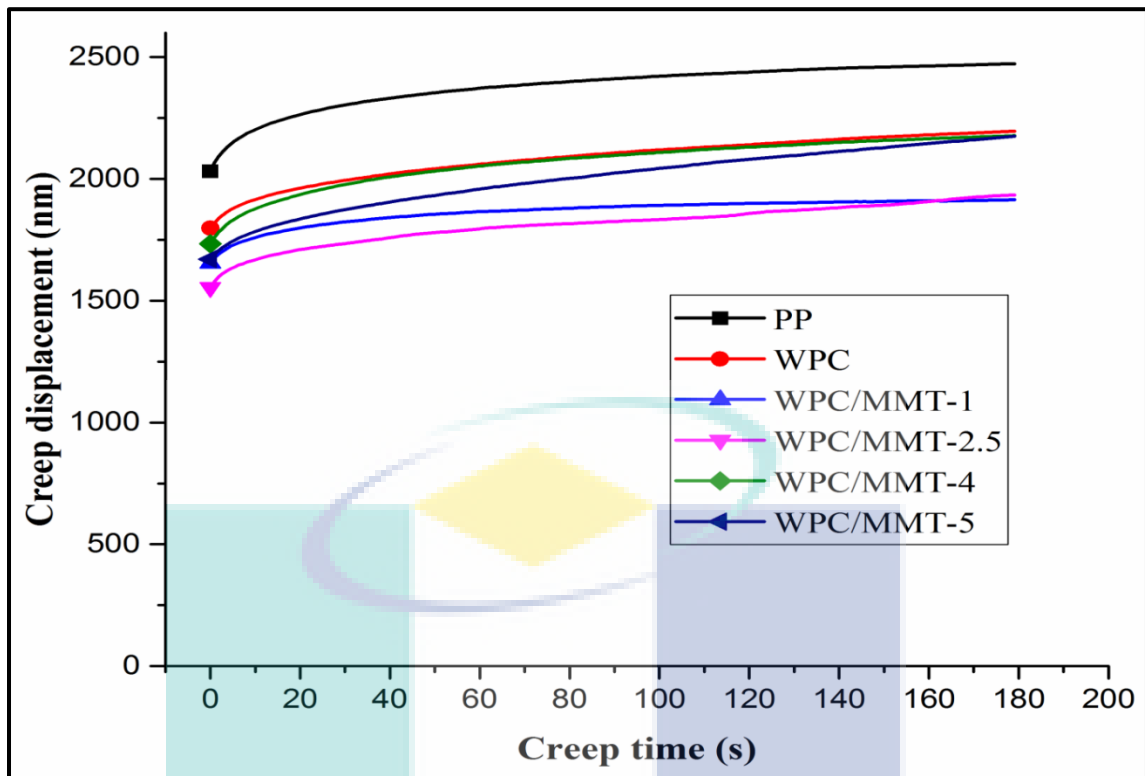


Figure 4.51 Creep displacement rate versus creep time for PP, WPC and WPC/MMT with different nanoclay concentrations

However, WPC with 4 and 5 wt% nanoclay shows higher creep displacement than the WPC with 1 and 2.5 wt% nanoclay. The increment of creep displacement with higher loading of nanoclay might be attributed by the formation of nanoclay agglomerates, as discussed earlier. Agglomeration of nanoclay does not just bring the slippage layers of nanoclay that results in insignificant constraint creep resistance but also interrupted interfacial interaction.

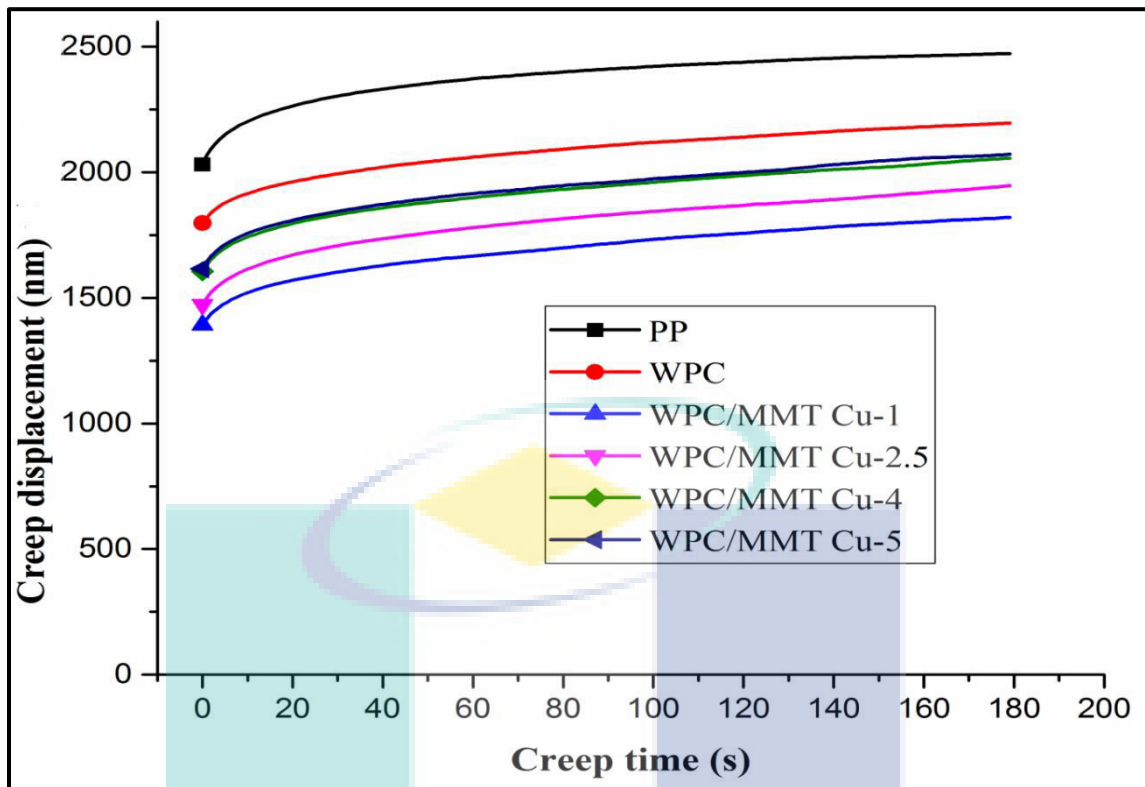


Figure 4.52 Creep displacement rate versus creep time for PP, WPC and WPC/MMT Cu with different nanoclay concentrations

Figure 4.52 exhibits the creep behaviour of modified nanoclay-based WPC (WPC/MMT-Cu). It can be seen that the creep displacement of WPC is significantly reduced by adding nanoclay into the composite. The reduction rate is higher as compared to the neat PP and WPC. The results exhibit that the creep displacement has reduced nearly by 22% for 1wt%, 13% for 2.5wt%, 7% for 4wt% and 6% for 5wt% nanoclay, respectively. The reduction of creep displacement with the addition of modified nanoclay suggests that development of nanoclay layer that permit more PP chains to enter into the nanoclay galleries and create strong interaction between nanoclay and the polymer matrix. Consequently, when the constant load is applied, it could retard the molecular mobility.

However, WPC prepared from modified nanoclay showed higher improvement in creep resistance over unmodified nanoclay-based WPC. With the loading of 1 wt% of unmodified nanoclay into the WPC, the creep displacement of the composite is decreased by around 15% over WPC. Whereas, with the addition of same content of TMI-modified nanoclay into the composite, these properties of WPC are decreased by

nearly 22%. Modification of nanoclay enhances the dispersion of nanoparticle into the composite. The large interfacial area of nanoclay are due the better dispersion of nanoparticles into the composite has contributed to the change of mobility and curing degree of polymer chains (Schadler, 2003).

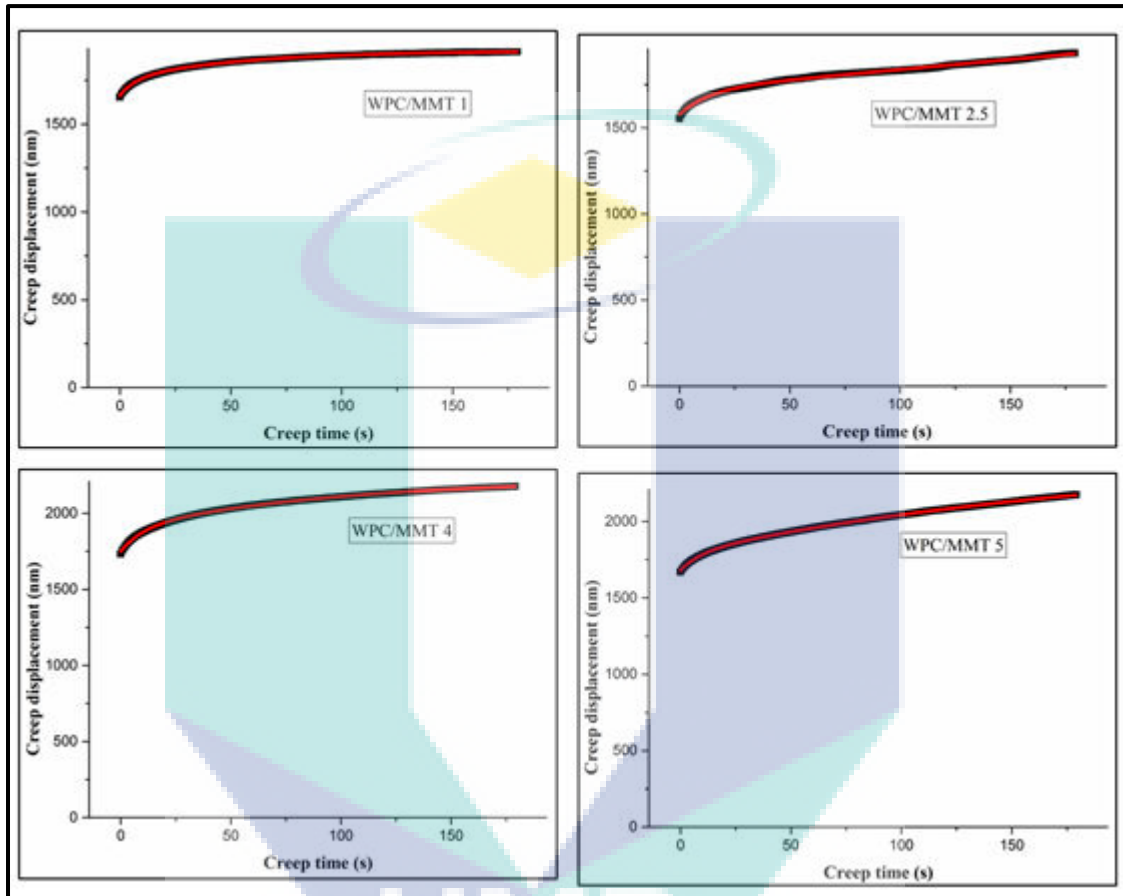


Figure 4.53 Creep displacement versus time for WPC/MMT with different nanoclay concentrations. Solid black line is experimental data and the thin red line is fitting results by Eq. (4.1)

The fitting results base on Eq. 4.1 for the indentation creep data are exhibited in Table 4.14 and Figure 4.53, 4.54. The incorporation of nanoclay into the WPC reduces the value of instantaneous displacement, h_e , which resulted from the elastic deformation. The decrement of instantaneous displacement indicating that the higher stiffness of composite. However, with increasing nanoclay content, the initial creep is slightly increased. As mentioned in previous result that the increase in h_e could be corresponded with agglomeration of nanoclay in the polymer matrix.

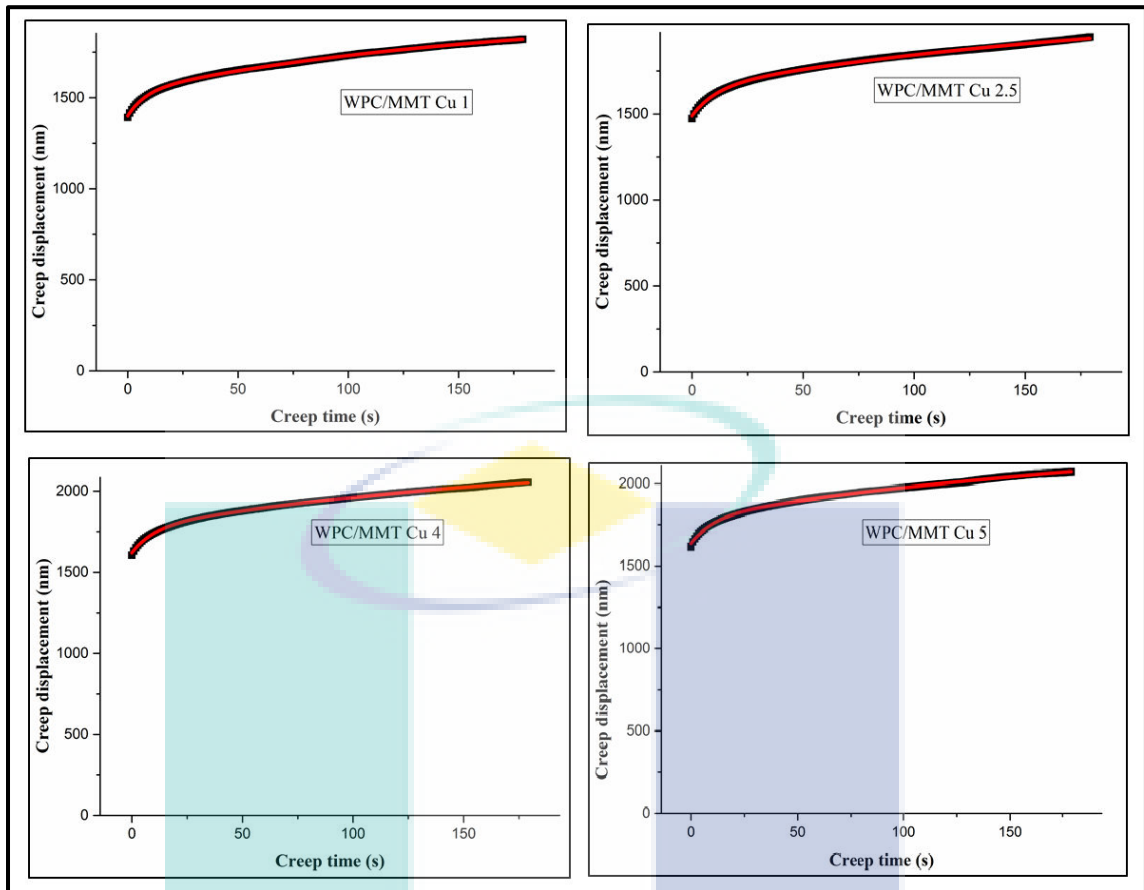


Figure 4.54 Creep displacement versus time for WPC/MMT Cu with different nanoclay concentrations. Solid black line is experimental data and the thin red line is fitting results by Eq. (4.1)

The WPC with less content of nanoclay show a lower value of h_e , indicating a higher stiffness of composite were developed. The higher initial displacement and elastic deformation at the early stage of creep increased due to the further increment in nanoclay loading. WPC/MMT Cu show better performance in creep resistant than WPC/MMT at the initial stage of creep due to a lower value of h_e . It shows that the incorporation of modified nanoclay into the polymer matrix plays a vital role in controlling creep at the initial stages.

Table 4.14 Fitting parameters from Eq. (4.1) for polypropylene, WPC, WPC/MMT and WPC/MMT Cu from indentation creep experiment

Parameters	WPC/MMT				WPC/MMTCu			
	1 wt%	2.5 wt%	4 wt%	5wt%	1 wt%	2.5 wt%	4 wt%	5wt%
h_e (nm)	1576	1662	1679	1748	1400	1489	1620	1634
h_1 (nm)	227	253	363	390	145	160	182	657
τ_1 (s)	161	189	207	257	13	55	99	207
h_2 (nm)	133	155	165	551	29	95	111	328
τ_2 (s)	8.21	8.35	8.43	8.67	8.12	8.18	8.26	8.29

For viscoelastic behaviour which is represented by h_1 and h_2 , the presence of nanoclay demonstrates some enhancement on the creep performance by decreased depth penetration in both MMT and MMT Cu nanoclay-based WPC. The retardant time became longer, especially in τ_1 , due to the increasing nanoclay content. The increase of retardation time represents the polymer matrix and nanoclay interactions. The τ_1 showed higher value than τ_2 , most probably associated with the movement of the polymer chains.

4.6 Optimization of TMI-modified nanoclay based wood-plastic composite by Response surface methodology (RSM)

4.6.1 Screening of WPC parameters by Fractional Factorial Design (FFD)

A screening experiment was carried out by following a 2^{5-1} factorial design and total 16 experiments were performed. An initial range for screening was chosen from the previous study (Mathuna and Li, 2004a). Polypropylene content (X1), Nanoclay content (X2), wood flour particle size (X3), Die temperature (X4), and Screw speed (X5) were the studied factors, while tensile strength (MPa) of WPC was the response. The factors and their ranges are summarized in Table 4.15 and the experimental design and the corresponded results are presented in Table 4.16.

Table 4.15 Factors and respected ranges for screening experiment

Factors	Unit	Minimum	Maximum
Polypropylene content	%	73	78
Nanoclay content	%	1	5
Wood flour particle size	μ	250	400
Die temperature	$^{\circ}\text{C}$	170	190
Screw speed	rpm	50	80

Table 4.16 Factorial design with response

Run	Polypropylene content (%)	Nanoclay content (%)	Wood flour particle size (μ)	Die temperature ($^{\circ}$ C)	Screw speed (rpm)	Tensile strength (MPa)
1	73.00	1.00	400	170.00	80.00	34.39
2	73.00	5.00	250	190.00	50.00	28.07
3	73.00	1.00	250	190.00	80.00	33.20
4	78.00	1.00	250	170.00	80.00	35.53
5	78.00	5.00	250	170.00	50.00	27.55
6	78.00	5.00	400	190.00	50.00	27.68
7	73.00	5.00	400	170.00	50.00	29.32
8	73.00	1.00	400	190.00	50.00	34.82
9	78.00	1.00	400	190.00	80.00	33.98
10	78.00	5.00	400	170.00	80.00	26.37
11	78.00	5.00	250	190.00	80.00	27.71
12	73.00	5.00	250	170.00	80.00	26.85
13	73.00	5.00	400	190.00	80.00	27.53
14	73.00	1.00	250	170.00	50.00	35.59
15	78.00	1.00	400	170.00	50.00	31.98
16	78.00	1.00	60	190.00	50.00	34.49

The ANOVA results was generated from the factorial design and it is presented in Table 4.17.

UMP

Table 4.17 Analysis of variance (ANOVA) table for the screening experiment of experimental factors with actual units and experimental responses

Source	Sum of Squares	df	Mean Square	F-Value	p-value Prob > F	
Model	185.0127	7	26.43039	39.72198	< 0.0001	significant
A-Polypropylene (X1)	1.2544	1	1.2544	1.885226	0.2070	
B-Nanoclay content (X2)	174.900625	1	174.9006	262.8565	< 0.0001	
C-Particle Size (X3)	0.5329	1	0.5329	0.80089	0.3970	
D- Extruder Die temperature (X4)	0.000625	1	0.000625	0.000939	0.9763	
E-Extruder Screw speed (X5)	0.970225	1	0.970225	1.458142	0.2617	
AC	3.629025	1	3.629025	5.454028	0.0478	
AE	3.7249	1	3.7249	5.598118	0.0455	
Residual	5.323075	8	0.665384			
Cor Total	190.335775	15				

The ANOVA results depicted in Table 4.17 showed that nanoclay content with P-value < 0.0001 has the most significant effect on the response. While Polypropylene content, particle size, extruder die temperature, extruder screw speed have P-value > 0.005, hence it did not have any significant effect on the response.

Statistical summary of the FFD is presented in Table 4.18. Parameters like F-value, probability > F, lack of fit, R-squared were obtained from the analysis of the data using Design expert software. An Adj. R-Squared value of 0.972 exhibited that the data is fitted well with the model. An adequate precision measures the signal to noise ratio and value of 15.759 was obtained (desired is > 4), it indicates that the signal is sufficient for the model to be used to navigate the design space.

Table 4.18 Statistical summary of screening result

Standard Deviation	Mean	Coefficient of Variation	R ²	Adjusted R ²	Adequate Precision
0.815	30.94	2.636	0.972	0.947	15.759

A linear regression equation obtained from the regression results of FFD could be expressed as Equation 4.2.

$$\text{Tensile strength (Y}_1\text{)} = 30.94 - 0.28 X_1 - 3.31 X_2 + 0.18 X_3 - (0.00625 - 003 X_4) - 0.25 X_5 \quad (4.2)$$

The obtained results from Fractional Factorial Design (FFD) is illustrated in Figure 4.54, 4.55, 4.56 and 4.57 which shows all the possible interactions of the five parameters. All parameters showed a high or a less influence on the tensile strength of WPC.

Figure 4.55 shows the interaction effect of Polypropylene content (73-78 wt%) and nanoclay content (1-5 wt%) on the tensile strength (response). The tensile strength of WPC was found remarkably higher at low content of nanoclay. This could be attributed to the well dispersed nanoparticles. However, Further addition of nanoclay (5 wt%) caused a decrement in tensile strength of composite. unlike to nanoclay content, high loading of polypropylene increased the tensile strength of WPC. The response value was observed up to 33.60 MPa at 78 wt% of polypropylene and 1 wt% of nanoclay but it started to reduce drastically and reached a minimum of 27.50 MPa at 73 wt% of polypropylene and 5 wt% of nanoclay. The reason might be the low interfacial interaction between polymer matrix and nanoclay (Javier et al., 2015). The better polypropylene-nanoclay interaction in the composite leads to strong interfacial adhesion. Another cause might be the agglomeration of nanoclay due to the high loading.

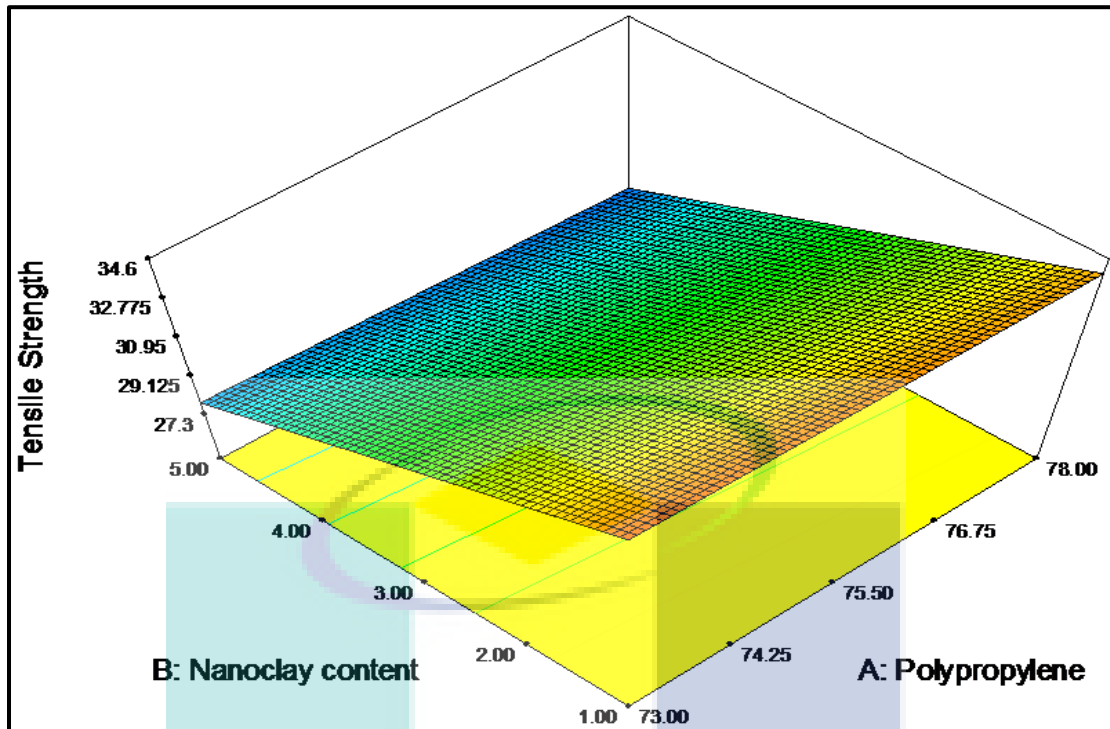


Figure 4.55 3D plot showing the interaction between polypropylene content and nanoclay

The polypropylene and wood flour particle size (μ) interaction graph is illustrated in Figure 4.56. It is noticed that polypropylene and wood flour particle size both have significant impact on tensile strength of WPC followed by nanoclay content. The response values were observed up to 31.30 MPa at 400 μ particle size and 73wt% of polypropylene. Nevertheless, it started to decrease and reached a minimum of 30.90 MPa at 250 μ particle size and 78 wt% of polypropylene. The reduction in response value was on account of high particle size which led to the impairment of interfacial interaction between polymer matrix and wood flour (Soccalingame et al., 2015).

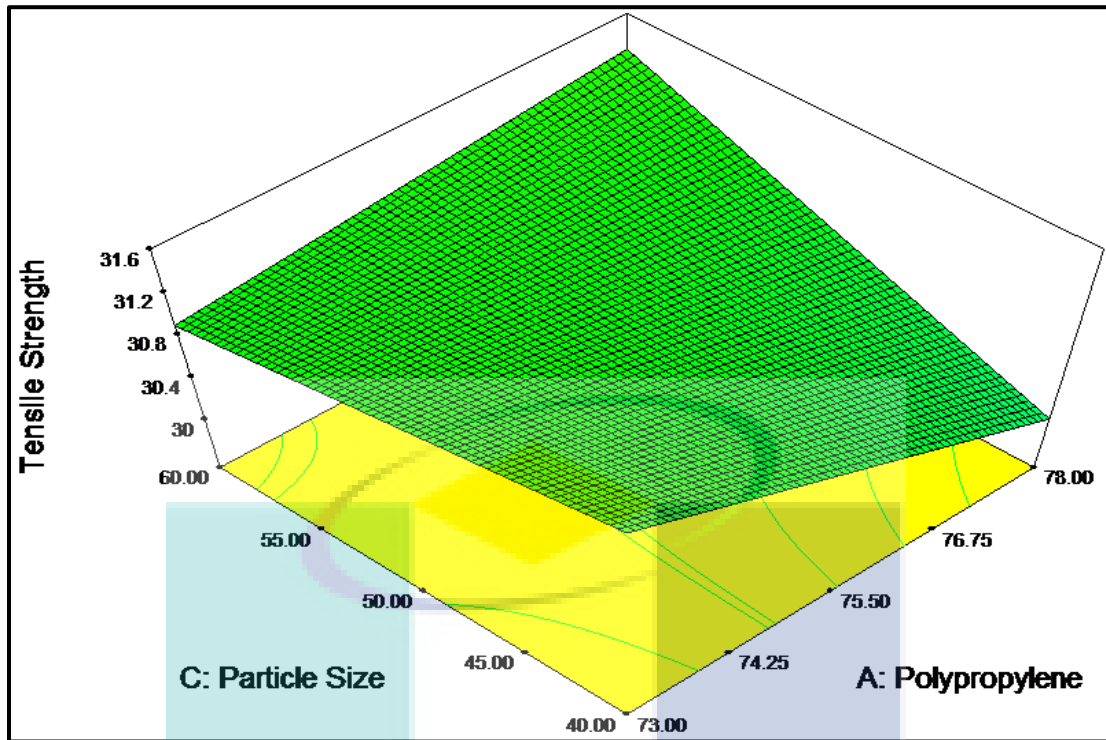


Figure 4.56 3D plot showing the interaction between polypropylene content and wood flour particle size

The nanoclay content and wood flour particle size interaction graph was illustrated in Figure 4.57. Nanoclay content and wood flour particle size had important effect on the tensile strength. The response value was observed to be maximized more than 34.50 MPa at 1 wt% of nanoclay and at 400 μ particle size, but it started to decrease slightly and to reach the maximum of 27.40 Mpa at 5 wt% of nanoclay and at 250 μ particle size. This was an improvement in tensile strength values, due to complete interaction between nanoclay and wood flour into the composite.

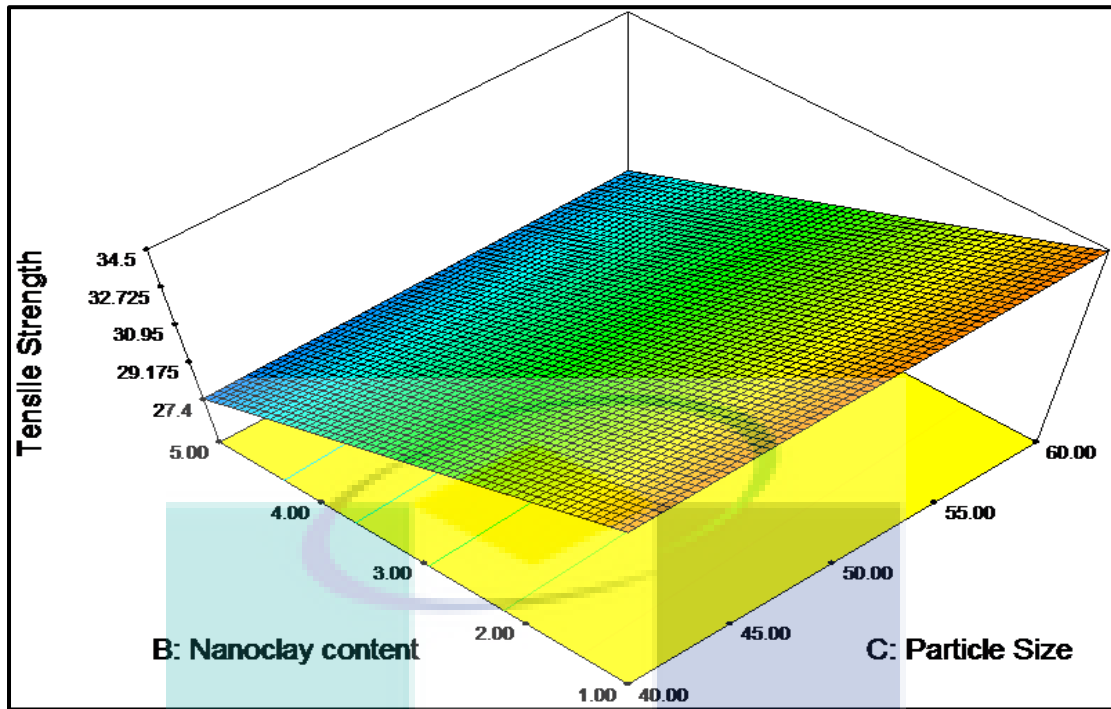


Figure 4.57 3D plot showing the interaction between nanoclay content and wood flour particle size

The screw speed and die temperature of extruder graph was illustrated in Figure 4.58. The screw speed had an important effect of more than the die temperature of extruder on tensile strength. The response value was observed to be maximized more than 31 MPa at 50 rpm of screw speed and 170 °C die temperature, but it started to decrease radically and to reach the minimum of 30.68 MPa at 80 rpm and 190 °C die temperature. This decline in tensile strength value of WPCs might be due to the improper dispersion or mixing of WPCs components at high screw speed of extruder. Matuana and Li, (2004) observed that processing at higher speed rate prevented the loss of wood flour moisture through the environment, thus the water vapour generated during processing creates bubbles into the composite and reduces the tensile strength of composite.

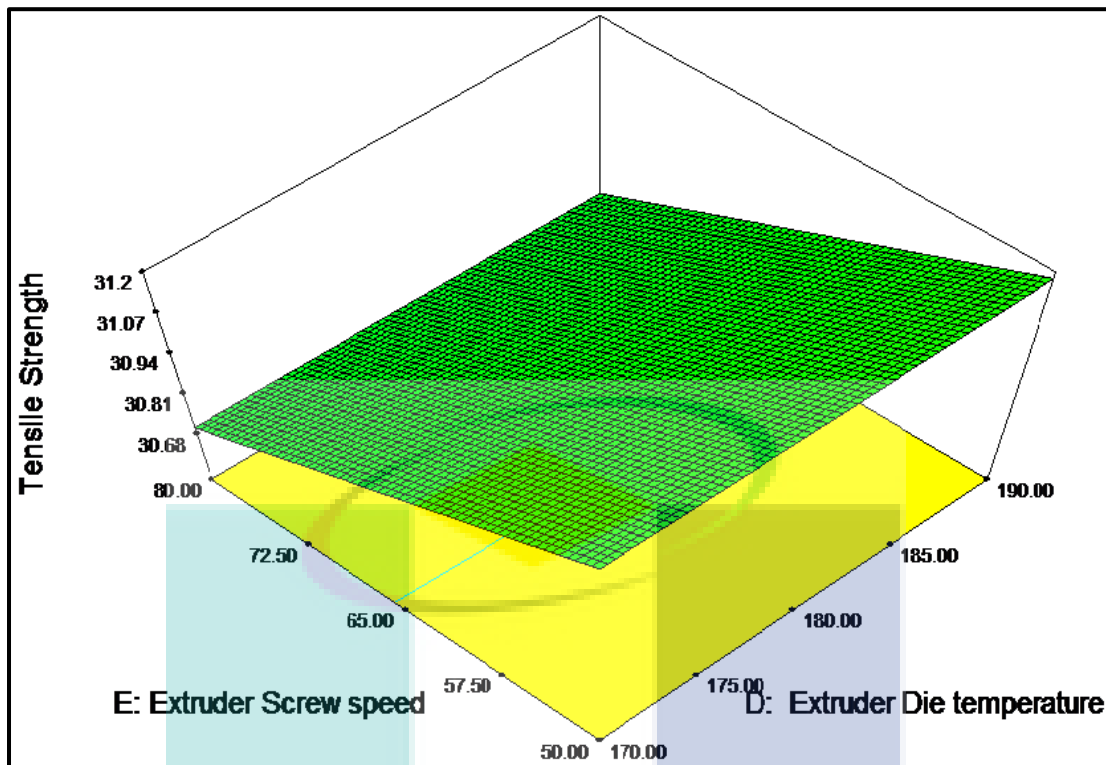


Figure 4.58 3D plot showing the interaction between extruder screw speed and die temperature

4.6.2 Augmentation of Central Composite Design (CCD)

In the final step of optimization process, the central composite design was employed to develop a quadratic model in order to obtain the true optimum condition for the fabrication of high performer WPC using nanoclay.

FFD exhibited that all five factors shown more or less influence on the tensile strength of WPC but as per FFD analysis data among all factors nanoclay content and polypropylene content had high contribution for tensile strength. Thus the new range ranges were calculated from screening to optimizing the fabrication conditions for WPC. Thirteen runs were executed to investigate the effect of nanoclay content and polypropylene content on tensile strength of composite. The CCD matrix with actual variables and response as tensile strength is presented in Table 4.19.

Table 4.19 Central composite design (CCD) with response

Run order	Nanoclay content (wt%)	Polypropylene content (wt%)	Tensile strength (MPa)
1	1.00	75.00	33.01
2	1.00	71.00	33.05
3	1.00	73.00	34.29
4	1.00	73.00	34.39
5	0.00	73.00	28.21
6	1.50	74.00	33.31
7	0.50	74.00	35.38
8	2.00	73.00	33.51
9	1.50	72.00	33.89
10	0.50	72.00	34.87
11	1.00	73.00	34.32
12	1.00	73.00	34.14
13	1.00	73.00	34.49

4.6.3 Fitting Model and Analysis Variance

Regression analysis was performed to fit the response function with the experimental information. The statistical significance of second-order model equation was checked by F-test is part of ANOVA. The statistical parameters obtained from the ANOVA have appeared in Table 4.20. As it can be seen that the model-F value for tensile strength was 21.52 which demonstrates the model is significant. An adequate precision measures the signal to noise proportion and proportion more prominent than 4 is desirable. The model showed adequate precision ratio of 16.310, means that this model can be utilized to explore the navigate design space (Drissen et al., 2007). The prob>F estimation of under 0.005 demonstrated that the model is significant. Here, the created model has a prob>F estimation of 0.0004, which demonstrated that the model is exceptionally significant. The "Lack of Fit F-quality" of 8.34 suggests the Lack of Fit is not significant, demonstrating that the model is fitted well.

Table 4.20 Analysis of variance (ANOVA) table of the quadratic model for tensile strength

Source	Sum of Squares	df	Mean Square	F-Value	p-value Prob > F	
Model	38.32	5	7.66	21.52	< 0.0004	significant
A-Nanoclay	22.55	1	22.55	63.32	< 0.0001	
B-Polypropylene	1.875SE-003	1	1.875E-003	5.265E-003	0.9442	
AB	0.30	1	0.30	0.83	0.3915	
A ²	9.06	1	9.06	25.44	0.0015	
B ²	2.48	1	2.48	6.95	0.0336	
Residual	2.49	7	0.36			
Lack of Fit	0.43	3	0.081	8.34	0.0913	Not significant
Pure error	0.067	4	0.017			
Cor Total	40.81	12				

The regression model is displayed in Table 4.21. The R² value of 0.9389 shows that the regression model fits to the experimental values well and it can give a helpful clarification to the connections between the independent variables and response. Equation 5.2 exhibits the model acquired from the Design Expert Software.

Table 4.21 Coefficient of variation, R², and adequate precision of the model

Standard Deviation	Mean	Coefficient of Variation	R ²	Adjusted R ²	Predicted R ²	Adequate precision
0.60	34.53	1.73	0.9389	0.8953	0.4093	16.310

$$\text{Tensile strength (MPa)} = + 34.25 - 1.37 X_1 - 0.013 X_2 - 0.27 X_1X_2 + 0.63 X_1^2 - 0.33 X_2^2$$

Where X1 and X2, represents the nanoclay and polypropylene content respectively.

4.6.4 Adequate Check Model

ANOVA was used to check the adequacy of the second-order model. The statistical properties of model can be checked by assessing different diagnostic plots, for example, plots of normal probability and studentized residuals. The most important diagnostic plot is the normal probability plot of the studentized residual (Korbahti and Rauf, 2008). The studentized residuals are defined as the residual divided by the calculated standard deviation of the residual, which measures the number of standard deviation isolating the actual and predicted values. Figure 4.59, displayed the normal probability plot, delineating about a straight line of studentized residuals distribution. It demonstrates that the error was uniformly circulated and supports the adequacy of the least square fit.

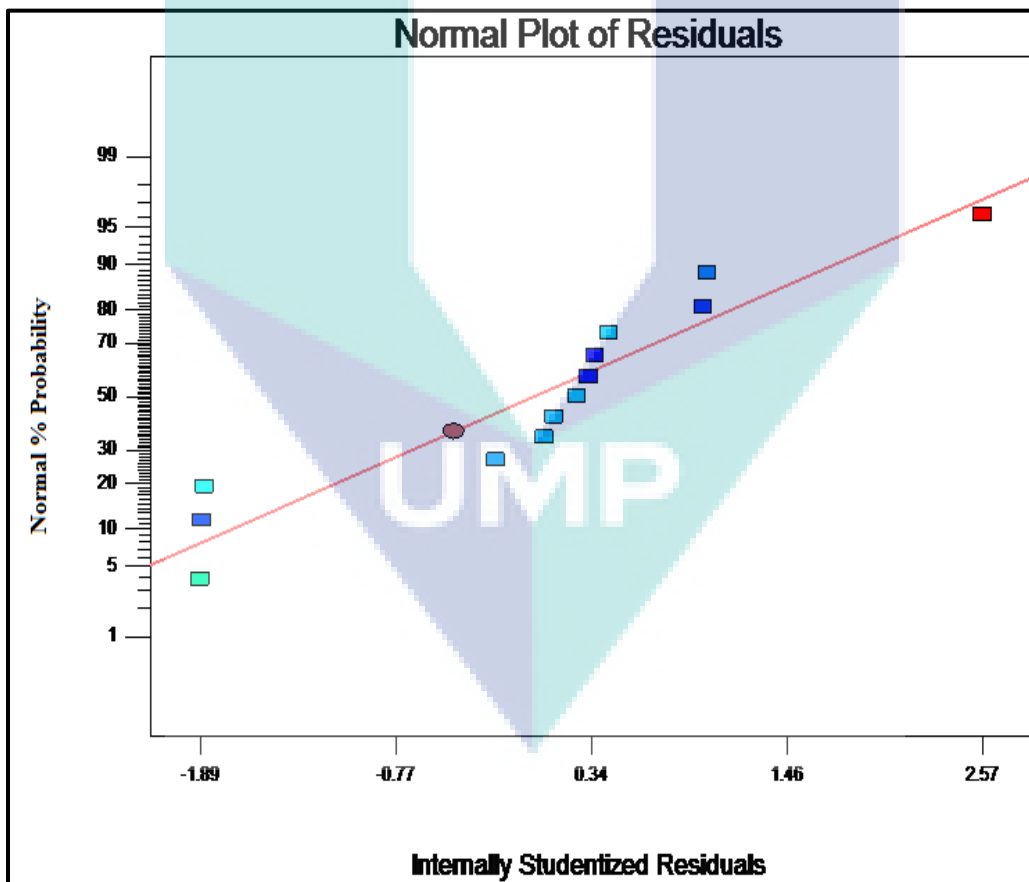


Figure 4.59 Normal plot of residuals generated from the model

Figure 4.60 outlines the studentized residual obtained from the analysis versus predicted value computed from the model. In a perfect world, the plot should be randomly scattered, proposing that the difference of real observations is consistent for all values of the response. The graph revealed that the proposed model is particularly adequate and reasonably free from any violation of the independence or constant value assumption, as studentized residuals lies in the range of ± 3 (Mason et al., 2003).

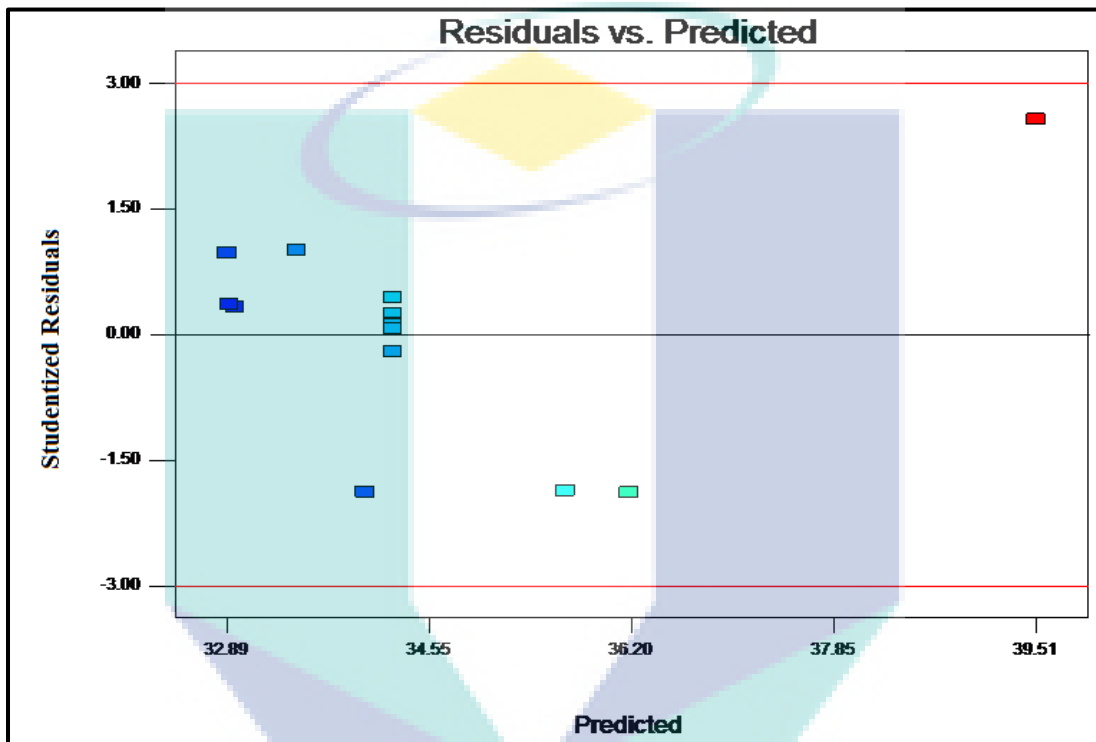


Figure 4.60 Diagnostic plot generated from the model for plot of Residual vs. Predicted

4.6.5 Optimization Condition for Response Surface analysis

The result of CCD is depicted in Figure 4.61. The possible interaction of two parameters is displayed in order to achieve maximum tensile strength. Figure 4.61 was plotted between nanoclay and polypropylene content by observing tensile strength (response) at range of nanoclay content (0-2 wt%) and polypropylene content (71-75 wt%). The tensile strength was found remarkably increasing at low nanoclay and high polypropylene content. Low content of nanoclay plays an important role of transferring maximum stress from polymer matrix to the wood flour. As discussed earlier, high content of nanoclay agglomerates during the compounding and reduces the strength of

the composite. During manufacturing of wood-plastic composite, the distribution of nanofillers is crucial because it significantly affects the tensile strength of the composite than other factors.

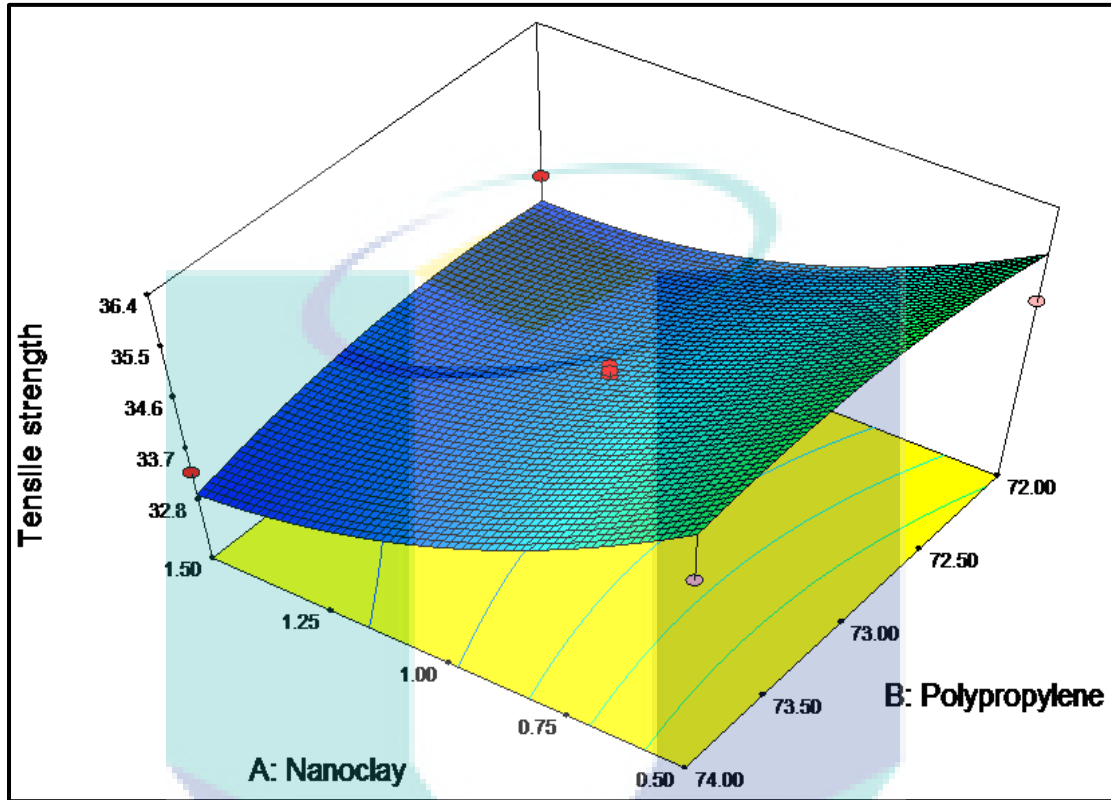


Figure 4.61 Nanoclay content vs. Polypropylene content

The effect of nanoclay and polypropylene content on response was drawn in Figure 4.61. The response surface of tensile strength was observed with maximum of 35.38 MPa at 0.50 wt% of nanoclay content and 74 wt% of Polypropylene content. A high degree of interaction was observed in these two factors.

4.6.6 Model Validation and Experimental Confirmation

Validation of the developed empirical model adequacy is important to justify the impact of nanoclay on tensile strength of wood-plastic composite. Based on the model and numerical optimization executed in the Design Expert ($D \times 7$) software, three suggested ideal conditions were chosen, which is exhibited in Table 4.22. The ideal optimum conditions were picked on the premise of economics of working feasibility

and maximum desirability of the response. In Table 4.22, the highlighted optimum conditions was chosen to optimize the tensile strength, where the initial parameters of conversion was set as wood flour particle size 40 mesh, die temperature of extrusion 186.17 °C, screw speed of extruder 50 rpm. To verify the predicted optimum condition three repeated experiments were performed and the tensile strength was observed as 34.21 MPa, 34.14 MPa, and 33.92 MPa.

The actual results were compared with the predicted value and % error was calculated by using Equation 4.3 and Equation 4.4. When compared to the actual tensile strength with the predicted value maximum percentage error was found as 0.021 %, 0.024%, and 0.023% respectively. The finding indicates that the developed model is reasonably accurate within 95% confidence interval and considerably adequate to give a precise result.

$$\text{Residual} = \text{Actual Value} - \text{Predicted value} \quad (4.3)$$

$$\% \text{ Error} = \frac{\text{Residual}}{\text{Actual Value}} \times 100 \quad (4.4)$$

Table 4.22 Optimum condition obtained from RSM

Number	Nanoclay (wt%)	content Polypropylene content (wt%)	Tensile strength (MPa)	Desirability
1	1.38	72.00	33.46	0.937
2	1.44	72.00	33.45	0.938
3	1.47	73.94	32.97	1.000

CHAPTER 5

CONCLUSIONS AND RECOMMENDATIONS

5.1 Conclusions

The research and development activities during this doctoral research brought important results which would eventually help the industry to develop high performance WPC. The primary hypothesis of this study has been confirmed, that adding nanoclay as filler in WPC improves the properties of WPC. During this work, such materials were successfully applied in the WPC and the hypothesis has been proved by demonstrating the targeted properties. This chapter briefly outlines the major conclusions of this doctoral research and its recommendations for further improvement.

All the objectives in this study were successfully achieved. The first objective was to fabricate and study the performance of WPC reinforced by organoclay. The incorporating of Organoclay into the WPC effectively improved the mechanical properties; this improvement comes at 1 wt% of Organoclay loading. The sample with 1 wt% Organoclay showed lower water absorption among other samples. The SEM and TEM micrographs showed that high contents of Organoclay (4-5 wt. %) were dispersed poorly and agglomerated easily and this caused the reduction in mechanical and physical properties of the composite. The highest improvement on the thermal stability of composites was achieved at 1wt% and 2.5 wt% of Organoclay loading. Fourier transform infrared spectroscopy (FT-IR) and XRD analysis showed that the layered silicates (Si-O) were able to disperse in WPC.

The second objective which was the modification of pristine nanoclay and it was successfully obtained using transition metal ion modification method, in which copper

chloride (CuCl_2) was used as a transition metal ion. The following objective was the incorporation of the pristine and TMI-modified nanoclay into the WPC and studying the properties of WPC. After the fabrication process, the presence of the nanoclay was confirmed through the silica peaks that appeared in the FTIR analysis. The obtained SEM images showed that the incorporation of pristine nanoclay into the WPC created number of holes, gaps, and cracks as well as large agglomerates in its structures. The modification proved to be successful as there were few numbers of holes, cracks and agglomerates present in the SEM micrographs of WPC reinforced copper modified nanoclay (WPC/MMT Cu). WPC loaded by copper modified nanoclay showed uniform dispersion of nanoclay particles over WPC/MMT and it was confirmed by TEM analysis.

Major improvements on the mechanical properties of the WPC was observed in WPC/MMT Cu whereby the tensile strength, flexural strength, elongation at break and impact strength of the WPC reinforced by modified nanoclay showed a significant increase compared to the WPC/MMT. 1 wt% and 2.5 wt% nanoclay loading of WPC/MMT Cu were the dominant of all samples were tested. In both the physical properties test, WPC/MMT Cu depicted the best improvements. Following that, improved thermal stability in the WPC with modified nanoclay could be seen from the TGA and DTG analysis. Higher thermal degradation temperature was obtained in the presence of WPC/MMT Cu. According to the DSC results, it can be observed that the degree of crystallinity was improved by the incorporation of the nanoclay. However, incorporation of nanoclay did not affect significantly on the melting temperature of WPC.

The fourth objective was to study the surface mechanical properties and surface creep behaviour of WPC which were studied by using nanoindentation technique. WPC reinforced with 1 wt% of organoclay and TMI-modified nanoclay significantly improved the hardness, elastic modulus and creep resistance of WPCs. The improvement was achieved at 43%, 42% and 15% for WPC/C20 and 44%, 45% and 21% for WPC/MMT Cu over WPC (control sample) respectively. However, higher loading of nanoclay dramatically decreased the surface mechanical properties and creep resistance of composite. WPCs reinforced with TMI-modified nanoclay showed greater

improvement than the WPC reinforced with organoclay and pristine nanoclay due to higher compatibility between the modified nanoclay and the polymer matrix. Moreover, WPCs reinforced by organoclay exhibited lower improvement than WPC/MMT Cu. The reason might be that the decomposition of organic surfactants in organoclay structure above 170 °C.

The fifth and the last objective was to optimize the best fabrication conditions for WPC/MMT Cu by using response surface methodology. The effects of tensile strength on the fabrication of WPC/MMT Cu were screened using FFD with five factors which were polypropylene content, nanoclay content, wood flour particle size, extruder die temperature and extruder screw speed and optimized using CCD with two factors which were polypropylene content, and nanoclay content. Based on FFD results, polypropylene content and nanoclay content were selected for CCD (optimization) analysis due to their high contribution towards the tensile strength among other factors. The optimum tensile strength was obtained i.e., 33.46 MPa at 72 wt% of polypropylene, 1.38 wt% of nanoclay, 40 mesh wood flour particle size, 186.17 °C die temperature of extrusion and 50 rpm screw speed of extruder.

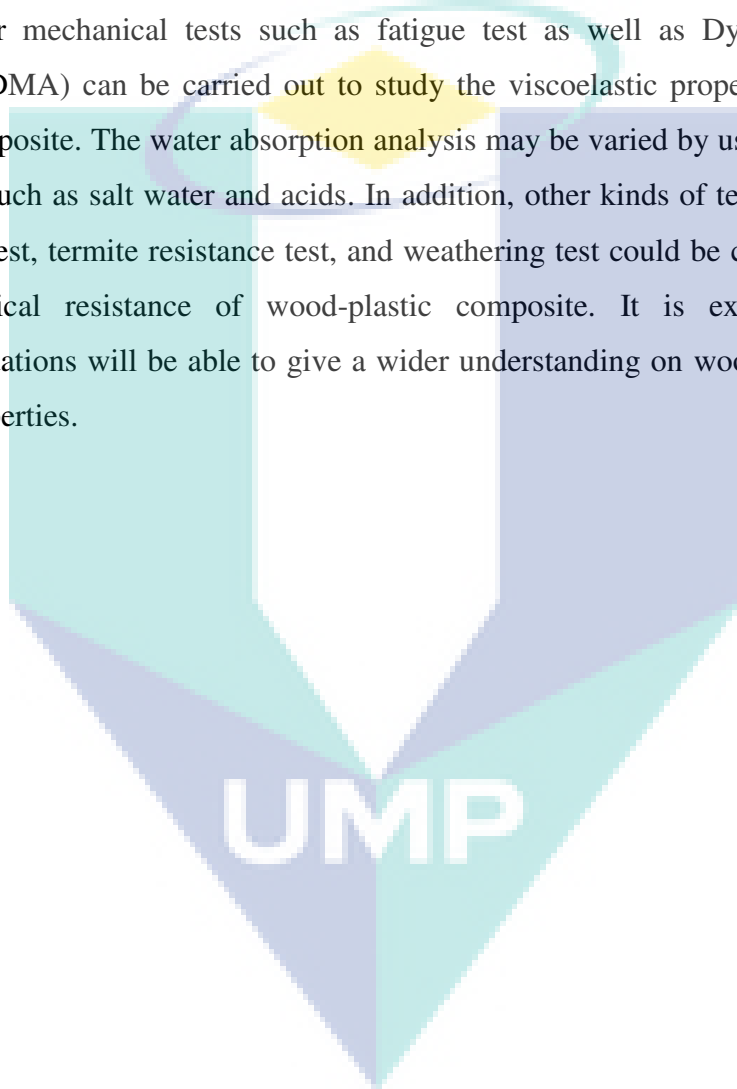
5.2 Recommendations for Future Work

In order to have a better understanding on the influence of the incorporation of conventional nanoclay and modified nanoclay on the properties of wood-plastic composite, different polymers could be used as the polymer matrix. For instance, polymer such as polyamide 6 (PA6) and polylactic acid (PLA) could be used and the property studies could be widened even further to biodegradability studies and rheological studies.

Apart from that, properties of WPC may be improved by employing different new kinds of nanofillers such as graphene, carbon nanotubes. It is important that the new nanofillers are able to produce good intercalated wood-plastic composite in a small amount in order to be cost efficient. In addition, varying nanoclay weight percentages should be done to understand more on the impact of the concentrations on the properties tested. In this work, the MMT nanoclay was modified using copper ions. It is

recommended that other types of transition metal ions such as Titanium and Zinc are used to modify the nanoclay to get a better understanding on the catalytic performance that this metal brings upon the nanoclay.

The surface mechanical study of the wood-plastic composite can be expanded even further by studying scratch behaviour to gain a better understanding of the scratch resistance of wood-plastic composite. In addition to the mechanical tests formed in this work, other mechanical tests such as fatigue test as well as Dynamic Mechanical Analysis (DMA) can be carried out to study the viscoelastic properties of the wood-plastic composite. The water absorption analysis may be varied by using different kinds of liquids such as salt water and acids. In addition, other kinds of testing such as fungi resistance test, termite resistance test, and weathering test could be carried out to study the biological resistance of wood-plastic composite. It is expected that these recommendations will be able to give a wider understanding on wood-plastic composite and its properties.



REFERENCES

- Abraham, R., Thomas, S.P., Kuryan, S., Isac, J., Varughese, K.T. and Thomas, S. (2009). Mechanical properties of ceramic-polymer nanocomposites. *Polymer*. 8, p.12.
- Advani, S.G. (2007). Processing and Properties of Nanocomposites, *World Scientific Publishing Co.*, Hackensack, NJ.
- Ahmadi, S.J. and A. Mohadespour, (2005). *Polymer Nanocomposites: Layered Silicate*. 1st Edn., Atomic Energy Organization of Iran, Tehran, Iran.
- Ahmadi, S.J., Yudong, H. and Li, W. (2004). Synthesis of EPDM/organoclay nanocomposites: effect of the clay exfoliation on structure and physical properties. *Iranian Polymer Journal*. 13, pp.415-422.
- Alamri, H. and Low, I.M. (2013). Effect of water absorption on the mechanical properties of nanoclay filled recycled cellulose fibre reinforced epoxy hybrid nanocomposites. *Composites Part A: Applied Science and Manufacturing*. 44, pp.23-31.
- Alexandre, M. and Dubois, P. (2000). Polymer-layered silicate nanocomposites: preparation, properties and uses of a new class of materials. *Materials Science and Engineering: R: Reports*. 28(1), pp.1-63.
- Alhuthali, A., Low, I.M. and Dong, C. (2012). Characterisation of the water absorption, mechanical and thermal properties of recycled cellulose fibre reinforced vinyl-ester eco-nanocomposites. *Composites Part B: Engineering*. 43(7), pp.2772-2781.
- AlMaadeed, M. a, Ouederni, M. and Noorunnisa Khanam, P. (2013). Effect of chain structure on the properties of Glass fiber/polyethylene composites. *Material and Design*. 47, 725–730. doi:<http://dx.doi.org/10.1016/j.matdes.2012.11.063>
- Arao, Y., Nakamura, S., Tomita, Y., Takakuwa, K., Umemura, T. and Tanaka, T. (2014). Improvement on fire retardancy of wood flour/polypropylene composites using various fire retardants. *Polymer Degradation Stability*. 100, 79–85. doi:[10.1016/j.polymdegradstab.2013.12.022](http://dx.doi.org/10.1016/j.polymdegradstab.2013.12.022)
- Asgary, A.R., Nourbakhsh, A. and Kohantorabi, M. (2013). Old newsprint/polypropylene nanocomposites using carbon nanotube: Preparation and characterization. *Composites Part B: Engineering*. 45(1), pp.1414-1419.
- Ashori, A. (2008). Wood-plastic composites as promising green-composites for automotive industries. *Bioresources Technology*, 99, 4661–4667. doi:[10.1016/j.biortech.2007.09.043](http://dx.doi.org/10.1016/j.biortech.2007.09.043)

- Ashori, A. and Nourbakhsh, A. (2011). Preparation and characterization of polypropylene/wood flour/nanoclay composites. *European Journal of Wood and Wood Products*. 69, 663–666. doi:10.1007/s00107-010-0488-9
- Ashori, A., Sheshmani, S. and Farhani, F. (2013). Preparation and characterization of bagasse/HDPE composites using multi-walled carbon nanotubes. *Carbohydrate Polymer*. 92, 865–871. doi:10.1016/j.carbpol.2012.10.010
- Awal, A., Ghosh, S. and Sain, M. (2009). Thermal properties and spectral characterization of wood pulp reinforced bio-composite fibers. *Journal of thermal analysis and calorimetry*. 99(2), pp.695-701.
- Ayrilmis, N., Dundar, T., Kaymakci, A., Ozdemir, F. and Kwon, J.H. (2014). Mechanical and thermal properties of wood-plastic composites reinforced with hexagonal boron nitride. *Polymer composites*. 35(1), pp.194-200.
- Ayrilmis, N., Jarusombuti, S., Fueangvivat, V. and Bauchongkol, P. (2011). Effect of thermal-treatment of wood fibers on properties of flat-pressed wood plastic composites. *Polymer Degradation Stability*. 96, 818–822. doi:10.1016/j.polymdegradstab.2011.02.005
- Azeredo, H.M. (2009). Nanocomposites for food packaging applications. *Food Research International*, 42(9), pp.1240-1253.
- Babaei, I., Madanipour, M., Farsi, M. and Farajpoor, A. (2014). Physical and mechanical properties of foamed HDPE / wheat straw flour / nanoclay hybrid composite. *Composite: Part B*. 56, 163–170. doi:10.1016/j.compositesb.2013.08.039
- Bakraji, E.H. and Salman, N. (2003). Properties of wood–plastic composites: effect of inorganic additives. *Radiation Physics and Chemistry*. 66(1), pp.49-53.
- Balasuriya, P.W., Ye, L. and Mai, Y. (2001). Mechanical properties of wood fake-polyethylene composites. Part I: effects of processing methods and matrix melt flow behaviour. *Composite: Part A*. 32, 619–629.
- Barone, J.R., Schmidt, W.F. and Liebner, C.F.E. (2005). Compounding and molding of polyethylene composites reinforced with keratin feather fiber. *Composite Science and Technology*. 65, 683–692. doi:10.1016/j.compscitech.2004.09.030
- Bas, D. and Boyaci, I.H. (2007). Modeling and optimization I: Usability of response surface methodology. *Journal of Food Engineering*. 78, 836–845. doi:10.1016/j.jfoodeng.2005.11.024
- Baysal, G., Aydin, H., Koytepe, S. and Seckin, T. (2013). Comparison dielectric and thermal properties of polyurethane/organoclay nanocomposites. *Thermochimica Acta*. 566: 305-313.
- Becker, O. and Simon, G.P. (2006). *Polymer Nanocomposites*. Mai, Y.W. and Yu, Z.Z. England; Woodhead Publishing Limited.

- Bengtsson, M., Gatenholm, P. and Oksman, K. (2005). The effect of crosslinking on the properties of polyethylene/wood flour composites. *Composite Science and Technology*. 65, 1468–1479. doi:10.1016/j.compscitech.2004.12.050
- Bengtsson, M. and Oksman, K. (2006). Silane crosslinked wood plastic composites: Processing and properties. *Composite Science Technology*. 66, 2177–2186. doi:10.1016/j.compscitech.2005.12.009
- Bezerra, M.A., Santelli, R.E., Oliveira, E.P., Villar, L.S. and Escaleira, L. a. (2008). Response surface methodology (RSM) as a tool for optimization in analytical chemistry. *Talanta*. 76, 965–977. doi:10.1016/j.talanta.2008.05.019
- Bhaskar, J., Haq, S., Pandey, A.K. and Srivastava, N. (2012). Evaluation of properties of propylene-pine wood Plastic composite. *Journal of Materials and Environmental Science*, 3(3), pp.605-612.
- Bishay, I.K., Abd-El-Messieh, S.L. and Mansour, S.H. (2011). Electrical, mechanical and thermal properties of polyvinyl chloride composites filled with aluminum powder. *Material and Design*. 32, 62–68. doi:10.1016/j.matdes.2010.06.035
- Biswal, M., Mohanty, S. and Nayak, S.K. (2009). Influence of organically modified nanoclay on the performance of pineapple leaf fiber-reinforced polypropylene nanocomposites. *Journal of applied polymer science*, 114(6), pp.4091-4103.
- Biswas, M. and Sinha, R.S. (2001). Recent progress and synthesis in evaluation of polymer montmorillonite nanocomposites. *Advanced Polymer Science*. 155: 167-221.
- Blumstein, A. (1965). Polymerization of adsorbed mono-layers. I. Preparation of the clay- polymer complex. *Journal of Polymer Science: Part A*. 3: 2653-2664.
- Bouafif, H., Koubaa, A., Perre, P. and Cloutier, A. (2009). Effects of fiber characteristics on the physical and mechanical properties of wood plastic composites. *Composites Part A: Applied Science and Manufacturing*, 40(12), pp.1975-1981.
- Bouafif, H., Koubaa, A., Perre, P. and Cloutier, A. (2008). Effects of Fiber Characteristics on the Physical and Mechanical Properties of wood plastic composite. *9 th International. Conference on Flow Process and Composite*. Material. 9.
- Breton, Y., Desarmot, G., Salvétat, J.P., Delpoux, S., Sinturel, C., Beguin, F. and Bonnamy, S. (2004). Mechanical properties of multiwall carbon nanotubes/epoxy composites: influence of network morphology. *Carbon*, 42(5), pp.1027-1030.

- Cahn, R.W. ed. (2005). *Concise encyclopedia of magnetic and superconducting materials*. 2nd Edition, Elsevier, Oxford.
- Chaharmahali, M., Hamzeh, Y., Ebrahimi, G., Ashori, A. and Ghasemi, I. (2014). Effects of nano-graphene on the physico-mechanical properties of bagasse/polypropylene composites. *Polymer Bulletin*. 71, 337–349. doi:10.1007/s00289-013-1064-3
- Chang, J.H., An, Y.U., Cho, D. and Giannelis, E.P. (2003). Poly(lactic acid) nanocomposites: comparison of their properties with montmorillonite and synthetic mica (II). *Polymer*. 44(13): 3715-3720.
- Chavooshi, A., Madhoushi, M., Navi, M. and Abareshi, M.Y. (2014). MDF dust/PP composites reinforced with nanoclay: Morphology, long-term physical properties and withdrawal strength of fasteners in dry and saturated conditions. *Construction and Building Materials*, 52, pp.324-330.
- Chen, L., Wong, S. C. and Pisharath, S. (2003). Fracture properties of nanoclay-filled polypropylene. *Journal of Applied Polymer Science*, 88(14), 3298-3305.
- Chavooshi, A., Madhoushi, M., Navi, M. and Abareshi, M.Y. (2014). MDF dust/PP composites reinforced with nanoclay: Morphology, long-term physical properties and withdrawal strength of fasteners in dry and saturated conditions. *Construction and Building Materials*, 52, pp.324-330.
- Clemons, C. (2002). Wood-plastic composites in the United States: The interfacing of two industries. *Forest Products Journal*, 52(6), p.10.
- Craig M. Clemons and Rebecca E. Iback, (2004). Effects of processing method and moisture history on laboratory fungal resistance of wood-HDPE composites. *Forest Product Journal*. 4, 50–57.
- Das, S., Sara, A, K., Choudhury, P.K., Basak, R.K., Mitra, B. and Todd, C, T. (2000). *Journal of Applied Polymer Science*. 76, 1652–1661.
- Deka, B.K. and Maji, T.K. (2010). Effect of coupling agent and nanoclay on properties of HDPE, LDPE, PP, PVC blend and Phargamites karka nanocomposite. *Composite Science and Technology*. 70, 1755–1761. doi:10.1016/j.compscitech.2010.07.010
- Dennis, H. R., Hunter, D. L., Chang, D., Kim, L., White, J. L., Cho, J. W. and Paul, D. R. (2001). Effect of Melt Processing Condition on the Extent of Exfoliation in Organoclay-Based Nanocomposites. *Polymer*. 42, pp. 9513 – 9522.
- Dhakal, H.N., Zhang, Z.Y. and Richardson, M.O.W. (2006). Nanoindentation behaviour of layered silicate reinforced unsaturated polyester nanocomposites. *Polymer testing*, 25(6), pp.846-852.
- Dias, R.C.M., Goes, A.M., Serakides, R., Ayres, E. and Orefice, R.L. (2010). Porous biodegradable polyurethane nanocomposites: preparation,

characterization, and biocompatibility tests. *Material Research*. 13(2): <http://dx.doi.org/10.1590/S1516-14392010000200015>.

- Dimitry, O.I., Abdeen, Z.I., Ismail, E.A. and Saad, A.L.G. (2010). Preparation and properties of elastomeric polyurethane/organically modified montmorillonite nanocomposites. *Journal of polymer research*, 17(6), pp.801-813.
- Ding, Z. and R.L. Frost. (2004). Thermal study of copper adsorption on montmorillonites. *Thermochimica Acta* .416(1-2):11-16.
- Doan, T.T.L., Gao, S.L. and Mader, E. (2006). Jute/polypropylene composites I. Effect of matrix modification. *Composite Science and Technology*. 66, 952–963. doi:10.1016/j.compscitech.2005.08.009
- Dobrev, D., Nenkova, S. and Vasileva, S. (2006). Morphology and mechanical properties of polypropylene-wood flour composites. *BioResources* 1, 209–219.
- Dowling, A.H., Stamboulis, A. and Fleming, G.J.P. (2006). The influence of montmorillonite clay reinforcement on the performance of a glass ionomer restorative. *Journal of Dentistry*. 34(10): 802-810.
- Downing, T.D., Kumar, R., Cross, W.M., Kjerengtroen, L. and Kellar, J.J. (2000). Determining the interphase thickness and properties in polymer matrix composites using phase imaging atomic force microscopy and nanoindentation. *Journal of adhesion science and technology*, 14(14), pp.1801-1812.
- Dutta, A.K., Penumadu, D. and Files, B. (2004). Nanoindentation testing for evaluating modulus and hardness of single-walled carbon nanotube–reinforced epoxy composites. *Journal of materials research*, 19(01), pp.158-164.
- Espert, A., Vilaplana, F. and Karlsson, S. (2004). Comparison of water absorption in natural cellulosic fibres from wood and one-year crops in polypropylene composites and its influence on their mechanical properties. *Composites Part A: Applied science and manufacturing*, 35(11), pp.1267-1276.
- Etmimi, H.M. (2012). *New approaches to the synthesis and exfoliation of polymer/functional graphene nanocomposites by miniemulsion polymerization*. PhD. University of Stellenbosch, South Africa.
- Fabiya, J.S., McDonald, A.G., Morrell, J.J. and Freitag, C. (2011). Effects of wood species on durability and chemical changes of fungal decayed wood plastic composites. *Composites Part A: Applied Science and Manufacturing*, 42(5), pp.501-510.
- Fabiya, J.S., McDonald, A.G., Wolcott, M.P. and Griffiths, P.R. (2008). Wood plastic composites weathering: Visual appearance and chemical changes. *Polymer Degradation Stability*. 93, 1405–1414. doi:10.1016/j.polymdegradstab.2008.05.024

- Fang, Y., Wang, Q., Guo, C., Song, Y. and Cooper, P.A. (2013). Effect of zinc borate and wood flour on thermal degradation and fire retardancy of polyvinyl chloride (PVC) composites. *Journal of Analytical and Applied Pyrolysis*, 100, pp.230-236.
- Farhadinejad, Z., Ehsani, M., Khosravian, B. and Ebrahimi, G. (2012). Study of thermal properties of wood plastic composite reinforced with cellulose micro fibril and nano inorganic fiber filler. *European Journal of Wood and Wood Products*. 70, 823–828. doi:10.1007/s00107-012-0630-y
- Farsheh, A.T., Talaeipour, M., Hemmasi, A.H., Khademieslam, H. and Ghasemi, I. (2011). Investigation on the mechanical and morphological properties of foamed nanocomposites based on wood flour/PVC/multi-walled carbon nanotube. *BioResources*. 6, 841–852.
- Faruk, O. and Matuana, L.M. (2008). Nanoclay reinforced HDPE as a matrix for wood-plastic composites. *Composite Science and Technology*. 68, 2073–2077. doi:10.1016/j.compscitech.2008.03.004.
- Fink, C.A., Caulfield, D.F. Sanadi, A.R. (2000). The interphase in natural fiber composites – transcrystallinity effects on thermomechanical properties. *In Proceeding of the 23rd annual meeting of the adhesion society*. "Adhesion Science for the 20th Century", Feb. 20-23, Carolina, USA.
- Finnigan, B., Martin, D., Halley, P., Truss, R. and Campbell, K. (2004). Morphology and properties of thermoplastic polyurethane nanocomposites incorporating hydrophilic layered silicates. *Polymer*. 45(7): 2249-2260.
- Fisher, T., Hajaligol, M., Waymack, B. and Kellogg, D. (2002). Pyrolysis behavior and kinetics of biomass derived materials. *Journal of analytical and applied pyrolysis*, 62(2), pp.331-349.
- Flores, A. and Calleja, F.B. (1998). Mechanical properties of poly (ethylene terephthalate) at the near surface from depth-sensing experiments. *Philosophical Magazine A*, 78(6), pp.1283-1297.
- Frankowski, D.J., Capracotta, M.D., Martin, J.D., Khan, S.A. and Spontak, R.J. (2007). Stability of organically modified montmorillonites and their polystyrene nanocomposites after prolonged thermal treatment. *Chemistry of materials*, 19(11), pp.2757-2767.
- Gan, K.S., Choo, T. and Lim, S.C. (2000). Timber Notes - Medium Hardwoods I.
- Gao, S.L. and Mader, E. (2002). Characterisation of interphase nanoscale property variations in glass fibre reinforced polypropylene and epoxy resin composites. *Composites Part A: applied science and manufacturing*, 33(4), pp.559-576.
- Garcia, M., Hidalgo, J., Garmendia, I. and García-Jaca, J. (2009). Wood–plastics composites with better fire retardancy and durability performance.

Composites Part A: Applied Science and Manufacturing, 40(11), pp.1772-1776.

- Gardner, D.J., Han, Y. and Wang, L. (2015). Wood–Plastic Composite Technology. *Current Forestry Reports*, 1(3), pp.139-150.
- Gardner, D.J. and Murdock, D. (2002). Extrusion of Wood Plastic Composites. *Advanced Engineering Wood Composite Center*. 1–6.
- Gassan, J. and Bledzki, a. K. (2000). Possibilities to improve the properties of natural fiber reinforced plastics by fiber modification - jute polypropylene composites. *Applied Composite Material*. 7, 373–385. doi:10.1023/A:1026542208108
- Gebhardt, A. (2011). Understanding Additive Manufacturing. *Underst. Addit. Manuf.* 1–29. doi:10.3139/9783446431621
- George, J., Bhagawan, S.S. and Thomas, S. (2000). Low-Density Polyethylene Composites Reinforced With Pineapple-Leaf Fiber. *Journal of Applied Polymer Science*. 57, 843–854.
- Georgopoulos, S.T., Tarantili, P.A., Avgerinos, E., Andreopoulos, A.G. and Koukios, E.G. (2005). Thermoplastic polymers reinforced with fibrous agricultural residues. *Polymer Degradation and Stability*, 90(2), pp.303-312.
- Ghasemi, I. and Kord, B. (2009). Long-term Water Absorption Behaviour of Polypropylene/Wood Flour/Organoclay Hybrid Nanocomposite. *Iranian Polymer Journal*. 18, 683–691.
- Giannelis, E.P. (1996). Polymer layered silicate nanocomposites. *Advanced Materials*. 8(1): 29-35.
- Gosseling, R.R.D.R.B. (2006). Injection Molding of Postconsumer Wood – Plastic Composites I: Morphology. *Journal of Thermoplastic Composite Material*. 19, 639– 657. doi:10.1177/0892-705706067484
- Griswold, B.M. (2006). Old computers to be recycled into decking. *Plastic News*, 1–3.
- Guo, C., Li, L. and Wang, Q. (2012). Investigation on the compatibilizing effect of m-isopropenyl- α , α -dimethylbenzyl isocyanate grafted polypropylene on polypropylene and wood flour composites. *Wood science and technology*, 46(1-3), pp.257-270.
- Guo, Z., Park, S., Wei, S., Pereira, T., Moldovan, M., Karki, A.B., Young, D.P. and Hahn, H.T. (2007). Flexible high-loading particle-reinforced polyurethane magnetic nanocomposite fabrication through particle-surface-initiated polymerization. *Nanotechnology*. 18 335704: 1-8.
- Gupta, R.K., Kennel, E. and Kim, K.J. eds. (2009). *Polymer nanocomposites handbook*. CRC press.

- Gusev, A.A. and Lusti, H.R. (2001). Rational design of nanocomposites for barrier applications. *Advanced Materials*, 13(21), pp.1641-1643.
- Gwon, J.G., Lee, S.Y., Chun, S.J., Doh, G.H. and Kim, J.H. (2010). Effects of chemical treatments of hybrid fillers on the physical and thermal properties of wood plastic composites. *Composites Part A: Applied Science and Manufacturing*, 41(10), pp.1491-1497.
- Hakamy, A., Shaikh, F. U. A., and Low, I. M. (2014). Thermal and mechanical properties of hemp fabric-reinforced nanoclay–cement nanocomposites. *Journal of Materials Science*, 49(4), 1684-1694.
- Han, G., Y. Lei, Q. Wu, Y. Kojima and S. Suzuki, (2008). Bamboo-fiber filled high density polyethylene composites: Effect of coupling treatment and nanoclay. *Journal of Polymer Environ.* 21: 1567-1582.
- Herrmann, a. S., Nickel, J. and Riedel, U. (2000). Construction materials based upon biologically renewable resources—from components to finished parts. *Polymer Degradation Stability*. 59, 251–261. doi:10.1016/S0141-3910(97)00169-9
- Hetzer, M. and De Kee, D. (2008). Wood/polymer/nanoclay composites, environmentally friendly sustainable technology: A review. *Chemical engineering research and design*, 86(10), pp.1083-1093.
- Hohne, G.W.H., Hemminger, W.F. and Flammersheim, H.J. (2003). *Differential Scanning Calorimetry*. 2. Germany; Springer-Verlag Berlin Heidelberg.
- Holbery, J. and Houston, D. (2006). Natural-fiber-reinforced polymer composites in automotive applications. *Jom*, 58(11), pp.80-86.
- Homami, S.S., Seydei, M.K. and Moradi, S. (2013). Preparation of Wood Plastic Composite with High Density Polyethylene and Bagasse. *World Applied Sciences Journal*. 21, 1302–1304. doi:10.5829/idosi.wasj.2013.21.9.2669
- Hosseinaei, O., Wang, S., Enayati, A.A. and Rials, T.G. (2012). Effects of hemicellulose extraction on properties of wood flour and wood–plastic composites. *Composites Part A: Applied Science and Manufacturing*, 43(4), pp.686-694.
- Huda, M.S., Drzal, L.T., Mohanty, A.K. and Misra, M. (2006). Chopped glass and recycled newspaper as reinforcement fibers in injection molded poly (lactic acid) (PLA) composites: A comparative study. *Composites Science and Technology* 66(11–12): 1813- 1824.
- Hussain, F., Hojjati, M., Okamoto, M. and Gorga, R.E. (2006). Review article: polymer-matrix nanocomposites, processing, manufacturing, and application: an overview. *Journal of composite materials*, 40(17), pp.1511-1575.

- Isik, I., Yilmazer, U. and Bayram, G. (2003). Impact modified epoxy/montmorillonite nanocomposites: synthesis and characterization. *Polymer*. 44(20): 6371-6377.
- J. Njuguna, K.P. and S.D. (2008). Nanofiller- reinforced polymer nanocomposites. *Polymer Advanced Technology*. 19, 947–959.
- Javier, C.S., Sergio, A.R., Roberto, Z.G. and Jorge, D.D. (2015). Optimization of the tensile and flexural strength of a wood-PET composite. *Ingeniería, Investigación y Tecnología*, 16(1), pp.105-112.
- Jayaraman, K. (2003). Manufacturing sisal-polypropylene composites with minimum fiber degradation. *Composite Science and Technology*. 63, 367–374. doi:10.1016/S0266-3538(02)00217-8
- Jin, J., Song, M., Yao, K.J. and Chen, L. (2006). A study on viscoelasticity of polyurethane–organoclay nanocomposites. *Journal of applied polymer science*, 99(6), pp.3677-3683.
- John, M.J. and Thomas, S. (2008). Biofibers and biocomposites. *Carbohydrate Polymer*. 71, 343–364. doi:10.1016/j.carbpol.2007.05.040
- Johnson, R.K., Zink-Sharp, A., Rennecker, S.H. and Glasser, W.G. (2008). Mechanical properties of wetlaid lyocell and hybrid fiber-reinforced composites with polypropylene. *Composites Part A: Applied Science and Manufacturing*, 39(3), pp.470-477.
- Jordens, C., Wietzke, S., Scheller, M. and Koch, M. (2010). Investigation of the water absorption in polyamide and wood plastic composite by terahertz time-domain spectroscopy. *Polymer Testing*. 29, 209–215. doi:10.1016/j.polymertesting.2009.11.003
- Kamar, N.T., Hossain, M.M., Khomenko, A., Haq, M., Drzal, L.T. and Loos, A. (2015). Interlaminar reinforcement of glass fiber/epoxy composites with graphene nanoplatelets. *Composites Part A: Applied Science and Manufacturing*, 70, pp.82-92.
- Kamdem, D.P., Jiang, H., Cui, W., Freed, J. and Matuana, L.M. (2004). Properties of wood plastic composites made of recycled HDPE and wood flour from CCA-treated wood removed from service. *Composites Part A: Applied Science and Manufacturing*, 35(3), pp.347-355.
- Kamel, S. (2007). Nanotechnology and its applications in lignocellulosic composites, a mini review. *Express Polymer Letter*. 1, 546–575. doi:10.3144/expresspolymlett.2007.78
- Kanny, K. and Moodley, V.K. (2007). Characterization of polypropylene nanocomposite structures. *Journal of Engineering Materials and Technology*, 129(1), pp.105-112.

- Karmaker, A.C. and Youngquist, J.A. (1996). Injection molding of polypropylene reinforced with short jute fibers. *Journal of Applied Polymer Science*, 62(8), pp.1147-1151.
- Karmarkar, A., Chauhan, S.S., Modak, J.M. and Chanda, M. (2007). Mechanical properties of wood–fiber reinforced polypropylene composites: Effect of a novel compatibilizer with isocyanate functional group. *Composites Part A: Applied Science and Manufacturing*, 38, 227–233. doi:10.1016/j.compositesa.2006.05.005
- Keener, T.J., Stuart, R.K. and Brown, T.K. (2004). Maleated coupling agents for natural fibre composites. *Composites Part A: Applied Science and Manufacturing*, 35(3), pp.357-362.
- Khademi-Eslam, H., Yousefnia, Z., Ghasemi, E. and Talaeipour, T. (2013). Investigating the mechanical properties of wood flour/polypropylene/ nanoclay composite. *Iran Journal of Wood Paper Sciences and Resources*, 28(1): 153-168.
- Khalid, M., Ali, S., Abdullah, L.C., Ratnam, C.T. and Thomas Choong, S. (2006). Effect of MAPP as coupling agent on the mechanical properties of palm fiber empty fruit bunch and cellulose polypropylene biocomposites. *International Journal of Engineering Technology*, 3, 79–84.
- Khosravian, B. (2009). *Investigating the mechanical, physical, thermal and morphological properties of polypropylene / wood flour / wollastonite hybrid composites*. MA Thesis, Department of Agriculture and Natural Resources, University of Tehran, Iran.
- Kim, J.P., Yoon, T.H., Mun, S.P., Rhee, J.M. and Lee, J.S. (2006). Wood-polyethylene composites using ethylene-vinyl alcohol copolymer as adhesion promoter. *Bioresources Technology*, 97, 494–499. doi:10.1016/j.biortech.2005.02.048
- Klyosov, A.A. (2007). *Wood Plastic Composites*. WileyInterscience, Hoboken, N.J.
- Korbahti, B.K. and Rauf, M.A. (2008). Response surface methodology (RSM) analysis of photoinduced decoloration of toluidine blue. *Chemical Engineering Journal*, 136(1), pp.25-30.
- Kord, B. (2011). Effect of bark flour content on mechanical properties of wood plastic composites. *World Applied Sciences Journal*, 14(3), pp.398-401.
- Kord, B. (2012). Effects of compatibilizer and nanolayered silicate on physical and mechanical properties of PP/bagasse composites. *Turkish Journal of Agriculture and Forestry*, 36(4), pp.510-517.
- Kord, B. (2010). Investigating the effect of nanoclay particles on the mechanical properties of woodplastic composite obtained from high density polyethylene- wood flour. Two Iran. Quart. *Journal of Wood Paper Sciences and Resources*, 25(1): 91-101.

- Kord, B. and Kiakojour, S. (2011). Effect of nanoclay dispersion on physical and mechanical properties of wood flour/polypropylene/glass fiber hybrid composites. *BioResources*. 6, 1741–1751.
- Kordkheili, H., Farsi, M. and Rezazadeh, Z. (2013). Physical, mechanical and morphological properties of polymer composites manufactured from carbon nanotubes and wood flour. *Composite Part B: Engineering*. 44, 750–755.
- Kordkheili, H.Y., Hiziroglu, S. and Farsi, M. (2012). Some of the physical and mechanical properties of cement composites manufactured from carbon nanotubes and bagasse fiber. *Material and Design*. 33, 395–398. doi:10.1016/j.matdes.2011.04.027
- Kornmann, X. (2001). *Synthesis and Characterization of Thermoset-Clay Nanocomposites*. Doctoral Thesis. Division of Polymer Engineering, Lulea University of Technology, Lulea, Sweden.
- Korol, J. (2012). Polyethylene matrix composites reinforced with keratin fibers obtained from waste chicken feathers. *Journal of Biobased Material Bioenergy* 6, 355–360. doi:10.1166/jbmb.2012.1237
- Krishnamoorti, R., Vaia, R.A. and Giannelis, E.P. (1996). Structure and Dynamics of Polymer-Layered Silicate Nanocomposites. *Chem Mater*. 8: 1728-1734.
- Kuo, P.Y., Wang, S.Y., Chen, J.H., Hsueh, H.C. and Tsai, M.J. (2009). Effects of material compositions on the mechanical properties of wood-plastic composites manufactured by injection molding. *Material and Design*. 30, 3489–3496. doi:10.1016/j.matdes.2009.03.012
- Lee, C.T., Lee, S.L., Ng, K.K.S., Faridah, Q.Z., Siraj, S.S. and Norwati, M. (2011). Estimation of outcrossing rates in *Koompassia malaccensis* from an open-pollinated population in Peninsular Malaysia using microsatellite markers. *Journal of Tropical Forest Science*. 23, 410–416.
- Lee, S.H. and Wang, S. (2006). Biodegradable polymers/bamboo fiber biocomposite with bio-based coupling agent. *Composites Part A: Applied Science and Manufacturing*, 37(1), pp.80-91.
- Lee, S.Y., Kang, I. a., Doh, G.H., Kim, W.J., Kim, J.S., Yoon, H.G. and Wu, Q. (2008). Thermal, mechanical and morphological properties of polypropylene/clay/wood flour nanocomposites. *Express Polymer Letter*. 2, 78–87. doi:10.3144/expresspolymlett.2008.11
- Lei, B., Zhang, Y., He, Y., Xie, Y., Xu, B., Lin, Z., Huang, L., Tan, S., Wang, M. and Cai, X. (2015). Preparation and characterization of wood–plastic composite reinforced by graphitic carbon nitride. *Materials & Design*, 66, pp.103-109.

- Lei, S. (2003). *Formulation and mechanical properties of polypropylene nanocomposites*. Doctoral dissertation, Concordia University.
- Lei, Y., Q. Wu, C.M. Celmons, F. Yao and Y. Xu. (2007). Influence of Nanoclay on properties of HDPE/wood composites. *Journal of Applied Polymer Science*. 106: 3958-3966.
- Li, X., Gao, H., Scrivens, W.A., Fei, D., Xu, X., Sutton, M.A., Reynolds, A.P. and Myrick, M.L. (2004). Nanomechanical characterization of single-walled carbon nanotube reinforced epoxy composites. *Nanotechnology*, 15(11), p.1416.
- Li, X., Lei, B., Lin, Z., Huang, L., Tan, S. and Cai, X. (2014). The utilization of bamboo charcoal enhances wood plastic composites with excellent mechanical and thermal properties. *Material and Design*. 53, 419–424. doi:10.1016/j.matdes.2013.07.028
- Li, X., Tabil, L.G. and Panigrahi, S. (2007). Chemical treatments of natural fiber for use in natural fiber-reinforced composites: A review. *J. Polym. Environ.* 15, 25–33. doi:10.1007/s10924-006-0042-3
- Loos, J., Alexeev, A., Grossiord, N., Koning, C.E. and Regev, O. (2005). Visualization of single-wall carbon nanotube (SWNT) networks in conductive polystyrene nanocomposites by charge contrast imaging. *Ultramicroscopy* 104, 160–167. doi:10.1016/j.ultramic.2005.03.007
- Lundin, T., Falk, R.H. and Felton, C. (2001). Accelerated Weathering of Natural Fiber-Thermoplastic Composites : Effects of Ultraviolet Exposure on Bending Strength and Stiffness. *Matrix*, 87–94.
- Lu, J. Z., Wu. Q. and McNabb H. S. (2000). Chemical Coupling in Wood Fiber and Polymer Composites: A Review of Coupling Agents and Treatments. *Wood Fiber Sci.* 32(1), pp 88 – 104.
- Lu, J.Z., Wu, Q. and McNabb, H.S. (2007). Chemical coupling in wood fiber and polymer composites: A review of coupling agents and treatments. *Wood and Fiber Science*, 32(1), pp.88-104.
- Magaraphan, R., Lilayuthalert, W. and Sirivat, A. (2001). Preparation , structure , properties and thermal behavior of rigid-rod polyimide / montmorillonite nanocomposites. *Compos. Sci. Technol.* 61, 1253–1264.
- Mai, Y.W. and Yu. Z. Z. (2010). *Polymer Nanocomposites* (Ed. 1st). New York: CRC Press.
- Markarian, J. (2008). Outdoor living space drives growth in wood-plastic composites. *Plast. Addit. Compd.* 10, 20–25. doi:10.1016/S1464-391X(08)70131-4
- Materials Evaluation and Engineering, Inc. (2009). *Handbook of analytical methods for materials* (online). <http://mee-inc.com/thermal-analysis.html>.

- Matuana, L.M. and Li, Q. (2004). Statistical modeling and response surface optimization of extruded HDPE/wood-flour composite foams. *Journal of Thermoplastic Composite Materials*, 17(2), pp.185-199.
- Messersmith, P.B. and Giannelis, E.P. (1995). Synthesis and barrier properties of poly (ϵ -caprolactone)-layered silicate nanocomposites. *Journal of Polymer Science Part A: Polymer Chemistry*, 33(7), pp.1047-1057.
- Metin, D., Tihminlioglu, F., Balkose, D. and Ulku, S. (2004). The effect of interfacial interactions on the mechanical properties of polypropylene/natural zeolite composites. *Compos. Part A Appl. Sci. Manuf.* 35, 23–32. doi:10.1016/j.compositesa.2003.09.021
- Migneault, S., Koubaa, A., Erchiqui, F., Chaala, A., Englund, K. and Wolcott, M.P. (2009). Effects of processing method and fiber size on the structure and properties of wood-plastic composites. *Compos. Part A Appl. Sci. Manuf.* 40, 80–85. doi:10.1016/j.compositesa.2008.10.004
- Mohan, T.P., Kuriakose, J. and Kanny, K. (2011). Effect of nanoclay reinforcement on structure, thermal and mechanical properties of natural rubber–styrene butadiene rubber (NR–SBR). *Journal of Industrial and Engineering Chemistry*, 17(2), pp.264-270.
- Mohanty, S., and Nayak, S. K. (2007). Effect of clay exfoliation and organic modification on morphological, dynamic mechanical, and thermal behavior of melt-compounded polyamide-6 nanocomposites. *Polymer Composites*, 28(2), 153-162.
- Morrell, J.J., Stark, N.M., Pendleton, D.E. and McDonald, A.G. (2009). *Durability of Wood-Plastic Composites*, 71–76.
- Mwaikambo, L.Y. and Ansell, M.P. (1999), June. The effect of chemical treatment on the properties of hemp, sisal, jute and kapok fibres for composite reinforcement. In *2nd international wood and natural fibre composites symposium*, Vol. 6.
- Naeemian, N. (2008). *Evaluating the properties of hybrid composition made of wood flour, hemp fibers/polypropylene*, Ph.D Thesis, Islamic Azad University, Science and Research Branch of Tehran.
- Nafchi, H.R., Abdouss, M., Najafi, S.K., Gargari, R.M. and Mazhar, M. (2015). Effects of nano-clay particles and oxidized polypropylene polymers on improvement of the thermal properties of wood plastic composite. *Maderas. Ciencia y tecnología*, 17(1), pp.45-54.
- Najafi, A., Kord, B., Abdi, A. and Ranaee, S. (2012). The impact of the nature of nanoclay on physical and mechanical properties of polypropylene/reed flour nanocomposites. *Journal of Thermoplastic Composite Materials*, 25(6), pp.717-727.

- Najafi, S.K. and Kordkheili, H.Y. (2011). Effect of sea water on water absorption and flexural properties of wood-polypropylene composites. *European Journal of Wood and Wood Products*, 69(4), pp.553-556.
- Nakas, G. I., and Kaynak, C. (2009). Use of different alkylammonium salts in clay surface modification for epoxy-based nanocomposites. *Polymer composites*, 30(3), 357-363.
- Nawani, P., Gelfer, M.Y., Hsiao, B.S., Frenkel, A., Gilman, J.W. and Khalid, S. (2007). Surface modification of nanoclays by catalytically active transition metal ions. *Langmuir*, 23(19), pp.9808-9815.
- Ndiaye, D., Diop, B., Thiandoume, C., Fall, P.A., Farota, A.K. and Tidjani, A. (2012). Morphology and Thermo Mechanical Properties of Wood / Polypropylene Composites. *Polypropylene*, 415–428.
- Ndiaye, D. and Tidjani, a. (2012). Effects of coupling agents on thermal behavior and mechanical properties of wood flour/polypropylene composites. *J. Compos. Mater.* doi:10.1177/0021998311435675
- Odenberger, P.T., Andersson, H.M. and Lundström, T.S. (2004). Experimental flow-front visualisation in compression moulding of SMC. *Compos. Part A Appl. Sci. Manuf.* 35, 1125–1134. doi:10.1016/j.compositesa.2004.03.019
- Okamoto, M. (2003). Polymer/Layered Silicate Nanocomposites. *Rapra Review Reports*. 14(7): 36.
- Olphen, H.V. (1977). *An Introduction to Clay Colloidal Chemistry*. New York. Wiley.
- Oliver, W.C. and Pharr, G.M. (1992). An improved technique for determining hardness and elastic modulus using load and displacement sensing indentation experiments. *Journal of materials research*, 7(06), pp.1564-1583.
- Panthapulakkal, S. and Sain, M. (2007). Agro-residue reinforced high-density polyethylene composites: Fiber characterization and analysis of composite properties. *Compos. Part A Appl. Sci. Manuf.* 38, 1445–1454. doi:10.1016/j.compositesa.2007.01.015
- Panthapulakkal, S., Zereskian, a. and Sain, M. (2006). Preparation and characterization of wheat straw fibers for reinforcing application in injection molded thermoplastic composites. *Bioresour. Technol.* 97, 265–272. doi:10.1016/j.biortech.2005.02.043
- Paul, S.A., Joseph, K., Mathew, G.D.G., Pothen, L. a. and Thomas, S. (2010). Influence of polarity parameters on the mechanical properties of composites from polypropylene fiber and short banana fiber. *Compos. Part A Appl. Sci. Manuf.* 41, 1380–1387. doi:10.1016/j.compositesa.2010.04.015
- Pavlidou, S. and Papaspyrides, C.D. (2008). A review on polymer-layered silicate nanocomposites. *Progress in Polymer Science*. 33(12): 1119-1198.

- Qin, H., Zhang, S., Zhao, C., Feng, M., Yang, M., Shu, Z. and Yang, S. (2004). Thermal stability and flammability of polypropylene/montmorillonite composites. *Polymer Degradation and Stability*, 85(2), pp.807-813.
- Rahman, K.-S., Islam, M.N., Rahman, M.M., Hannan, M.O., Dungani, R. and Khalil, H.A. (2013). Flat-pressed wood plastic composites from sawdust and recycled polyethylene terephthalate (PET): physical and mechanical properties. *Springerplus* 2, 629. doi:10.1186/2193-1801-2-629
- Ramos Filho, F.G., Melo, T.J.A., Rabello, M.S. and Silva, S.M. (2005). Thermal stability of nanocomposites based on polypropylene and bentonite. *Polymer Degradation and Stability*, 89(3), pp.383-392.
- Ratanawilai, T., Thanawattanasirikul, N. and Homkhiew, C. (2012). Mechanical and thermal properties of oil palm wood sawdust reinforced post-consumer polyethylene composites. *ScienceAsia*, 38, 289–294. doi:10.2306/scienceasia1513-1874.2012.38.289.
- Ray, D., Sarkar, B.K. and Bose, N.R. (2002). Impact fatigue behaviour of vinylester resin matrix composites reinforced with alkali treated jute fibers. *Compos. - Part A Appl. Sci. Manuf.* 33, 233–241. doi:10.1016/S1359-835X(01)00096-3
- Ray, S.S. and Okamoto, M. (2003). Polymer / Layered Silicate Nanocomposites: A Review from Preparation to Processing, *Prog. Polym. Sci.* 28, pp 1539 – 1641.
- Razavi-Nouri, M., Jafarzadeh-Dogouri, F., Oromiehie, A. and Langroudi, A.E. (2006). Mechanical properties and water absorption behaviour of chopped rice husk filled polypropylene composites. *Iranian Polymer Journal*, 15(9), pp.757-766.
- Royan, N., Ng, Y., Ghani, M.A., Ahmad, S. and Lumpur, K. (2014). Study of the Mechanical and Morphology Properties of Recycled HDPE Composite using Rice Husk Filler. *Av. Mater. Sci.* 1–10.
- Rossi, L. M. and Morton, J. (2006). WPCs: Putting Innovation on a Faster Track. *International Conference on Wood fiber-Plastic Composites*. 8th. Madison, WI, May 23 – 25.
- Rude, E.F. a Y. (2007). *Evaluation of Coupling Mechanisms in Wood Plastic Composites*.
- Sain, M., Park, S.H., Suhara, F. and Law, S. (2004). Flame retardant and mechanical properties of natural fiber-PP composites containing magnesium hydroxide. *Polym. Degrad. Stab*, 83, 363–367. doi:10.1016/S0141-3910(03)00280-5
- Salah, M. and Mokhtar, a. (2009). *Wood Plastic Composites*. *Www.Intechopen.Com* 325–344.

- Salmah, H., Ruzaidi, C.M. and Ghani, S. a. (2007). the Effect of Coupling Agent on Thermal Properties and Morphology of Paper Sludge Filled Polypropylene (Pp)/ Ethylene Propylene Diene Terpolymer (Epdm) Composites. *Composites Part A: Applied Science and Manufacturing*, 29(8), pp.1632-1637.
- Schadler, L.S. (2003). *Polymer-Based and Polymer-Filled Nanocomposites* (pp. 77-153). Wiley-VCH Verlag GmbH & Co. KGaA.
- Schadler, L.S., Brinson, L.C. and Sawyer, W.G. (2007). Polymer nanocomposites: A small part of the story. *Jom*, 59, 53–60. doi:10.1007/s11837-007-0040-5
- Schut, J.H. (2004). Beyond Decking. *Plastic Technology*, 50(8), pp50-55.
- Segerholm, K. (2007). Wood Plastic Composites made from Modified Wood - Aspects on moisture sorption, micromorphology and durability. *Composites Part A: Applied Science and Manufacturing*, 29(9), pp.1632-1637.
- Sgriccia, N., Hawley, M.C. and Misra, M. (2008). Characterization of natural fiber surfaces and natural fiber composites. *Composites Part A: Applied Science and Manufacturing*, 39(10), pp.1632-1637.
- Shamini, G. (2014). *Barrier, thermal and mechanical properties of polyurethane-modified clay nanocomposites for thermal insulation material*. PhD thesis, Universiti Malaysia Pahang, Malaysia.
- Shen, L., Phang, I.Y., Chen, L., Liu, T. and Zeng, K. (2004). Nanoindentation and morphological studies on nylon 66 nanocomposites. I. Effect of clay loading. *Polymer*, 45(10), pp.3341-3349.
- Sherman, L. M. (2004). Wood-Filled Plastics - They Need the Right Additives for Strength, Good Looks & Long Life. *Plast. Technol.* 50(7), pp 52 – 59.
- Sheshmani, S., Ashori, A. and Fashapoyeh, M.A. (2013). Wood plastic composite using graphene nanoplatelets. *International journal of biological macromolecules*, 58, pp.1-6.
- Shokrieh, M. and S.E. Sonbolestan, (2007). The effect of structural factors on the mechanical properties of polymer-clay nanocomposites. *Journal of Polymer Science and Technology*. 20(2): 187-195.
- Sihombing, H., Rassiah, K., Ashaari, Z. and Y, M.Y. (2012). Analysis and development of recycled materials for wood plastic composite product. *Elixir Mech. Engg*, 51, 10834–10840.
- Silva, M.J.D., Kanda, D.H.F. and Nagashima, H.N. (2012). Mechanism of charge transport in castor oil-based polyurethane/carbon black composite. *Journal of Non-Crystalline Solids*, 358(2): 270-275.

- Singh-Beemat, J. and Iroh, J.O. (2012). Characterization of corrosion resistant clay/epoxy ester composite coatings and thin films. *Prog. Org. Coatings* 74, 173–180. doi:10.1016/j.porgcoat.2011.12.006
- Soccalingame, L., Bourmaud, A., Perrin, D., Benezet, J.C. and Bergeret, A. (2015). Reprocessing of wood flour reinforced polypropylene composites: Impact of particle size and coupling agent on composite and particle properties. *Polymer Degradation and Stability*, 113, pp.72-85.
- Soury, E., Behraves, a. H., Rouhani Esfahani, E. and Zolfaghari, a. (2009). *Design, optimization and manufacturing of wood-plastic composite pallet*. Mater. Des. 30, 4183–4191. doi:10.1016/j.matdes.2009.04.035
- Stark, N.M., Matuana, L.M. and Clemons, C.M. (2004). Effect of processing method on surface and weathering characteristics of wood-flour/HDPE composites. *Journal of Applied Polymer Science*, 93, 1021–1030. doi:10.1002/app.20529
- Stark, N.M. and Rowlands, R.E. (2003). Effects of Wood Fiber Characteristics on Mechanical Properties of Wood/Polypropylene Composites. *Wood Fiber Sci.* 35, 167–174. doi:10.1016/S0008-8846(03)00193-5
- Stark, N.M., White, R.H., Mueller, S. a. and Osswald, T. a. (2010). Evaluation of various fire retardants for use in wood flour-polyethylene composites. *Polym. Degrad. Stab.* 95, 1903–1910. doi:10.1016/j.polymdegradstab.2010.04.014
- Sun, S., Li, C., Zhang, L., Du, H.L. and Burnell-Gray, J.S. (2006). Interfacial structures and mechanical properties of PVC composites reinforced by CaCO₃ with different particle sizes and surface treatments. *Polymer international*, 55(2), pp.158-164.
- Svab, I., Musil, V. and Leskovac, M. (2005). The adhesion phenomena in polypropylene/wollastonite composites. *Acta Chim. Slov*, 52, pp.264-271.
- Sykacek, E., Hrabalova, M., Frech, H. and Mundigler, N. (2009). Extrusion of five biopolymers reinforced with increasing wood flour concentration on a production machine, injection moulding and mechanical performance. *Compos. Part A Appl. Sci. Manuf*, 40, 1272–1282. doi:10.1016/j.compositesa.2009.05.023
- Tabari, H.Z., Nourbakhsh, A. and Ashori, A. (2011). Effects of nanoclay and coupling agent on the physico-mechanical, morphological, and thermal properties of wood flour/polypropylene composites. *Polymer Engineering & Science*, 51(2), pp.272-277.
- Taib, R.M., Zauzi, N.S.A., Ishak, Z. a M. and Rozman, H.D. (2010). Effects of Photo-Stabilizers on the Properties of Recycled High-Density Polyethylene (HDPE)/ Wood Flour (WF) Composites Exposed to Natural Weathering. *PRIM Malaysia Polymer Journal*, 5, 193–203.

- Tajan, M., Chaiwutthinan, P. and Leejarkpai, T. (2008). Thermal and Mechanical Properties of Wood-Plastic Composites from Iron Wood Flour and Recycled Polypropylene Foam. *J. Met. Mater. Miner.* 18, 53–56.
- Theng, B.K.G. (1979). *Formation and properties of clay-polymer complexes*. Elsevier:Amsterdam.
- Thio, Y.S., Argon, a. S. and Cohen, R.E. (2004). Role of interfacial adhesion strength on toughening polypropylene with rigid particles. *Polymer (Guildf)*, 45, 3139–3147. doi:10.1016/j.polymer.2004.02.064
- Tjong, S.C. (2009). *Carbon nanotube reinforced composites: metal and ceramic matrices*. John Wiley & Sons.
- Vaia, R.A., Price, G., Ruth, P.N., Nguyen, H.T. and Lichtenhan, J. (1999). Polymer/layered silicate nanocomposites as high performance ablative materials. *Applied Clay Science*, 15: 67-92.
- Varghese, S., Kocsis, J.K. and Gatos, K.G. (2003). Melt compounded epoxidised natural rubber/layered silicate nanocomposites: Structure-properties relationships. *Polymer*, 44: 3977-3983.
- Vitkauskiene, I., Makuska, R., Stirna, U. and Cabulis, U. (2011). Thermal properties of polyurethane-polyisocyanurate foams based on Poly(ethylene terephthalate) waste. *Materials Science*. 17(3): 249-253.
- Wang, K.H., Choi, M.H., Koo, C.M., Xu, M., Chung, I.J., Jang, M.C., Choi, S.W. and Song, H.H. (2002). Morphology and physical properties of polyethylene/silicate nanocomposite prepared by melt intercalation. *Journal of Polymer Science Part B: Polymer Physics*, 40(14), pp.1454-1463.
- Wang, Y. (2007). Morphological characterization of wood plastic composite (WPC) with advanced imaging tools: developing methodologies for reliable phase and internal damage characterization. *Adv. Imaging*.
- Wang, Z. and Pinnavaia, T.J. (1998). Nanolayer reinforcement of elastomeric polyurethane. *Chemistry of Materials*, 10: 3769-3771.
- Wang, Z., Wang, X., Li, G. and Zhang, Z. (2008). Enhanced exfoliation of montmorillonite prepared by hydrothermal method. *Applied Clay Science*, 42: 146-150.
- Waste, T., Programme, R.A. and Academy, T.O. (2003). *Wood Plastic Composites Study - Technologies and Uk*.
- Wenhan Ren, Dan Zhang, Ge Wang, and H.C. (2014). Mechanical and Thermal Properties of Bamboo Pulp Fiber Reinforced Polyethylene Composites. *BioResources*, 9, 4117–4127.
- Wolcott, M.P. (1999). A technology review of WPC. *33rd Int. Part. Mater. Symp.*

- Wolcott, M. P., Smith, P. M. and Hermanson, J. (2006). Opportunities and Challenges for WPC's in Emerging Product Areas. *International Conference on Wood fiber-Plastic Composites*. 8th, Madison, WI, May 23 – 25, 134.
- Wunderlich, B. (1980). *Crystal melting*. Macromolecular physics, vol. 3. New York: Academic Press.
- Xie, Y., Hill, C. a S., Xiao, Z., Miltz, H. and Mai, C. (2010). Silane coupling agents used for natural fiber/polymer composites: A review. *Compos. Part A Appl. Sci. Manuf.* 41, 806–819. doi:10.1016/j.compositesa.2010.03.005
- Yang, B.Z., Seale, R.D., Dahlen, J., Shmulsky, R. and Jones, P.D. (2014). Bending properties of a novel engineered composite from southern pine lumber. *Eur. J. Wood Wood Prod.* 72, 601–607. doi:10.1007/s00107-014-0821-9
- Yang, S., Zhang, Y.W. and Zeng, K. (2004). Analysis of nanoindentation creep for polymeric materials. *Journal of applied physics*, 95(7), pp.3655-3666.
- Yang, T.H., Leu, S.Y., Yang, T.H. and Lo, S.F. (2012). Optimized material composition to improve the physical and mechanical properties of extruded wood-plastic composites (WPCs). *Constr. Build. Mater.* 29, 120–127. doi:10.1016/j.conbuildmat.2011.09.013
- Yao, K.J., Song, M. Hourston, D.J. and Luo, D.Z. (2002). Polymer/layered clay nanocomposites: 2 polyurethane nanocomposites. *Polymer*, 43: 1017-1020.
- Yapar, S. (2009). Physicochemical study of microwave-synthesized organoclays. *Colloid Surface A*, 345: 75-81.
- Yeh, S.-K. (2007). *Polypropylene-Based Wood-Plastic Composites Reinforced With Nanoclay*. PhD Dissertation.
- Yeh, S.K., Agarwal, S. and Gupta, R.K. (2009). Wood-plastic composites formulated with virgin and recycled ABS. *Compos. Sci. Technol.* 69, 2225–2230. doi:10.1016/j.compscitech.2009.06.007
- Yeh, S.K. and Gupta, R.K. (2008). Improved wood-plastic composites through better processing. *Compos. Part A Appl. Sci. Manuf.* 39, 1694–1699. doi:10.1016/j.compositesa.2008.07.013
- Yeh, S.K. and Gupta, R.K. (2010). Nanoclay-reinforced, polypropylene-based wood-plastic composites. *Polymer Engineering & Science*. 50(10), pp.2013-2020.
- Yeh, S.K., Kim, K.J. and Gupta, R.K. (2013). Synergistic effect of coupling agents on polypropylene-based wood-plastic composites. *Journal of Applied Polymer Science*. 127(2), pp.1047-1053.

- Yeh S-K, Ortiz D, Al-Mulla A and Gupta R.K. (2005). Mechanical and thermal properties of wood/layered silicate/ plastic composites. *In: 8th International Conference on Woodfiber–Plastic Composites (and other natural fibers)*, Madison, Wisconsin, USA, 23–25.
- Yildiz, S. and Gumuskaya, E. (2007). The effects of thermal modification on crystalline structure of cellulose in soft and hardwood. *Building and Environment*. 42(1), pp.62-67.
- Yusoh, K. (2010). *Subsurface and bulk mechanical properties of polyurethane nanocomposite films*. Doctoral dissertation, © Kamal Yusoh.
- Zhao, Y., Wang, K., Zhu, F., Xue, P. and Jia, M. (2006). Properties of poly (vinyl chloride)/wood flour/montmorillonite composites: Effects of coupling agents and layered silicate. *Polymer Degradation and Stability*. 91(12), pp.2874-2883.
- Ziaei, T.H., M.A. Danesh, R. Hosseinpour Pia and A. Nourbakhsh, (2011). Evaluation of mechanical and morphological behavior of polypropylene/ wood fiber nanocomposite prepared by melt compounding. *Proceeding of the 2010 International Conference on Nanotechnology and Biosensors IPCBEE*, IACSIT Press, Singapore, 2: 20-23.
- Zolfaghari, A., Behraves, A.H. and Adli, A. (2013). Continuous glass fiber reinforced wood plastic composite in extrusion process: Mechanical properties. *Mater. Des.* 51, 701–708. doi:10.1016/j.matdes.2013.04.08.

The logo of UMPA (Universiti Malaysia Perlis) is a large, stylized shield shape. It is divided into four quadrants by a white 'V' shape pointing downwards. The top-left quadrant is light blue, the top-right is light purple, the bottom-left is light green, and the bottom-right is light blue. The letters 'UMPA' are written in white, bold, sans-serif font across the center of the shield.

UMPA

APPENDIX

A: MECHANICAL PROPERTIES OF WOOD-PLASTIC COMPOSITE

A-1: Tensile properties of PP and WPC with different concentrations of organoclay

Samples	Tensile strength (MPa)	Tensile modulus (MPa)
PP	32.77 ± 0.1	347.26 ± 2.6
WPC	27.98 ± 0.1	449.52 ± 2.4
WPC-1	32.21 ± 0.1	549.65 ± 1.2
WPC-2.5	31.48 ± 0.1	552.56 ± 1.0
WPC-4	31.02 ± 0.2	560.41 ± 1.2
WPC-5	30.71 ± 0.2	577.97 ± 1.3

A-2: Flexural properties of PP and WPC with different concentrations of organoclay

Samples	Flexural strength (MPa)	Flexural modulus (MPa)
PP	48.28 ± 0.3	1449.39 ± 0.6
WPC	54.82 ± 0.2	1823.95 ± 0.4
WPC-1	59.45 ± 0.2	1903.16 ± 0.4
WPC-2.5	58.76 ± 0.1	1918.65 ± 0.2
WPC-4	58.56 ± 0.1	1958.57 ± 0.2
WPC-5	57.13 ± 0.1	1965.23 ± 0.3

A-3: Effect of organoclay on Elongation at Break

Sample	Elongation at break (%)
PP	28.39 ± 0.3
WPC	12.03 ± 0.1
WPC-1	12.10 ± 0.2
WPC-2.5	11.54 ± 0.3
WPC-4	11.40 ± 0.1
WPC-5	11.40 ± 0.2

A-4: Effect of organoclay on impact strength

Sample	Izod impact strength (J/m)
PP	21.83 ± 0.2
WPC	19.42 ± 0.3
WPC-1	17.83 ± 0.2
WPC-2.5	15.75 ± 0.3
WPC-4	14.43 ± 0.3
WPC-5	14.25 ± 0.3

A-5: Tensile strength of PP and WPC with different concentrations of MMT and MMT Cu

Samples	Tensile strength (MPa)	
	WPC/MMT	WPC/MMT Cu
PP	32.77 ± 0.1	
WPC	27.98 ± 0.3	
WPC- 1	29.99 ± 0.2	32.31 ± 0.2
WPC- 2.5	30.07 ± 0.3	31.98 ± 0.3
WPC- 4	29.89 ± 0.3	30.14 ± 0.2
WPC-5	29.47 ± 0.3	29.32 ± 0.3

A-6: Tensile modulus of PP and WPC with different concentrations of MMT and MMT Cu

Samples	Tensile modulus (MPa)	
	WPC/MMT	WPC/MMT Cu
PP	347.26 ± 2.6	
WPC	449.52 ± 2.4	
WPC- 1	502.37 ± 2.6	558.71 ± 2.3
WPC- 2.5	525.11 ± 2.5	567.14 ± 2.1
WPC- 4	556.96 ± 2.2	571.04 ± 2.3
WPC-5	579.68 ± 2.3	594.10 ± 2.4

A-7: Flexural strength of PP and WPC with different concentrations of MMT and MMT Cu

Samples	Flexural strength (MPa)	
	WPC/MMT	WPC/MMT Cu
PP	48.28 ± 0.1	
WPC	54.82 ± 0.2	
WPC - 1	57.02 ± 0.3	59.46 ± 0.3
WPC- 2.5	57.12 ± 0.1	57.42 ± 0.1
WPC- 4	55.21 ± 0.3	56.66 ± 0.1
WPC-5	55.11 ± 0.2	55.76 ± 0.1

A-8: Flexural modulus of PP and WPC with different concentrations of MMT and MMT Cu

Samples	Flexural modulus (MPa)	
	WPC/MMT	WPC/MMT Cu
PP	1449.39 ± 0.6	
WPC	1823.95 ± 0.4	
WPC - 1	1889.50 ± 2.6	1923.37 ± 2.7
WPC- 2.5	1901.10 ± 2.7	1939.43 ± 2.5
WPC- 4	1931.16 ± 2.4	1959.42 ± 3.0
WPC-5	1958.97 ± 2.4	1965.74 ± 2.8

A-9: Elongation at break of PP and WPC with different concentrations of MMT and MMT Cu

Samples	Elongation at break (%)	
	WPC/MMT	WPC/MMT Cu
PP	28.39 ± 0.2	
WPC	12.03 ± 0.1	
WPC - 1	10.31 ± 0.1	13.16 ± 0.1
WPC- 2.5	9.76 ± 0.1	12.66 ± 0.2
WPC- 4	9.49 ± 0.2	12.62 ± 0.1
WPC-5	9.15 ± 0.1	9.93 ± 0.2

A-10: Impact strength of PP and WPC with different concentrations of MMT and MMT Cu

Samples	Izod impact strength (J/m)	
	WPC/MMT	WPC/MMT Cu
PP	21.83 ± 0.2	
WPC	19.42 ± 0.2	
WPC - 1	15.45 ± 0.1	17.92 ± 0.1
WPC- 2.5	14.72 ± 0.2	15.86 ± 0.1
WPC- 4	13.97 ± 0.1	15.06 ± 0.2
WPC-5	11.22 ± 0.2	12.84 ± 0.2

APPENDIX B

B: PHYSICAL PROPERTIES OF WOOD-PLASTIC COMPOSITE

B-1: Density of PP and WPC with different concentrations of MMT and MMT Cu

Samples	Density (g/cm ³)	
	WPC/MMT	WPC/MMT Cu
PP	0.89 ± 0.02	
WPC	0.99 ± 0.01	
WPC - 1	1.09 ± 0.01	1.26 ± 0.02
WPC- 2.5	1.079 ± 0.01	1.20 ± 0.01
WPC- 4	1.074 ± 0.01	1.16 ± 0.01
WPC-5	1.04 ± 0.02	1.15 ± 0.02

B-2: Water absorption of PP and WPC with different concentrations of MMT and MMT Cu

Samples	Water absorption (%)			
	WPC/MMT		WPC/MMT Cu	
	15 days	30 days	15 days	30 days
PP	0.034 ± 0.01	0.037 ± 0.01		
WPC	0.842 ± 0.02	1.039 ± 0.02		
WPC - 1	0.578 ± 0.01	0.661 ± 0.01	0.477 ± 0.01	0.532 ± 0.01
WPC- 2.5	0.673 ± 0.01	0.782 ± 0.01	0.563 ± 0.01	0.592 ± 0.02
WPC- 4	0.796 ± 0.02	0.861 ± 0.02	0.696 ± 0.02	0.730 ± 0.01
WPC-5	0.840 ± 0.02	0.974 ± 0.02	0.731 ± 0.01	0.789 ± 0.02

PUBLICATIONS

CONFERENCE PROCEEDING

1. Yadav, S. M., & Yusoh, K. B. (2015). MECHANICAL AND PHYSICAL PROPERTIES OF WOOD-PLASTIC COMPOSITES MADE OF POLYPROPYLENE, WOOD FLOUR AND NANOCLAY. *Proceeding-Kuala Lumpur International Agriculture, Forestry and Plantation September*, 12-13.

JOURNAL PAPERS

1. Yadav, S. M., & Yusoh, K. B. Modification of pristine nanoclay and its application in wood-plastic composite. *e-Polymers*. **Impact factor: 0.812.**

2. Yadav, S. M., & Yusoh, K. B. Preparation and characterization of wood plastic composite reinforced by organoclay. *Journal of the Indian Academy of Wood Science*, 1-14. **Impact factor: 0.34.**

3. Yadav, S. M., & Yusoh, K. B. (2015). MECHANICAL AND PHYSICAL PROPERTIES OF WOOD-PLASTIC COMPOSITES MADE OF POLYPROPYLENE, WOOD FLOUR AND NANOCLAY. *International Journal of Agriculture, Forestry and Plantation*. Vol.1, September, 52-58.

4. Yadav, S. M., & Yusoh, K. B. Subsurface mechanical properties and subsurface creep behaviour of TMI-modified nanoclay reinforced wood - plastic composite studied by nanoindentation. Submitted to the *Holzforschung* (**under review**). **Impact factor: 1.7**

5. Yadav, S. M., & Yusoh, K. B. Sub-surface mechanical properties and sub-surface creep behaviour of wood-plastic composites reinforced by organoclay. Submitted to the *Polymer engineering* (**under review**). **Impact factor: 0.68**